

C852
6
o.132
969

Atmospheric Transport Processes

Elmar R. Reiter

*Part 1:
Energy Transfers and
Transformations*

AEC CRITICAL REVIEW SERIES

*Atmospheric
Transport
Processes*

*Part 1: Energy
Transfers and
Transformations*

Elmar R. Reiter

Department of Atmospheric Science
Colorado State University, Fort Collins, Colorado

U. S. ATOMIC ENERGY COMMISSION Division of Technical Information

1969

Available as TID-24868
from Clearinghouse for Federal Scientific and Technical Information
National Bureau of Standards, U. S. Department of Commerce
Springfield, Virginia 22151 \$3.00

Library of Congress Catalog Card Number: 76-603262

Printed in the United States of America
USAEC Division of Technical Information Extension
Oak Ridge, Tennessee
December 1969

FOREWORD

“Every now and then you have to stop and put things together.” The staff member who made that statement described well the process of the “critical, creative review.” The next step—of forming conclusions and recommendations for action—is unavoidable to the creative mind, and Dr. Reiter has taken it in this series of four parts on Atmospheric Transport Processes. His conclusions form a new foundation on which to build.

In preparing this review for the AEC Division of Biology and Medicine, Dr. Reiter has encountered a vast number of publications and research projects—far more than any of us had expected. Many of the papers are controversial, and sometimes their evidence is contradictory. About them the observation can be made that the meteorologists and dynamicists on the one hand and the chemists on the other have not been sufficiently cognizant of the other’s field. I believe this review will contribute toward improving the awareness of both and, with that, man’s knowledge of the atmosphere and his ability to predict the movement of tracers within it.

John R. Totter, *Director*
Division of Biology and Medicine
U. S. Atomic Energy Commission

PREFACE

The atmosphere surrounding our globe in a relatively thin “skin” can be looked at from various points of view: The dynamic meteorologist will mainly be interested in the interplay of forces that bring about the various large-scale and small-scale flow patterns which may be observed on a day-to-day basis. He will utilize his systems of equations to arrive at objective forecasts of such motion patterns and of the structure of the atmosphere. The atmospheric chemist will explore the various constituents that make up the body of air in which the dynamicist revels. The turbulence and diffusion expert will take these constituents and spread them about according to laws that infringe upon the realm of the dynamicist. There are also the even more specialized fields of radiation and thermodynamics that deal with energy fluxes received from and returned to sources and sinks beyond the physical extent of the earth’s atmosphere and with the redistribution of these energies within the atmosphere.

This review, which is Part 1 of a series on atmospheric transport processes, adopts its own idiosyncratic point of view: It deals with the properties of the atmosphere that are capable of transporting atmospheric characteristics, be it chemical constituents or dynamic properties. Thus, in essence, it deals with a description of the general circulation of the atmosphere. More specifically, however, it is concerned with the aspects of the general circulation—beyond a descriptive phenomenology—that serve as sources of its maintenance.

An understanding of atmospheric transport processes entails an understanding of the general circulation itself. However, such a grasp of the subject material will have profound practical applications. In recent years the atmosphere has been considered more and more as one of the world’s natural resources that is suffering increasingly

from contamination by anthropogenic pollutants. These impurities, radioactive or not, will be carried over large distances by atmospheric motions. Therefore the transport processes described in this review will be of vital interest to air-pollution control and planning, including not only industrial pollution but also contamination of the atmosphere by nuclear experiments, by aviation, and by space technology.

I compiled the major part of this review during a year of sabbatical leave which I spent at European universities and libraries. I am especially indebted to Prof. Dr. Herfried Hoinkes, head of the Department of Meteorology and Geophysics, University of Innsbruck, Austria, for making available to me the extensive and well-stocked library facilities of that department. Similar appreciation is due Prof. Dr. Hermann Flohn, head of the Department of Meteorology, University of Bonn, Germany, for putting his fine institute at my disposal. I also wish to thank the many individuals, too numerous to be listed here, with whom I had stimulating discussions, which in no small way helped to clarify and generate ideas put down in this review.

Sandra Olson and Peggy Stollar typed the manuscript, including the many cumbersome equations. Dennis Walts took on the tasks of supervising the redrafting of figures and of editing and proofreading the manuscript.

This review, sponsored by the U.S. Atomic Energy Commission under Contract No. AT(11-1)-1340, expresses my views and not necessarily those of the sponsoring agency.

Elmar R. Reiter, *Head*
Department of Atmospheric Science
Colorado State University

October 1969

CONTENTS

Foreword	iii
Preface	v
1. Introduction	1
Mathematical Symbolism	6
2. Angular Momentum Balance	9
Theoretical Considerations	9
Computational Results	12
3. Energy Fluxes and Transformations in the General Circulation of the Atmosphere	33
Theoretical Considerations	33
Computational Results	48
4. Spectral Considerations of Eddy Transports	161
General Remarks	161
Theoretical Background	162
Computational Results	165
5. Geographic and Curvilinear Coordinate Systems	201
6. Conclusions and Outlook	213
References	217
Author Index	243
Subject Index	249

1 INTRODUCTION

This review is the first of several monographs on atmospheric transport processes. The discussion in Part I will not deal with details, such as individual jet-stream systems, or with various case studies; it will focus on global aspects of transport processes.

In a later part several "quasi-conservative" air-mass properties will be derived from hydrodynamic and thermodynamic equations. Absolute angular momentum, total energy of an air column, and potential vorticity can be listed among the parameters used most effectively in tracing large-scale air motions in the general circulation of the atmosphere. These conservative parameters will be used in detailed qualitative and quantitative descriptions of atmospheric circulation features (Reiter, 1961, 1963b, 1968a).

In studies of the general circulation, it has long been recognized that the transport processes that maintain the climatic balance of the atmosphere occur not only in mean meridional motions but also in horizontal "austausch" or eddy-exchange processes, which involve the big whirls of cyclones and anticyclones (Defant, 1921; Jeffreys, 1933). Which of the two processes was the more important long remained a matter of argument. With the improvement of the aerological network after World War II, computations of transport quantities from actual observations tipped the scales in favor of the eddy transport, at least in the middle and high latitudes.

Riehl and Fultz (1957, 1958) used geophysical-model experiments to demonstrate that the relative efficiency of mean and eddy transports is of secondary importance. A meandering jet stream in a "dishpan" experiment with a symmetric three-wave configuration showed, for instance, that the circulation in middle latitudes underneath the mean jet-stream position is indirect if flux terms are averaged along

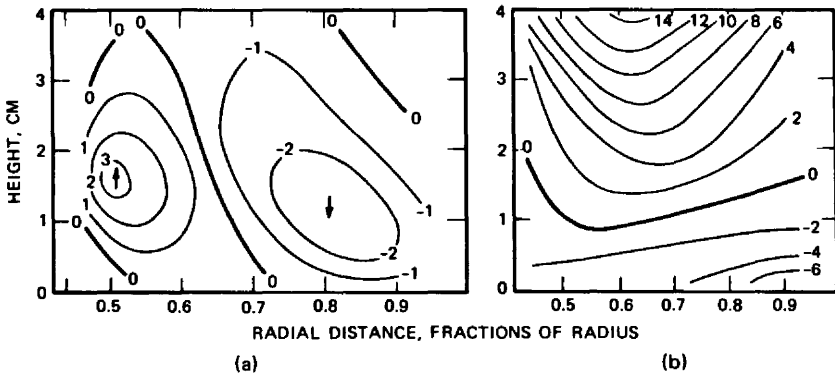


Fig. 1.1 Zonal average of (a) vertical motions (per mille of linear speed of equator) and (b) horizontal motions (percent of linear speed of equator) for the case of three symmetric waves in a dishpan. [From H. Riehl and D. Fultz, *Quarterly Journal of the Royal Meteorological Society (England)*, 83(356): 228 (1957).]

latitude circles (Fig. 1.1). Mean meridional cross sections through such a flow configuration show three circulation cells, such as those postulated by Palmén (1954) and shown in Fig. 1.2, for the earth's atmosphere. (In Fig. 1.2, rising motion along the outer rim of the dishpan and sinking motion along the inner rim are assumed because of the heating at the "equator" and the cooling at the "pole" of the pan.)

However, if the hydrodynamic variables are averaged with respect to a coordinate system whose point of origin is located in the jet axis, following its meanders a totally different circulation pattern evolves (Fig. 1.3). In this curvilinear coordinate system, one single direct circulation cell now occupies the space between the equator and the pole of the dishpan.

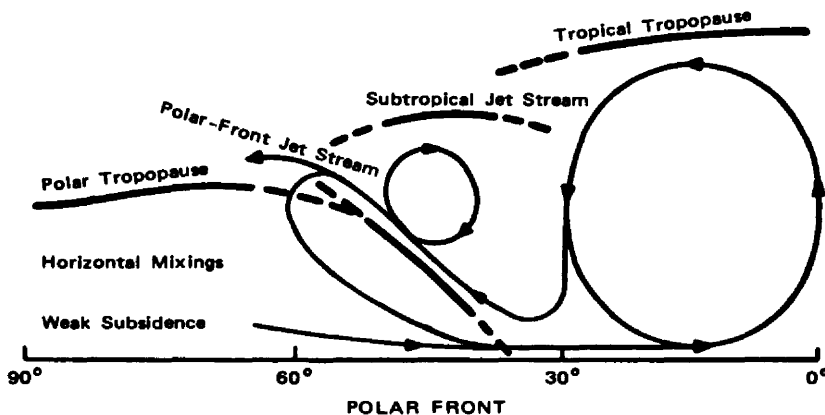


Fig. 1.2 Schematic diagram of the mean meridional circulation in the northern hemisphere during winter. Heavy lines indicate tropopauses and the polar front. (After E. Palmén, 1954.)

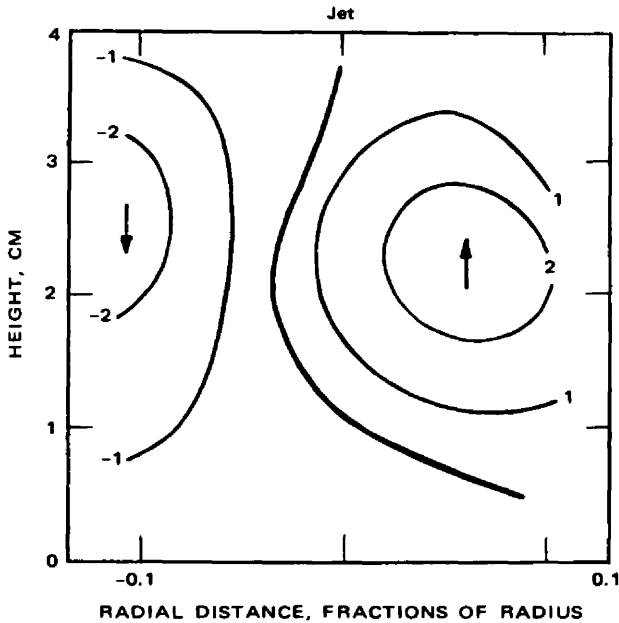


Fig. 1.3 Vertical motions (per mille of linear speed of equator) in a curvilinear coordinate system for three symmetric waves in a dishpan. [From H. Riehl and D. Fultz, *Quarterly Journal of the Royal Meteorological Society (England)*, 83(356): 228 (1957).]

In the geographic coordinate system, the indirect-circulation cell underneath the jet stream implies that the jet stream continuously loses kinetic energy and generates potential energy. Similar considerations could be made for the polar-front jet stream in Fig. 1.2. For this jet stream to be sustained against frictional dissipation as well as the loss of kinetic energy in the indirect circulation, eddy-transport processes must resupply this energy.

The curvilinear system, on the other hand, follows the large-scale eddy motions prescribed by the jet axis, thus filtering the influence of these eddies from the transport computations. The task of maintaining the jet stream against frictional dissipation falls now to the mean cross-axis circulation. Only at some distance from the jet axis will eddy motions gain some importance because of departures of the wind vectors there from the wind direction in the jet axis. Examples for heat transports are given in Figs. 1.4 and 1.5. These two figures refer to a steady three-wave pattern in a dishpan experiment. The pattern migrates slowly eastward, showing only rather diffuse jet maxima. Circles and crosses in these two diagrams refer to actual measurements in the dishpan, obtained from thermistors at various depths and from "winds" at the surface of the pan made visible by floating aluminum powder. "Winds" at depth were computed from the thermal wind equation. Some smoothing of these measured data, indicated by the heavy curves, proved to be necessary in order to approxi-

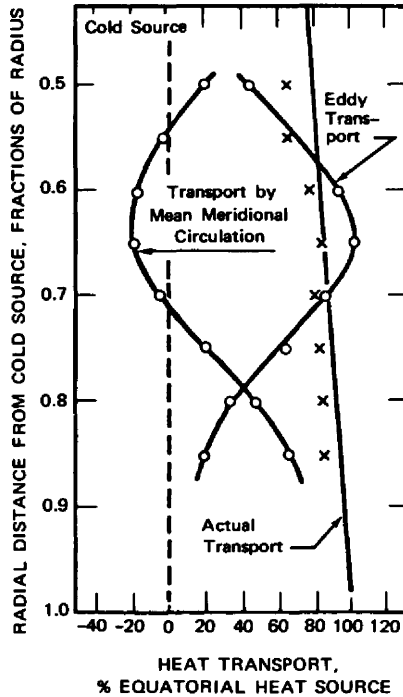


Fig. 1.4 Mean meridional heat transport in cylindrical (geographical) coordinates (percent of the equatorial heat source) for three symmetric waves in a dishpan. The ordinate marks the radial distance from the cold source (total distance cold source–equator = 1). \circ , transports by mean meridional circulation and by the wave motion (eddy transport). \times , observed total transport. The straight line is the computed total transport. This line is not vertical because it incorporates heat losses at the free-water surface of the dishpan. [From H. Riehl and D. Fultz, *Quarterly Journal of the Royal Meteorological Society (England)*, 84(362): 390 (1958).]

mate the theoretical magnitude of the transports given by the straight, slightly slanting lines. In the real atmosphere, where well-developed jet maxima lead to appreciable magnitudes of the departures of velocities from the mean velocity measured along reference lines parallel to the jet axis, one should expect eddy-transport terms of some size, even in the jet axis, more so than indicated in Fig. 1.5. This will not distract, however, from the fact that the mean mass circulation across the jet axis will carry the bulk of the flux of quasi-conservative air-mass characteristics across the jet stream.

From the studies by Riehl and Fultz (1957, 1958), it appears that the relative importance of mean- and eddy-transport terms depends decisively on the choice of the coordinate system. The total transport, as the sum of mean and eddy transports, remains unaffected by the choice of reference frame, however.

Even though only the magnitude of the combined transport processes is important in maintaining the general circulation, there are some far-reaching implications on the

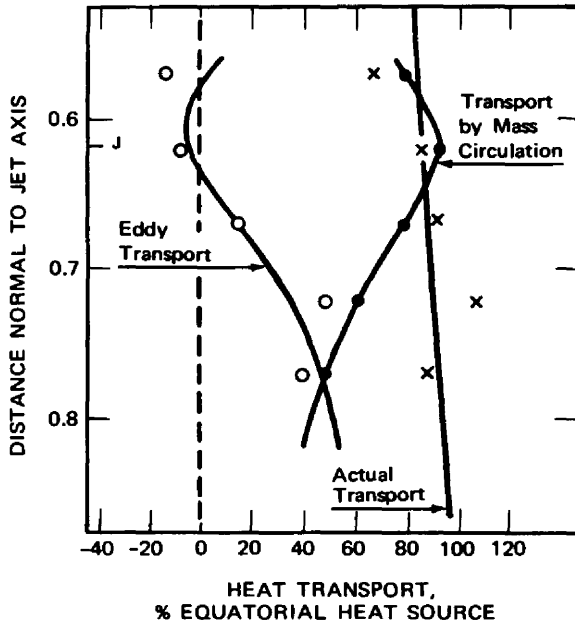


Fig. 1.5 Same as Fig. 1.4 except curvilinear coordinate system. Ordinate shows relative distance from mean jet axis (J). [From H. Riehl and D. Fultz, *Quarterly Journal of the Royal Meteorological Society (England)*, 84(362): 397 (1958).]

transport of nuclear debris associated with the various modes of these processes. For instance, if the total transport of heat, momentum, and trace substances were carried out solely by a mean meridional (Hadley) circulation—as it would be in a slowly rotating dishpan—the trajectories of contaminated air parcels would follow a spiral motion: ascent near the equator, northeastward displacement aloft, sinking near the pole, and southwestward flow near the surface of the earth. The gradual spread of an injection of nuclear or other debris along these spiral paths would be controlled mainly by small-scale diffusion processes.

This rather unrealistic model of an atmospheric circulation will now be modified by introducing a number of symmetric planetary waves, such as in the experiments by Riehl and Fultz (1957, 1958). The effect is a certain distortion of the original spiral trajectories by the regular wave pattern. The gradual spread of a plume of debris still is controlled largely by the small-scale diffusion processes. The large-scale eddy motions in the symmetric wave pattern, as well as local horizontal and vertical wind shears, produce distortions in the plume only when the diffusion processes reach dimensions commensurate with the scale of these local shears and of the large waves. The absence of eddies or waves in the spectrum range between the long planetary waves and the small-scale (molecular) diffusion processes would make the spreading of a plume of contaminants an extremely slow process.

Conditions become more realistic if we allow a continuous spectrum of eddies in our model atmosphere, ranging from planetary waves to cyclone waves to meso-scale disturbances and to small-scale turbulent eddies and molecular diffusion (Kao, 1962; Vinnichenko, 1969). Such a continuous spectrum of perturbation motions will cause a rather rapid diffusion of any trace substance. The diffuse depletion of radioactivity concentrations and of the concentrations of any other tracer will strongly depend on the intensity, or kinetic energy, of the eddy motions in the wavelength band commensurate with the scale of the diffusing plume. Eddies smaller than those in this wavelength band will contribute toward homogeneity of the tracer within the contaminated volume of air that vacillates in its motion around the hemisphere. Thus, with the increase in size of a debris cloud, its further spread can be controlled by a changing range of eddy scales. Discussion in subsequent chapters will show that the kinetic energies contained in the various "wave bands" of large-scale eddies cannot be assumed to be constant. They depend strongly on the state of the general circulation and on the processes that generate, dissipate, and redistribute these kinetic energies. A better understanding of the energetics of the general circulation, therefore, will aid in the comprehension of the intricate mechanisms that control the global and small-scale spread of atmospheric contaminants.

From this rather general discussion, we may arrive at the following statements:

1. The relative magnitudes of eddy and mean meridional transport processes are important in the spread of aerosols. These relative magnitudes affect the large-scale diffusion and the latitudinal and vertical displacement of the debris.
2. The spectrum distribution of the eddy motions in the atmosphere affects the time and space scales of diffusion processes.
3. Standing and transient eddies will have different effects on diffusion. (In transient eddy motions trajectories will be different from streamlines.) The two types of eddies, therefore, may well be considered separate from each other.

MATHEMATICAL SYMBOLISM

In reviewing a number of references on the subject of eddy-transport processes in the atmosphere, one cannot help being frustrated by the maze of symbols denoting the various averaging processes. As long as only time-averaged values and departures therefrom are considered, bars and primes may well suffice in marking atmospheric variables in the conventional way. Matters become increasingly confusing, however, when longitudinal, latitudinal, vertical, and time averages and departures must be accounted for simultaneously and when each author defines his own usage of brackets, asterisks, double and triple primes, tildes, wavy lines, etc.

There is no way of sparing the reader the trouble of studying each author's individualistic approach to mathematical symbolism when he wishes to refer to the original papers. Nevertheless, to simplify matters in this review, which deals with a

variety of averaging aspects, a new symbolic language is introduced which circumvents the problem of running short of different notations (Reiter, 1969b).

1. Average values are indicated by brackets and departures therefrom by parentheses.

2. The ordinates along which averages and departures are computed are indicated by subscripts in parentheses.

3. Subscripts *not* in parentheses have their usual meaning, such as that of a vector component or a differentiation. Brackets or parentheses *without* subscripts or with subscripts *not* in parentheses retain their usual mathematical meaning and do *not* indicate averaging procedures or departures therefrom.

For example, longitudinal averaging produces

$$v = [v]_{(\lambda)} + (v)_{(\lambda)} \tag{1.1}$$

where v is the meridional velocity component and λ is the geographic longitude. Averaging with respect to time, t , yields

$$v = [v]_{(t)} + (v)_{(t)} \tag{1.2}$$

The first terms on the right-hand sides of Eqs. 1.1 and 1.2 indicate the mean values; the second terms indicate the departures from the mean. The terms on the left-hand sides are spot values or instantaneous values.

Averaging with respect to time *and* longitude results in the following terms:

$$v = [v]_{(\lambda,t)} + [(v)_{(\lambda)}]_{(t)} + ([v]_{(\lambda)})_{(t)} + (v)_{(\lambda,t)} \tag{1.3}$$

Here the first term on the right-hand side indicates a zone- and time-averaged value. It might also be written as $[[v]_{(\lambda)}]_{(t)}$, or as $[[v]_{(t)}]_{(\lambda)}$, unless the order in which averaging steps must be taken is of significance. If that is not true, $[v]_{(\lambda,t)} = [v]_{(t,\lambda)}$, where the order in which the subscripts appear indicates the sequence of averaging steps. The second term in Eq. 1.3 is the time average of the departures from the zonal average, the third term represents the departures of the zone-averaged instantaneous values from the time average, and the last term is the departure of instantaneous and local values from the zonal and time average.

It is easily seen that

$$[u v]_{(t)} \neq [u]_{(t)} [v]_{(t)} \tag{1.4}$$

however

$$[u]_{(t)} [v]_{(t)} = [[u]_{(t)} [v]_{(t)}]_{(t)} \tag{1.5}$$

The preceding notation may be slightly longer than the symbolism that it is designed to replace. It is easy to read and write, however. It clearly indicates the

averaging process that must be performed over certain variables or products of variables. It also does not preempt the normal use of subscripts, parentheses, or brackets. This notation is also somewhat easier to read than a multiple-index notation proposed earlier by Lorenz (1953). For further details see Reiter (1969b).

2 ANGULAR MOMENTUM BALANCE

THEORETICAL CONSIDERATIONS

If we consider the earth and its atmosphere as a closed system, i.e., if we neglect the very small effects of tidal friction, the total absolute angular momentum, G_a , per unit mass of this system will be conserved:

$$\int_v \rho G_a dV = \int_{v_E} \rho G_{aE} dV + \int_{v_A} \rho G_{aA} dV + \int_{v_O} \rho G_{aO} dV \quad (2.1)$$

Subscripts E, A, and O refer to the solid earth, the atmosphere, and the ocean, respectively. The integral on the left-hand side of Eq. 2.1 expresses the total absolute angular momentum of this closed system and hence should be regarded as a constant. Departures from the mean value of each of the integrals on the right-hand side will result in adjustments of the values of the remaining two integrals. Specifically, changes in the total absolute angular momentum of the atmosphere will be compensated for by changes in the earth's angular momentum, i.e., by small changes in its rate of rotation or in a slight wobble of the axis of rotation, or both. Changes in the total absolute angular momentum of the oceans contribute a negligibly small amount to Eq. 2.1. Comparisons between changes in the atmospheric angular momentum and fluctuations in the length of day give a surprisingly good correlation (Rudloff, 1950, 1963; see also Sutcliffe, 1950; Dungen, Cox, and Mieghem, 1950, 1956, 1959; Hassan, 1961; Mieghem, 1952b).

The exchange of absolute angular momentum between earth (or ocean) and atmosphere takes place by surface friction. In the trade-wind region and in the area of

polar easterlies, westerly angular momentum is generated. In the westerlies of temperate latitudes, this angular momentum is returned to the earth. If a balance between generation and dissipation is to be maintained, sources and sinks of angular momentum at the earth's surface must equal each other in total strength when integrated over a period of time long enough to span positive and negative fluctuations in the earth's rate of rotation mentioned previously. Furthermore, transport processes must carry absolute angular momentum from the source regions to the sinks.

The absolute angular momentum of a traveling air parcel is conserved only if no external forces, such as pressure forces, are acting on it. This is generally not the case for individual air parcels. However, for the atmosphere as a whole, the assumption is justified (neglecting again seasonal differences in the zonal circulation of the total atmosphere which lead to variations in the length of day). The total budget of the atmospheric absolute angular momentum depends on the frictional exchange with the earth's surface. Table 2.1 shows values of this budget computed by Dungen, Cox, and Mieghem (1952). In this table the differences in the frictional characteristics of the northern and the southern hemispheres are quite obvious.

Table 2.1
MOMENTUM BUDGET OF THE ATMOSPHERE* (10^{32} g-cm²/sec)

	Deviation from the annual average			Momentum transport from the earth's surface to the atmosphere (plus sign)		
	Northern hemisphere	Southern hemisphere	Global	Northern hemisphere	Southern hemisphere	Global
February	-0.6	+2.0	+1.4	+13.7	-12.3	+1.4
May	-1.4	-3.2	-4.6	+4.2	-8.8	-4.6
August	+0.4	-0.8	-0.4	+0.8	-1.2	-0.4
November	+1.4	+2.2	+3.6	+13.3	-9.7	+3.6

*From F. H. van den Dungen, J. F. Cox, and J. van Mieghem, *Tellus*, 4(1): 5 (1952).

The circulations which transport absolute angular momentum across latitude circles and which are necessitated by the source and sink distribution will carry other atmospheric characteristics as well, such as mass, heat, and aerosol concentrations. Consideration of the absolute-angular-momentum transport, therefore, will yield valuable clues on the transport processes governing the spread of atmospheric admixtures, such as atomic debris from nuclear experiments, industrial waste, or naturally generated aerosols.

As pointed out in Chap. 1, transport processes can occur in mean meridional motions as well as in horizontal and vertical eddies. Palmén's circulation scheme (Fig. 1.2) accounts for the mean motions only and not for eddy processes.

The balance of the angular momentum of the atmosphere can be written as (Widger, 1949; Tucker, 1960):

$$\frac{\partial}{\partial t} \int_V \rho G_A dV = \int_S \rho G_A V_n dS + \int_\sigma pr d\sigma + \int_S r\tau_x dS \quad (2.2)$$

In this equation

$$G_A = ur + \Omega r^2 \quad (2.3)$$

is the absolute angular momentum per unit mass, V_n is the inward component of velocity across the surface dS , $d\sigma$ is the projection of dS on the meridional plane, $r (= a \cos \phi)$ is the distance from the earth's axis, and τ_x is the total zonal (eastward) frictional stress at the boundary. The term $\int_\sigma pr d\sigma$ represents the torque caused by pressure differences across mountain ranges (White, 1949). Integrals are taken over a complete latitude belt and from the bottom to the top of the atmosphere.

We can assume that the long-term average, $[\rho G_A]_{(t)}$, in a latitude belt is constant. The left-hand side of Eq. 2.2 vanishes under this assumption. The first integral term on the right-hand side indicates the transfer of absolute angular momentum by advective processes across the boundaries of the latitude belt under consideration. We can expand this term into the transport across horizontal surfaces, H , at pressure levels p_1 and p_2 , and across vertical surfaces, A , at latitudes ϕ_1 and ϕ_2 , and furthermore into transports by mean and by eddy motions. This yields, because of Eq. 2.3,

$$\left\{ \int_A \rho r [u]_{(t)} [v]_{(t)} dA + \Omega \int_A \rho r^2 [v]_{(t)} dA \right\}_{\phi_1}^{\phi_2} + \left\{ \int_H \rho r [u]_{(t)} [w]_{(t)} dH + \Omega \int_H \rho r^2 [w]_{(t)} dH \right\}_{p_1}^{p_2} \quad (2.4a)$$

$$+ \left\{ \int_A \rho r [(u)_{(t)}(v)_{(t)}]_{(t)} dA \right\}_{\phi_1}^{\phi_2} \quad (2.4b)$$

$$+ \left\{ \int_H \rho r [(u)_{(t)}(w)_{(t)}]_{(t)} dH \right\}_{p_1}^{p_2'} \quad (2.4c)$$

$$+ \int_\sigma pr d\sigma \quad (2.4d)$$

$$+ \int_H r\tau_x dH \quad (2.4e)$$

Expression 2.4a constitutes the angular-momentum transport by mean meridional and mean vertical motions, as expressed in Palmén's circulation scheme (Fig. 1.2). Expressions 2.4b and 2.4c describe transport processes by horizontal and vertical eddies. Term 2.4d is the torque due to pressure differences across mountains (White, 1949), and term 2.4e represents the exchange of absolute angular momentum due to frictional interaction with the earth's surface. (The top of the atmospheric layer at p_2 is assumed to be frictionless.)

COMPUTATIONAL RESULTS

Momentum Flux

Work by Starr (1948, 1954a, 1954b, 1956), Starr and White (1951), Palmén (1951), Palmén and Alaka (1952), Priestley and Troup (1954), Bjerknes and Mintz (1955), Mieghem (1956a, 1956b), and Zubyan (1959) stresses the important fact that eddy-transport processes carry the bulk of momentum poleward in the troposphere. The relative importance of the mean meridional circulation decreases rapidly in extratropical latitudes (Riehl, 1962b; Pfeffer, 1964). This is confirmed by recent computations by Holopainen (1965, 1967). (For more details, see Chap. 3.) Kuo (1960) also demonstrated by theoretical considerations that with increasing rate of rotation (hence with increasing Coriolis parameter) eddy processes should dominate over mean meridional transports. Dishpan experiments have corroborated this conclusion (Reiter, 1961, 1963b). Thus it appears that the so-called " β -effect," i.e., the effect of the change of the Coriolis parameter with latitude ($\beta = \partial f / \partial y$), plays an important role in suppressing mean meridional circulation processes in favor of eddy processes in the earth's atmosphere.

According to Palmén and Alaka (1952), the ratio between mean meridional transport and eddy transport is 44% at 20°N, 23% at 25°N, and only 11% at 30°N. These computations are based on eddy-transfer data published by Mintz (1951) and on values of frictional transfer of momentum between the earth and the atmosphere given by Widger (1949). They show that even in the Hadley cell eddy-transport processes are dominant.

Other computations of the mean meridional circulation in the lower troposphere of the trade-wind region, based on wind observations, have been made by Riehl (1950), Riehl and Yeh (1950), Palmén (1955), Tucker (1957), and Palmén, Riehl, and Vuorela (1958). Rao and Ramanadham (1963) published data on eddy momentum flux over India.

Priestley and Troup (1964) pointed out that estimates of the poleward flux of angular momentum based on actual wind observations may contain a slow-wind bias because data are frequently missing in the upper troposphere and stratosphere when winds are strong. Angell (1964) comes to the same conclusion from transosonde measurements, which show stronger winds on the average than radiosonde observations or geostrophic- and gradient-wind calculations. His data indicate an ageostrophic northward eddy flux in middle latitudes that may amount to as much as one-fourth the geostrophic flux.

Tucker (1960) set out to estimate various eddy-flux terms given in Eq. 2.4. He had to contend with the sparsity of data in tropical regions, and he also was forced to omit the Asian sector between 40°E and 160°W (Tucker, 1959). Especially because of the omissions, Tucker's results [computed for summer (June, July, and August) and winter (December, January, and February), starting with December 1949 and ending with August 1951] may need some systematic adjustments. It is well known that the missing sector contributes significantly toward meridional momentum transports by

the monsoonal circulation systems (see, e.g., Keshava, 1968). Nevertheless, several of Tucker's results will be mentioned briefly. The earlier conclusion of Palmén and Alaka (1952), that the mean meridional circulation of the troposphere is of relative importance only at low latitudes, appears justified from Tucker's computations. Tucker's computations are based on values of $[v]_{(\lambda,t)}$ given in Fig. 2.1, with longitude λ excluding the Asian sector and time t extending over the three-month periods mentioned previously. Meridional flux terms, such as those given in Eq. 2.4, were computed from these basic data. Results are given in Tables 2.2 to 2.5. The importance of horizontal eddy fluxes is clearly evident from these values (Table 2.4). The horizontal eddy fluxes were considered as residual between total (F_T) and mean meridional fluxes (F_M) and were adjusted to computations by Starr (1951a) and Starr and White (1952a, 1952b). Tucker infers from the tabulated values the presence of two direct-circulation cells, one on each side of an indirect cell. This conforms to the schematic diagram shown in Fig. 1.2. Confirmation of this three-cell pattern has been obtained by Starr (1968), Murgatroyd (1969), and Vernekar (1967).

Mieghem and Hamme (1962), however, using the same basic data as Tucker (1959), obtained the more complex mean circulation shown in Fig. 2.2, where J_1 and J_2 are the mean positions of the subtropical and polar-front jet streams. The term C_1 indicates the center of the Hadley cell; C_2 , the center of the indirect Ferrel cell; C_3 and C_4 , a direct and an indirect upper-tropospheric cell; and C_5 , a direct cell in polar latitudes.

Terms C_3 and C_4 may be an effect of the large meanders in the polar-front jet. Owing to the asymmetric distribution of the cyclonic and anticyclonic horizontal wind shears about individual jet streams, the mean position of the jet will appear close to the equatorward edge of the latitude belt over which it fluctuates during the time period of averaging (Davis, 1951; Reiter, 1961, 1963b, 1963c). Within this belt of fluctuations, one should expect sinking motions on the west side of troughs. In the zonal-averaging process, the sinking motions, in the mean, occur farther south than the rising motions, thus simulating an indirect-circulation cell, C_4 . The same effect leads to the three-cell pattern observed in dishpan experiments with a "geographic" coordinate system (Fig. 1.1). In addition, the presence of an arctic-front jet stream may contribute to the complexity of the mean meridional circulation pattern obtained by Mieghem and Hamme, especially to cells C_4 and C_5 .

Table 2.4 shows that the jet-stream level dominates in the horizontal eddy transport of momentum (see also Kao, 1954b). According to Holopainen (1967), this eddy momentum flux is mainly carried out by *transient eddies*. These transient eddies account for almost 90% of the total poleward flux at the latitude of peak flux (about 30°N). Figure 2.3 shows the seasonal variation of the total flux. Figure 2.4 gives a comparison between Holopainen's annual average values and earlier studies by Buch (1954), Mintz (1955a), and Wiin-Nielsen, Brown, and Drake (1963, 1964). The effects of *standing eddies*, according to Holopainen, are small and tend to balance against the flux accomplished by the mean meridional circulation (see also Gilman, 1964; Wiin-Nielsen and Vernekar, 1967). Murray et al. (1969), on the other hand, conclude that at 30°N standing eddies play almost as large a role in angular momentum

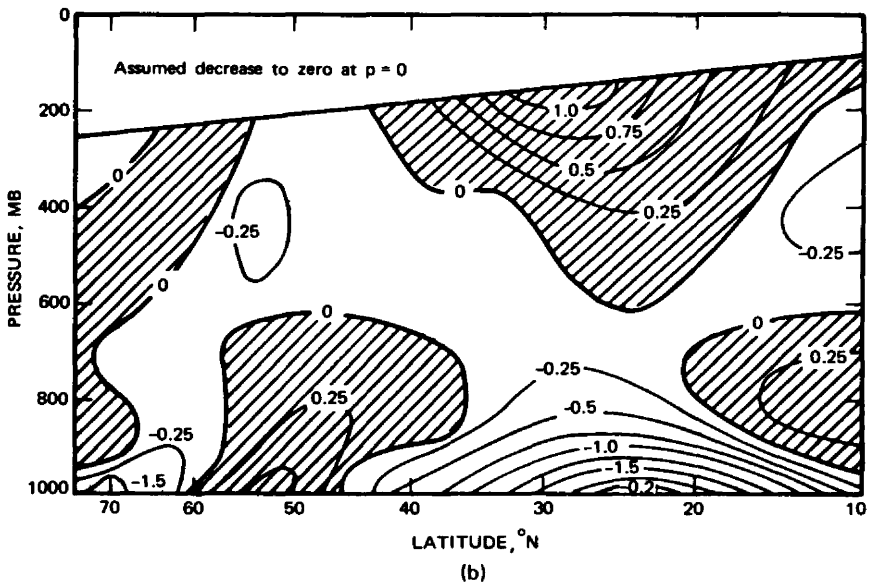
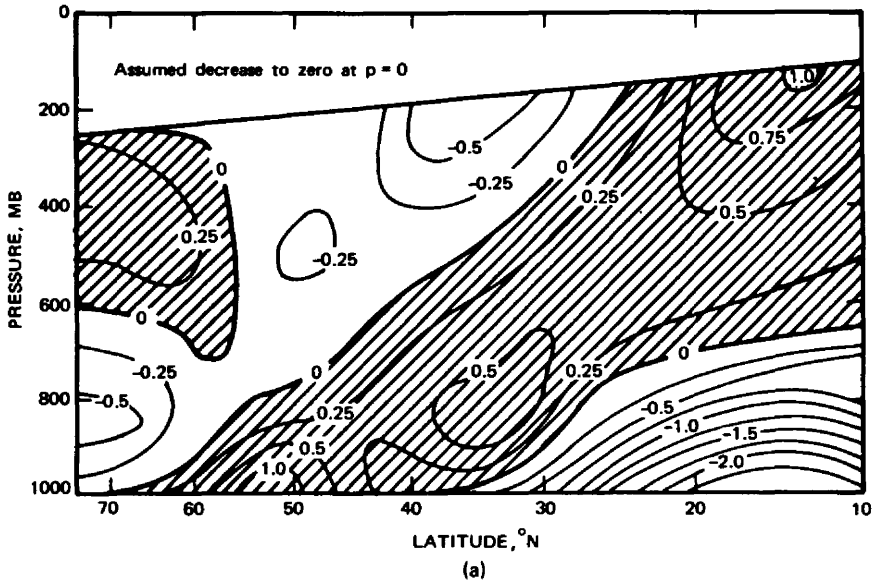


Fig. 2.1 Mean meridional velocity (m/sec), southerlies shaded. (a) Winter. (b) Summer. [From G. B. Tucker, *Tellus*, 12(2): 134 (1960).]

Table 2.2
 NORTHWARD MASS TRANSPORT (10^6 tons/sec) BETWEEN 1000 AND 700 MB*

	Latitude, °N												
	60	55	50	45	40	35	30	25	20	15	10	5	0
Palmén and Alaka (1952)							-58	-84	-126	-183	-190	-134	-67
Winter	-2	+12	+18	+21	+40	+46	-8	-49	-92	-110			
Summer	-7	+8	+21	+15	+2	-30	-72	-77	-46	-1			

*From G. B. Tucker, *Tellus*, 12(2): 137 (1960).

Table 2.3
CONTRIBUTION OF THE MEAN MERIDIONAL CIRCULATION (F_M)(10^{25} g-cm²/sec²)
TO THE TOTAL HORIZONTAL FLUX OF ANGULAR MOMENTUM (F_T)
ACROSS A LATITUDE CIRCLE*

	Latitude, °N											
	65	60	55	50	45	40	35	30	25	20	15	
Winter												
F_M	+0.2	-0.1	-0.5	-0.8	-1.1	-2.4	-3.1	-1.0	+2.3	+5.5	+6.5	
100 F_M/F_T	-20	-20	-20	-8	-5	-10	-9	-2	+6	+18	+36	
F_M	Using values of $[u]_{(\lambda,t)}$				-2.3	-2.9	-4.8	+2.9	+5.5	+13.1	+16.4	
100 F_M/F_T	obtained by Petterssen (1950)				-11	-13	-14	+7	+14	+42	+91	
F_M	Palmén and Alaka							+6	+11	+14		
100 F_M/F_T	(1952)							+10	+19	+30		
Summer												
F_M	0	+0.1	-0.1	-0.8	-0.8	0	+1.3	+2.0	+1.7	+0.8	+0.4	
100 F_M/F_T	0	+20	-4	-11	-7	0	+7	+11	+12	+18	+40	

*From G. B. Tucker, *Tellus*, 12(2): 139 (1960).

Table 2.4
PERCENTAGE OF TOTAL HORIZONTAL EDDY
TRANSFER ALLOCATED TO EACH LAYER*

Layer, mb	Latitude, °N				
	15	20	25	30	35
Winter					
0 to 200	10	20	25	30	30
200 to 400	60	50	50	45	45
400 to 600	20	20	20	20	20
600 to 800	10	10	5	5	5
800 to 1000	0	0	0	0	0
Summer					
0 to 200	0	15	20	25	25
200 to 400	70	55	55	50	50
400 to 600	15	15	15	15	15
600 to 800	10	10	10	5	5
800 to 1000	5	5	0	5	5

*From G. B. Tucker, *Tellus*, 12(2): 140 (1960).

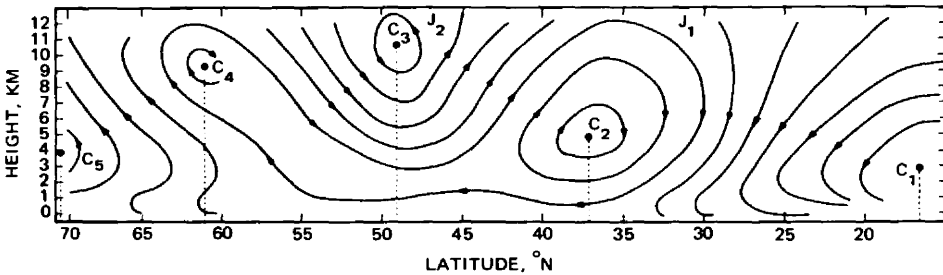


Fig. 2.2 Mean meridional circulation. Streamlines define the centers of the Hadley cell (C_1), of the Ferrel cell (C_2), of two cells of the upper troposphere (C_3 and C_4), and of a direct cell north of 65°N (C_5). (After Mieghem and Hamme, 1962.)

transport as transient eddies. The mean meridional circulation at this latitude makes a significant contribution toward the momentum flux at jet-stream level only during winter and spring. During summer the subtropical jet stream, which dominates this latitude region near 30°N , does not exist as a hemispheric entity. (More about the effects of transient and standing eddies will be reported in Chap. 4.) The preceding

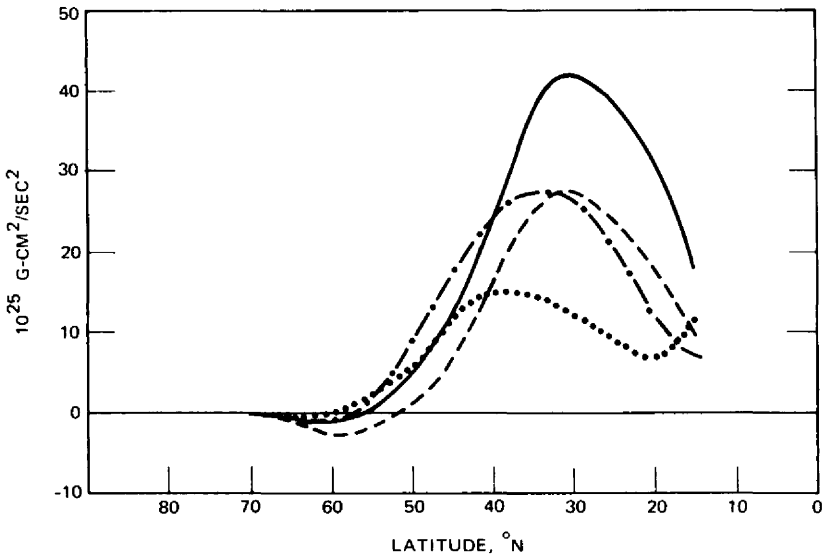


Fig. 2.3 The total poleward flux of angular momentum ($10^{25} \text{ g-cm}^2/\text{sec}^2$) over the northern hemisphere in winter (heavy line), in spring (dashed line), in summer (dotted line), and in fall (dashed-dotted line). (Adapted from Holopainen, 1967.)

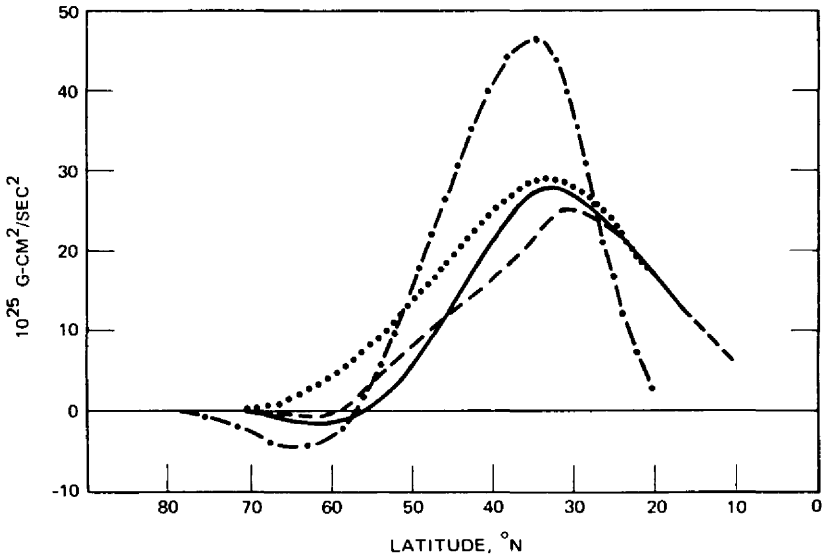


Fig. 2.4 The annual mean poleward flux of angular momentum ($10^{25} \text{ g-cm}^2/\text{sec}^2$) over the northern hemisphere according to Holopainen (1967) (heavy line), Buch (1954) (dashed line), Mintz (1955a) (dotted line), and Wiin-Nielsen et al. (1963, 1964) (dashed-dotted line). (Adapted from Holopainen, 1967.)

Table 2.5
SURFACE-FRICTION TORQUE (S) AND TORQUE DUE TO
PRESSURE DIFFERENCE ACROSS THE MOUNTAINS (M) (10^{25} g-cm²/sec²)*†
(Also conversion table for 1 dyne/cm² throughout a 5° latitude belt)

	Latitude, °N										
	70-65	65-60	60-55	55-50	50-45	45-40	40-35	35-30	30-25	25-20	20-15
Winter											
S	(0)	(-1.0)	-3.0	-6.0	-9.0	-10.5	-10.5	-10.5	+1.5	+6.0	+12.0
M	(+1.0)	+0.5	0	-1.0	-2.0	-2.0	0	+1.5	+2.0	+2.0	(+1.0)
Summer											
S	(-0.5)	-1.5	-1.5	-3.0	-3.0	-1.5	-1.5	0	+4.5	+7.5	+4.5
M	(+1.0)	+0.5	-0.5	-1.5	-2.0	-2.0	-1.5	-0.5	+0.5	+2.0	(+1.0)
Conversion table											
1 dyne equals	2.1	3.0	4.1	5.3	6.5	7.7	8.9	10.3	11.6	12.3	12.9

*Parentheses indicate extrapolated values.

†From G. B. Tucker, *Tellus*, 12(2): 136 (1960).

results are characteristic for a geographic coordinate system. In a curvilinear system, eddy transports reveal a different distribution (see Chap. 5).

In Table 2.5 are given values for Eqs. 2.2d and 2.2e, torques due to horizontal pressure differences across mountain ranges (White, 1949; see also Kao, 1960; Saltzman, 1961b; Kung, 1968) and frictional torque, respectively. Data compiled by Priestley (1951) for surface drag have been used in Tucker's tabulation. They were multiplied, however, by a factor of 1.5 since they appeared to be too low. More recently Kung (1968) compiled data on surface friction. From these data it appears that the zonal surface stress over the Atlantic is of the same order of magnitude as that over the North American continent. In middle latitudes during winter the oceanic stress is even significantly larger than the continental one. (For stress data over the oceans and in the southern hemisphere, see Hellermann, 1967.)

Aside from acting as momentum sinks in middle latitudes, large mountain ranges have an even more important effect on atmospheric transport processes. By generating specific patterns of standing planetary waves, these ranges contribute significantly to large-scale eddy processes. Such effects will be considered in detail in Chap. 4.

The *vertical transfer of momentum* in the atmosphere is accomplished by *small-scale* shearing stresses as well as by *large-scale* mean and eddy motions. Sheppard (1953) estimated the former to be most important for the angular-momentum flux at low levels. This is where the rotating earth imparts its angular momentum to the atmosphere by frictional forces. In first approximation, the eddy exchange coefficients of momentum, heat, and inert admixtures to the atmosphere, which control such small-scale fluxes, may be considered equal, or at least to be of the same order of magnitude. It is obvious, therefore, that the momentum-exchange processes between earth and atmosphere have a direct bearing on transports of other quantities, such as natural radioactivity generated in the soil or of ozone destroyed at the ground.

Defant and Boogaard (1963) arrived at numerical estimates of the large-scale *mean* vertical mass transport in the Hadley cell for a single day (Dec. 12, 1957) (Fig. 2.5). The values given in this figure may be considered as slightly too small to characterize average conditions because the simultaneously estimated horizontal transport values are lower than those obtained by other investigators who extended their computations over longer time periods (Palmén, 1966a). The pattern in Fig. 2.5, nevertheless, appears to be typical.

The large-scale vertical *eddy* transport of zonal momentum has been estimated by White and Cooley (1952) and later, from more reliable data, by Starr and Dickinson (1963). In the set of computations by Starr and Dickinson, the effects of standing eddies and of transient disturbances have been considered separately. The standing eddies are given by

$$[[w]_{(t)}]_{(\lambda)}([u]_{(t)}]_{(\lambda)})_{(\lambda)} = [[w]_{(t)}[u]_{(t)}]_{(\lambda)} - [[w]_{(t)}]_{(\lambda)}[[u]_{(t)}]_{(\lambda)} \quad (2.5)$$

and the transient eddies by

$$[[w]_{(t)}(u)_{(t)}]_{(t)}]_{(\lambda)} \quad (2.6)$$

(For a breakdown into fast- and slow-moving transient modes, see Bradley, 1968.)

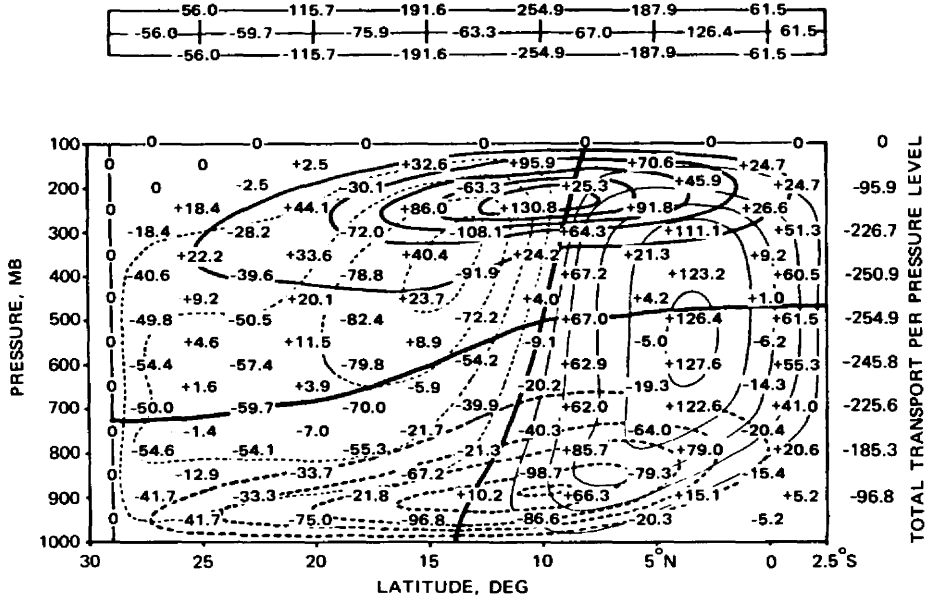


Fig. 2.5 Horizontal and vertical mass transports (10^6 tons/sec) in the Hadley cell on Dec. 12, 1957. The table at the top of the figure shows the mass balance between the layers above and below the line of zero horizontal transport as well as the horizontal-flux-divergence values, which are balanced by vertical flow through this line of zero horizontal transport. [From F. Defant and H. M. E. van de Boogaard, *Tellus*, 15(2): 260 (1963).]

Computational results are shown in Fig. 2.6 for January and April 1958. Analyses have been prepared after tabulated values given by Starr and Dickinson (1963). During the first month the transient eddies seem to prevail. During the second month the main transport seems to be accomplished by the standing eddies. During January the standing-eddy effects are quite strong in the subtropical jet stream (see also Krishnamurti, 1961a, 1961b; Murray et al., 1969) and in the stratosphere of high latitudes. During the same month the vertical momentum transport by transient eddies particularly dominates the latitudes in which the polar-front and arctic-front jet streams have to be sought. Transient eddies also have a strong effect in the upper troposphere of the latitudes characteristic of the subtropical jet stream. By comparison, Krishnamurti (1961b) finds for winter 1955–1956 that in *horizontal* kinetic-energy transport, standing eddies, on the average, are dominating over transient eddies. This apparent discrepancy may have three reasons: First, horizontal and vertical eddy-transport processes may show different ratios of standing vs. transient eddy transports. Second, Krishnamurti's calculations refer to a curvilinear coordinate system whose origin follows the jet axis of the subtropical jet, whereas the results obtained by Starr and Dickinson were in a geographic coordinate system (see Chap. 1). The two coordinate systems should be expected to have different filtering effects on

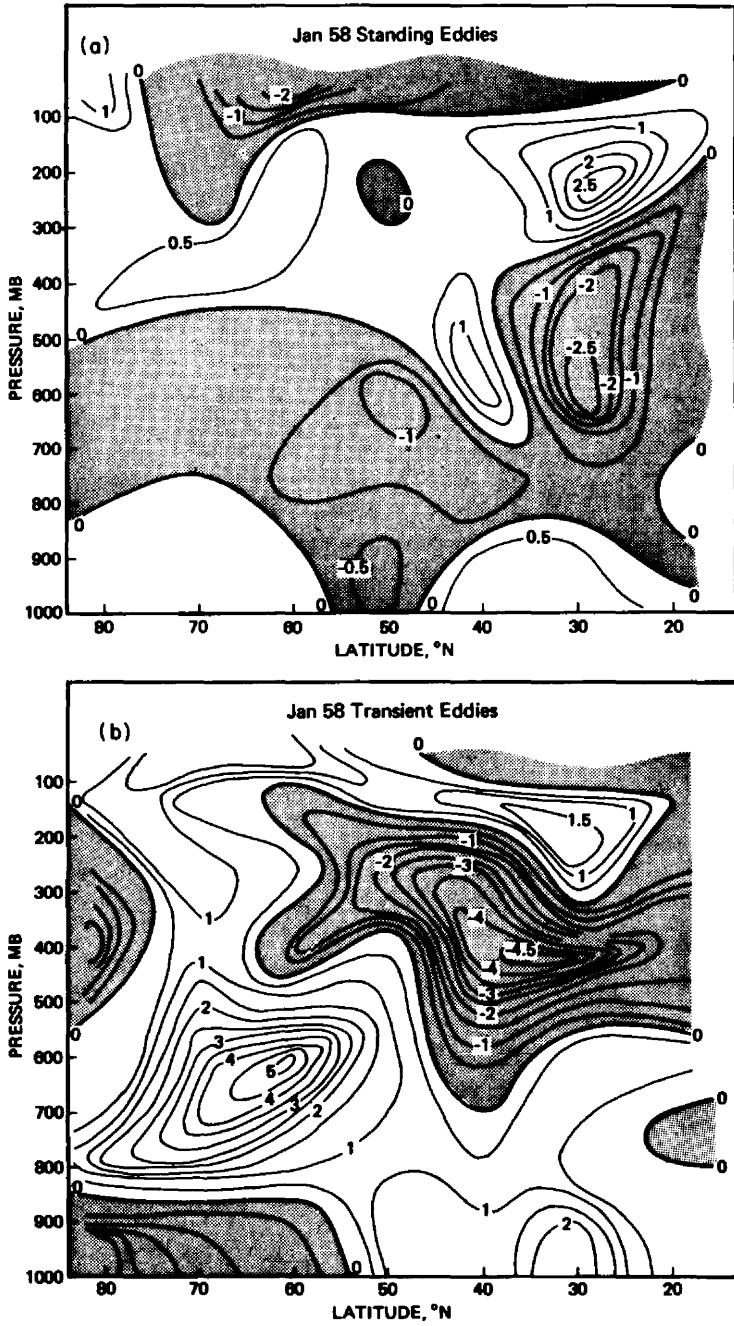


Fig. 2.6 (See page 23 for legend.)

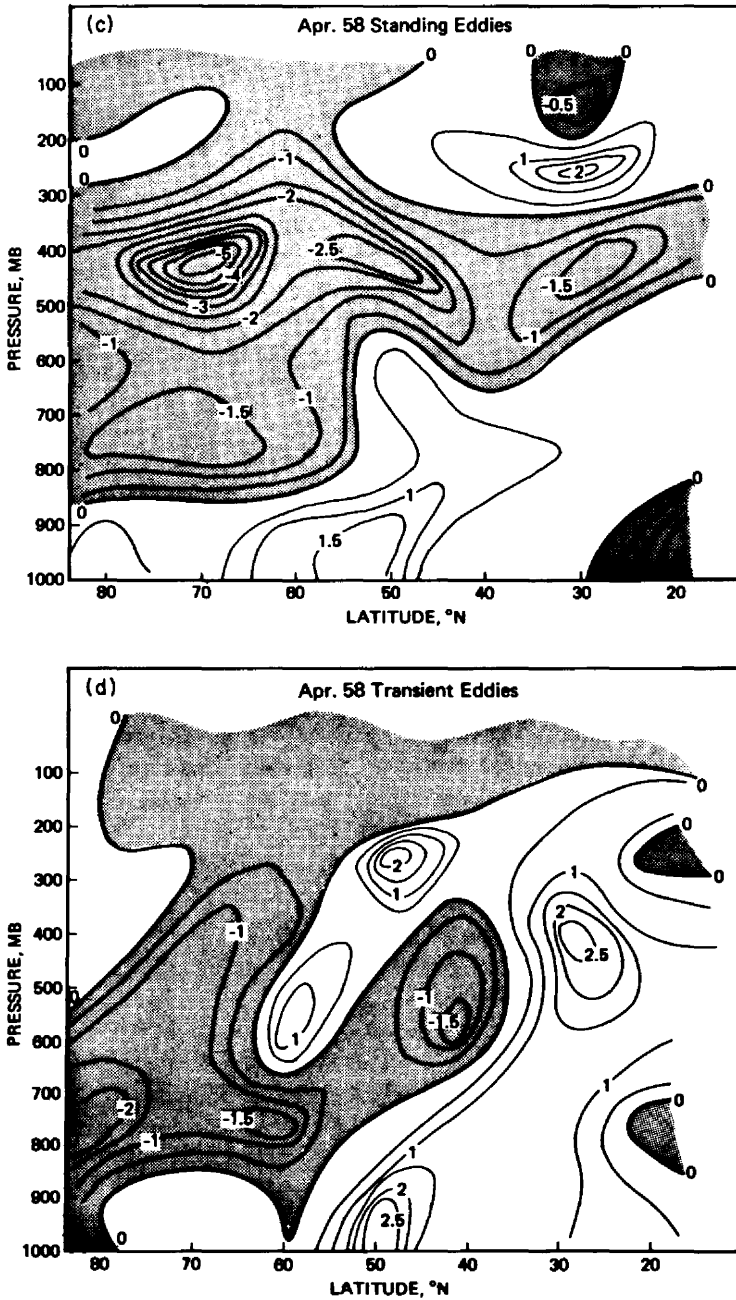


Fig. 2.6 Vertical transport of zonal momentum by large-scale standing and transient eddies (cm^2/sec^2) during January 1958 (a and b) and during April 1958 (c and d). (Adapted from Starr and Dickinson, 1963.)

standing and transient eddies. Third, there seem to be strong variations in the relative magnitudes of standing and transient eddy transports between individual months. January 1956, in Krishnamurti's study, for instance, reveals a slight excess of transient eddy transport over standing eddy transport, in contrast to the other winter months that entered into the *average* conditions for the winter 1955–1956.

Standard Deviations of Velocity Components

For order-of-magnitude estimates on angular momentum or heat transport by eddy motions, or both, the standard deviations, σ , of wind components and of temperature fluctuations may be considered (see, e.g., Saltzman and Vernekar, 1968). According to Rao (1967),

$$[(a)_{(t)}(b)_{(t)}]_{(t)} \leq \sigma_a \sigma_b \quad (2.7)$$

where a and b are meteorological parameters. Thus substitution of standard deviations for the mean fluctuations in the equations governing the eddy-transport processes will yield estimates of the upper limits of these processes. By such studies the important role of the eddies in maintaining the mean circulation of the atmosphere can easily be corroborated.

A number of statistics on standard deviations of meteorological parameters are available in the literature. Goldie, Moore, and Austin (1957) have published standard deviations of temperature. Crossley (1950) pointed out that the standard deviation of temperature is smaller on a constant-pressure surface than on a constant-height surface. Such effects must be considered when applying σ_T to eddy-transport estimates (Rao, 1967).

Flohn (1961) published values of the standard deviation of the meridional wind component in the northern hemisphere during winter and summer (Fig. 2.7), using data by Crutcher (1958, 1959) and Faust et al. (1959). The large eddy transports in the region of the polar front and subtropical jet streams are evident. Surprising are the small values of σ_v in and above the tropical easterly jet stream of summer (see also Flohn, 1964). In the subtropical stratosphere of summer, the standard deviations of the meridional components of the geostrophic wind (computed from data by Lahey et al., 1960) seem to be larger than those of actual winds; elsewhere there is good agreement between the two quantities.

Newell (1963c) (see also Newell et al., 1966) considers spatial standard deviations of the meridional velocity component,

$$[(\overline{v})_{(t)}]_{(\lambda)}^2 \quad (2.8)$$

where λ indicates longitude and t is taken over three-month periods. He takes these deviations as indicators for the meridional transport by standing eddies. The transient eddy transport can be estimated from the zonal mean of the time standard deviations

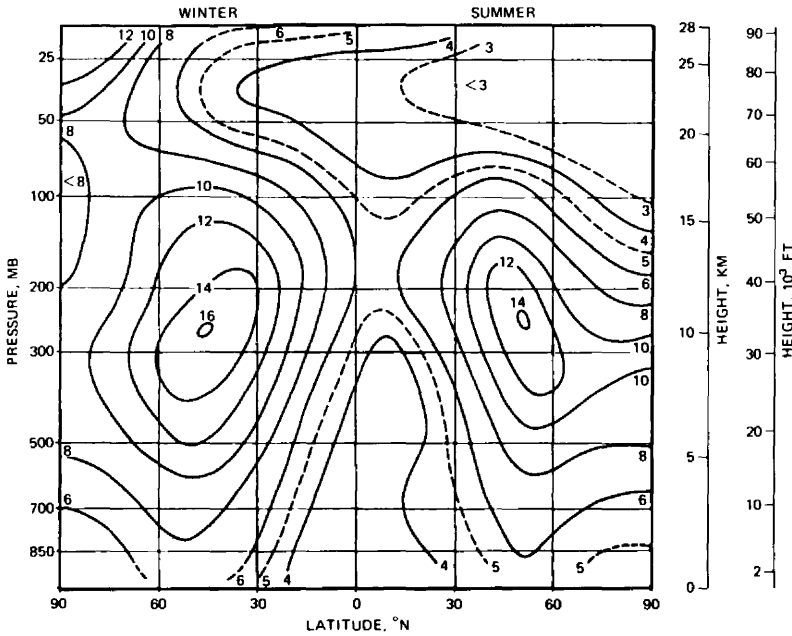


Fig. 2.7 Standard deviation of the meridional component of flow (v) (m/sec) for average conditions in summer and winter of the northern hemisphere. [From H. Flohn, *Geofisica Pura e Applicata*, 50(1961/111), 232 (1961).]

$$[(v)^2(t)]^{1/2}(t, \lambda) \tag{2.9}$$

A comparison of Eqs. 2.8 and 2.9 with Eqs. 2.5 and 2.6 reveals the analogy of the averaging processes involved, indicated by the same sequences of brackets, parentheses, and subscripts. Results obtained by Newell (1963c) are shown in Fig. 2.8. They are based on analyses by Murakami (1962) and Oort (1962) (see also Peng, 1963, 1965b). From these data it appears that standing and transient eddy transports are comparable in magnitude, the latter being slightly larger. (This is in agreement with the vertical transports discussed with Fig. 2.6.) The effects of the tropopause jet streams and of the stratospheric polar-night jet on meridional eddy motions are clearly indicated.

There is considerable seasonal variation in the horizontal transport by standing eddies. The time standard deviations reveal less variability (Newell et al., 1966). Estimates of the time standard deviations for the upper stratosphere are shown in Fig. 2.9. Data from the Meteorological Rocket Network were used in the preparation of this diagram. Because of the sparsity of information from the high atmosphere, these analyses may still be subject to revision, especially since they may contain a certain bias with respect to tidal motions (see also Part 2 and Newell 1963b, 1965a).

An order-of-magnitude estimate of vertical eddy fluxes can be obtained from the variance or from the standard deviations of vertical velocities. The latter can be

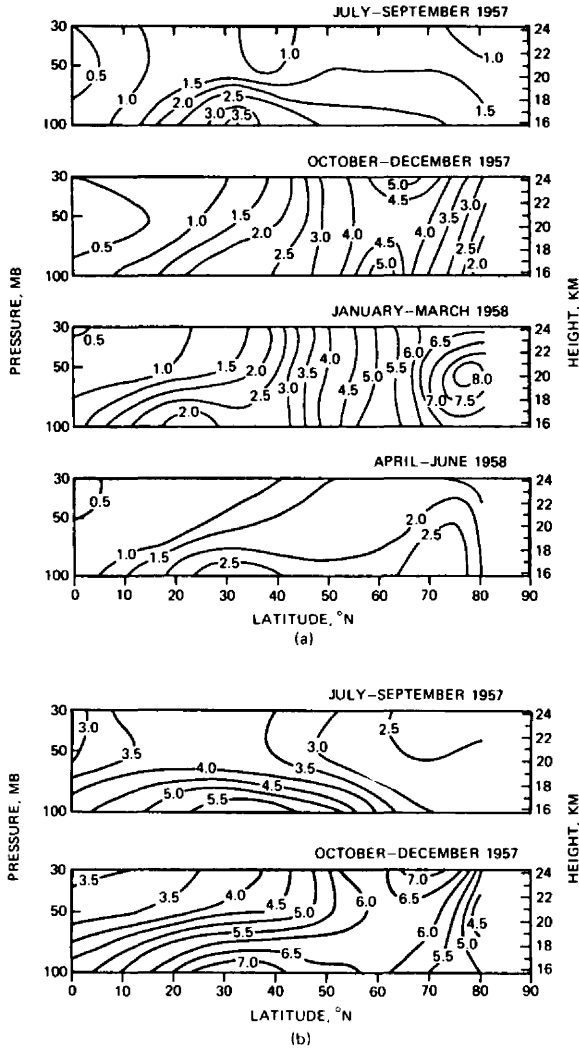


Fig. 2.8 Spatial standard deviation of standing eddy components of the meridional component of velocity (a) and zonal mean of time standard deviations of transient eddy components of the meridional component of velocity (b) (m/sec). [From R. E. Newell, *Journal of Geophysical Research*, 68(13): 3954-3955 (1963).]

computed under the assumption of adiabatic motions (Jensen 1960, 1961). Such *eddy* fluxes appear to be larger than fluxes by *mean* vertical velocities as computed by Tucker (1959) or Barnes (1963) (see Newell, 1963c).

Data on angular momentum transports in the upper stratosphere and mesosphere are anything but abundant. From analyses by Teweles (1961), Teweles and Finger (1962), and Keegan (1961, 1962), one can conclude that eddy-transport processes also play a dominant role at these high levels of the atmosphere. Tilting troughs and ridges are discernible from these analyses and would, at least qualitatively, account for large magnitudes of eddy momentum flux in the domain of long planetary waves (see Newell 1963b, 1963c; Reiter 1961, 1963b).

Vorticity Transport

The vorticity equation in the simplified form

$$\frac{dQ_z}{dt} = -D_h Q_z \quad (2.10)$$

where Q_z is the vertical component of the absolute vorticity and D_h is the horizontal divergence, shows that the absolute vorticity of an air mass is not too effective a tracer for atmospheric motions because of its nonconservative nature under divergent flow conditions. Nevertheless, it is reasonable to assume that the total absolute vorticity within the polar cap of cold air on the cyclonic side of the polar-front jet stream is nearly conserved because the total divergence or convergence of this air mass is close to zero. Under this assumption the meridional wind profile that would result under a redistribution by turbulent mixing of this absolute vorticity contained in the cap of polar air can be computed. The mixing will proceed until the absolute vorticity is constant everywhere in this volume of cold air. At the same time the total angular momentum of the polar air mass will be conserved. Such constant absolute vorticity wind profiles have been considered by the Chicago meteorological school in explaining the jet-stream phenomenon (Rossby, 1947; University of Chicago, 1947; A. Defant, 1949) (for further details see Reiter, 1961, 1963b). This so-called "mixing theory" of jet-stream formation tacitly assumes large-scale eddy processes to be effective agents in stirring the absolute vorticity on the cyclonic side of the polar-front jet within the cap of cold polar air into a constant value. Synoptic studies have shown, however, that strong maxima of positive absolute vorticity are associated with the cyclonic sides of well-developed jet maxima. This suggests that the postulated eddy mixing processes are not strong enough to generate a uniform vorticity distribution as postulated by Rossby and his collaborators. Only when flow conditions are averaged over several days, or over a broad hemispheric sector, will the absolute vorticity on the cyclonic side of the mean jet-stream position assume a nearly constant value.

Kao (1960) considers the so-called momentum vorticity, defined as

$$\nabla \times \rho \vec{v}_a$$

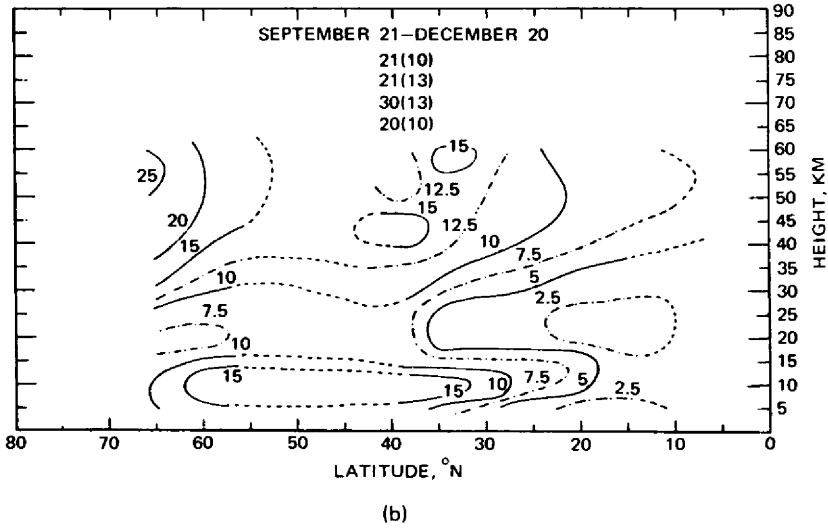
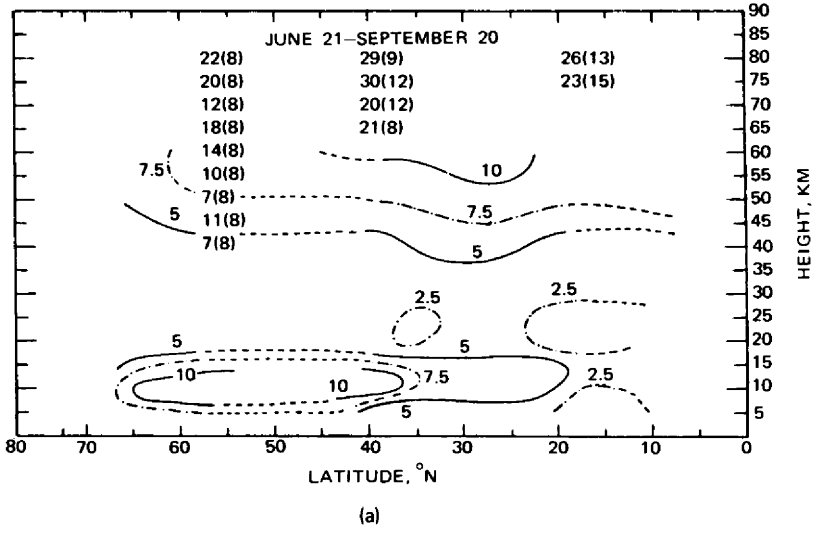


Fig. 2.9 (See page 29 for legend.)

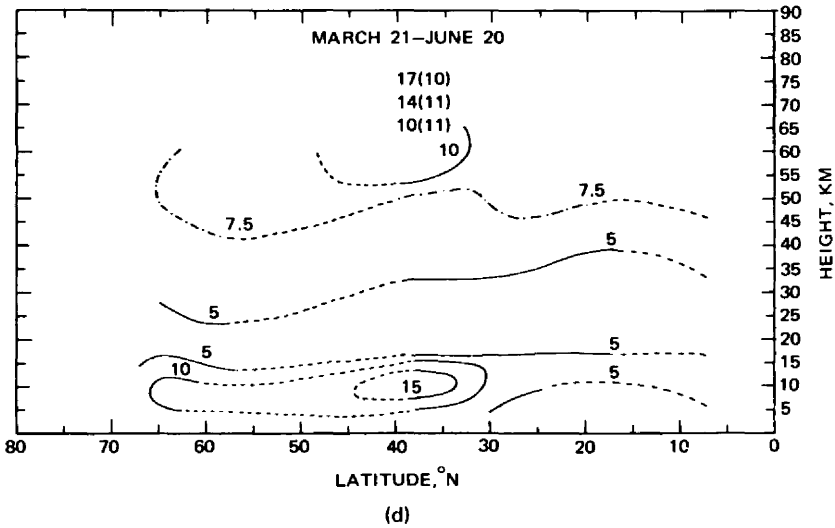
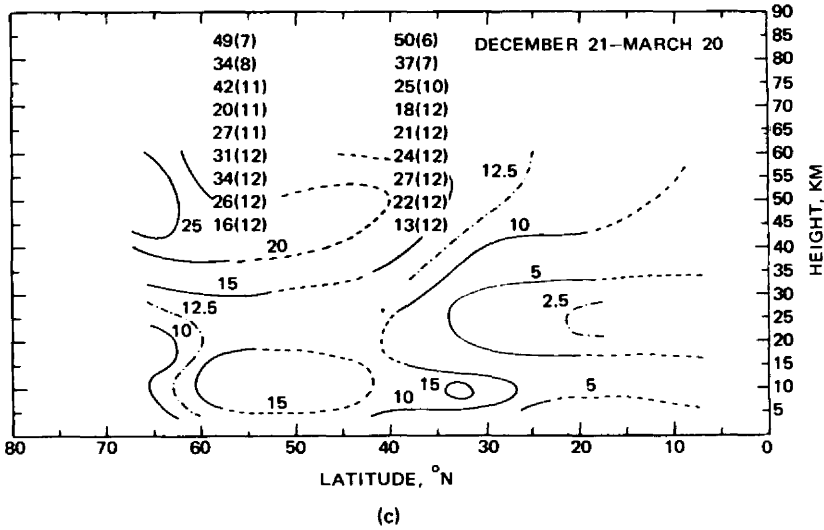


Fig. 2.9 Temporal standard deviation of the meridional wind component as deduced from the Meteorological Rocket Network data. (a) Summer. (b) Autumn. (c) Winter. (d) Spring. Additional numerical values, listing standard deviations and number of observations, are from rocket grenade [left-hand column of (a) and both columns of (c)] and chaff (all other columns) data. [From R. E. Newell, J. M. Wallace, and J. R. Mahoney, *Tellus*, 18(2-3): 369; 370 (1966).]

where \vec{v}_a is the absolute velocity vector measured with respect to an inertial coordinate system. The complicated nature of the balance requirements of this momentum vorticity can be seen if the operator $\nabla \times$ is applied to the full equation of motion, which will produce the complete vorticity equation. Simplifying conditions can be assumed, such as the total momentum vorticity of the polar cap poleward of latitude ϕ being equal to the total zonal angular momentum integrated over the vertical surface at latitude ϕ , extending from the bottom to the top of the atmosphere. Kao (1960) also considered pressure effects at the bottom boundary of the atmosphere which are produced by mountains and which may generate or dissipate momentum vorticity. He arrives at sources of momentum vorticity between latitude 15°N and 50°N and between 80°N and the pole. Sinks of momentum vorticity are found between the equator and 15°N and between latitudes 50°N and 80°N with corresponding transport processes in between. Latitudes of zero mean meridional transport of momentum

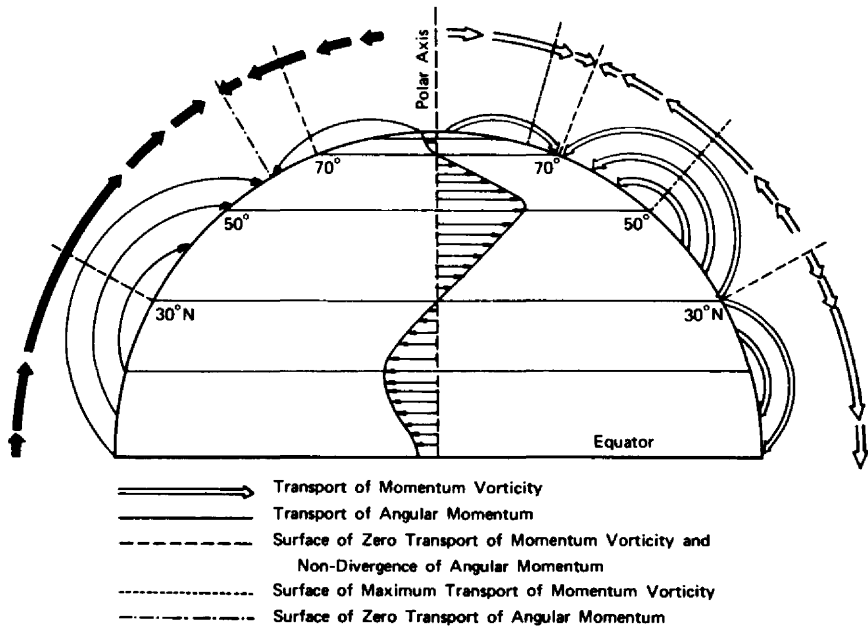


Fig. 2.10 Schematic diagram showing the mean zonal surface-wind distribution in the northern hemisphere and the corresponding meridional transports of the vertical component of momentum vorticity and angular momentum. [From S.-K. Kao, *Journal of Meteorology*, 17(2): 129 (1960).]

vorticity are placed schematically at 30°N and 70°N (Fig. 2.10). Corresponding considerations of angular momentum transport show a sink of this quantity between 30°N and 70°N in the region of surface westerlies. The tropical and polar regions with easterlies act as a source for angular momentum. These theoretical patterns of momentum vorticity flux appear to agree well with computations from actual data of geostrophic winds (Kao, 1953).

Instead of absolute vorticity, the use of potential vorticity

$$P = \frac{1}{\rho} Q_z \frac{\partial \theta}{\partial z} \quad (2.11)$$

where θ is the potential temperature, appears more rewarding in tracing adiabatic atmospheric motions. This quantity can be used as an effective tracer in identifying stratospheric and tropospheric air masses in their transition through the tropopause, especially in the vicinity of jet streams. More about the use of potential vorticity as an air-mass tracer will be given in Part 3 of this review. However, I have no knowledge that *statistical* transport studies of potential vorticity have been made as yet, probably because of the rather involved computational and analysis work required to arrive at reliable hemispheric distributions of this quantity (Danielsen, 1967a, 1967b).

3 ENERGY FLUXES AND TRANSFORMATIONS IN THE GENERAL CIRCULATION OF THE ATMOSPHERE

THEORETICAL CONSIDERATIONS

The following discussion is restricted to a few classical derivations of energy-transfer processes. These derivations have been refined considerably by the various authors pursuing specialized aspects of atmospheric energetics. For mathematical and computational details, the reader should consult the original papers referenced in this and subsequent chapters. Excellent summaries by Lorenz (1967) and by Dutton and Johnson (1967) have become available recently.

The study of the balance of potential (P), internal (I), and kinetic (K) energy in the general circulation of the atmosphere has a long history. Margules (1903) considered changes in the total potential energy (i.e., the sum of potential and internal energy) and its conversion into kinetic energy as the driving mechanism of storms. The combining of P and I energies into one quantity is usually justified since

$$P = \int_0^{\infty} g \rho z \, dz = \int_0^{\infty} p \, dz \quad (3.1)$$

and

$$I = \int_0^{\infty} c_v T \rho \, dz = \frac{c_v}{R} \int_0^{\infty} p \, dz \quad (3.2)$$

where ρ = density

g = acceleration of gravity

z = height
 p = pressure
 T = temperature
 c_v = specific heat at constant volume
 c_p = specific heat at constant pressure
 R = gas constant

P and I differ only by a constant factor. Since $R = c_p - c_v$,

$$P + I = \frac{c_p}{R} \int_0^{\infty} p \, dz = \frac{c_p}{g} \int_0^{p_0} T \, dp \quad (3.3)$$

Margules (1903) pointed out that only a small fraction of this total potential energy ($P + I$) may actually be converted into kinetic energy. In an atmosphere with horizontal density stratification, none of its potential energy is available for transformation into kinetic energy (Lorenz, 1955a, 1955b). In a baroclinic atmosphere, in which the density stratification is different from horizontal, adiabatic redistribution of mass will change the total potential energy and generate kinetic energy until a statically stable horizontal stratification has been achieved in which the total potential energy reaches a minimum value. Only the amount of total potential energy that is in excess of this minimum value is available for conversion into kinetic energy. This quantity is called "available potential energy," A .

Lorenz (1955a) describes the following properties of A :

1. The sum of the available potential energy and the kinetic energy is conserved under adiabatic flow.
2. The available potential energy is completely determined by the distribution of mass.
3. The available potential energy is zero if the stratification is horizontal and statically stable.
4. The available potential energy is positive if the stratification is not both horizontal and statically stable.

For potential energy to be released, the flow of air must be inclined at an angle against the isentropic surfaces. (Adiabatic flow along an isentropic surface does not consume potential energy.) According to Eady (1950) and Green (1960), optimum efficiency of this release is reached when the slope of the motions in the eddies is approximately one-half the slope of the mean isentropes. The isentropes would tend to flatten under the influence of eddy motions; differential heating, however, would tend to steepen them (see also Newell, 1963c).

Although A is the only source of K , it is not its only sink. Friction destroys kinetic energy and generates internal energy, which, in turn, increases the minimum total potential energy as well as the existing total potential energy. The increase in minimum total potential energy, however, is unavailable for conversion into kinetic energy. Thus the loss of kinetic energy by friction exceeds the gain in available

potential energy. For a climatological balance of the general circulation of the atmosphere to be maintained against friction, available potential energy must be resupplied continuously by radiation processes.

The whole amount of available potential energy need not necessarily be converted into kinetic energy. We realize, for instance, that in zonal flow of a baroclinic atmosphere, which is dynamically stable, no kinetic energy is generated. This makes the treatment of energy fluxes and conversions in the atmosphere quite complicated. The following is a short résumé of some of the considerations that enter into a quantitative treatment of the atmospheric circulation. The original paper by Lorenz (1955a) contains additional detail.

Substitution of Poisson's equation

$$T = \theta p^\kappa 1000^{-\kappa} \quad (3.4)$$

where θ is the potential temperature and the Poisson constant (κ) = $R/c_p \approx 2/7$, into Eq. 3.3 and integration by parts yields

$$P + I = (1 + \kappa)^{-1} \frac{c_p}{g} 1000^{-\kappa} \int_0^\infty p^{1+\kappa} d\theta \quad (3.5)$$

The minimum total potential energy that cannot be converted into kinetic energy is achieved if everywhere on the globe $p = [p]_{(\lambda, \phi)}$, where the subscripts indicate global averaging. Thus, per unit area of the earth's surface,

$$(P + I)_{\min} = (1 + \kappa)^{-1} \frac{c_p}{g} 1000^{-\kappa} \int_0^\infty [p]_{(\lambda, \phi)}^{1+\kappa} d\theta \quad (3.6)$$

The average available potential energy, $[A]_{(\lambda, \phi)}$, per unit area can be written as the difference between Eqs. 3.5 and 3.6:

$$[A]_{(\lambda, \phi)} = (1 + \kappa)^{-1} \frac{c_p}{g} 1000^{-\kappa} \int_0^\infty ([p^{1+\kappa}]_{(\lambda, \phi)} - [p]_{(\lambda, \phi)}^{1+\kappa}) d\theta \quad (3.7)$$

where $[p^{1+\kappa}]_{(\lambda, \phi)}$ again denotes an area average over an isobaric surface. Unless $p \equiv [p]_{(\lambda, \phi)}$, the integral term in parentheses is greater than zero since $(1 + \kappa) > 1$. It is difficult, however, to compare the average available potential energy, $[A]_{(\lambda, \phi)}$, in the form of Eq. 3.7 with the average total potential energy, $([P]_{(\lambda, \phi)} + [I]_{(\lambda, \phi)})$. For such a comparison, $p = [p]_{(\lambda, \phi)} + (p)_{(\lambda, \phi)}$ is substituted into $[p^{1+\kappa}]_{(\lambda, \phi)}$, and this expression is expanded into a power series

$$p^{1+\kappa} = [p]_{(\lambda, \phi)}^{1+\kappa} \left\{ 1 + (1 + \kappa) \frac{(p)_{(\lambda, \phi)}}{[p]_{(\lambda, \phi)}} + \frac{\kappa(1 + \kappa)}{2!} \frac{(p)_{(\lambda, \phi)}^2}{[p]_{(\lambda, \phi)}^2} + \dots \right\} \quad (3.8)$$

From this series, according to Eq. 3.7, the value $[p]_{(\lambda,\phi)}^{1+\kappa}$ must be subtracted. When performing the area-averaging operation, the second term in parentheses containing $[(p)_{(\lambda,\phi)}]_{(\lambda,\phi)}$ will vanish. Lorenz (1955a) showed that this series, in general, will converge rapidly so that Eq. 3.7 is approximated well by

$$[A]_{(\lambda,\phi)} = \frac{1}{2} \kappa \frac{c_p}{g} 1000^{-\kappa} \int_0^{\infty} [p]_{(\lambda,\phi)}^{1+\kappa} \left[\frac{(p)_{(\lambda,\phi)}^2}{[p]_{(\lambda,\phi)}^2} \right]_{(\lambda,\phi)} d\theta \quad (3.9)$$

Thus $[A]_{(\lambda,\phi)}$ depends on the variance of pressure over isentropic surfaces. This variance, however, is closely represented by the variance of potential temperature on an isobaric surface

$$(p)_{(\lambda,\phi)} \approx -(\theta)_{(\lambda,\phi)} \frac{\partial p}{\partial \theta} \quad (3.10)$$

[Dutton and Johnson (1967) retained a usually neglected isentropic boundary term in their computations.]

Thus

$$[A]_{(\lambda,\phi)} = \frac{1}{2} \kappa \frac{c_p}{g} 1000^{-\kappa} \int_0^{p_0} [p]_{(\lambda,\phi)}^{-(1-\kappa)} [\theta]_{(\lambda,\phi)}^2 \left\{ -\frac{\partial [\theta]_{(\lambda,\phi)}}{\partial p} \right\}^{-1} \times \left[\frac{(\theta)_{(\lambda,\phi)}^2}{[\theta]_{(\lambda,\phi)}^2} \right]_{(\lambda,\phi)} dp \quad (3.11)$$

From Poisson's equation, in the form

$$\frac{\partial \theta}{\theta} - \frac{\partial T}{T} = -\kappa \frac{\partial p}{p} \quad (3.12)$$

and because the dry-adiabatic lapse rate is $\Gamma_d = \frac{g}{c_p}$, one arrives at

$$\frac{\partial \theta}{\partial p} = -\kappa \frac{\theta}{p} \frac{(\Gamma_d - \Gamma)}{\Gamma_d} \quad (3.13)$$

where $\Gamma = -\partial T/\partial z$ is the actual lapse rate. Since the variance of potential temperature along an isobaric surface also resembles the variance of temperature along the same surface, $(\theta)_{(\lambda,\phi)}/\theta = (T)_{(\lambda,\phi)}/T$, Eq. 3.11 can be transformed, with the use of Eq. 3.13, into

$$[A]_{(\lambda,\phi)} = \frac{1}{2} \int_0^{\infty} [T]_{(\lambda,\phi)} \{ \Gamma_d - [\Gamma]_{(\lambda,\phi)} \}^{-1} \left[\frac{(T)_{(\lambda,\phi)}^2}{[T]_{(\lambda,\phi)}^2} \right]_{(\lambda,\phi)} dp \quad (3.14)$$

For $[\Gamma]_{(\lambda, \phi)} \approx \frac{2}{3} \Gamma_d$ and $[(T)_{(\lambda, \phi)}^2]_{(\lambda, \phi)} \approx (15^\circ)^2$, Lorenz arrives at an estimate of

$$\frac{[A]_{(\lambda, \phi)}}{[P]_{(\lambda, \phi)} + [I]_{(\lambda, \phi)}} \approx \frac{1}{200} \quad (3.15)$$

Mieghem (1956b, 1957) showed that the available potential energy as formulated by Lorenz in Eq. 3.14 constitutes a minimum value for an incompressible atmosphere. Mieghem's additional term, entering under the integral of Eq. 3.14, $(1/2)[p/(\rho C^2)_e]$, where C is the speed of sound and subscript e denotes conditions of hydrostatic equilibrium, turns out to be one order of magnitude smaller for large-scale atmospheric motions than Lorenz's term. Thus, for transformation processes of at least synoptic scale, Lorenz's formulation can be considered adequate.

The mean kinetic energy of the atmosphere per unit area of the earth's surface can be written as

$$[K]_{(\lambda, \phi)} = \frac{1}{2g} \int_0^{[p_0]_{(\lambda, \phi)}} [V^2]_{(\lambda, \phi)} dp \quad (3.16)$$

Considering the square of the speed of sound given by

$$C^2 = \frac{c_p}{c_v} RT \quad (3.17)$$

Eq. 3.3 can be transformed into

$$[P]_{(\lambda, \phi)} + [I]_{(\lambda, \phi)} = \frac{c_v}{gR} \int_0^{[p_0]_{(\lambda, \phi)}} [C^2]_{(\lambda, \phi)} dp \quad (3.18)$$

Since in the atmosphere $[V]_{(\lambda, \phi)} = [C]_{(\lambda, \phi)}/20$, one can estimate that

$$\frac{[K]_{(\lambda, \phi)}}{[P]_{(\lambda, \phi)} + [I]_{(\lambda, \phi)}} \approx \frac{1}{2000} \quad (3.19)$$

and, from Eq. 3.15, that

$$\frac{[K]_{(\lambda, \phi)}}{[A]_{(\lambda, \phi)}} \approx \frac{1}{10} \quad (3.20)$$

Thus it is easily seen that not nearly all available potential energy is converted into kinetic energy (see also Hollmann, 1959).

From the thermodynamic equation

$$dh = c_p dT - \alpha dp \quad (3.21)$$

where h is the amount of heat added to the system per unit of mass and $\alpha = 1/\rho$ is the specific volume, one arrives at

$$\frac{\partial \theta}{\partial t} + \mathbf{v} \cdot \nabla \theta + \omega \frac{\partial \theta}{\partial p} = \frac{\theta}{c_p T} \frac{dh}{dt} \quad (3.22)$$

where \mathbf{v} and ∇ are horizontal vectors and $\omega = dp/dt$. Multiplication by θ and addition of the continuity equation in the form

$$\frac{1}{2} \theta^2 \left(\frac{\partial \omega}{\partial p} + \nabla \cdot \mathbf{v} \right) = 0 \quad (3.23)$$

yields

$$\frac{1}{2} \frac{\partial \theta^2}{\partial t} + \frac{1}{2} \nabla (\theta^2 \mathbf{v}) + \frac{1}{2} \frac{\partial}{\partial p} (\theta^2 \omega) = \frac{\theta^2}{c_p T} \frac{dh}{dt} \quad (3.24)$$

If these terms are averaged over the whole extent of an isobaric surface, the second term on the left-hand side of this equation (divergence term) will give no contribution. In our notation we will indicate the global area-averaging process over an isobaric surface by the subscript (λ, ϕ) .

$$\frac{1}{2} \frac{\partial}{\partial t} [\theta^2]_{(\lambda, \phi)} + \frac{1}{2} \frac{\partial}{\partial p} [\theta^2 \omega]_{(\lambda, \phi)} = \left[\frac{\theta^2}{c_p T} \frac{dh}{dt} \right]_{(\lambda, \phi)} \quad (3.25)$$

If Eq. 3.22 is added to the continuity equation, $\theta(\partial \omega / \partial p + \nabla \cdot \mathbf{v}) = 0$, after isobaric area averaging, the following is obtained

$$\frac{\partial [\theta]_{(\lambda, \phi)}}{\partial t} + \frac{\partial}{\partial p} [\omega \theta]_{(\lambda, \phi)} = \left[\frac{\theta}{c_p T} \frac{dh}{dt} \right]_{(\lambda, \phi)} \quad (3.26)$$

Multiplication of this expression by $[\theta]_{(\lambda, \phi)}$ yields

$$\frac{1}{2} \frac{\partial}{\partial t} [\theta]_{(\lambda, \phi)}^2 + [\theta]_{(\lambda, \phi)} \frac{\partial}{\partial p} [\omega \theta]_{(\lambda, \phi)} = [\theta]_{(\lambda, \phi)} \left[\frac{\theta}{c_p T} \frac{dh}{dt} \right]_{(\lambda, \phi)} \quad (3.27)$$

One may now substitute the perturbation notation into Eq. 3.25, keeping in mind that $[\theta^2]_{(\lambda, \phi)} = [\theta]_{(\lambda, \phi)}^2 + [(\theta)^2]_{(\lambda, \phi)}$. If Eq. 3.27 is subtracted from the result of this substitution, one arrives at

$$\begin{aligned} \frac{1}{2} \frac{\partial}{\partial t} [(\theta)^2]_{(\lambda, \phi)} &= -[\theta \omega]_{(\lambda, \phi)} \frac{\partial [\theta]_{(\lambda, \phi)}}{\partial p} - \frac{1}{2} \frac{\partial}{\partial p} [(\theta)^2 \omega]_{(\lambda, \phi)} \\ &\quad + \frac{[\theta]_{(\lambda, \phi)}}{c_p [T]_{(\lambda, \phi)}} \left[(\theta)_{(\lambda, \phi)} \frac{d(h)_{(\lambda, \phi)}}{dt} \right]_{(\lambda, \phi)} \end{aligned} \quad (3.28)$$

Lorenz (1955a) neglects the second term on the right-hand side of this equation. Multiplication of Eq. 3.28 by $[\Gamma]_{(\lambda,\phi)} / \{[\theta]_{(\lambda,\phi)}^2 (\Gamma_d - [\Gamma]_{(\lambda,\phi)})\}$ and integration over $\int_0^{[p_0]_{(\lambda,\phi)}} dp$ yields

$$\frac{\partial [A]_{(\lambda,\phi)}}{\partial t} = -C + G \tag{3.29}$$

since $(\theta)_{(\lambda,\phi)} / [\theta]_{(\lambda,\phi)} = (T)_{(\lambda,\phi)} / [T]_{(\lambda,\phi)}$. In this expression C represents the energy transformation,

$$C = \int_0^{[p_0]_{(\lambda,\phi)}} [\theta\omega]_{(\lambda,\phi)} \frac{\partial [\theta]_{(\lambda,\phi)}}{\partial p} \frac{[T]_{(\lambda,\phi)}}{[\theta]_{(\lambda,\phi)}^2 (\Gamma_d - [\Gamma]_{(\lambda,\phi)})} dp \tag{3.30}$$

or

$$C = -\frac{R}{g} \int_0^{[p_0]_{(\lambda,\phi)}} \frac{[T\omega]_{(\lambda,\phi)}}{p} dp \tag{3.31}$$

or

$$C = -\int_0^{[p_0]_{(\lambda,\phi)}} [v \cdot \nabla z]_{(\lambda,\phi)} dp \tag{3.32}$$

Equation 3.32 is obtained from Eq. 3.31 by means of the continuity equation and the hydrostatic equation.* Furthermore, the generation of available potential energy can be written as

$$G = \int_0^{[p_0]_{(\lambda,\phi)}} \frac{[\theta]_{(\lambda,\phi)}}{c_p [T]_{(\lambda,\phi)}} \left[(\theta)_{(\lambda,\phi)} \frac{d(h)_{(\lambda,\phi)}}{dt} \right]_{(\lambda,\phi)} \times \frac{[T]_{(\lambda,\phi)}}{[\theta]_{(\lambda,\phi)}^2 (\Gamma_d - [\Gamma]_{(\lambda,\phi)})} dp \tag{3.33}$$

$$\left. \begin{aligned} * \frac{\partial(\omega z)}{\partial p} + \nabla \cdot (vz) &= 0 \\ -z \frac{\partial \omega}{\partial p} - z \nabla \cdot v &= 0 \end{aligned} \right\}$$

$$\omega \frac{\partial z}{\partial p} + v \cdot \nabla z = 0$$

Furthermore,

$$\frac{\partial z}{\partial p} = -\frac{1}{g\rho} \quad \text{and} \quad \frac{R[T]_{(\lambda,\phi)}}{pg} = \frac{1}{\rho g}$$

or

$$G = \frac{1}{g} \int_0^{[p_0]_{(\lambda, \phi)}} \frac{\Gamma_d}{\Gamma_d - [\Gamma]_{(\lambda, \phi)}} \frac{1}{[T]_{(\lambda, \phi)}} \left[(T)_{(\lambda, \phi)} \frac{d(h)_{(\lambda, \phi)}}{dt} \right]_{(\lambda, \phi)} dp \quad (3.34)$$

The generation of available potential energy thus relies on diabatic heating and cooling (Mieghem, 1962). Estimates indicate that the maximum possible rate of generation lies between 0.01 and 0.04 of the incoming solar radiation energy (Lorenz, 1960). See Dutton and Johnson (1967) for a different definition of an "efficiency factor" in the generation of available potential energy.

If the equations for horizontal motion are written

$$\frac{\partial \mathbf{v}}{\partial t} + (\mathbf{v} \cdot \nabla) \mathbf{v} + \omega \frac{\partial \mathbf{v}}{\partial p} = -g \nabla z - 2\Omega \times \mathbf{v} + \mathbf{F} \quad (3.35)$$

where \mathbf{F} is the frictional force, one obtains in similar fashion, by multiplication with $(\cdot \mathbf{v})$ and by application of the appropriate form of the continuity equation,

$$\frac{\partial [K]_{(\lambda, \phi)}}{\partial t} = C - D \quad (3.36)$$

where

$$D = -\frac{1}{g} \int_0^{[p_0]_{(\lambda, \phi)}} [\mathbf{v} \cdot \mathbf{F}]_{(\lambda, \phi)} dp \quad (3.37)$$

is the dissipation of kinetic energy.

For adiabatic and frictionless flow, generation G and dissipation D vanish, and thus the sum of $[A]_{(\lambda, \phi)}$ and $[K]_{(\lambda, \phi)}$ is conserved. Under such conditions, available potential energy must be increased through decreases in kinetic energy and vice versa. If both quantities increase or decrease together, nonadiabatic effects must be involved. This is the case for the observed large increase of $[A]_{(\lambda, \phi)}$ from summer to winter, when $[K]_{(\lambda, \phi)}$ increases at the same time (Spar, 1949).

Available potential energy and kinetic energy are generated, dissipated, and transformed by the *mean zonal* structure and motion of the atmosphere and by *eddies* superimposed upon these mean conditions. Lorenz (1955a) therefore considers separately the zonal and eddy available potential energies, $[A_Z]_{(\lambda, \phi)}$ and $[A_E]_{(\lambda, \phi)}$, and the zonal and eddy kinetic energies, $[K_Z]_{(\lambda, \phi)}$ and $[K_E]_{(\lambda, \phi)}$. In the following these terms are written in the form used by Muench (1965b); however, they are adapted to our present notation, which is described in Chap. 2. Subscript (λ) indicates a longitudinal (or zonal) average defined, for instance, as

$$[T]_{(\lambda)} = \frac{1}{2\pi} \int_0^{2\pi} T d\lambda \quad (3.38)$$

Subscript (λ, ϕ) represents a “spatial average,” defined as

$$[T]_{(\lambda, \phi)} = \frac{1}{1 - \sin \phi_s} \int_{\phi_s}^{\pi/2} [T]_{(\lambda)} \cos \phi \, d\phi \quad (3.39)$$

where ϕ_s is the latitude confining the polar cap over which the averaging operation is performed. The sequence of the two subscript letters indicates that average values $[T]_{(\lambda)}$ are computed first and then a second averaging process with respect to geographic latitude is applied. Departures from these averages are indicated by appropriate terms in parentheses, as described in Chap. 2. Specifically,

$$\begin{aligned} T &= [T]_{(\lambda)} + (T)_{(\lambda)} \\ [T]_{(\lambda)} &= [T]_{(\lambda, \phi)} + ([T]_{(\lambda)})_{(\phi)} \end{aligned} \quad (3.40)$$

The spatially averaged static stability is abbreviated by

$$[\sigma]_{(\lambda, \phi)} = \left[T \left(\frac{g}{c_p} - \frac{\partial T}{\partial z} \right) \right]_{(\lambda, \phi)} \quad (3.41)$$

With this the terms for mean zonal and eddy energies can be written as

$$\begin{aligned} A_E &= \int_{p_1}^{p_2} \frac{[(T)_{(\lambda)}^2]_{(\lambda, \phi)}}{2[\sigma]_{(\lambda, \phi)}} \, dp \\ A_Z &= \int_{p_1}^{p_2} \frac{[[T]_{(\lambda)}^2]_{(\lambda, \phi)}}{2[\sigma]_{(\lambda, \phi)}} \, dp \end{aligned} \left. \vphantom{\int_{p_1}^{p_2}} \right\} A_E + A_Z = A$$

$$\begin{aligned} K_E &= \int_{p_1}^{p_2} \frac{[(u)_{(\lambda)}^2 + (v)_{(\lambda)}^2]_{(\lambda, \phi)}}{2g} \, dp \\ K_Z &= \int_{p_1}^{p_2} \frac{[[u]_{(\lambda)}^2 + [v]_{(\lambda)}^2]_{(\lambda, \phi)}}{2g} \, dp \end{aligned} \left. \vphantom{\int_{p_1}^{p_2}} \right\} K_E + K_Z = K \quad (3.42)$$

For convenience the averaging notation has been omitted from A_E , A_Z , K_E , and K_Z . The original papers by Muench (1965b) and Lorenz (1955a) contain further details on the derivation of these terms.

For conditions in a closed system (achieved by integrating over the whole hemisphere), Lorenz (1955a) arrived at the following equations describing the changes of zonal and eddy available potential and kinetic energies. The sign of $\langle K_Z, A_Z \rangle$ has been changed from Lorenz’s original notation to make it conform to the direction of arrows in Fig. 3.1.

$$\begin{aligned}
\frac{\partial A_Z}{\partial t} &= \langle K_Z, A_Z \rangle - \langle A_Z, A_E \rangle + G_Z \\
\frac{\partial A_E}{\partial t} &= -\langle A_E, K_E \rangle + \langle A_Z, A_E \rangle + G_E \\
\frac{\partial K_Z}{\partial t} &= -\langle K_Z, A_Z \rangle + \langle K_E, K_Z \rangle - D_Z \\
\frac{\partial K_E}{\partial t} &= \langle A_E, K_E \rangle - \langle K_E, K_Z \rangle - D_E
\end{aligned} \tag{3.43}$$

In these expressions the notation for the energy-transformation terms adopted by a number of American authors has been used instead of C . The term $\langle K_Z, A_Z \rangle$, for instance, indicates the transformation of K_Z into A_Z . Allowing for the direction in which these energy transformations proceed, one can write

$$\langle K_Z, A_Z \rangle = -\langle A_Z, K_Z \rangle \tag{3.44}$$

These transformation terms are given explicitly in Table 3.1, following the form proposed by Muench (1965b). They are similar to those described earlier by Miller (1950). The terms G_Z and G_E describe the generation (or destruction) of zonal and eddy available potential energy, respectively. The terms D_Z and D_E are the zonal and eddy dissipation of kinetic energy by friction, respectively. Each of the energy-transformation terms contains vertical or horizontal transports of momentum or of sensible heat. Miegheem (1952a) also allows for the transport of latent heat.

Similar transport terms will also govern the large-scale motions of aerosols. Thus a better understanding of the energy transports and conversions in the atmosphere will also further our knowledge of the transport mechanisms controlling the spread of radioactive debris and of other artificial and natural contaminants of the atmosphere.

As shown in Eq. 3.40, such transport processes can become quite involved in their mathematical treatment. Let us consider, as an example, the zonally averaged vertical transport of sensible heat, $[T\omega]_{(\lambda)}$. Since

$$T = [T]_{(\lambda, \phi)} + ([T]_{(\lambda)})_{(\phi)} + (T)_{(\lambda)} \tag{3.45}$$

and

$$\omega = [\omega]_{(\lambda, \phi)} + ([\omega]_{(\lambda)})_{(\phi)} + (\omega)_{(\lambda)} \tag{3.46}$$

we arrive at

$$\begin{aligned}
[T\omega]_{(\lambda)} &= [T]_{(\lambda, \phi)}[\omega]_{(\lambda, \phi)} + [T]_{(\lambda, \phi)}([\omega]_{(\lambda)})_{(\phi)} \\
&\quad + ([T]_{(\lambda)})_{(\phi)}[\omega]_{(\lambda, \phi)} + ([T]_{(\lambda)})_{(\phi)}([\omega]_{(\lambda)})_{(\phi)} + [(T)_{(\lambda)}(\omega)_{(\lambda)}]_{(\lambda)}
\end{aligned} \tag{3.47}$$

The first four terms on the right of Eq. 3.47 are not affected by the additional zonal-averaging process since all their factors already contain zonal mean values. An additional bracket, $[]_{(\lambda)}$, therefore, has not been written. Terms containing only one factor, $()_{(\lambda)}$, vanish in a zonal-averaging process. Only the last term on the right

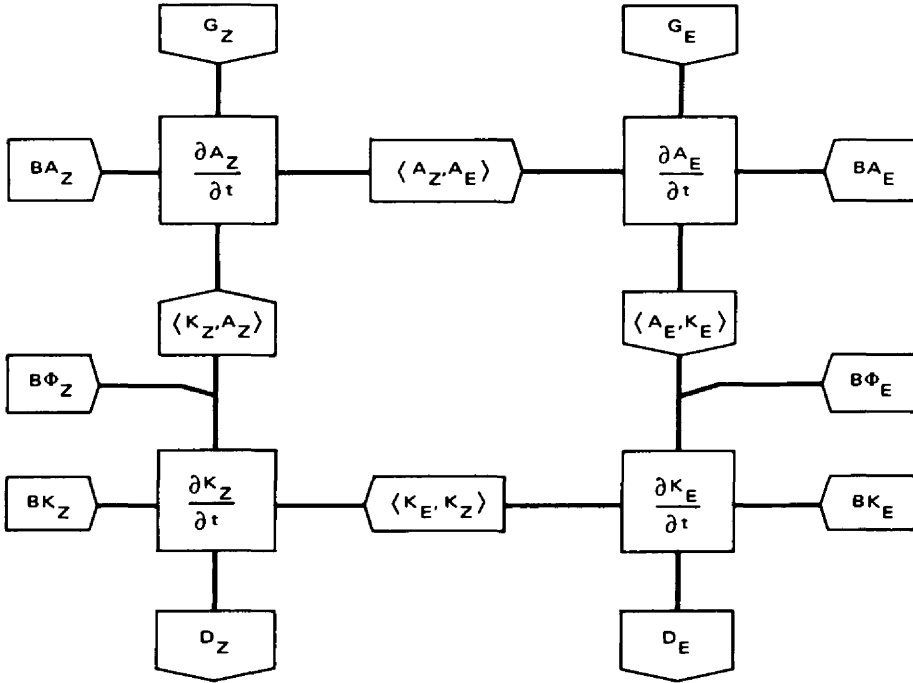


Fig. 3.1 Schematic diagram of energy balance. Pentagons are pointed in the direction of energy transfer for positive values of these processes. (Adapted from Muench, 1965b.)

remains as a result of possible correlations between departures from the zonal mean in temperatures and in vertical motions. Terms two and three would vanish in an additional latitudinal-averaging process, $[]_{(\phi)}$. Term four would be retained even after such latitudinal averaging as an effect of a possible correlation between the two factors. It contributes toward the mean meridional circulation. For a large enough latitude interval ϕ , we can assume that $[\omega]_{(\lambda, \phi)} = 0$. Hence the first term on the right should vanish. If the averaging interval ϕ is too small to allow this assumption, the first term will contribute, together with term four, toward the mean meridional circulation. If the latitude interval ϕ of averaging is quite small, the contribution from the averaged term four will be negligible, and term one on the right of Eq. 3.47 will account for the total mean meridional circulation.

From the foregoing one can deduce that, by simultaneous application of longitudinal and latitudinal averaging, transport processes can be resolved into

1. Transports by mean meridional circulations (first and/or fourth term on the right side of Eq. 3.47).
2. Eddy transports whose values per unit area are independent of latitude (last term on right side of Eq. 3.47).
3. Eddy transports whose values vanish when averaged over latitude (second and third terms in Eq. 3.47).

This short example reveals the complexity of mean and eddy transports. If, in addition, time-averaging and vertical-averaging operations are considered, further complications arise, as will be demonstrated in subsequent chapters (see also Reiter, 1969b).

Transport terms similar to the ones derived previously are distributed characteristically in the various energy-transformation functions derived by Lorenz (1955a) and Muench (1965b) (see Table 3.1). This has also been recognized by other authors (Mieghem, 1952a, 1956a; Kuo, 1951a; Starr, 1953).

So far we have considered the atmosphere as a closed system, following the approach by Lorenz (1955a). The closed system is achieved by integrating the energy equations over the entire surface of the globe and the whole depth of the atmosphere. Practical computations of energy-transformation processes usually depend on data from specific regions, or layers, in the atmosphere. In such cases energy fluxes across the boundaries of the system become important, and thus the new balance requirements become even more complicated (Mieghem, 1958, 1967). Muench (1965a, 1965b), therefore, proposes transformation equations of the form

$$\begin{aligned}
 \frac{\partial A_Z}{\partial t} &= BA_Z + \langle K_Z, A_Z \rangle - \langle A_Z, A_E \rangle + G_Z \\
 \frac{\partial A_E}{\partial t} &= BA_E - \langle A_E, K_E \rangle + \langle A_Z, A_E \rangle + G_E \\
 \frac{\partial K_Z}{\partial t} &= BK_Z - \langle K_Z, A_Z \rangle + \langle K_E, K_Z \rangle + B\phi_Z - D_Z \\
 \frac{\partial K_E}{\partial t} &= BK_E + \langle A_E, K_E \rangle - \langle K_E, K_Z \rangle + B\phi_E - D_E
 \end{aligned} \tag{3.48}$$

The terms containing the letter B indicate energy fluxes across the boundaries of the area and layer under consideration. They are listed explicitly in Table 3.1.

Figure 3.1 describes schematically the functions of the various energy-transformation and -flux terms. It follows a flow diagram originally proposed by Phillips (1956). Since it became evident from observational data that, on the average,

the large-scale eddies of the general circulation feed the mean zonal flow—contrary to the concepts of turbulence theory according to which the mean motion feeds the eddies—the transformation term $\langle K_E, K_Z \rangle$ has been entered as positive in Eqs. 3.43 and 3.48 and in Fig. 3.1. Also, $\langle K_Z, A_Z \rangle$ has been entered instead of $\langle A_Z, K_Z \rangle$, which Muench (1965b, 1966) used in his original concept, to preserve a clockwise energy flux in Fig. 3.1, even though, on the average, the general circulation follows $\langle A_Z, K_Z \rangle$.

Many authors have added considerable refinement to these energy-transformation and flux considerations. It would be far beyond the scope of this review to follow all these derivations in detail. Most of these refinements will be listed briefly in the subsequent chapters. For further information, however, consult the original publications.

Table 3.1

**ENERGY-TRANSFORMATION TERMS AND FLUX TERMS AS DERIVED BY
MUENCH (M) (1965b) AND LORENZ (L) (1955a)**

(a is the radius of the earth and Q is the rate of diabatic heat addition per unit of mass)

$$\begin{aligned}
 \text{(M)} \quad \langle A_Z, A_E \rangle &= \int_{p_1}^{p_2} \left\{ \left[\frac{(\overline{T})_{(\lambda)}(\overline{v})_{(\lambda)}}{2[\sigma]_{(\lambda, \phi)} a} \frac{\partial ([\overline{T}]_{(\lambda)}(\phi))}{\partial \phi} \right]_{(\lambda, \phi)} \right. \\
 &\quad \left. + \left[(\overline{T})_{(\lambda)}(\overline{\omega})_{(\lambda)} P^{-\kappa} \frac{\partial}{\partial p} \left(\frac{([\overline{T}]_{(\lambda)}(\phi) P^\kappa)}{[\sigma]_{(\lambda, \phi)}} \right) \right]_{(\lambda, \phi)} \right\} dp \\
 \text{(M)} \quad \langle A_E, K_E \rangle &= - \int_{p_1}^{p_2} [(\overline{\omega})_{(\lambda)}(\overline{T})_{(\lambda)}]_{(\lambda, \phi)} \frac{R}{pg} dp \\
 \text{(M)} \quad \langle K_E, K_Z \rangle &= \int_{p_1}^{p_2} \frac{1}{g} \left\{ \left[\frac{\cos \phi}{a} (\overline{u})_{(\lambda)}(\overline{v})_{(\lambda)} \frac{\partial}{\partial \phi} \left(\frac{[\overline{u}]_{(\lambda)}}{\cos \phi} \right) \right]_{(\lambda, \phi)} \right. \\
 &\quad \left. + \frac{1}{a} \left[(\overline{v})_{(\lambda)}^2 \frac{\partial [\overline{v}]_{(\lambda)}}{\partial \phi} \right]_{(\lambda, \phi)} + [\tan \phi (\overline{u})_{(\lambda)}^2 [\overline{v}]_{(\lambda)}]_{(\lambda, \phi)} \right. \\
 &\quad \left. + \left[(\overline{\omega})_{(\lambda)}(\overline{u})_{(\lambda)} \frac{\partial [\overline{u}]_{(\lambda)}}{\partial p} \right]_{(\lambda, \phi)} \right. \\
 &\quad \left. + \left[(\overline{\omega})_{(\lambda)}(\overline{v})_{(\lambda)} \frac{\partial [\overline{v}]_{(\lambda)}}{\partial p} \right]_{(\lambda, \phi)} \right\} dp \\
 \text{(L)} \quad \langle K_Z, A_Z \rangle &= \frac{R}{g} \int_{p_1}^{p_2} \frac{1}{p} [\overline{T}]_{(\lambda, \phi)} [\overline{\omega}]_{(\lambda, \phi)} dp
 \end{aligned}$$

or

(Table continues on page 46.)

$$\frac{R}{g} \int_{p_1}^{p_2} \frac{1}{p} [([T]_{(\lambda)})(\phi) ([\omega]_{(\lambda)})(\phi)]_{(\phi)} dp$$

(see remarks subsequent to Eq. 3.47)

$$(M,L) \quad G_Z = \int_{p_1}^{p_2} \frac{[(Q)_{(\lambda)})(\phi) ([T]_{(\lambda)})(\phi)]_{(\phi)}}{c_p [\sigma]_{(\lambda, \phi)}} dp$$

(for alternate equation, see preceding expression and remarks to Eq. 3.47)

$$(M) \quad G_E = \int_{p_1}^{p_2} \frac{[(Q)_{(\lambda)}(T)_{(\lambda)}]_{(\lambda, \phi)}}{c_p [\sigma]_{(\lambda, \phi)}} dp$$

$$(M) \quad D_Z = \int_{p_1}^{p_2} \frac{1}{g} \{ [u]_{(\lambda)} [F_\lambda]_{(\lambda)} + [v]_{(\lambda)} [F_\phi]_{(\lambda)} \}_{(\lambda, \phi)} dp$$

(subscripts without parentheses indicate components of the frictional force)

$$(M) \quad D_E = \int_{p_1}^{p_2} \frac{1}{g} \{ [(u)_{(\lambda)}(F_\lambda)_{(\lambda)} + (v)_{(\lambda)}(F_\phi)_{(\lambda)}]_{(\lambda, \phi)} \} dp$$

$$(M) \quad \begin{aligned} BA_Z = & \frac{\cos \phi_s}{a(1 - \sin \phi_s)} \int_{p_1}^{p_2} \frac{1}{2[\sigma]_{(\lambda, \phi)}} \{ 2[(T)_{(\lambda)}(v)_{(\lambda)}]_{(\lambda)} ([T]_{(\lambda)})(\phi) \\ & + ([T]_{(\lambda)})_{(\phi)}^2 [v]_{(\lambda)} \}_{\phi_s} dp \\ & + \left\{ \frac{1}{2[\sigma]_{(\lambda, \phi)}} [2[(\omega)_{(\lambda)}(T)_{(\lambda)}]_{(\lambda)} ([T]_{(\lambda)})(\phi) \right. \\ & \left. + ([T]_{(\lambda)})_{(\phi)}^2 [\omega]_{(\lambda)} \right\}_{(\lambda, \phi)} \Big|_{p_1} \\ & - \left\{ \frac{1}{2[\sigma]_{(\lambda, \phi)}} [2[(\omega)_{(\lambda)}(T)_{(\lambda)}]_{(\lambda)} ([T]_{(\lambda)})(\phi) \right. \\ & \left. + ([T]_{(\lambda)})_{(\phi)}^2 [\omega]_{(\lambda)} \right\}_{(\lambda, \phi)} \Big|_{p_2} \end{aligned}$$

(ϕ_s is the latitude confining the polar cap over which the latitudinal averaging operation is performed. Subscripts without parentheses indicate boundaries at which computations must be carried out.)

$$(M) \quad BA_E = \frac{\cos \phi_s}{a(1 - \sin \phi_s)} \int_{p_1}^{p_2} \frac{1}{2[\sigma]_{(\lambda, \phi)}} \{ [(T)_{(\lambda)}^2 v]_{(\lambda)} \}_{\phi_s} dp$$

(Table continues on page 47.)

$$+ \left\{ \frac{[\omega(T)_{(\lambda)}^2]_{(\lambda, \phi)}}{2[\sigma]_{(\lambda, \phi)}} \right\}_{p_1} - \left\{ \frac{[\omega(T)_{(\lambda)}^2]_{(\lambda, \phi)}}{2[\sigma]_{(\lambda, \phi)}} \right\}_{p_2}$$

where $v = [v]_{(\lambda)} + (v)_{(\lambda)}$
 $\omega = [\omega]_{(\lambda)} + (\omega)_{(\lambda)}$, etc.

$$(M) \quad BK_Z = \frac{\cos \phi_s}{a(1 - \sin \phi_s)} \int_{p_1}^{p_2} \frac{1}{2g} \{[(u^2 + v^2 - (u)_{(\lambda)}^2 - (v)_{(\lambda)}^2)v]_{(\lambda)}\}_{\phi_s} dp$$

$$+ \frac{1}{2g} \{[(u^2 + v^2 - (u)_{(\lambda)}^2 - (v)_{(\lambda)}^2)\omega]_{(\lambda, \phi)}\}_{p_1}$$

$$- \frac{1}{2g} \{[(u^2 + v^2 - (u)_{(\lambda)}^2 - (v)_{(\lambda)}^2)\omega]_{(\lambda, \phi)}\}_{p_2}$$

$$(M) \quad BK_E = \frac{\cos \phi_s}{a(1 - \sin \phi_s)} \int_{p_1}^{p_2} \frac{1}{2g} \{[(u)_{(\lambda)}^2 + (v)_{(\lambda)}^2]v\}_{(\lambda)}\}_{\phi_s} dp$$

$$+ \frac{1}{2g} \{[(u)_{(\lambda)}^2 + (v)_{(\lambda)}^2]\omega\}_{(\lambda, \phi)}\}_{p_1}$$

$$- \frac{1}{2g} \{[(u)_{(\lambda)}^2 + (v)_{(\lambda)}^2]\omega\}_{(\lambda, \phi)}\}_{p_2}$$

$$(M) \quad B\Phi_Z = \frac{\cos \phi_s}{a(1 - \sin \phi_s)} \int_{p_1}^{p_2} \frac{1}{g} \{[v]_{(\lambda)}([\Phi]_{(\lambda)}(\phi))\}_{\phi_s} dp$$

$$+ \frac{1}{g} \{[([\omega]_{(\lambda)}(\phi) ([\Phi]_{(\lambda)}(\phi))]_{(\lambda, \phi)}\}_{p_1}$$

$$- \frac{1}{g} \{[([\omega]_{(\lambda)}(\phi) ([\Phi]_{(\lambda)}(\phi))]_{(\lambda, \phi)}\}_{p_2}$$

(Φ is the geopotential)

$$(M) \quad B\Phi_E = \frac{\cos \phi_s}{a(1 - \sin \phi_s)} \int_{p_1}^{p_2} \frac{1}{g} \{[(v)_{(\lambda)}(\Phi)_{(\lambda)}]_{(\lambda)}\}_{\phi_s} dp$$

$$+ \frac{1}{g} \{[(\omega)_{(\lambda)}(\Phi)_{(\lambda)}]_{(\lambda, \phi)}\}_{p_1} - \frac{1}{g} \{[(\omega)_{(\lambda)}(\Phi)_{(\lambda)}]_{(\lambda, \phi)}\}_{p_2}$$

COMPUTATIONAL RESULTS

The numerical evaluation of the terms in Table 3.1 turns out to be a monumental task, not so much as far as computational work is concerned—large electronic calculators usually will handle the equations with ease—but with respect to data preparation. It is unfortunate that the results will depend to a considerable degree on data density and on the analysis techniques involved. This is one of the reasons why results obtained by various authors are not always comparable with each other. Further complications arise from the use of different averaging techniques (Oort, 1964b).

Since the atmosphere seldom presents itself with model simplicity, computations conducted for relatively short time periods are expected to yield strongly varying results, depending on the state of the atmosphere. Many studies are available on the mean and eddy fluxes in the troposphere and stratosphere for limited periods of time. Attempts have been made to piece together from this wealth of information a “seasonal mean state” of energies and energy transformations in the atmosphere (Oort, 1964a; for meridional kinetic energy at 500 mb, see Shapiro and Ward, 1963). Doing so, it became apparent that even relatively long periods of time may show an abnormal behavior in the energy-transformation processes that drive the general circulation of the atmosphere (Shapiro and Ward, 1963; Wiin-Nielsen, 1965).

The subsequent résumé will outline the results of a number of such studies on the energetics of the atmosphere. Since these studies involve estimates on mean meridional and eddy motions in the atmosphere, they will further the understanding of the mechanisms of large-scale transport processes of aerosols as well.

Mean and Eddy Kinetic-Energy Distributions

Mean values of the transfer of eddy kinetic into mean kinetic energy were computed by Saltzman and Fleisher (1960a) for the 500-mb surface and by Starr (1953, 1959a) for the entire depth of the northern hemispheric atmosphere. Saltzman and Fleisher used a geostrophic approximation for their computations, whereas Starr based his investigations on actual wind data. (For more details on the calculations by Saltzman and Fleisher, see Chap. 4.)

If the 500-mb values by Saltzman and Fleisher (1960a) are representative for the entire depth of the atmosphere, the values given in Table 3.2 can be obtained. These values compare with computations carried out by Starr (1953, 1959a), see Table 3.3, for (i) the first six months of 1950, (ii) the second six months of 1950, (iii) for January 1949, and (iv) for the year 1951—the same year used in the study by Saltzman and Fleisher (1960a). In these computations it was assumed that $[u]_{(\lambda)}$ and $[(u)_{(\lambda)} - (v)_{(\lambda)}]_{(\lambda)}$ are zero at the equator.

These studies lead to the important conclusion that, on the average, the net transfer of energy is directed from the eddies to the zonal flow (see also Rossby, 1949;

Table 3.2
MEAN VALUES OF THE TRANSFER OF EDDY KINETIC
ENERGY INTO MEAN KINETIC ENERGY AT THE 500-mb
SURFACE, NORTHERN HEMISPHERE*

(i)	5.8×10^{20} ergs/sec = 5.8×10^{10} kilojoules/sec (Winter average)
(ii)	1.8×10^{20} ergs/sec = 1.8×10^{10} kilojoules/sec (Summer average)
(iii)	3.8×10^{20} ergs/sec = 3.8×10^{10} kilojoules/sec (Annual average)

*Adapted from Saltzman and Fleisher, 1960a.

Arakawa, 1953; Kuo, 1953; Miegheem, 1956a; Murakami, 1963; Starr, 1959b). For more details on countergradient flux, see Starr (1968). Webster (1961, 1965) and Oort (1964c) found a similar energy transfer from the eddies to the mean flow in the Gulf Stream.

A transfer in this direction is indicated by a positive sign for $\langle K_E, K_Z \rangle$ (see Fig. 3.1). This is contrary to the experience gained from small-scale turbulence, where, according to L. F. Richardson, "Big whirls have little whirls that feed on their velocity, and little whirls have lesser whirls and so on to viscosity." Saltzman and Fleisher (1960a) paraphrased this verse in the form, "All whirls do trade their velocity—but the biggest whirl exacts its cut."

The smaller values of energy transfer obtained by Saltzman and Fleisher (1960a) as compared to those computed by Starr (1953, 1959a) are attributed to the additional smoothing introduced by the geostrophic approximations (Starr, 1959a). The effect of smoothing is also indicated by the fact that transfer values computed from daily wind data are larger than those computed from time-averaged and vertically averaged data (Table 3.3). The effect of different smoothing techniques has been considered by Oort (1964b) and will be described later.

Stratospheric Energy Conversions with Special Reference to Warming Periods

Complete consideration of all energy-transformation terms listed in Table 3.1 was given by Muench (1965b) for stratospheric flow conditions during January 1958. A period of stratospheric warming between January 22 and January 24 was preceded by a slight increase in eddy available potential energy (Fig. 3.2). The eddy kinetic energy showed a continuous rise during the second half of the month (see also Matsuno and Hirota, 1966). The energy-conversion term $\langle A_E, K_E \rangle$ (Fig. 3.3) increased strongly during the warming episode. The term $B\Phi_Z$ behaved quite erratically. One possible source of error in its computation was the difficulty in estimating accurately the zonally averaged vertical motions at low latitudes. Relatively large values of $B\Phi_E$ appeared several days before the warming. The energy transferred by this term came almost entirely from the troposphere through the 100-mb surface. Before the onset of

Table 3.3

**MEAN VALUES OF THE TRANSFER OF EDDY KINETIC ENERGY INTO
MEAN KINETIC ENERGY FOR THE ENTIRE DEPTH OF
THE ATMOSPHERE IN THE NORTHERN HEMISPHERE*†**

(i)	(a) 4.2×10^{20} ergs/sec	For vertically averaged winds and transports
	(b) 3.9×10^{20} ergs/sec	For calculations performed at individual levels and for mean conditions, integrated vertically as final step
	(c) $(4.5 \pm 1.0) \times 10^{20}$ ergs/sec	From vertically integrated zonal-wind profiles under instantaneous daily conditions, the long-term mean being formed by averaging the daily figures for the production (excluding data for 70°N)
	(d) 9.8×10^{20} ergs/sec	For individual levels and daily conditions. The long term mean is obtained by averaging the daily production figures (excluding data from 70°N)
(ii)	(a) 4.6×10^{20} ergs/sec	See (i) (a) above
	(b) 5.5×10^{20} ergs/sec	See (i) (b) above
(iii)	(a) 10.5×10^{20} ergs/sec	See (i) (a) above
	(b) 9.8×10^{20} ergs/sec	See (i) (b) above
(iv)	(c) $(4.8 \pm 0.7) \times 10^{20}$ ergs/sec	See (i) (c) above
	(d) $(5.8 \pm 1.0) \times 10^{20}$ ergs/sec	See (i) (d) above (70°N data are included)
	(e) 4.6×10^{20} ergs/sec	From mean wind profiles averaged vertically and with respect to time. (This value for 1950 would be 4.4×10^{20} ergs/sec)
	(f) $(6.2 \pm 1.2) \times 10^{20}$ ergs/sec	From 500-mb daily winds, assumed to be representative of the average atmosphere [compare with values (iii) in Table 3.2 obtained by Saltzman and Fleisher (1960a)]

*Adapted from Starr, 1953, 1959a.

†Letters (i), (ii), etc., refer to various periods of investigation as mentioned in the text. Letters (a), (b), etc., pertain to different modes of computation described in the table.

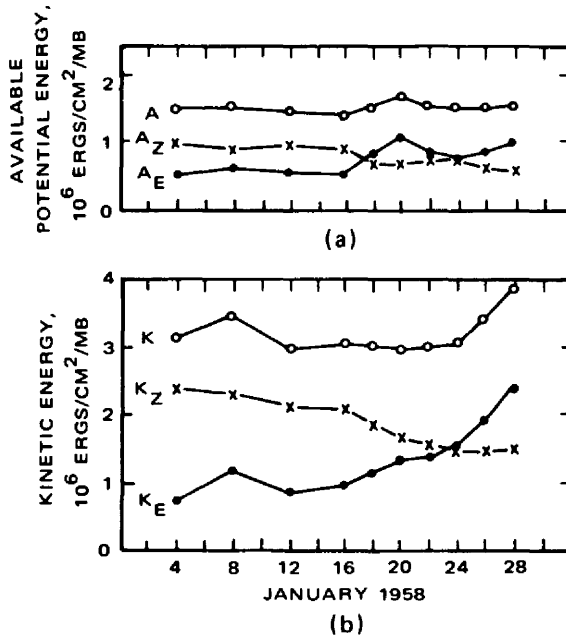


Fig. 3.2 Available potential energy (a) and kinetic energy (b) in the stratosphere during January 1958. (Adapted from Muench, 1965b.)

the warming, $\langle A_E, K_E \rangle$ was virtually nil in the stratosphere; nevertheless, K_E showed a pronounced increase during that period. This suggests that the energy increase was caused almost entirely by a transfer of energy from the troposphere to the stratosphere. A report by Hirota (1967) on an observed upward propagation of stratospheric warming events supports this conclusion. Thus the stratospheric eddy motions might, at least in part, be considered as a “driven circulation” produced by tropospheric motions. White and Nolan (1960) and also Julian and Labitzke (1965) arrived at similar conclusions, as shown in the following. Oort (1965) and Newell (1964d) also arrived at a countergradient flux of momentum and heat in the lower stratosphere, which confirms the conclusion that these eddies are forced by the tropospheric circulation (see also Newell, 1965b; Newell and Miller, 1965; Peng, 1965a,c; Starr, 1968).

The monthly mean energy cycle for January 1958, according to Muench (1965b, 1966), is shown in Fig. 3.4. Numbers in circles indicate an imbalance in each of the four energy equations, produced by computational techniques. Frictional dissipation terms were not computed. They are probably smaller than the estimate of $D = 2.6$ ergs/sec/g made by Saltzman (1961a) for the troposphere and—because of the stresses at the lower boundary of the stratosphere—would even be negative (Oort, 1964a; Julian and Labitzke, 1965), i.e., kinetic energy would be fed into the stratosphere by frictional forces. The estimates by Muench (1965b) and also by Reed et al. (1963) differ from the results by Oort (1964a), mainly in the magnitude and sign of $\langle A_E, K_E \rangle$

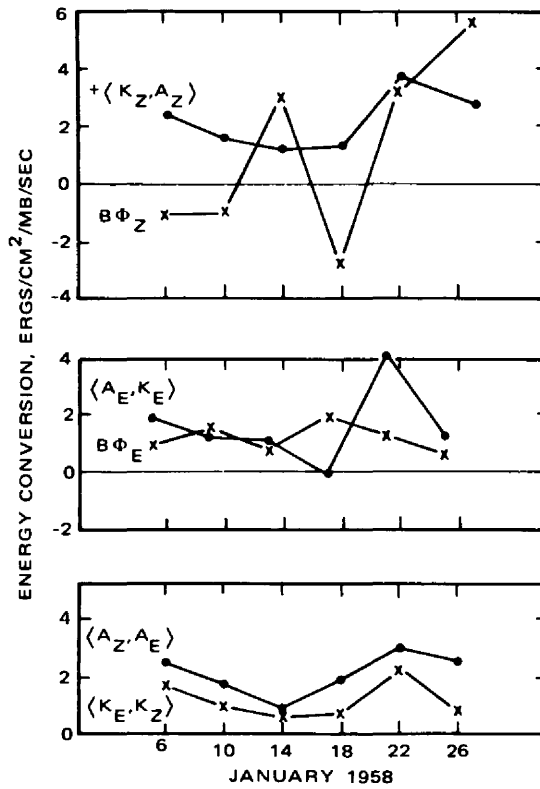


Fig. 3.3 Energy conversions in the stratosphere during January 1958. (Adapted from Muench, 1965b.)

and $\langle A_Z, A_E \rangle$, probably because Oort included in his period (January through March 1958) conditions that no longer were characteristic of the winter stratosphere.

In Table 3.4, a few computational results by various authors are summarized. Positive signs correspond to conversions in the direction of pentagons shown in Fig. 3.4. The values obtained by Muench (1965b) characterize, as mentioned, stratospheric results during a month of warming. In his computations of $\langle A_E, K_E \rangle$, effects of diabatic heating or cooling were neglected.

Reed, Wolfe, and Nishimoto (1963) analyzed the energy conversions at 50 mb for the period Jan. 25, 1957, to Feb. 9, 1957 (see also Lateef, 1964). This was a period of sudden warming which produced a split in the polar vortex (Craig and Hering, 1959). During the first part of the period under investigation, the meridional temperature gradient had its normal poleward direction at high latitudes. During the second part of the period, however, the gradient reversed. Typical flow patterns before and after the breakdown of the polar vortex are shown in Figs. 3.5 and 3.6, respectively. In either of the two maps, planetary wave-number 2 appears to dominate. This fact will be stressed again in Chap. 4.

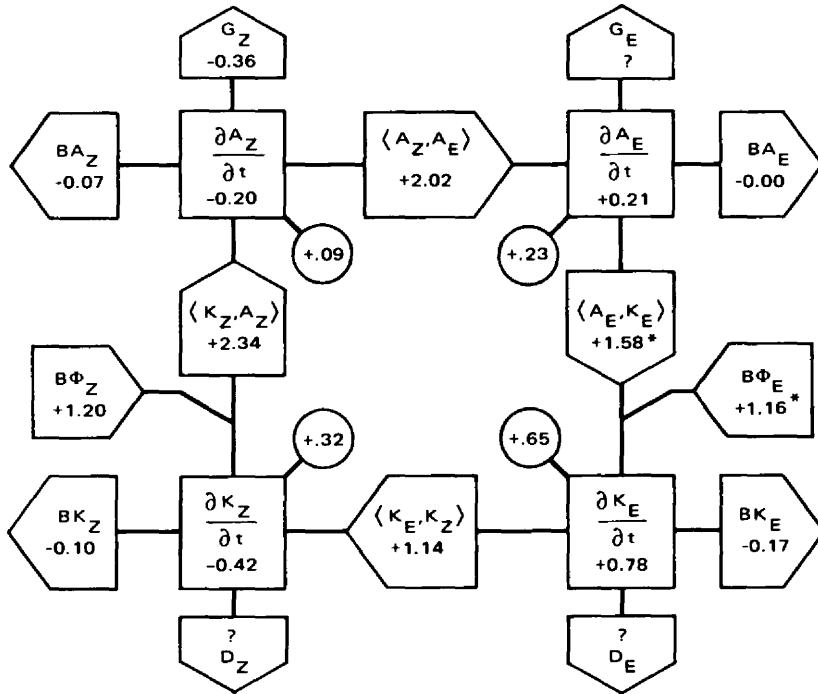


Fig. 3.4 Monthly mean stratosphere energy diagram for January 1958. Pentagons point in direction of energy transfer. Numerical values of energy processes (ergs/cm²/mb/sec) are shown inside. Circled values indicate the imbalance for the energy equation. Asterisk indicates that effects of diabatic heating were assumed to be negligible. (Adapted from Muench, 1965b.)

The energy distribution during this period of warming is shown in Fig. 3.7. Initially it seems that K_Z was four times as large as A_Z . Reed, Wolfe, and Nishimoto consider this to be typical for the wintertime stratosphere, in contrast to the winter troposphere, where, according to Saltzman and Fleisher (1960b), A_Z is about five times the value of K_Z (see also Reed, 1963b). The smaller temperature variance with latitude and the greater static stability apparently reduce the potential energy in the stratosphere relative to that in the troposphere. The kinetic energy per unit of mass in both regions appears to be about the same, probably even larger in the stratosphere during periods of a well-developed polar-night jet stream.

As shown in Fig. 3.7, K_Z decreased steadily throughout the period of investigation; however, K_E and A_E both increased during the first part of the period and then decreased during the second part [the parallel behavior of K_E and A_E within the same eddy has been considered theoretically by Kuo (1959)].

Computations by Oort (1964a) are shown in Table 3.4. They cover the stratosphere between 100 and 30 mb for the IGY period July 1957 to June 1958. Thus they represent a rather long time period. $K_Z > A_Z$, as postulated by Reed, Wolfe, and Nishimoto for the winter stratosphere, is not realized in Oort's sample,

Table 3.4
ESTIMATES OF ENERGY TRANSFORMATION BY VARIOUS AUTHORS*

Authors	Period	Units	G_Z	$\frac{\partial A_Z}{\partial t}$	$\langle A_Z, A_E \rangle$	G_E	$\frac{\partial A_E}{\partial t}$
Muench (1965b)	1/58	ergs/cm ² /mb/sec	-0.36	-0.20	2.02	-?	0.21
Reed et al. (1963)	1/25/57 to 2/4/57	ergs/cm ² /mb/sec	(-1.0)	-1.0	8.9	-?	2.4
Reed et al. (1963)	2/4/57 to 2/9/57	ergs/cm ² /mb/sec	(<-1.0)	4.7	-8.3	-?	-3.0
Oort (1964a)	7/57 to 6/58	10 ¹⁸ ergs/sec* or 10 ²⁵ ergs	-187	[23.6]	-53.1	(27.7)	[6.95]
Miyakoda (1963)	1/15/58 to 1/23/58	ergs/cm ² /mb/sec			2.4		
Sekiguchi (1963)	1/15/58 to 1/25/58	ergs/cm ² /mb/sec			4.0		
Julian and Labitzke (1965)	1/2/63 to 1/27/63	10 ⁷ ergs/cm ²	-31	-5	78	-7	8
Julian and Labitzke (1965)	1/27/63 to 2/26/63	10 ⁷ ergs/cm ²	-6	-2	-16	-28	-12
Julian and Labitzke (1965)	1/2/63 to 1/27/63	10 ⁷ ergs/cm ²	(+)	-132	1430	(-)	48
Julian and Labitzke (1965)	1/27/63 to 2/26/63	10 ⁷ ergs/cm ²	(+)	83	1067	(-)	-42

Table 3.4 (Continued)

	$\langle A_E, K_E \rangle$	$\frac{\partial K_E}{\partial t}$	D_E	$\langle K_E, K_Z \rangle$	$\frac{\partial K_Z}{\partial t}$	D_Z	$\langle K_Z, A_Z \rangle$	Remarks
Muench (1965b)	1.58	0.78	?	1.14	-0.42	?	+2.34	Stratosphere
Reed et al. (1963)	8.3	1.4	(-19.3)	5.8	-2.9	(10.7)	+6.5	Stratosphere
Reed et al. (1963)	-5.0	-3.0	(-14.3)	5.4	-2.2	(7.7)	-1.6	Stratosphere
Oort (1964a)	-25.4	[8.95]	(-47.5)	+22.1	[4.10]	?	?	Stratosphere
Miyakoda (1963)	0.2		-5.2	-2.2		?	1.0	Stratosphere
Sekiguchi (1963)	3.0		?	0.6		?	?	Stratosphere
Julian and Labitzke (1965)	68	13	-147	87	-15	46	98	Stratosphere
Julian and Labitzke (1965)	-44	-18	-75	3	+1	26	-13	Stratosphere
Julian and Labitzke (1965)	1205	11	147	-137	14	-46	389	Troposphere
Julian and Labitzke (1965)	816	-31	75	-72	0	-26	526	Troposphere

(Table continues on page 56.)

Table 3.4 (Continued)

Author: Richards (1967); Period: IQSY 1965; Units: 10^{18} ergs/sec

	Month											
	Jan.	Feb.	Mar.	Apr.	May	June	July	Aug.	Sept.	Oct.	Nov.	Dec.
$\langle A_Z, A_E \rangle$												
by transient eddies												
100 to 50 mb	18.4	11.4	6.2	-20.1	-10.9	-9.8	-6.1	-9.7	-15.9	-14.6	-9.9	-9.7
50 to 30 mb	22.2	11.2	0.97	-1.8	-1.9	-1.4	-1.1	-1.2	-1.3	-0.34	3.0	0.53
30 to 10 mb	33.8	18.1	2.3	-0.74	-1.1	-0.69	-0.40	-0.44	0.25	3.5	8.3	5.6
$\langle A_Z, A_E \rangle$												
by standing eddies												
100 to 50 mb	45.2	18.8	-5.4	-24.5	-37.1	-14.9	-9.6	-10.0	-17.7	-12.3	-7.3	-44.4
50 to 30 mb	49.1	18.1	3.3	-4.2	-1.6	-0.05	-0.85	-0.46	-1.4	2.7	22.9	-7.4
30 to 10 mb	96.4	43.3	6.5	-3.9	0.30	0.32	0.13	0.21	0.76	6.2	55.7	36.9
$\langle K_E, K_Z \rangle$												
by transient eddies												
100 to 50 mb	16.4	1.2	0.74	-2.8	1.2	0.42	-1.8	3.3	1.9	6.1	1.8	11.9
50 to 30 mb	15.8	5.9	7.4	2.0	-3.6	-0.12	-0.21	0.18	0.19	1.5	1.9	3.0
30 to 10 mb	58.8	27.0	31.0	3.6	-1.7	0.28	-0.42	0.22	1.5	5.2	15.7	-1.4
$\langle K_E, K_Z \rangle$												
by standing eddies												
100 to 50 mb	-14.6	-7.6	11.8	-0.21	4.2	-3.0	7.9	5.6	9.9	17.5	14.1	8.5
50 to 30 mb	-13.9	-0.07	25.9	-0.23	-0.59	-2.1	0.19	0.10	0.96	5.9	6.6	0.42
30 to 10 mb	39.7	28.5	68.2	-0.54	-0.88	-3.3	-0.57	0.09	1.9	13.9	3.1	-15.7
$\langle K_Z, A_Z \rangle$												
100 to 50 mb	91.6			22.0			47.7					
50 to 30 mb	49.8			6.4			12.1					
30 to 10 mb	134.1			-5.3			6.6					

* 10^{18} ergs/sec refers to the conversion terms. 10^{25} ergs are the units of energy written in brackets and entered into the spaces provided for the rate of change of energies.

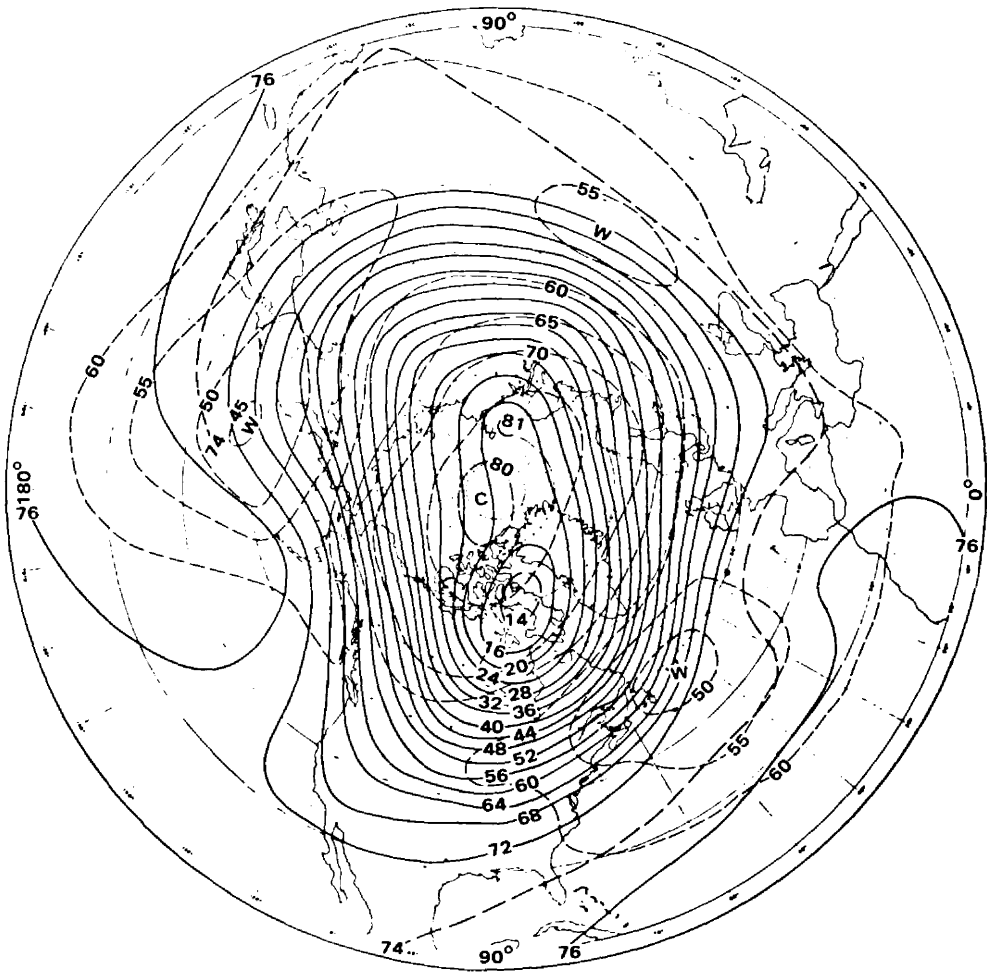


Fig. 3.5 Flow pattern before breakdown of polar vortex, 50-mb chart, Jan. 25, 1957. Contours (full line) in 100's of feet; isotherms (dashed lines) in degrees Centigrade. [From R. J. Reed, J. Wolfe, and H. Nishimoto, *Journal of the Atmospheric Sciences*, 20(4): 262 (1963).]

probably because of the inclusion of summertime conditions when weak easterlies offset the effect of the strong polar-night jet stream. The large negative value of $\langle A_Z, A_E \rangle$ can be produced by conditions during the transition seasons when eddy-transport processes carry heat against the mean temperature gradient. The negative sign of $\langle A_E, K_E \rangle$ also appears to correspond to conditions either after the polar-vortex breakdown or before its establishment. Negative values of G_Z indicate destruction of A_Z by radiative processes. The large values of G_Z also seem to be produced during the transition seasons when the polar regions are warming. Negative

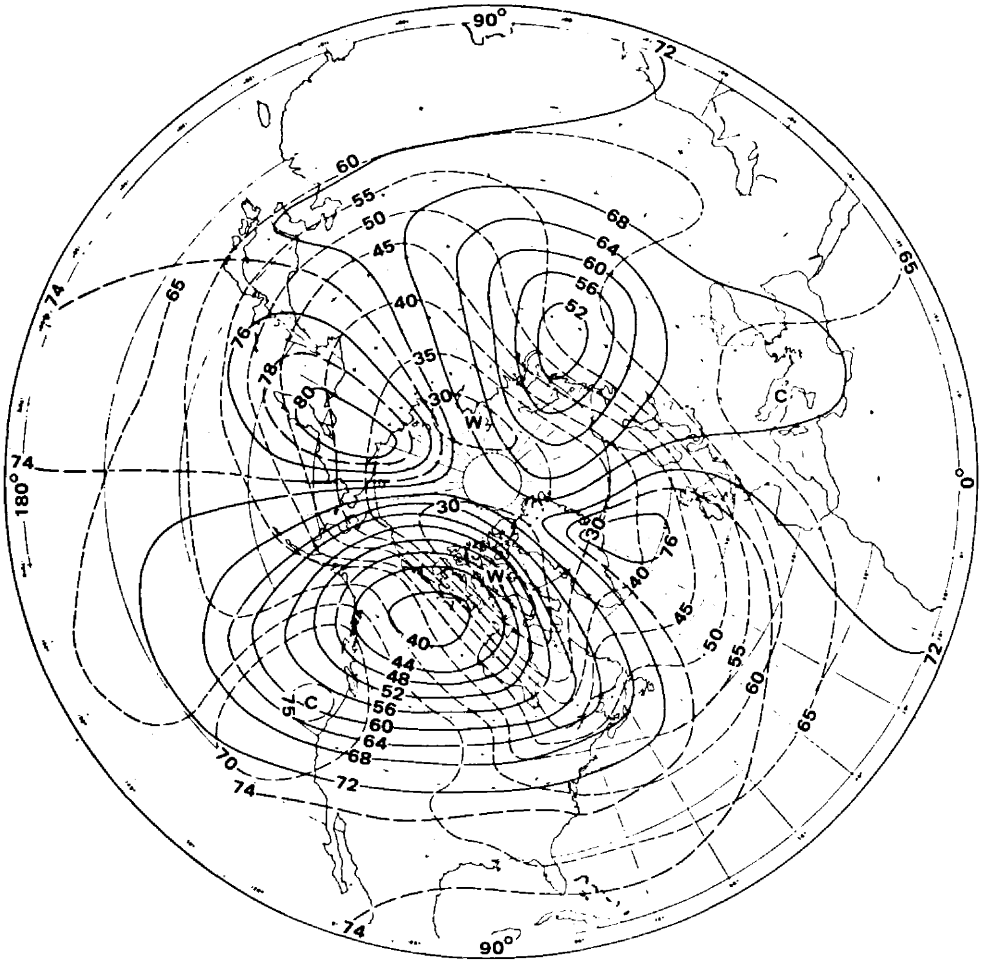


Fig. 3.6 Flow pattern after breakdown of polar vortex, 50-mb chart, Feb. 9, 1957. Contours (full line) in 100's of feet; isotherms (dashed lines) in degrees Centigrade. [From R. J. Reed, J. Wolfe, and H. Nishimoto, *Journal of the Atmospheric Sciences*, 20(4): 264 (1963).]

values of D_E express the action of the tropospheric and high-stratospheric eddies upon the eddy flow in the lower and middle stratosphere. (In Table 3.4, parentheses indicate that numerical estimates are unreliable.)

A recent study by Richards (1967), utilizing IQSY-1965 data, confirms the existence of negative values $\langle A_Z, A_E \rangle$ in the middle stratosphere during part of the year. This indicates that a self-contained source of eddy potential energy is converted into zonal available potential energy in this region. The latter may constitute a significant source of kinetic energy. Richards arrived at the values listed in Table 3.4, which differ considerably from those given by Oort (1964a).

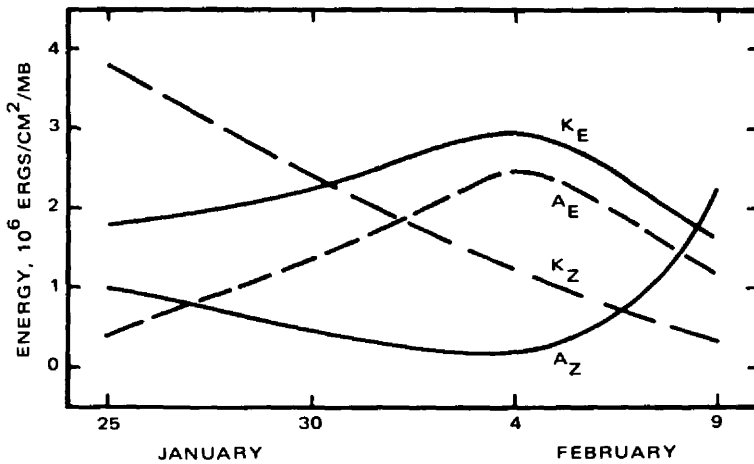


Fig. 3.7 Variations of zonal (A_Z) and eddy (A_E) potential energies and zonal (K_Z) and eddy (K_E) kinetic energies during period Jan. 25, 1957, to Feb. 9, 1957. [From R. J. Reed, J. Wolfe, and H. Nishimoto, *Journal of the Atmospheric Sciences*, 20(4): 265 (1963).]

Mean Vertical Motions in the Extratropical Stratosphere

Energy conversions in the stratosphere are shown in Fig. 3.8 for early 1957. Except for the conversion of K_E into K_Z , all conversion processes reverse their direction between the first and the second part of the warming period (see Table 3.4). During the first 10 days, A_Z fed into A_E (this means that the eddy heat transport was in the direction of the mean meridional temperature gradient), A_E was converted into K_E (sinking cold air and rising warm air in the eddy disturbances), K_E contributed to K_Z (eddy momentum flux directed against the mean meridional wind gradient), and K_Z was converted into A_Z (sinking of warm air and rising of cold air in a meridional plane). The fact that K_Z was converted into A_Z is also evident from Fig. 3.9, which shows zonally averaged vertical motions $[\omega]_{(\lambda)}$ in part b and zonally averaged temperature $[T]_{(\lambda)}$ in part a. Even though the sense of rotation in the vertical plane remains unchanged during the period—maximum downward motion ($\omega > 0$) near 50°N and maximum upward motion ($\omega < 0$) near 70°N —the circulation changes from indirect to direct because of the reversal in the mean meridional temperature gradient (see also Craig and Lateef, 1962; Reed, 1963b). Similar results were obtained by Mahlman (1966) for a stratospheric warming period in January and February 1958 (Fig. 3.10), which was described synoptically by Teweles and Finger (1958). London (1963) studied the same warming period and found good correlation between the migrating center of the “warm pool” and excess amounts of ozone, which suggested a dominant effect of subsidence motion in the stratospheric warming trend.

Results obtained by Anderson (1964) for 1960, Murakami (1965) for 1958, and Perry (1967) for 1963 confirm this vertical-motion pattern. A summary by Teweles

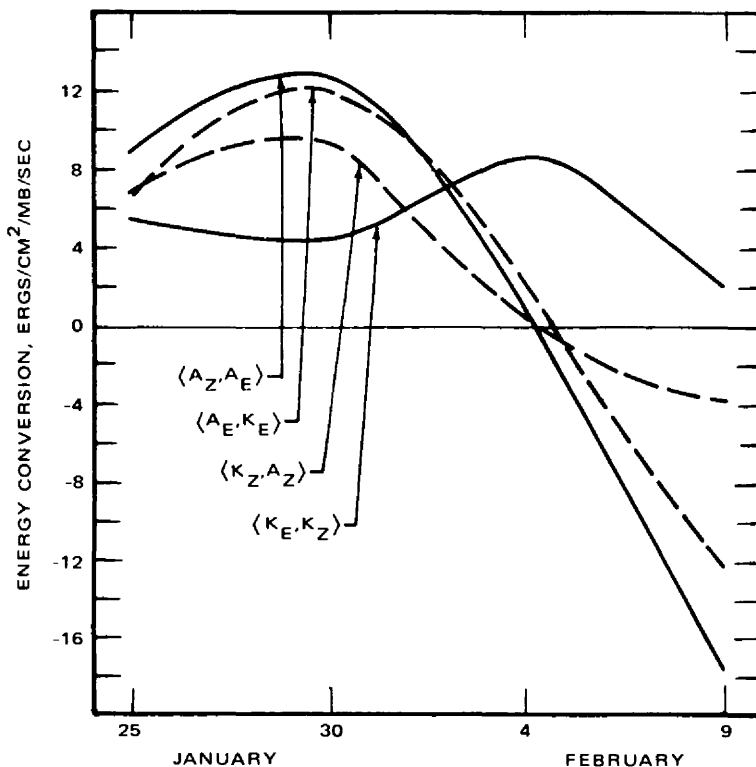


Fig. 3.8 Variations of energy conversions during period Jan. 25, 1957, to Feb. 9, 1957. $\langle A_Z, A_E \rangle$ denotes conversion from zonal potential energy to eddy potential energy, etc. [From R. J. Reed, J. Wolfe, and H. Nishimoto, *Journal of the Atmospheric Sciences*, 20(4): 265 (1963).]

(1964) for the 1957–1958 winter season is shown in Fig. 3.11. According to Murgatroyd (1969), the tropospheric three-cell pattern may extend as high as 20 km, at least during the transition seasons, diminishing in intensity above the tropopause. The “Junge aerosol layer” (see Part 2 of this review, *Chemical Tracers*) near 18 to 20 km probably signifies the transition region between the tropospheric and lower-stratospheric three-cell regime and the upper-stratospheric two-cell pattern. As shown in Fig. 3.12, the zonally averaged temperature gradient reversed during the breakdown period of 1958, as it did in 1957.

Recently Hirota (1967) and Walts (1968) studied the same stratospheric warming period of January–February 1958. Hirota investigated the synoptic movement of the temperature wave associated with the warming trend. He found that during the intensification stage of the warming trend the disturbance propagated upward from the lower to the upper stratosphere. During the subsequent migratory stage, the disturbance traveled westward, in accordance with the findings of Labitzke (1965a, 1965b) shown in Fig. 3.63. Walts (1968) investigated the vertical-motion pattern and

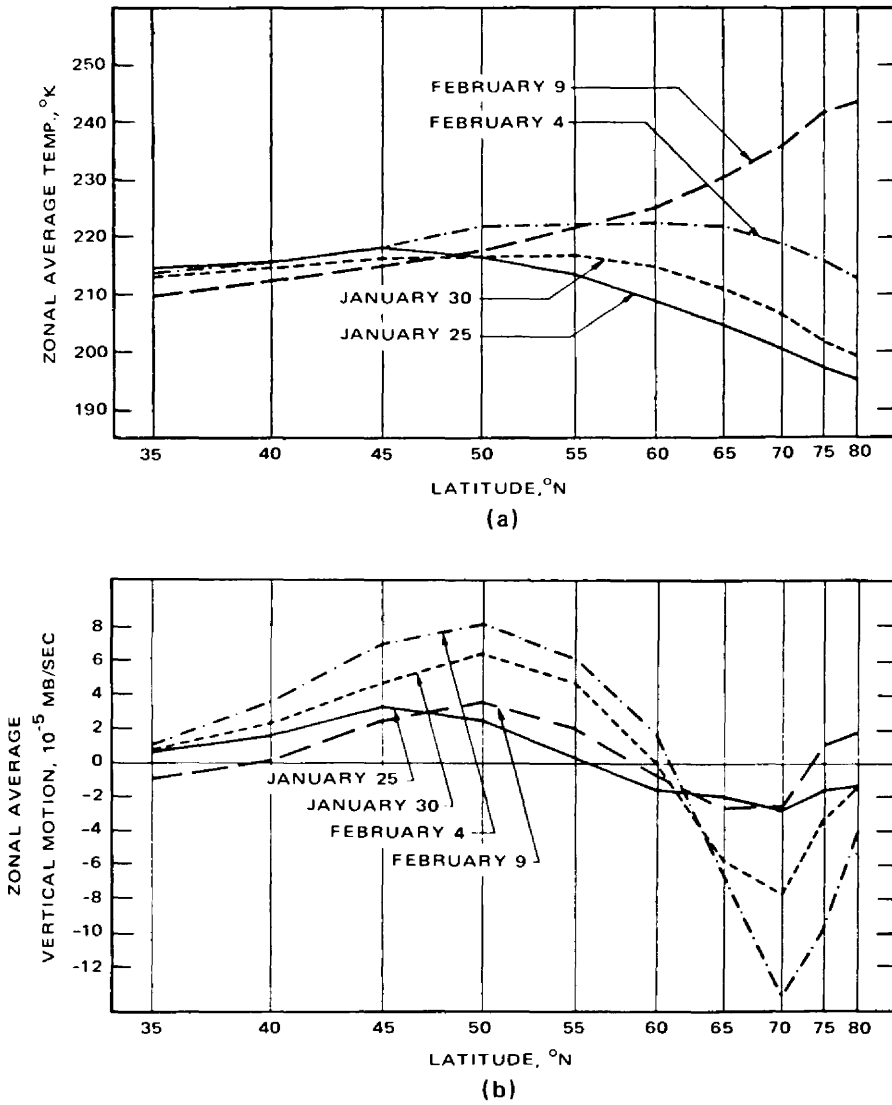


Fig. 3.9 (a) Variation of zonal average temperature with latitude and time at the 50-mb level during the sudden warming of early 1957 and (b) variation of the zonal average vertical motion with latitude at the same pressure level and during the same period. [From R. J. Reed, J. Wolfe, and H. Nishimoto, *Journal of the Atmospheric Sciences*, 20(4): 265 (1963).]

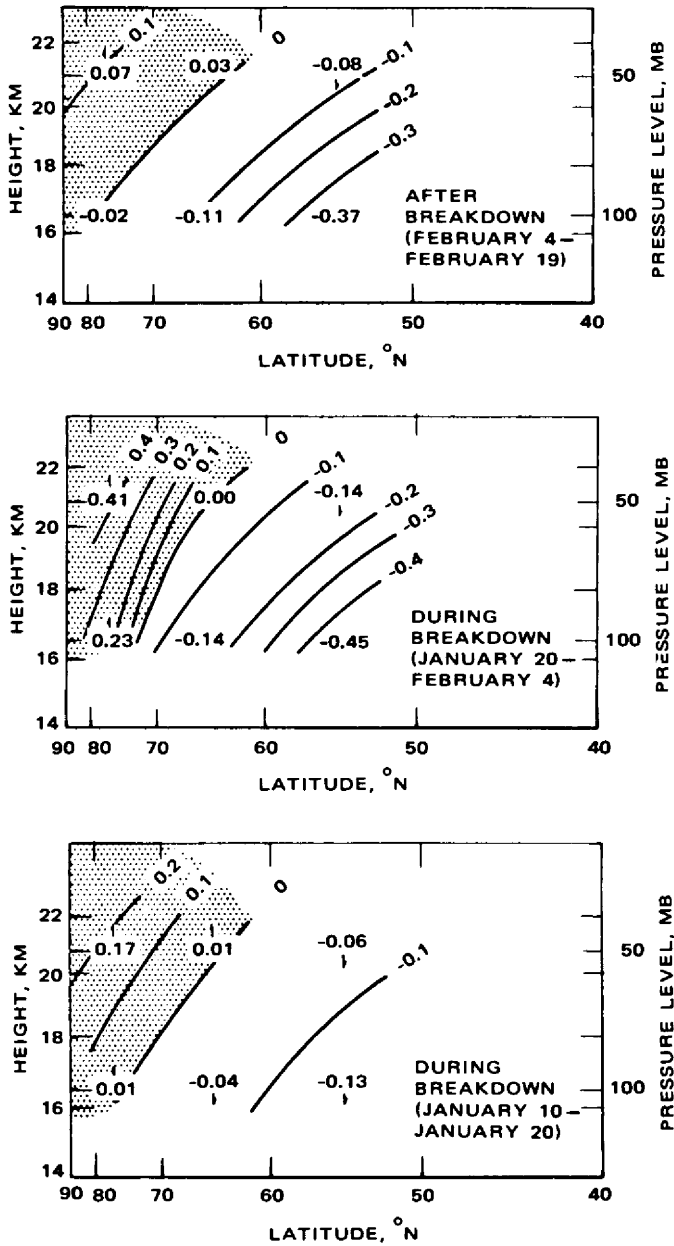


Fig. 3.10 Area-averaged vertical motion, $[w]_{(\lambda, \phi)}$ (km/day), for indicated periods before, during, and after polar-night vortex breakdown of January–February 1958. Hatching denotes area of rising motion. Numerical values are plotted in the centers of the latitude belts, ϕ , of averaging (Mahlman, 1966).

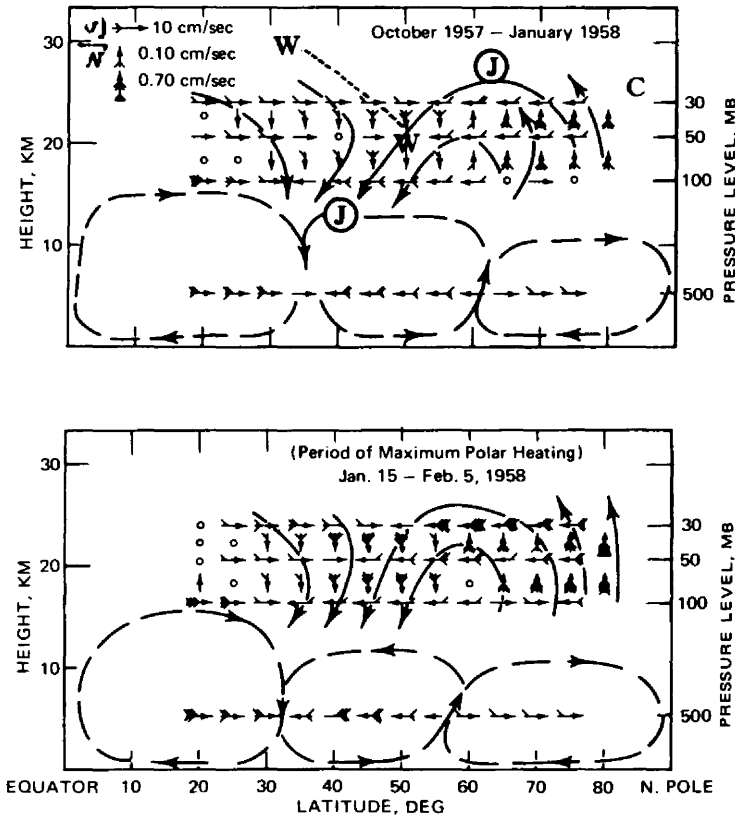


Fig. 3.11 Cross section of time and zonally averaged vertical, $[w]_{(t,\lambda)}$, and meridional, $[v]_{(t,\lambda)}$, wind components. Arrows give schematically the streamlines (not trajectories) of the mean circulation in the meridional plane. C, cold, W, warm. J, jet axis. [From S. Teweles, *Research in Geophysics*, Vol. 2, H. Odishaw (Ed.), p. 513, The Massachusetts Institute of Technology Press, 1964.]

the possible causes of the observed temperature changes in three separate regions of the northern hemisphere, two of them characterized by warming and one by cooling. The long-term temperature changes in these regions are shown in Fig. 3.13. The average temperature change in each of these areas was considered as a result of horizontal advection into the area under consideration and of the effects of adiabatic vertical motions. Results for Areas I, II, and III shown in Fig. 3.13 are given in Fig. 3.14 for the 50-mb surface. The patterns evolving for the 100-mb surface (not shown here) were similar. However, the numerical values, in general, revealed smaller amplitudes. In Fig. 3.14, $[]_{(A)}$ denotes area-averaged values, $()_{(t)}$ denotes departures of the mean value along the boundary of the area under consideration, and v_n is the velocity component normal to the area boundary.

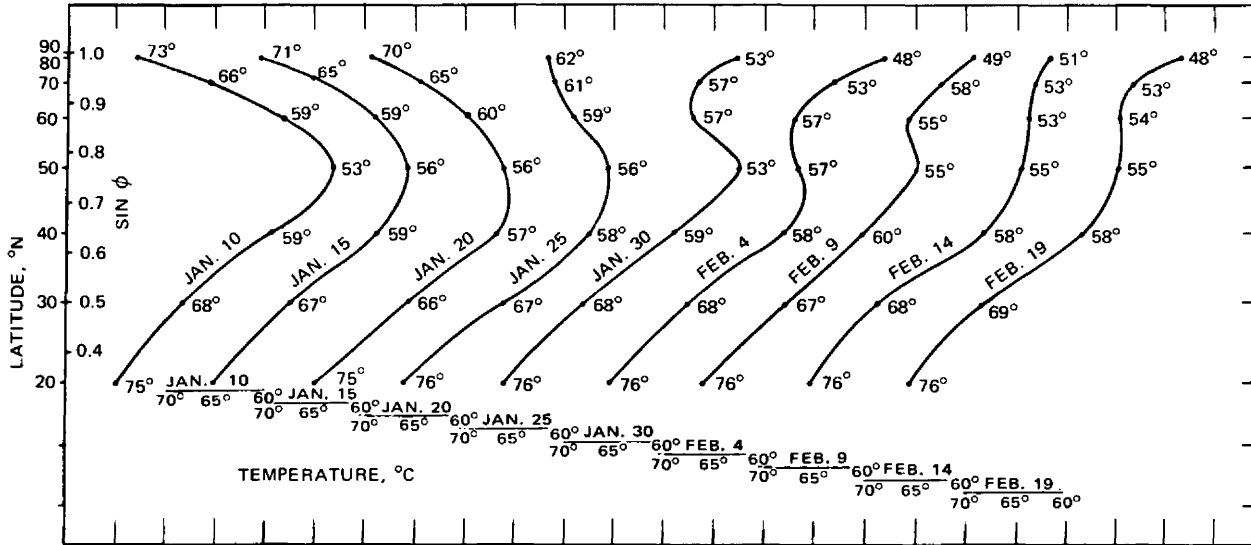


Fig. 3.12 Zonal mean temperatures, $[T](\lambda)$, plotted as a function of sine latitude (ϕ) for 100 mb. Abscissa scale is shifted 10 degrees to the right for each five-day interval. Numerical values of zonal mean temperatures are given at each point (Mahlman, 1966).

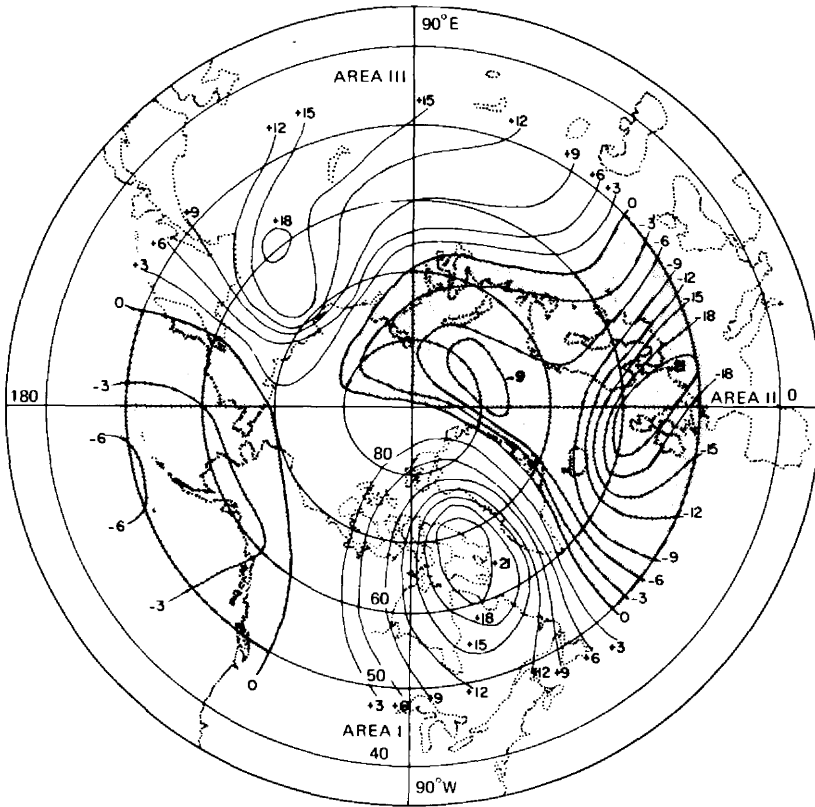
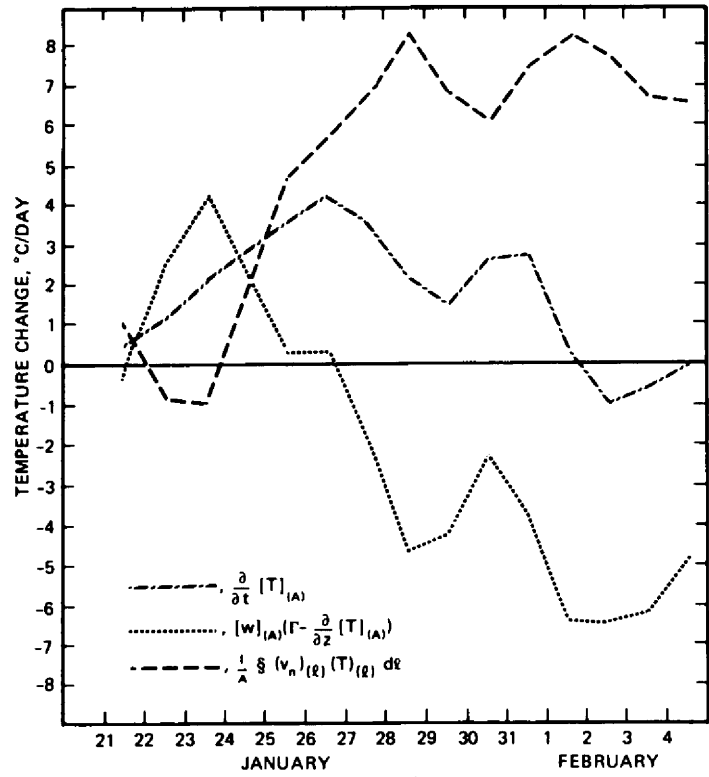


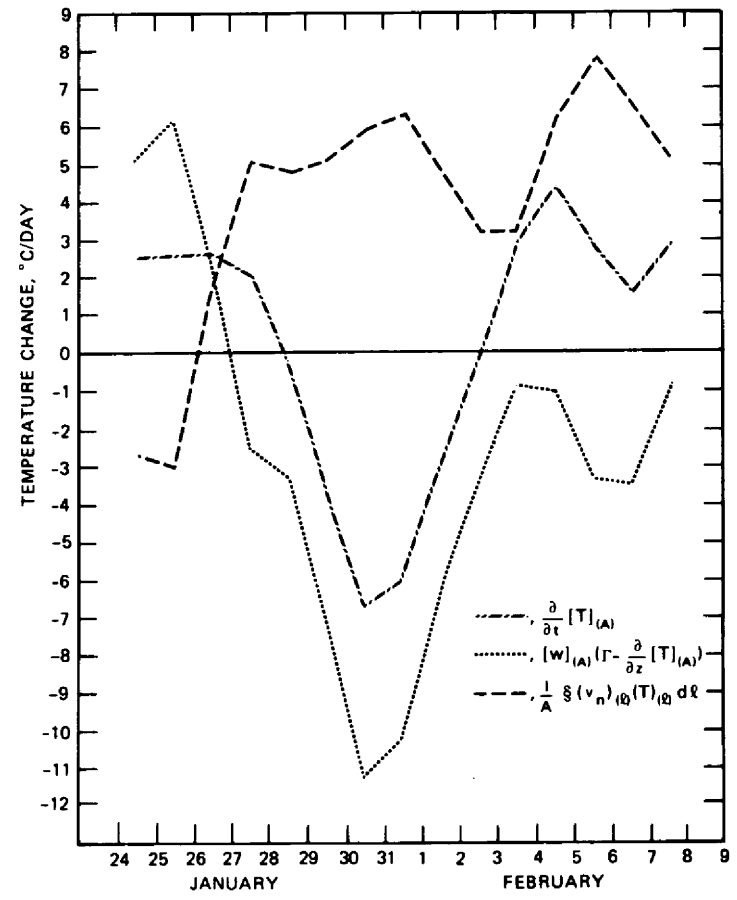
Fig. 3.13 Analysis of temperature change (ΔT) ($^{\circ}\text{C}$) from January 29–February 1, 1958, at 50 mb. Shaded area indicates cooling (Walts, 1968).

The striking result of Walts' investigation is that the main warming trends in Areas I and III do not seem to be caused by prolonged sinking motions, as London (1963) has suggested for hemispheric average conditions. Instead, this warming seems to be mainly resulting from the horizontal eddy flux of heat across the boundaries of the two regions under consideration (see also Anderson, 1964). However, the region of intense "sudden" cooling, which Walts investigated, was mainly caused by rising motions and by adiabatic expansion. The horizontal eddy flux of heat was directed into Area II (positive sign of the flux in part b of Fig. 3.14) even during the period of strongest cooling. The two mechanisms of temperature change—adiabatic vertical motions and horizontal advection—appear to be closely related to each other but tend to offset each other, at least partially, during the period and in the regions investigated by Walts.

The study by Walts (1968) comprised only a few isolated cases of stratospheric temperature changes during 1958 (see also Mieghem et al., 1966). Additional studies



(a)



(b)

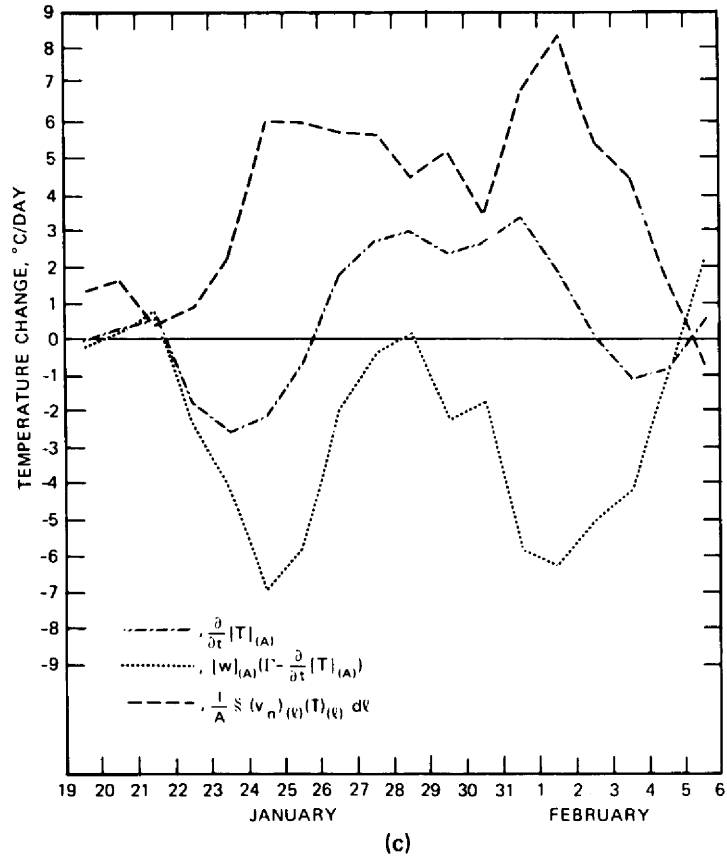


Fig. 3.14 Daily numerical values for mean temperature change, mean vertical flux, and horizontal eddy flux. (a) Area I (50 mb). (b) Area II (50 mb). (c) Area III (50 mb) (Walts, 1968).

will be needed before general conclusions can be drawn. Nevertheless, we will attempt to interpret London's (1963) findings on the correlation between excess amounts of ozone and "warm pools" in the light of Walts' findings: If horizontal heat advection imported from low latitudes is mainly responsible for the warming trend, ozone-rich air imported from tropical latitudes can cause the observed rise of ozone concentration in the warming regions (see also Part 2 of this review, *Chemical Tracers*). The strong ascending motions observed by Walts in the cooling region would tend to cause a negative departure of total ozone observed in this area, especially since the horizontal advection fails to offset the effect of these rising motions.

The area- and time-averaged vertical motions, $[w]_{(A,t)}$, computed by Walts (1968) for the regions indicated in Fig. 3.13 are shown in Fig. 3.15. In general, again, the ascending motions over the polar regions evolve from this study, which other investigators have commented on. However, in the regional treatment of these motions made by Walts, the "two-cell" structure of the stratospheric circulation (see p. 69) is not as clear cut as in hemispheric-average presentations. Since Walts' treatment of the stratospheric circulation problem filters out the large-scale eddy effects (by considering several of these large eddies individually), it is concluded that the stratospheric "two-cell structure" is—at least in part—simulated by these large-scale eddies. Miyakoda (1963) and Sekiguchi (1963) have published energy-flux data for the same stratospheric warming period of 1958 (see Table 3.4). Miyakoda's data cover the period Jan. 15 to 23, 1958, and the layer 189 to 9 mb. In his computation of $\langle K_E, K_Z \rangle$, he included terms that involve the mean meridional circulation. Computations by Sekiguchi (1963) were made on the 50-mb surface for the period Jan. 15 to 25, 1958. The presence of an indirect meridional circulation, found by Mahlman (1966), is confirmed by the calculations by Miyakoda (1963) and also by Julian and Labitzke (1965).

If diabatic effects were considered in the preceding computations, they would tend to increase the estimate of vertical motions in the indirect-circulation cell at high latitudes since, according to Manabe and Möller (1961), the stratosphere near the 50-mb level receives a net radiative heating south of 35°N and a cooling at higher latitudes.

Mean Vertical Motions in the Tropical Stratosphere

As indicated in Fig. 3.11 and by mass continuity, upward motion must exist in tropical regions of the stratosphere. This would suggest a two-cell structure of the meridional circulation in the winter stratosphere, with ascending motions near the equator and at high latitudes and descending motions in the warm belt of middle latitudes (see also Tucker, 1959; Barnes, 1963; Dickinson, 1962). This pattern is significantly different from the single-cell scheme suggested by Kellogg and Schilling (1951), with rising motion in the stratosphere over the summer pole and sinking over the winter pole, nor does it conform to the earlier model by Faust (1963a, 1963b, 1963c), who postulated rising motion over the equator and sinking motion over the

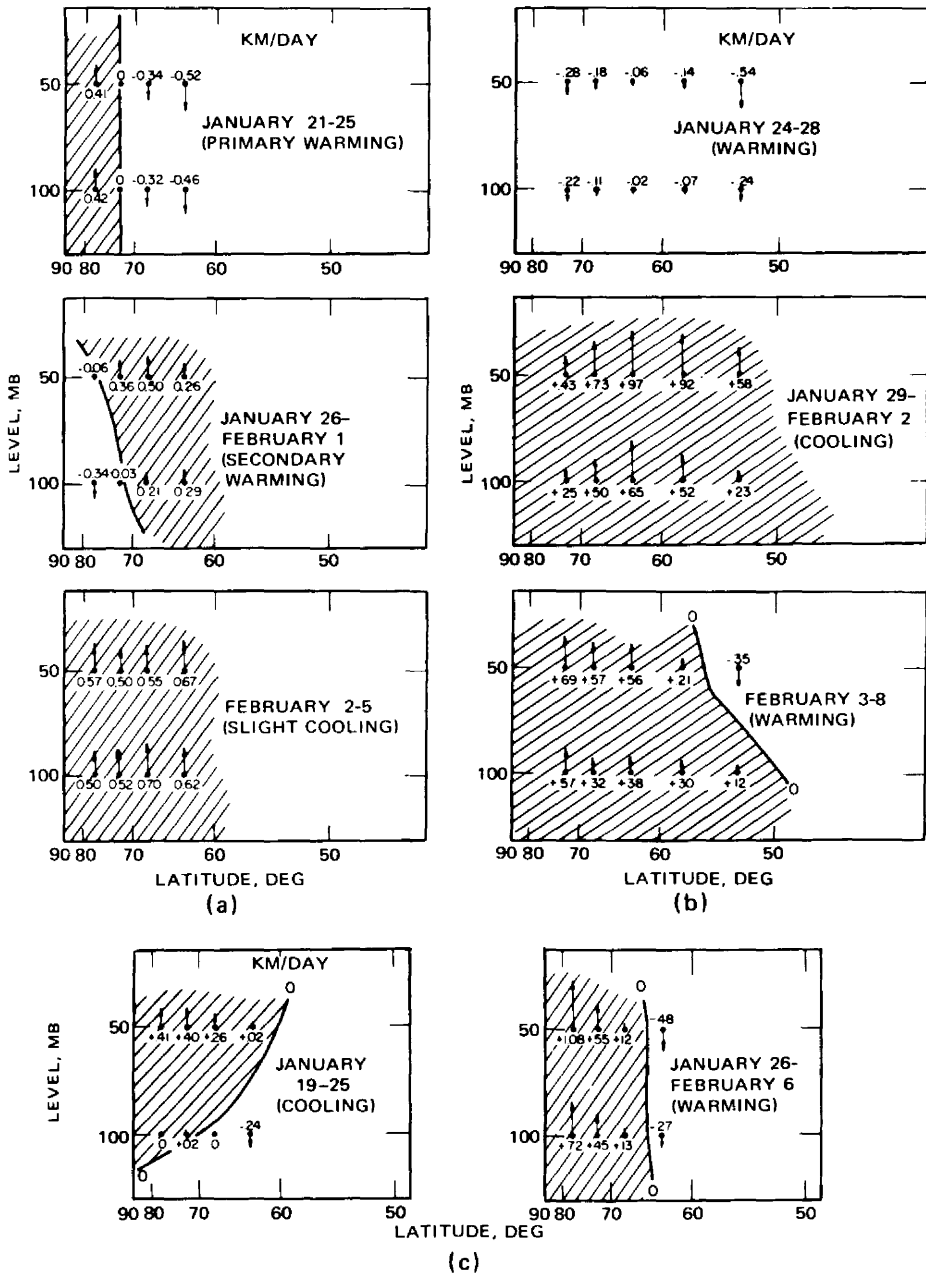


Fig. 3.15 Area- and time-averaged vertical motion, $[w](A,t)$, for dates indicated. (a) Area I. (b) Area II. (c) Area III. Shaded area indicates rising motion (Walts, 1968).

pole in the upper troposphere and the inverse pattern in the stratosphere between approximately 20 and 60 km height (see also Faust, 1961; Faust and Attmannspacher, 1961). Faust (1967) later revised his schematic model of atmospheric layers to include the two-cell structure described previously.

From momentum-balance requirements, Tucker (1964) concluded that upward vertical velocities over the equator should reach a maximum (0.04 cm/sec, or 35 m/day at 17 km) just above the tropopause. Above 19 or 20 km, a downward motion is required for momentum balance (maximum value 0.05 cm/sec, or 43 m/day at 23 km). This vertical velocity agrees with the assumed rate of descent of the velocity patterns in the 26-month oscillation that will be described later. The reversal of vertical motions near 20 km would agree with the model by Brewer (1949) for the vertical distribution of water vapor (see also Newell, 1963a) and with vertical ozone distributions reported by Griggs (1963) and Hering (1963).

The model by Reed (1964) of vertical motions in the tropical stratosphere (Fig. 3.16) confirms conclusions by Tucker (1964) only partially. The conclusions by Tucker hold for the time at which the easterly wind maximum is located near 20 km and the westerly wind maximum near 30 km. The downward shift of these maxima in the course of the biennial oscillation concurs with a shift of the levels at which vertical motions reverse their sign. Wallace and Newell (1966) voiced some criticism to Reed's circulation model, which may entail adjustments in the circulation model shown in Fig. 3.16. More details on the quasi-biennial oscillation in the tropical stratosphere will be given later in this chapter.

The Two-Cell Structure of the Stratosphere

The two-cell structure of the middle and upper stratospheric circulation described previously must be considered as an effect of eddy-transport processes [see earlier remarks on Walts (1968)]. Murgatroyd and Singleton (1961, 1962) have shown that a single meridional cell would result in the stratosphere (rising at the equator and sinking at both poles) if a mean meridional circulation alone were held responsible for the heat transport between radiation sources and sinks (see also Murgatroyd and Goody, 1958; Murgatroyd, 1957; Ohring, 1958; Sawyer, 1965). In the mesosphere (55 to 80 km), such a postulated mean meridional circulation would show rising over the summer pole and descent over the winter pole.

From Fig. 3.5 and from the foregoing discussion, it is evident that the effects of a mean meridional circulation are strongly overshadowed by the presence of planetary eddies. According to Molla and Loisel (1962) and Miller (1967), eddy transports in the layer 100 to 50 mb are such that northward-moving air subsides and southward-moving air rises. Such eddy motions would agree with the observed northward transport of ozone (Martin, 1956; Newell, 1961). Both standing and transient eddies (for definition, see p. 20) appear to have the same sign in the correlation between vertical-motion and meridional-motion components, although, according to Miller (1967), the transport patterns generated by standing eddies appear to be less regular

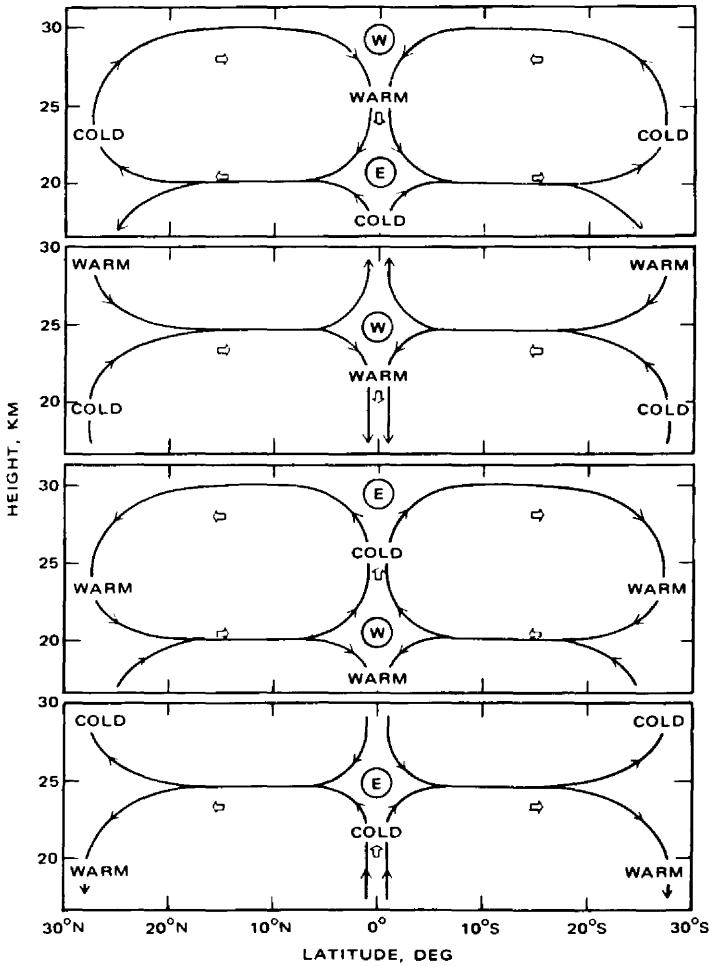


Fig. 3.16 Schematic model of the 26-month oscillation. E and W indicate locations of cores of easterly and westerly currents, respectively. Regions of warm and cold anomalies are marked appropriately. Arrows give directions of meridional circulations. The blocks and discrete arrows are located at points where the temperature and velocity components are maximums (or minimums) in time but not necessarily in space. [From R. J. Reed, *Quarterly Journal of the Royal Meteorological Society*, 90(386): 461 (1964).]

than the ones produced by transient eddies. The transport patterns generated by transient eddies reveal a poleward transport of conservative atmospheric properties from the equator to about 50°N, with a late winter maximum of transport appearing at the 45-mb level but not at the 75-mb level. This maximum is significant when considering the observed spring maxima of ozone and of radioactive fallout. Below 100 mb northward flow is associated with rising motion (Molla and Loisel, 1962).

A schematic model developed by Doporto (1964) is in disagreement, however, with the findings by Molla and Loisel. Doporto divides the atmosphere into quasi-horizontal "slabs" separated by "null layers." In the null layers the vertical velocity is assumed to be zero (these null layers correspond to the location of isopycnic levels). The horizontal slabs are subdivided into cells of sinking and rising motions. The sinking motions in the lower and middle troposphere to the rear of a cyclone and in a high-pressure ridge are superimposed by cells of rising motion between the upper tropospheric isopycnic level at approximately 8 to 10 km and another such level characterized by minimum horizontal winds near 18 km. Above this level and throughout the upper stratosphere, sinking motion again is superimposed over the low tropospheric subsidence region. Analog conditions are assumed to hold for regions with low tropospheric rising motions. Thus southward flow in the lower troposphere and in the stratosphere would be correlated with sinking motion. In my opinion more credence should be given to the results presented by Molla and Loisel (1962), which show an opposite correlation in the stratosphere above 100 mb, since their conclusions are based on sound observational evidence.

The two-cell structure of the stratosphere, although it appears to be characteristic of the stratospheric warming periods, does not seem to prevail throughout the year. Murgatroyd (1969) has shown that a three-cell pattern exists in the lower stratosphere during the transition seasons (see p. 60). Analyses of the mean meridional circulation for the IGY period indicate the presence of a three-cell pattern, at least through part of the year (Oort, 1964d), although the third cell [sinking over the equator and rising near 15°N, deduced from a convergence in the mean meridional circulation near the latter latitude] appears to be very weak. From the analysis by Oort (1964d), it is also interesting to note that the mean motion, $[v]_{(\lambda,t)}$, at 50 to 30 mb is directed toward the south in the yearly average except for latitudes greater than 70°N. The observed northward transport of ozone from equatorial regions, therefore, must be accomplished by eddy processes.

Stream Function and Velocity Potential

One of the problems in dealing with stratospheric flow patterns is how to obtain horizontal and vertical winds from sparse data. In estimating horizontal wind components, Julian and Labitzke (1965) use a modified stream function defined as

$$\nabla^2 S = \nabla \cdot \left(\frac{\nabla Z}{f} \right) \quad (3.49)$$

where Z denotes geopotential height. Table 3.4 contains only these stream-function estimates of energy transformations. (For systematic errors in geostrophic estimates of such transformations, see Bjerknes, 1960.)

Following Wiin-Nielsen (1964), vertical motions were computed adiabatically by Julian and Labitzke using the equation

$$\omega_a = \frac{\left(\frac{\partial T}{\partial t} + \mathbf{v} \cdot \nabla T\right)}{\left(\frac{\alpha}{c_p} - \frac{\partial T}{\partial p}\right)} \quad (3.50)$$

and the so-called “omega equation”

$$\nabla^2 \omega + \frac{f^2}{\sigma} \frac{\partial^2 \omega}{\partial p^2} = \frac{f}{\sigma} \left(\frac{\partial}{\partial p} \mathbf{v} \cdot \nabla Q - \nabla^2 \mathbf{v} \cdot \nabla \frac{\partial S}{\partial p} \right) \quad (3.51)$$

where Q is the absolute vorticity, $\sigma = \alpha(\partial \ln \theta)/\partial p$ is the static stability, and S is the stream function defined by Eq. 3.49.

By comparing the differences in mass transport resulting from Eqs. 3.50 and 3.51, the diabatic generation term, G_Z , could be estimated.

Wippermann (1957) proposed another treatment by considering the stream-function portion (ψ) and the velocity-potential portion (χ) of the flow. The horizontal wind vector \mathbf{v} can be defined as

$$\mathbf{v} = \mathbf{k} \times \nabla \psi + \nabla \chi \quad (3.52)$$

where \mathbf{k} is a unit vector along the vertical coordinate. From this he derives the transformation equation

$$\frac{\partial}{\partial t} [A]_{(F,p)} = [\nabla \chi \nabla \Phi]_{(F,p)} + [dh]_{(F,p)} \quad (3.53)$$

averaged over the surface of the earth, F , and over pressure. The term A contains both potential and internal energy, Φ is the geopotential, and dh is the nonadiabatic heat supply. According to Eq. 3.52, the relative vorticity is

$$q = \nabla^2 \psi \quad (3.54)$$

and the divergence is

$$D = \nabla^2 \chi \quad (3.55)$$

With these expressions Wippermann (1957) arrives at separate energy changes of the divergent and the rotational part of the flow in the form:

$$\frac{\partial}{\partial t} \left[\frac{(\nabla\psi)^2}{2} \right]_{(F,p)} = - [(f + \nabla^2\psi)\nabla\chi\nabla\psi]_{(F,p)} - \left[\nabla^2\chi \frac{(\nabla\psi)^2}{2} \right]_{(F,p)} - \left[\omega\mathbf{k} \left(\nabla\psi \times \nabla \frac{\partial\chi}{\partial\mathbf{p}} \right) \right]_{(F,p)} \quad (3.56)$$

$$\frac{\partial}{\partial t} \left[\left(\frac{\nabla\chi}{2} \right)^2 \right]_{(F,p)} = - [\nabla\chi\nabla\Phi]_{(F,p)} + [(f + \nabla^2\psi)\nabla\chi\nabla\psi]_{(F,p)} + \left[\nabla^2\chi \frac{(\nabla\psi)^2}{2} \right]_{(F,p)} + \left[\omega\mathbf{k} \left(\nabla\psi \times \nabla \frac{\partial\chi}{\partial\mathbf{p}} \right) \right]_{(F,p)} \quad (3.57)$$

From Eqs. 3.53, 3.56, and 3.57, it follows that

$$\frac{\partial}{\partial t} \left\{ [A]_{(F,p)} + \left[\frac{(\nabla\psi)^2}{2} \right]_{(F,p)} + \left[\frac{(\nabla\chi)^2}{2} \right]_{(F,p)} \right\} = [dh]_{(F,p)} \quad (3.58)$$

This means that the total energy of the earth's atmosphere changes only by the amount of mean diabatic heat added or subtracted. It follows, furthermore, that mean potential energy is transformed only in mean nonrotational (divergent-flow) kinetic energy. The latter, then, may be transformed into divergence-free (rotational) kinetic energy. This transformation appears to find more favorable conditions in cyclones ($\nabla^2\psi > 0$) than in anticyclones ($\nabla^2\psi < 0$), according to the first term on the right side of Eq. 3.56 (assuming equal magnitudes of f , $\nabla\psi$, and $\nabla\chi$ in cyclones and anticyclones).

Stratospheric—Tropospheric Interrelations

An interesting case of stratospheric warming, that of Jan. 25, 1963, to Feb. 4, 1963, was studied in detail by Julian and Labitzke (1965) (see also Warnecke, 1966; Webb, 1966; Perry, 1967). The synoptic events of this case have been described by Finger and Teweles (1964).

The patterns of mean meridional temperature profiles during this period follow very closely the ones described by Reed, Wolfe, and Nishimoto (1963) and by Mahlman (1966): The meridional temperature gradient, at first directed toward the pole, reverses after the polar vortex breaks down (Fig. 3.17). Mean vertical motions also reveal the two-cell structure of the stratospheric circulation mentioned previously, with an indirect cell at high latitudes. Tropospheric conditions in this diagram show the indirect Ferrel cell of middle latitudes and the direct cell of polar regions underneath the stratospheric indirect cell (see Fig. 3.11 for comparison). The tropical Hadley cell is not evident from the data presented in Fig. 3.17. It should be located underneath the direct stratospheric cell inferred from continuity considerations. Theoretical derivations of a forced meridional circulation by Kuo (1956) are, at least partially, substantiated by these actual observations.

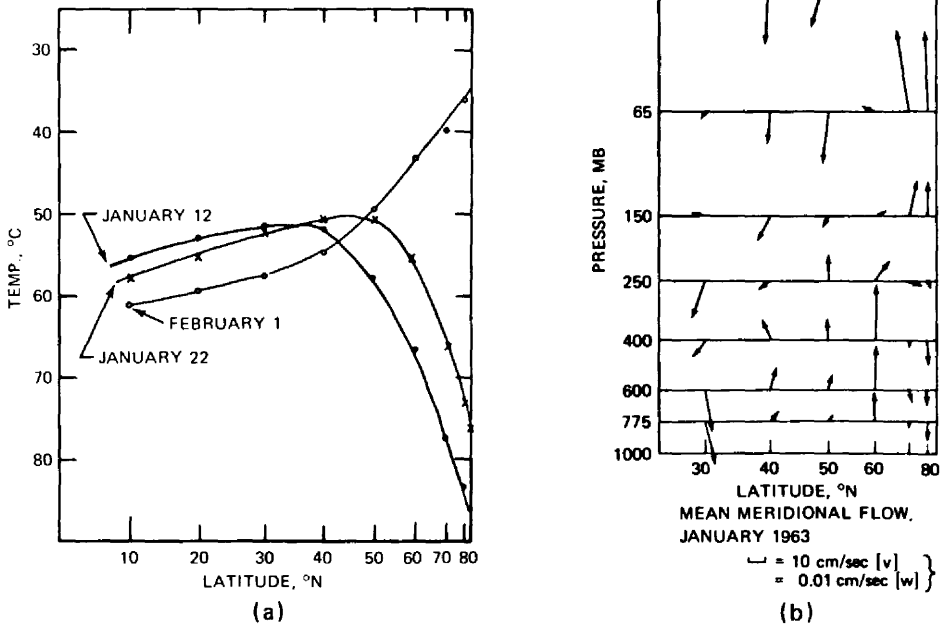


Fig. 3.17 (a) Zonally averaged 30-mb temperature shown as a function of the sine at the latitude for three selected days and (b) mean meridional circulation for January 1963 obtained by the application of the continuity equation to the solution of the omega equation. Vertical exaggeration, 1000 : 1. [From P. R. Julian and K. B. Labitzke, *Journal of the Atmospheric Sciences*, 22(6): 601; 607 (1965).]

Maximum eddy kinetic energy is reached before the reversal of the meridional temperature gradient takes place, as shown in Fig. 3.18 (compare with Fig. 3.7). The transport processes, again, reveal significant differences before and after the warming period (Fig. 3.19) (compare with Fig. 3.8).

Julian and Labitzke compared conditions in the stratosphere with those in the troposphere. The results are summarized in Fig. 3.20. Subscript "g" refers to geostrophic estimates of the horizontal wind components and subscript "s" refers to estimates using the modified stream function, S, defined by Eq. 3.49. Julian and Labitzke (1965) used objectively analyzed charts prepared on a routine basis by the National Meteorological Center (NMC) as basis for their tropospheric data. Recently, Hayden and Wiin-Nielsen (1968) pointed out that the objective analysis system used at NMC before 1965 contained inconsistencies that may lead to exaggerated values of the absolute values of wind components. This error is carried over into mean zonal wind speeds and into momentum transport estimates. In my opinion, such errors will have no drastic effect on the findings by Julian and Labitzke.

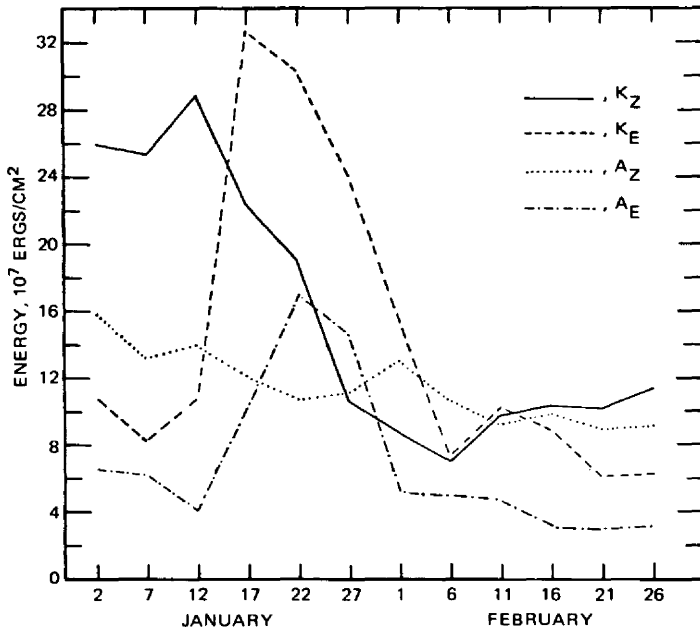


Fig. 3.18 Time variation of stratospheric zonal (K_Z) and eddy (K_E) kinetic and zonal (A_Z) and eddy (A_E) available potential energy for January–February 1963. [From P. R. Julian and K. B. Labitzke, *Journal of the Atmospheric Sciences*, 22(6): 600 (1965).]

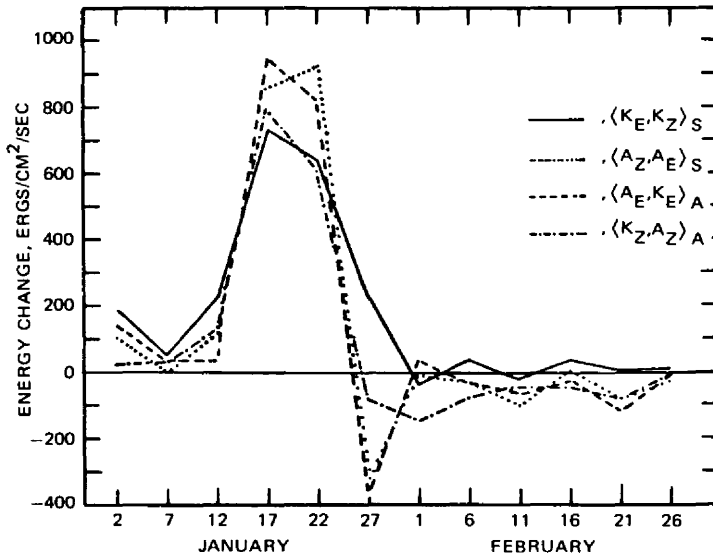


Fig. 3.19 Time variation of the stratospheric energy-transfer and energy-conversion processes, indicated as positive for January–February 1963. [From P. R. Julian and K. B. Labitzke, *Journal of the Atmospheric Sciences*, 22(6): 600 (1965).]

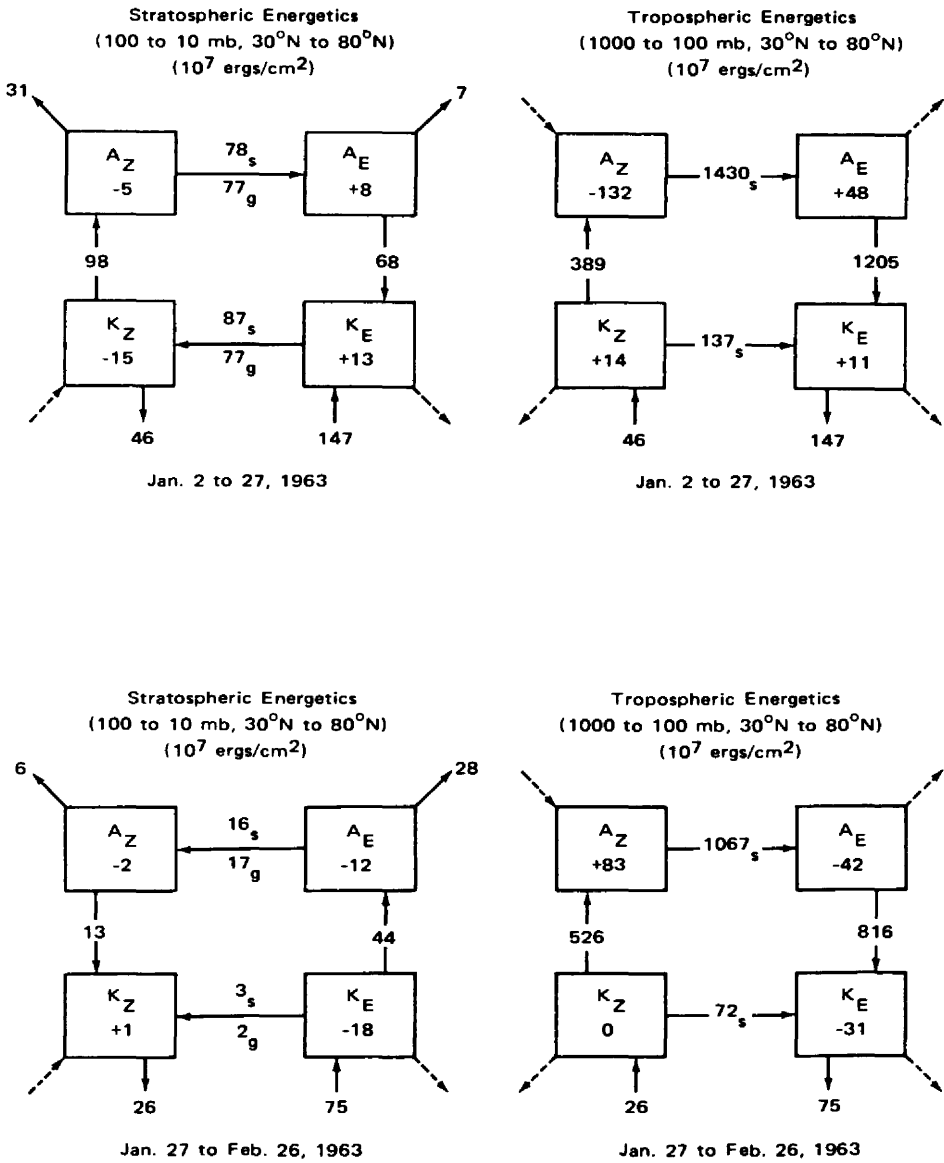


Fig. 3.20 Energy flow diagram for layers and periods as indicated. Arrows indicate total energy converted or transferred in the interval given by integration of energy exchange rates. Actual energy changes estimated from conditions on January 2 and 27 are shown in the boxes. Arrows projecting from the corners of the boxes represent generative or dissipative processes. The values of the surface boundary integrals representing the net vertical flux of kinetic energy are entered beneath the kinetic-energy boxes. Dashed arrows are inferred from balance requirements. [From P. R. Julian and K. B. Labitzke, *Journal of the Atmospheric Sciences*, 22(6): 601; 603 (1965).]

As in the computations by other authors mentioned previously, the stratosphere loses A_Z by radiative processes ($G_Z < 0$) because warm air to the south radiates more than cold air near the pole. (More about these radiative processes will be discussed on p. 125.) This loss of G_Z is considerably smaller after the vortex breakdown. Julian and Labitzke attribute the net loss of A_Z by radiative processes to integration over pressure, which was performed in arriving at the given results: Even though a net generation of A_Z occurs at levels above 25 to 30 km, the presence of a warm belt in middle latitudes in the more massive lower stratosphere—even after the warming—produces a net loss of A_Z when integrating between 100 and 10 mb.

The energy transformations and changes (see Fig. 3.20 and Table 3.4) again indicate—even more strikingly than the results by Reed et al. (1963)—that the stratospheric circulation is to a considerable degree influenced by eddy processes in the troposphere. This is expressed by the dominantly large (negative) values of D_E , which are produced mainly by upward flux of K_E through the 100-mb surface. This fact would render the lower and middle stratosphere a “steered” rather than a “steering” layer (see also Newell, 1963b, and theoretical work by Mieghem, 1963, who also provides a survey of literature on upward wave energy flux in the atmosphere). According to Charney and Drazin (1961), an atmospheric “index of refraction” for wave perturbations can be defined, which depends on the speed of the basic current, vertical wind shear, wave number, latitude, stability, and scale height. If this index is real, internal waves and vertical-energy propagation are possible. If it is imaginary, the waves are external, they will be reflected at the controlling layer, and vertical-energy propagation through this layer will be inhibited (see also Boville, 1963). According to Dickinson (1969), upward propagation of planetary-wave energy is enhanced during winter and is greatly attenuated during the equinoxes. The implications of these findings on long-range weather forecasting have yet to be explored.

Conditions in the troposphere (defined as the layer between 1000 and 100 mb) during the two January periods investigated by Julian and Labitzke (1965) are also given in Fig. 3.20 and Table 3.4. Part of these data for January 1963 have been given by Wiin-Nielsen, Brown, and Drake (1964). Since the region under consideration is bounded by the latitude circle 30°N , the influence of the direct meridional circulation in the Hadley cell is not included in these diagrams. It would have reduced the large positive value of $\langle K_Z, A_Z \rangle$. These data show that the vertical energy fluxes, as expressed by the boundary terms D_E and D_Z , represent relatively small items in the energetics of the troposphere, whereas in the stratosphere they become rather dominant. These terms produce a certain coupling effect between tropospheric and stratospheric circulations. Such coupling appears to exist also during stratospheric warming epochs. It seems to influence the eccentricity of the tropospheric polar vortex (wave No. 1) (Julian, 1965). See Chap. 4 for a discussion of processes in the wave-number space.

Energy Fluxes Above the Middle Stratosphere

Conditions in the higher atmosphere are not yet firmly established because of the sparsity of data. Newell (1963b) attempted first estimates of G_Z , A_Z , and K_Z ,

averaged for winter and summer, respectively, mainly from Meteorological Rocket Network data. From these rather crude data, he arrived at the following conclusions:

1. The layer between 30 and 60 km seems to be able to run on its own supply of energy during winter without the benefit of energy advection from below. This is in agreement with theoretical considerations by Charney and Drazin (1961) (see also Charney and Pedlosky, 1963). The layers between 60 and 80 km appear to need advection of energy, presumably from below, to supply their kinetic energy.

2. The eddy disturbances transport heat and relative angular momentum poleward in the region 30 to 60 km and are responsible for the formation of the high-level jet stream. Eddy kinetic energy seems to feed into the mean zonal kinetic energy at a rate that is about the same as the rate at which the eddy kinetic energy is generated. Eddy transport also appears to be responsible for the relatively high mesospheric temperatures in winter. Available potential energy is generated in this layer by radiation processes ($G_z > 0$). Chemical processes, such as the recombination of oxygen atoms, and descending motions from the lower ionosphere should be considered in explaining relatively high mesospheric temperatures near 80 km during the polar night (Kellogg, 1961; Haurwitz, 1961; Newell, 1964c; Maeda, 1963).

Estimates of frictional effects have the right magnitude to account for mass convergence and divergence associated with such vertical motions (Haurwitz, 1961). The meridional component of flow that results from the frictional effects in the zonal wind can be expressed by

$$v = \frac{1}{f} \frac{\mu}{\rho} \frac{\partial^2 u_g}{\partial z^2}$$

where u_g is the geostrophic wind produced by the meridional pressure gradient. The observed distributions of the curvature of the zonal wind profiles, which enters the preceding expression, are shown in Fig. 3.21, and the resulting frictionally induced portion of the mean meridional circulation is given schematically in Fig. 3.22.

According to Roper and Elford (1963), frictional dissipation of kinetic energy at heights of 70 to 110 km, as determined from meteor-trail observations, undergoes diurnal variations as well as a marked seasonal change. Thus, for instance, over Adelaide, Australia, turbulent dissipation appears to be strongest during March and September and weakest during May and November.

3. The heat and momentum budgets appear to be dominated by eddy processes rather than by meridional circulations as previously suggested.

4. If the northern hemispheric winter and summer conditions presented by Newell (1963b), mainly on the basis of North American and Pacific data, are assumed to be representative for the whole globe, there should be a quasi-horizontal flux of heat and relative angular momentum across the equator from the summer to the winter hemisphere in the 30- to 60-mb layer if this layer were indeed energetically independent from the lower atmosphere. Newell's (1963b) rocket data were probably biased by tidal effects. More about these effects will be presented in Part 2 of this review, *Chemical Tracers*.

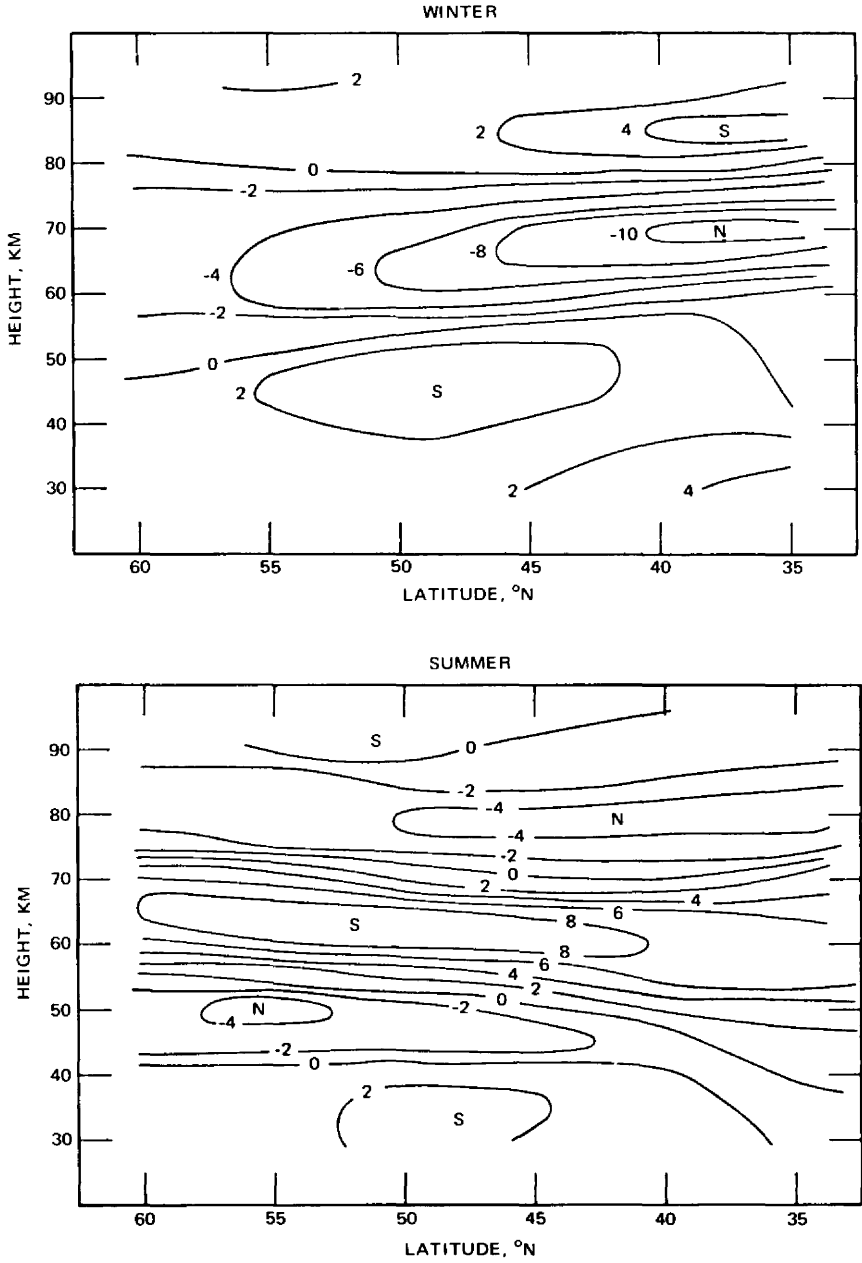


Fig. 3.21 Meridional distribution of the curvature of the vertical zonal wind profile (4×10^{-10} /cm/sec), with $\nu = 10^7$ cm²/sec and $f = 10^{-4}$ /sec, corresponding to a meridional velocity of 40 cm/sec (f is the Coriolis parameter and $\nu = \mu/\rho$ is the kinematic viscosity). Positive and negative values imply a frictional wind component to the south and north, respectively. [From B. Haurwitz, *Journal of Geophysical Research*, 66(8): 2386; 2387 (1961).]

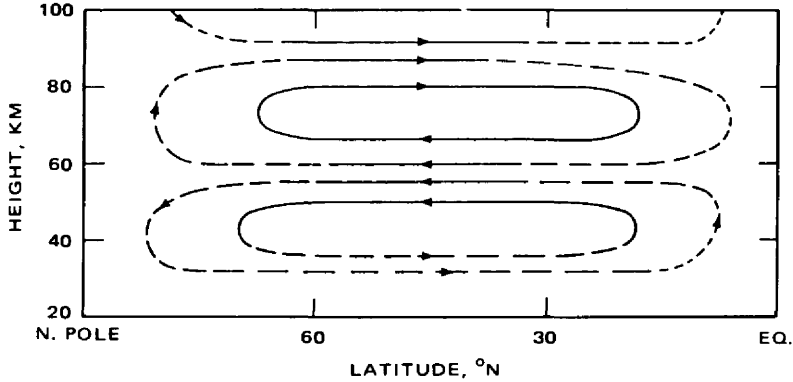


Fig. 3.22 Schematic diagram of meridional circulation in winter. [From B. Haurwitz, *Journal of Geophysical Research*, 66(8): 2388 (1961).]

More sophisticated measurements hopefully might shed additional light on the energetics of the high atmosphere.

Circulations in the Stratosphere and Mesosphere Derived from Heat Transport

Studies of sources and sinks of radiative energy between 30 and 100 km by Murgatroyd and Goody (1958) and by Ohring (1958) were used by Murgatroyd and Singleton (1961) as a basis for estimating the meridional circulation necessary to maintain the mesospheric and stratospheric temperature distributions. The results are shown in Fig. 3.23.

The fact that the one-cell circulation pattern of the stratosphere, shown in this figure for midsummer and midwinter, is not substantiated from actual wind data has already been discussed. As mentioned previously, owing to the strong effect of eddy motions, a two-cell pattern appears with rising motion over the pole. This pattern is especially well established during late winter and in periods of a polar-vortex breakdown. In view of this discrepancy between the conclusions reached by Murgatroyd and Singleton from heat-transport considerations and those reached from meridional-circulation patterns derived from stratospheric wind observations, the validity of the meridional and vertical fluxes shown in Fig. 3.23 for the mesosphere can also be questioned. However, these fluxes may well suffice for a first approximation of the flow patterns at these altitudes. The southward flow during midsummer near the mesopause is corroborated from noctilucent-cloud-drift observations (see Part 2 of this review, *Chemical Tracers*). The ascending motions shown for this season and these levels also agree with the postulated moisture distribution

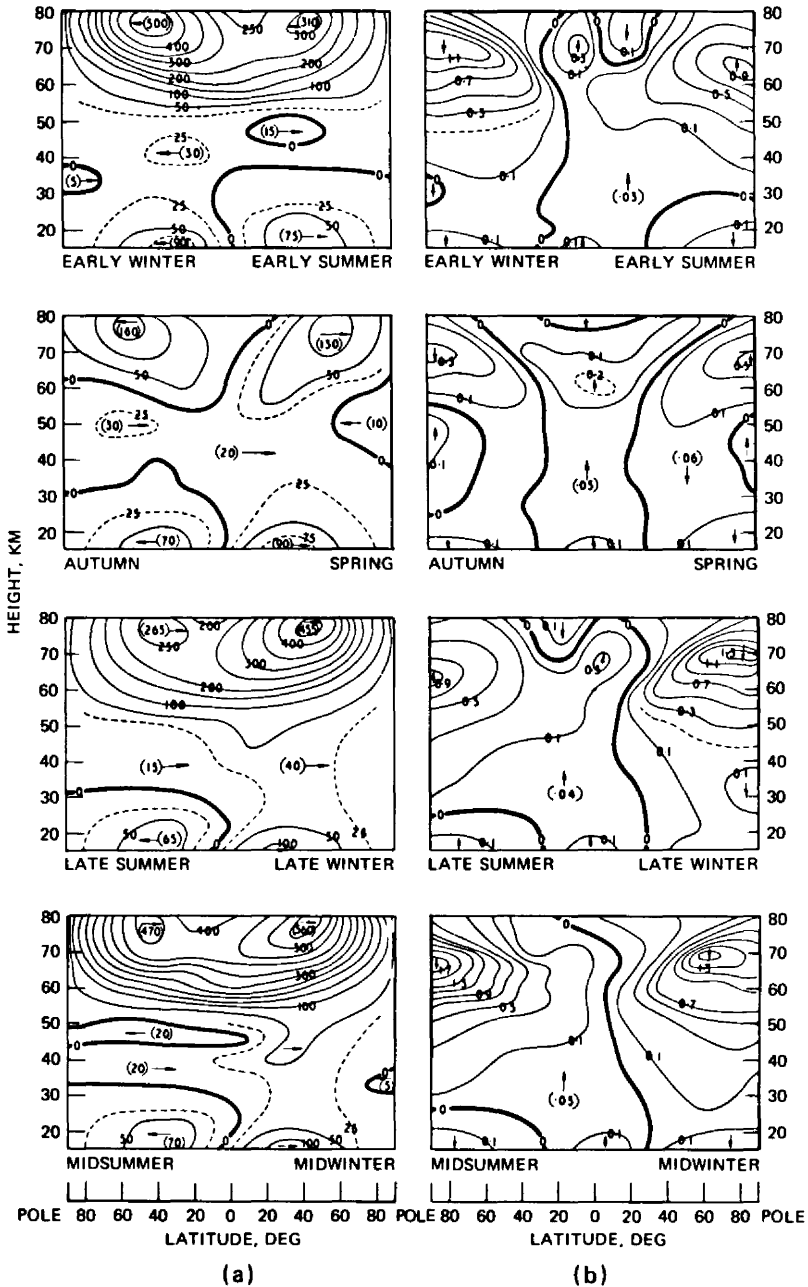


Fig. 3.23 Cross sections of (a) meridional and (b) vertical velocities (in cm/sec) from pole to pole at different times of the year. [From R. J. Murgatroyd and F. Singleton, *Quarterly Journal of the Royal Meteorological Society*, 87(372): 130 (1961).]

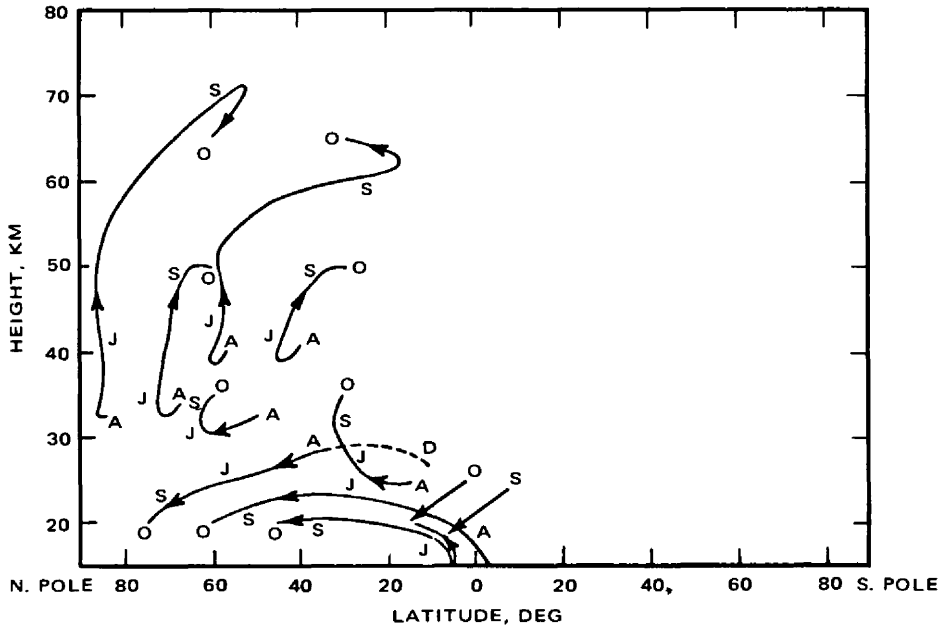
necessary for noctilucent-cloud formation. Adiabatic cooling associated with this upward flow will help to account for the low mesopause temperatures at high latitudes in the summer hemisphere.

The suspicion that Fig. 3.23 does not reveal the complete picture of meridional motions is hardened by the fact that the mesospheric easterlies of the summer hemisphere and the westerlies of the winter hemisphere are not nearly strong enough to conform to a simple Hadley cell under conservation of absolute angular momentum. As in the cases of tropopause and stratopause jet streams, eddy motions may, at least in part, be held responsible for these strongly reduced wind speeds. This fact has also been stressed by Haurwitz (1961), who computed the meridional flow components produced by frictional effects (see Figs. 3.18 and 3.19).

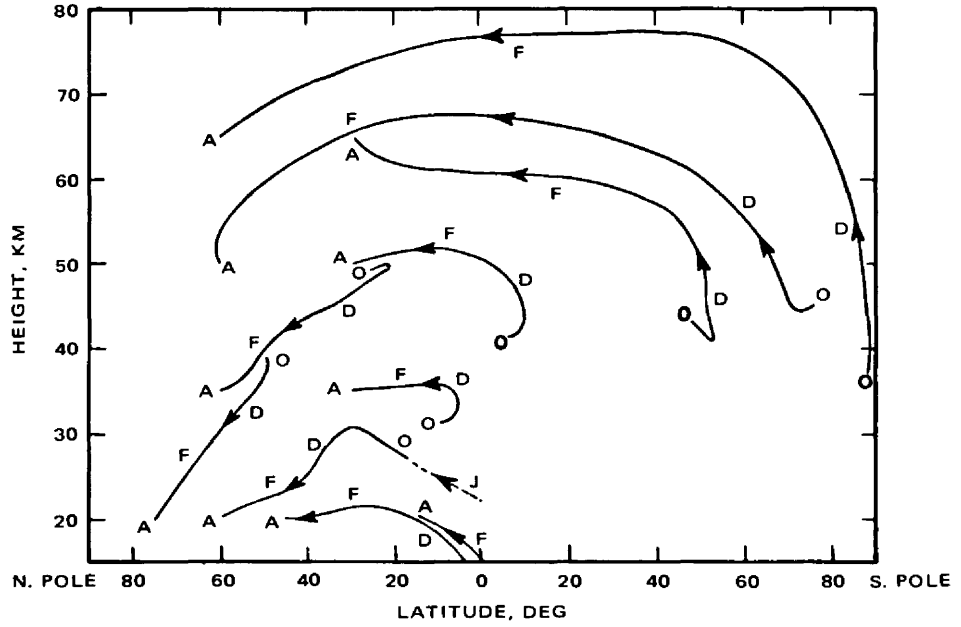
Murgatroyd and Singleton (1961) used the data shown in Fig. 3.23 for computing air trajectories over six-month periods (Fig. 3.24). From these estimates it appears that tropospheric air ascends into the higher atmosphere only in equatorial regions. The descent of air from the high atmosphere into the lower stratosphere is confined to the polar regions of the winter hemisphere. These trajectories agree, at least qualitatively, with the observed dryness of the middle stratosphere (see Part 2), which may be thought of as the result of a dehumidifying effect of the cold tropical tropopause region. The sinking motions shown in Fig. 3.21 for the middle and high stratosphere over the mid-latitude and polar regions of winter are corroborated by the subsequent spring maximums of ozone and of radioactive fallout.

Leovy's (1964) dynamic models of mesospheric circulations consider the effects of eddy fluxes of angular momentum and of sensible heat. The resulting motions are assumed to be in hydrostatic and geostrophic balance. They are considered to be small perturbations about a state of rest that is defined as the horizontal average of the radiative equilibrium temperature. Good agreement was reached with observed zonal wind distributions if eddy viscosity and conductivity parameters were assumed to be about 5×10^6 cm²/sec. Figure 3.25 shows the results for a vertically bounded model atmosphere in which pressure variations are required to vanish at the two isobaric boundary surfaces. This model also includes the latitudinal variations of the heating function.

Although Leovy's model portrays the zonal velocity distributions for summer and winter reasonably well, vertical velocities are probably too small to account for the noctilucent-cloud phenomenon described in Part 2. Meridional velocities also are probably too low. The temperature distribution shown in Fig. 3.25, obtained by adding the perturbation temperature field to the horizontally averaged radiative equilibrium temperature field, indicates low mesopause temperatures during summer, in agreement with noctilucent-cloud observations. Thus the mean meridional circulation would produce a countergradient heat flux. This indirect circulation would arise from the fact that the motions in the upper mesosphere are driven by the heat sources at lower levels, as mentioned earlier (Newell, 1963b). The sinking motion computed for the winter months will contribute to a certain extent to the relatively high mesospheric temperatures observed during that season.



(a)



(b)

Fig. 3.24 Selected air trajectories over six monthly periods. (a) Trajectories ending in autumn. (b) Trajectories ending in spring in the northern hemisphere. Dashed lines indicate movement in preceding six months. F, February. A, April. J, July. S, September. O, October. D, December. [From R. J. Murgatroyd and F. Singleton, *Quarterly Journal of the Royal Meteorological Society*, 87(372): 132 (1961).]

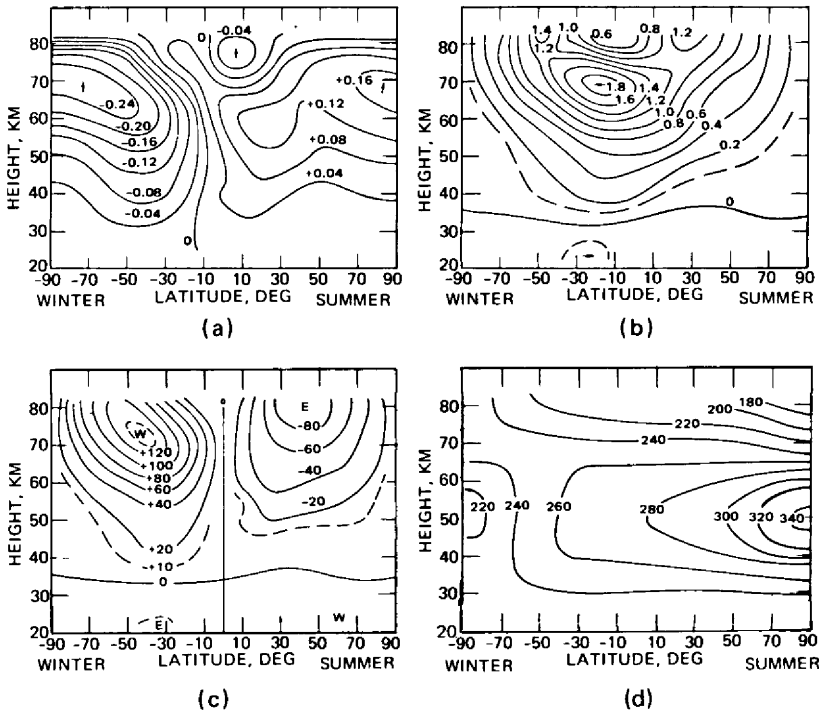


Fig. 3.25 Distribution of zonally averaged vertical (cm/sec) (a), meridional (m/sec) (b), and zonal velocity (m/sec) (c) and of temperature ($^{\circ}$ K) (d) in a theoretical circulation model. (Adapted from Leovy, 1964.)

The Index Cycle

The conversion term $\langle K_E, K_Z \rangle$ appears with a negative sign in the computational results by Julian and Labitzke (1965) for the troposphere. This is contrary to the model of the general circulation proposed earlier (Saltzman and Fleisher, 1960b, 1961; Phillips, 1956; Wiin-Nielsen, 1959; Wiin-Nielsen, Brown, and Drake, 1963), according to which K_E is transformed into K_Z . From earlier investigations of the index cycle* (Namias, 1950; Riehl, Yeh, and LaSeur, 1950; Mintz and Kao, 1952; for further remarks see Reiter, 1961, 1963b), periods in which the mean amplitudes of tropospheric disturbances increase and other periods in which they decrease can be distinguished. Minimum amplitudes are characteristic of the so-called high-index stage when the (zonally averaged) mean meridional profile of the westerly wind component shows maximum velocities. Maximum amplitudes, on the other hand, characterize the

*The index cycle is defined as the quasi-periodic or aperiodic variation of the general circulation of the atmosphere between high- and low-index stages.

low-index stage. During the transition from high to low index, a transfer of energy from K_Z to K_E should be expected. Thus the atmosphere seems to be able to operate in at least two different schemes as far as the maintenance of its kinetic energy is concerned.

A two-level quasi-geostrophic model of planetary flow, according to Eliassen (1961), yields a vacillating pattern in which kinetic energy is alternately transferred between the mean zonal flow and the eddies (see also Kuo, 1951b; Wippermann, 1956).

Dishpan experiments by Pfeffer and Chiang (1967) also reveal a distinct vacillation in the amplitudes of steady waves (i.e., waves that do not change their wave number throughout the experiment). This would not necessarily mean a reversal in the sign of $\langle K_E, K_Z \rangle$ but, with sufficiently large values of G_Z , could signify a quasi-periodic pumping in the conversion rates $\langle A_Z, A_E \rangle$ and $\langle A_E, K_E \rangle$, whereby $\langle A_Z, A_E \rangle$ periodically changes from values smaller than G_Z to values larger than G_Z and vice versa.

In the real atmosphere we should not expect to find an index cycle with regular periodicities between high and low indexes (Kress, 1965). Namias and Clapp (1951) have already pointed out the irregularity of index cycles. In an objective study of cross-spectra of the zonal index in polar, temperature, and subtropical latitudes as well as of coherence statistics of these indexes, Julian (1966) finds no preferred periodicity of an index cycle. Furthermore, Winston and Krueger (1961) demonstrated that the buildup and breakdown of A_Z (and K_Z) can be confined to a certain longitude sector. Integration over the whole hemisphere may not reveal these characteristic cycles in the energy transformations unless they are viewed in the wave-number space (see Chap. 4).

With this degree of freedom in the sign of energy-conversion processes available to the atmosphere, a certain variability in these energy conversions might be expected, even over monthly averaging periods and from one year to the next. Wiin-Nielsen (1965) has pointed out the pitfalls of drawing hasty conclusions on atmospheric energetics and transport processes from limited data samples. "Typical" winter and summer conditions are shown in Fig. 3.26. These conditions were inferred from computations by Wiin-Nielsen and Drake (1965) and by other authors (Krueger, Winston, and Haines, 1965; Wiin-Nielsen and Brown, 1962; Brown, 1964; Wiin-Nielsen, Brown, and Drake, 1963, 1964; Peixoto, 1961; Wiin-Nielsen, 1959; Saltzman and Fleisher, 1960b, 1961; for more details, see Wiin-Nielsen, 1965). As shown in Fig. 3.27, the January 1963 energy conversion differs drastically from these "normal" conditions. Wiin-Nielsen (1965) pointed out that the abnormality of January 1963 was also reflected in the distribution of $A_E(n)$ and $K_E(n)$ as functions of wave number n (see Chap. 4). Wave numbers 2 and 3 were more dominant during that month than during the preceding year (see also Murakami and Tomatsu, 1965).

Vertically Averaged Mean Flow and Shear Flow

In Figs. 3.25 and 3.26 an additional refinement has been included by considering the vertically averaged mean—or barotropic—kinetic energy, K_M , separately from

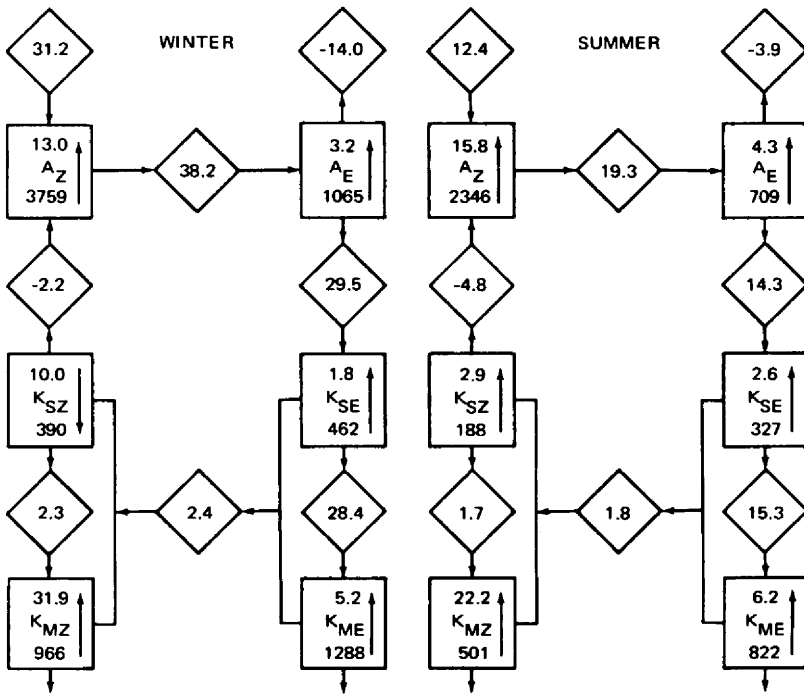


Fig. 3.26 Averaged energy diagram for winter and summer showing amounts of energy (kilojoules/m²) (lower numbers in the boxes), energy generations and conversions (10⁻⁴ kilojoules/m²/sec) (numbers in the diamonds), and decay times (days) (upper numbers in the boxes). The arrows after the decay times indicate that the times were computed from the energy inflow (↑) or the energy outflow (↓) (Wiin-Nielsen, 1965).

the kinetic energy of the (baroclinic) shear flow, K_S (Wiin-Nielsen, 1962; Wiin-Nielsen and Drake, 1965, 1966a). The former is defined as

$$K_M \equiv [K]_{(p,s)} = \frac{P_0}{2g} \int_s ([u]_{(p)}^2 + [v]_{(p)}^2) ds \tag{3.59}$$

where s indicates the surface over which the integral is evaluated and

$$[u]_{(p)} = \frac{1}{P_0} \int_0^{P_0} u dp \tag{3.60}$$

is the vertically averaged u component of flow. An analogous expression can be written for $[v]_{(p)}$. The kinetic energy of the shear flow is given by

$$K_S \equiv [(K)_{(p)}]_{(s)} = \frac{1}{2g} \int_0^{P_0} \int_s \{(u)_{(p)}^2 + (v)_{(p)}^2\} ds dp \tag{3.61}$$

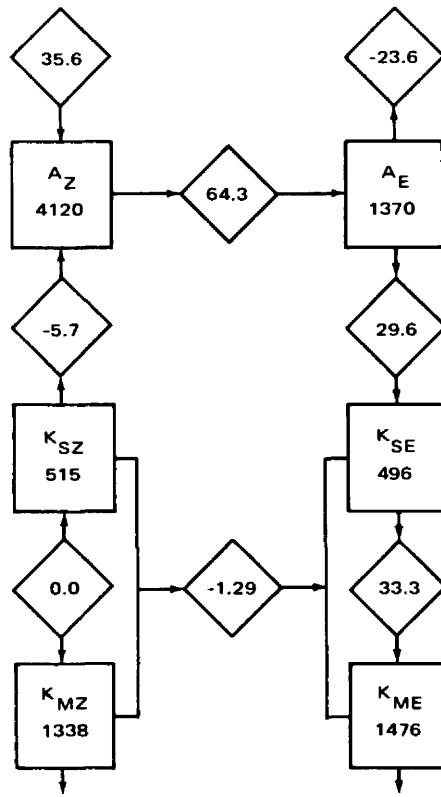


Fig. 3.27 Averaged energy diagram for January 1963. Arrangement as in Fig. 3.26 (Wiin-Nielsen, 1965).

for

$$u = [u]_{(p)} + (u)_{(p)} \text{ and } v = [v]_{(p)} + (v)_{(p)} \tag{3.62}$$

where $(u)_{(p)}$ and $(v)_{(p)}$ are the departures of wind speeds from the vertically averaged mean wind. The conditions hold that

$$[(u)_{(p)}]_{(p)} = [(v)_{(p)}]_{(p)} = 0 \tag{3.63}$$

and

$$K = [K]_{(p)} + (K)_{(p)} \equiv K_M + K_S \tag{3.64}$$

The conversion of the kinetic energy of shear flow into kinetic energy of mean flow is given by

$$\langle K_S, K_M \rangle = - \frac{P_0}{g} \int_S \{ [\mathbf{v}]_{(p)} \cdot [(\nabla \cdot \mathbf{v})_{(p)}(\mathbf{v})_{(p)}]_{(p)} + ([\mathbf{v}]_{(p)} \times \mathbf{K}) \times [(\mathbf{q})_{(p)}(\mathbf{v})_{(p)}]_{(p)} \} ds \quad (3.65)$$

where $(\mathbf{q})_{(p)}$ is the relative vorticity of the shear flow. The averaging subscript S has been omitted on the left side of this equation for the sake of convenience. Both quantities, K_M and K_S , can be considered with respect to their zonal and eddy components. This has been done in Figs. 3.26 and 3.27. The behavior of the four resulting components of kinetic energy during the abnormal period of January 1963 is shown in Fig. 3.28.

Typical values and ratios of K_M and K_S are given in Tables 3.5 through 3.7 (Wiin-Nielsen and Drake, 1965). As should be expected, both modes of kinetic energy attain maximum values during the winter months when tropospheric jet streams reach their peak intensity. The kinetic energy of shear flow, K_S , is mainly contributed from levels below 700 mb and above 200 mb. These are the regions where maximum baroclinicity is reached in the atmosphere (for further details on shears near jet streams, see Reiter 1961, 1963a, 1963b).

Table 3.8 contains values of the zonal mean and eddy modes of K_M and K_S . Numerical values for the eddy modes have been obtained by summation over the effects from wave numbers 1 to 15, measured on a hemispheric basis. In this table results by Wiin-Nielsen and Drake (1965) are compared with those from Smagorinsky's (1963) theoretical model. Smagorinsky's values for $K_S = K_{SZ} + K_{SE}$ are higher than those obtained by Wiin-Nielsen and Drake because Smagorinsky considers the total energy in the horizontal motions but Wiin-Nielsen and Drake only regard the nondivergent part of the motion. (The same explanation cannot hold for the discrepancies in $K_M = K_{MZ} + K_{ME}$ because the vertically averaged mean motion is essentially nondivergent in both sets of computations.)

This further differentiation of the kinetic energy into its divergent and nondivergent parts was proposed by Wiin-Nielsen (1962) (see also the work by Wippermann, 1957). Equation 3.65 indicates the conversion between the kinetic energies of (baroclinic) shear flow, K_S , and (barotropic) mean flow, K_M . Of the two terms under the integral in Eq. 3.65, the first contains divergence but the second does not. The conversion $\langle K_S, K_M \rangle$ thus can be broken down into a divergent and a nondivergent part

$$\langle K_S, K_M \rangle = \langle K_S, K_M \rangle_D + \langle K_S, K_M \rangle_{ND} \quad (3.66)$$

Using a two-parameter quasi-nondivergent model of the atmosphere (Eliassen, 1956; Phillips, 1958), Wiin-Nielsen (1962) estimated the effects of the nondivergent and divergent components of this energy conversion. In the simplified model adopted by him, the divergent components amount to only 10% of the nondivergent ones. Thus the largest part of the conversion processes should be presented adequately by a quasi-nondivergent general-circulation model.

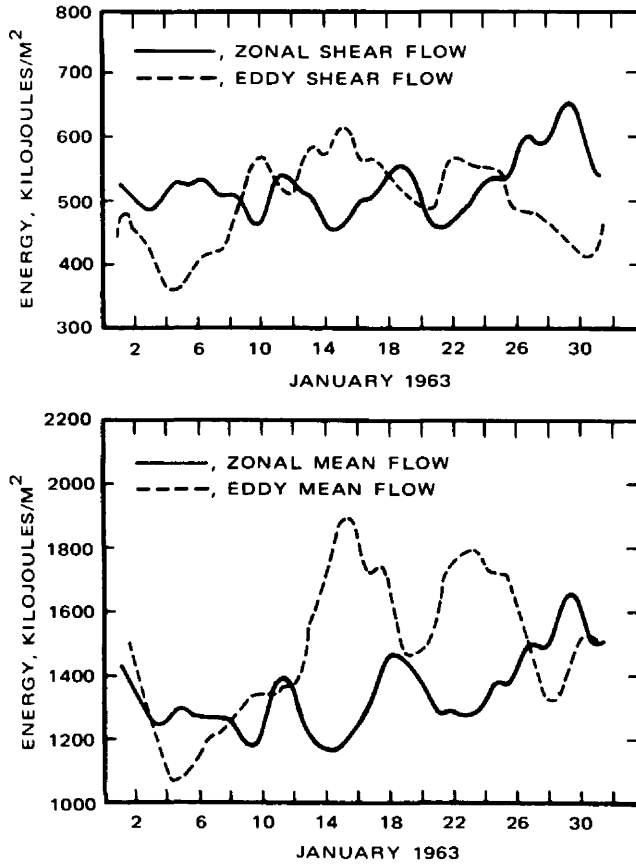


Fig. 3.28 Zonal and eddy shear flow and mean flow kinetic energies as functions of time during January 1963 (Wiin-Nielsen, 1965).

As indicated in Figs. 3.26 and 3.27, the kinetic energy gained by the conversion of eddy available potential energy, A_E , goes into eddy kinetic energy of the shear flow. A part of this energy, $(K)_{(p,\lambda)} \equiv K_{SE}$, converts by means of nondivergent and divergent flow processes as indicated previously into eddy kinetic energy of the mean flow $([K]_{(p)})_{(\lambda)} \equiv K_{ME}$. (In Figs. 3.26 and 3.27, only the total conversion, (K_S, K_M) , has been plotted.) According to Wiin-Nielsen (1962), this conversion reaches a peak at wave number 7 (see Chap. 4). Figure 3.29 indicates that this conversion undergoes a marked seasonal trend as well as short-term fluctuations.

In a later paper, Wiin-Nielsen and Drake (1966b) considered in detail the rather complex modes of energy transformation between zonal and eddy mean shear flows. In Fig. 3.30 their computational results for January 1963 are compared with those from Smagorinsky's (1963) numerical experiment. The term ND indicates the contribution from a quasi-nondivergent formulation; the term D depends on the

Table 3.5
MONTHLY MEAN VALUES OF THE KINETIC ENERGY IN THE
VERTICAL MEAN FLOW (K_M)*

	Values, kilojoules/m ²					
	January 1962	April 1962	July 1962	October 1962	January 1963	Average
K_M	2752	1832	891	1678	2814	1796

*From A. Wiin-Nielsen and M. Drake, *Monthly Weather Review*, 93(2): 85 (1965).

Table 3.6
MONTHLY MEAN VALUES OF THE KINETIC ENERGY OF THE
VERTICAL SHEAR FLOW (K_S) AND THE
CONTRIBUTIONS FROM THE DIFFERENT LEVELS*

Pressure level, mb	Values, kilojoules/m ²					
	January 1962	April 1962	July 1962	October 1962	January 1963	Average
850	361	244	112	198	343	226.50
700	125	84	44	72	119	80.50
500	24	16	13	17	30	18.25
300	140	106	49	90	138	96.00
200	393	258	155	226	382	256.63
Total	1048	708	373	604	1011	678.00

*From A. Wiin-Nielsen and M. Drake, *Monthly Weather Review*, 93(2): 85 (1965).

Table 3.7
RATIO OF K_S TO K_M FOR THE DIFFERENT
MONTHS AND THE ANNUAL AVERAGE*

K_S/K_M					
January 1962	April 1962	July 1962	October 1962	January 1963	Average
0.38	0.39	0.42	0.36	0.36	0.38

*From A. Wiin-Nielsen and M. Drake, *Monthly Weather Review*, 93(2): 85 (1965).

Table 3.8

MONTHLY MEAN VALUES, ANNUAL AVERAGE, AND MEAN VALUES
 COMPUTED BY SMAGORINSKY (1963) FOR ZONAL MEAN (K_{MZ}),
 EDDY MEAN (K_{ME}), ZONAL SHEAR (K_{SZ}), AND
 EDDY SHEAR (K_{SE}) FLOW KINETIC ENERGIES*

	Values, kilojoules/m ²						
	January 1962	April 1962	July 1962	October 1962	January 1963	Average	Smagorinsky
K_{MZ}	1240	732	310	648	1338	745	1842
K_{ME}	1512	1100	580	1030	1476	1051	208
K_{SZ}	515	313	110	218	515	289	884
K_{SE}	532	395	263	386	496	390	132

*From A. Wiin-Nielsen and M. Drake, *Monthly Weather Review*, 93(2): 87 (1965).

divergent component of the wind. The agreement between numerical model and observational data in the relative magnitudes and in the signs of the conversion processes is rather remarkable. Only the sign of $\langle [(K)_{(p)}]_{(\lambda)}, [K]_{(p,\lambda)} \rangle \equiv \langle K_Z, K_{MZ} \rangle$ shows a discrepancy, probably attributable to the omission of low-latitude data from Wiin-Nielsen's study and hence a partial suppression of the effects of the Hadley cell.

The discrepancy in $\langle (K)_{(p,\lambda)}, ([K]_{(p)})_{(\lambda)} \rangle \equiv \langle K_{SE}, K_{ME} \rangle$ between model and real atmosphere (Smagorinsky's results yield a substantially smaller value than those obtained by Wiin-Nielsen and Drake) probably is caused by a lack of truly planetary-scale waves in the model. The inclusion of mountain effects and of ocean-continent effects into the model might remedy this.

From Fig. 3.27, one would conclude that the zonal kinetic energy, K_Z , should decrease during the month of January 1963 because of the adverse transformation processes, $\langle K_Z, A_Z \rangle$ and $\langle K_E, K_Z \rangle$, affecting it. From Fig. 3.28, however, this appears not to be the case. A slight increase of $K_Z = K_{MZ} + K_{SZ}$ is even indicated from this diagram. There also appears to be a tendency for K_E and K_Z to be out of phase. This is particularly true for the barotropic components K_{ME} and K_{MZ} . Therefore, a major part of the energy cycle during this month might be ascribed to barotropic processes.

The Effect of Averaging on Energy Transformations

The different effect of space and time averaging on atmospheric energetics and energy-transfer mechanisms, earlier referred to by Starr (1953, 1959a) and Starr and White (1952c, 1952d), was treated systematically by Oort (1964b). Especially when long-time averages are involved, the pitfalls of short data samples mentioned by

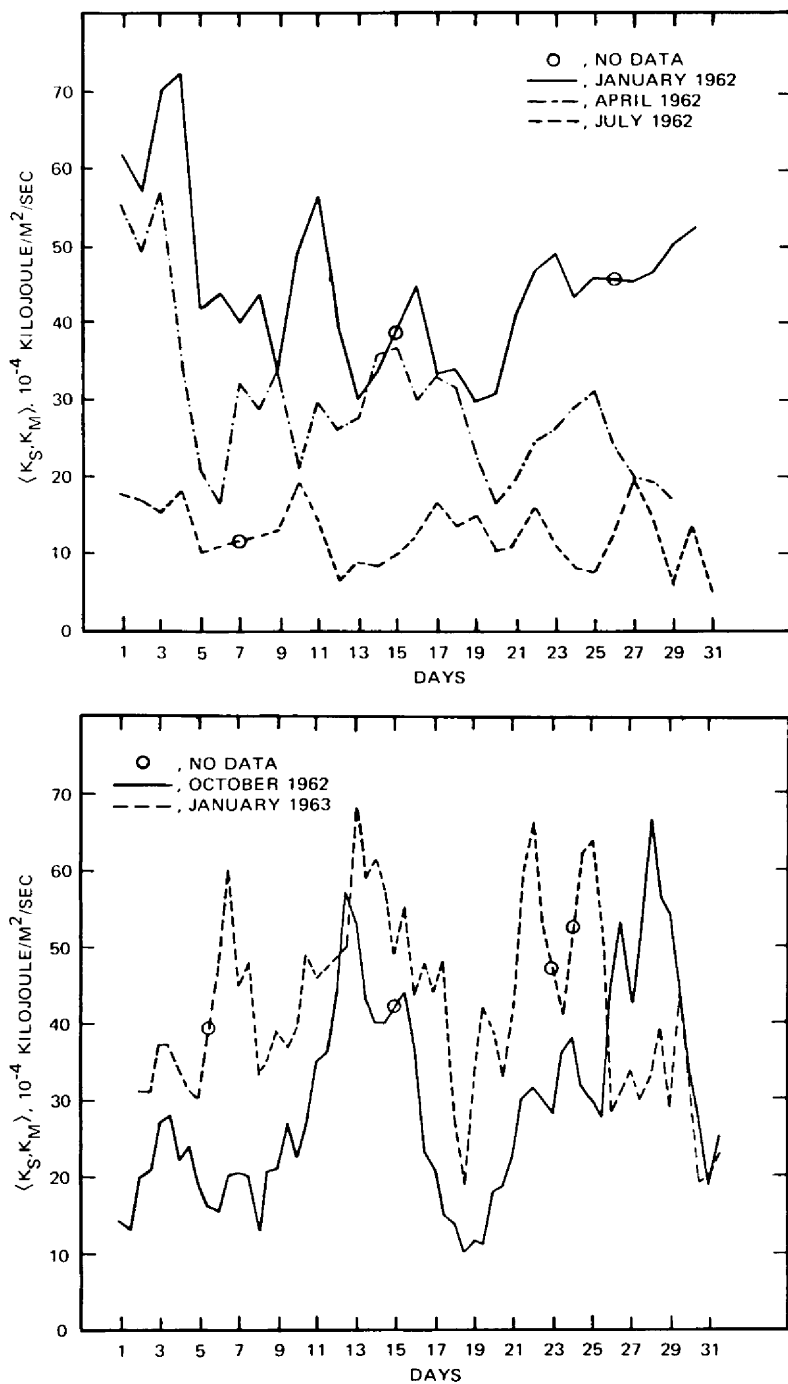


Fig. 3.29 Energy conversion, $\langle K_S, K_M \rangle$, as a function of time. [From A. Wiin-Nielsen and M. Drake, *Monthly Weather Review*, 93(2): 87 (1965).]

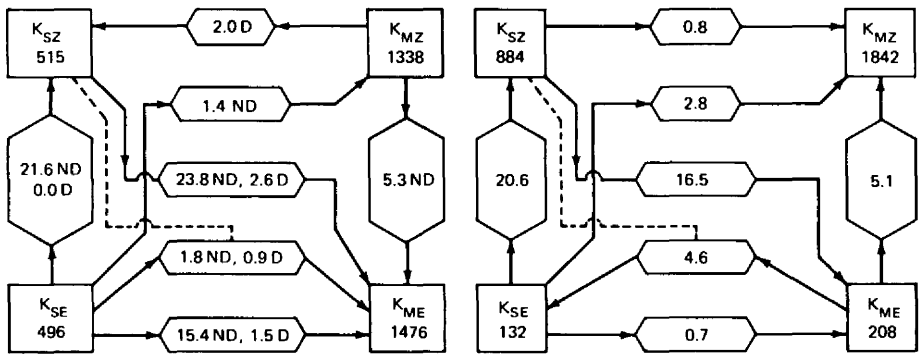


Fig. 3.30 Comparison of energy conversion obtained by Wiin-Nielsen and Drake for January 1963 (left) with that obtained by Smagorinsky (1963) (right). [From A. Wiin-Nielsen and M. Drake, *Monthly Weather Review*, 94(4): 227 (1966).]

Wiin-Nielsen (1964), which are apparent from the January 1963 period, should be avoided. From a survey of literature, Oort arrives at the “typical” annual flow diagrams of atmospheric energetics integrated over the entire atmosphere shown in Figs. 3.31 and 3.32. [Work of the following authors has been considered by Oort (1964b) in these summarized results: Brown, 1964; Brunt, 1926; Buch, 1954; Crutcher, 1961; Holopainen, 1964; Jensen, 1961; Krueger, Winston, and Haines, 1965; Murakami, 1960; Peixoto, 1960, 1961; Phillips, 1956; Saltzman, 1961a; Saltzman and Fleisher, 1960a, 1961, 1962; Smagorinsky, 1963; Starr, 1953, 1959b; Starr and White, 1954; Suomi and Shen, 1963; Teweles, 1963a; Wiin-Nielsen, 1959; Wiin-Nielsen, Brown, and Drake, 1963.]

In agreement with the notation defined in Chap. 1, wind components and temperatures can be expressed as

$$\begin{aligned}
 u &= [u]_{(\lambda,t)} + ([u]_{(t)}_{(\lambda)} + ([u]_{(\lambda)}_{(t)} + (u)_{(t,\lambda)}) \\
 v &= [v]_{(\lambda,t)} + ([v]_{(t)}_{(\lambda)} + ([v]_{(\lambda)}_{(t)} + (v)_{(t,\lambda)}) \\
 T &= [T]_{(\lambda,t)} + ([T]_{(t)}_{(\lambda)} + ([T]_{(\lambda)}_{(t)} + (T)_{(t,\lambda)}) \quad (3.67)
 \end{aligned}$$

The kinetic and potential energies connected with the four perturbation components on the right-hand sides of Eq. 3.67 are indicated in the following by subscripts 1 to 4.

Oort (1964b) defines mean (subscript M) and eddy (subscript E) energies in the space domain by

$$\begin{aligned}
 K_M &= K_1 + K_3 = \frac{1}{2} \int \{ [(u)_{(\lambda)}^2 + (v)_{(\lambda)}^2]_{(t)} \} dm \\
 K_E &= K_2 + K_4 = \frac{1}{2} \int \{ [(u)_{(\lambda)}^2]_{(\lambda)} + [(v)_{(\lambda)}^2]_{(\lambda)} \}_{(t)} dm
 \end{aligned}$$

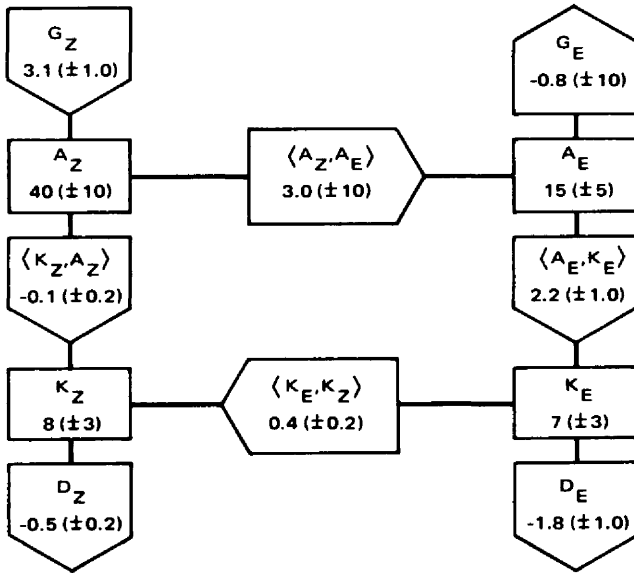


Fig. 3.31 Tentative flow diagram of the atmospheric energy in the space domain. Values are averages over a year for the northern hemisphere. Energy units are in 10^5 joules/m² ($= 10^8$ ergs/cm²); energy-transformation units are in watts/m² ($= 10^3$ ergs/cm²/sec). (Adapted from Oort, 1964b.)

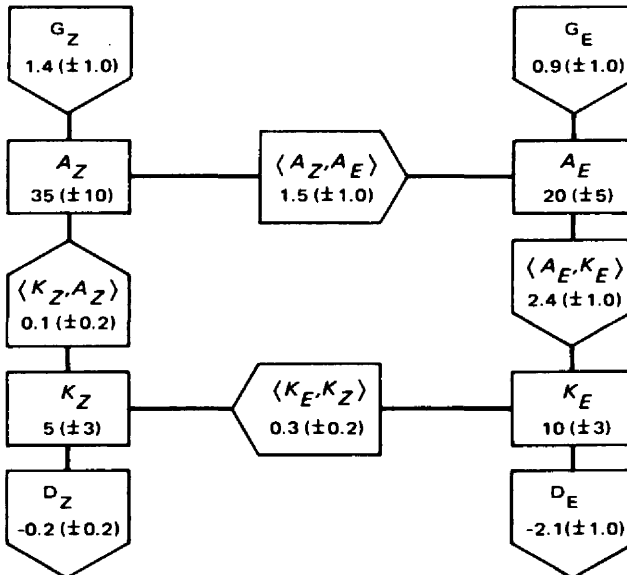


Fig. 3.32 Tentative flow diagram of the atmospheric energy in the mixed space-time domain. Values are averages over a year for the northern hemisphere. Energy units are in 10^5 joules/m²; energy-transformation units are in watts/m² (Adapted from Oort, 1964b.)

$$\begin{aligned}
 A_M &= A_1 + A_3 = \frac{c_p}{2} \int [\gamma([T]_{(\lambda)}^2)_{(A)}]_{(t)} dm \\
 A_E &= A_2 + A_4 = \frac{c_p}{2} \int [\gamma([T]_{(\lambda)}^2)_{(\lambda)}]_{(t)} dm
 \end{aligned}
 \quad (3.68)$$

where dm indicates integration over the mass of the entire atmosphere and

$$\gamma = -\left(\frac{\theta}{T}\right)^2 \frac{R}{c_p p_0} \int_0^{p_0} \left(\frac{T}{\theta}\right) \frac{1}{p} \left(\frac{\partial[\theta]_{(A)}}{\partial p}\right)^{-1} dp
 \quad (3.69)$$

Subscript A indicates an area average over a constant-pressure surface and the departure from this area average.

In the time domain, Oort defines

$$\begin{aligned}
 K_M &= K_1 + K_2 = \frac{1}{2} \int [[u]_{(t)}^2 + [v]_{(t)}^2]_{(\lambda)} dm \\
 K_E &= K_3 + K_4 = \frac{1}{2} \int [[(u)_{(t)}^2]_{(t)} + [(v)_{(t)}^2]_{(t)}]_{(\lambda)} dm \\
 A_M &= A_1 + A_2 = \frac{c_p}{2} \int \gamma [[T]_{(t)}^2]_{(A)}_{(\lambda)} dm \\
 A_E &= A_3 + A_4 = \frac{c_p}{2} \int \gamma [[(T)_{(t)}^2]_{(t)}]_{(\lambda)} dm
 \end{aligned}
 \quad (3.70)$$

For the mixed space–time domain, he arrives at

$$\begin{aligned}
 K_M &= K_1 = \frac{1}{2} \int \{[u]_{(t,\lambda)}^2 + [v]_{(t,\lambda)}^2\} dm \\
 K_E &= K_2 + K_3 + K_4 = \frac{1}{2} \int [[(u)_{(t)}^2]_{(t)} + [(v)_{(t)}^2]_{(t)} + ((u)_{(t)})_{(\lambda)}^2 \\
 &\quad + ((v)_{(t)})_{(\lambda)}^2]_{(\lambda)} dm \\
 A_M &= A_1 = \frac{c_p}{2} \int \gamma ([T]_{(\lambda,t)})_{(A)}^2 dm \\
 A_E &= A_2 + A_3 + A_4 = \frac{c_p}{2} \int \gamma [[(T)_{(t)}^2]_{(t)} + ([T]_{(t)})_{(\lambda)}^2]_{(\lambda)} dm
 \end{aligned}
 \quad (3.71)$$

The space domain is defined in terms of the potential and kinetic energy of the zonally averaged motion. All integrals entering the expressions for energy changes and transformations are computed daily. Time averaging is performed as a final step. The

energy cycle in this domain thus considers the maintenance of the zonal mean state and of the eddies superimposed upon this state.

The time domain is defined in terms of energies of the mean time motion and of the eddies superimposed upon it. The energy cycle in this domain thus considers the maintenance of the time-averaged state and of the transient (in time) eddies. (For slow- and fast-moving transient modes, see Bradley, 1968.)

The mixed space–time domain finally considers the energetics of the zonal—mean and time—mean motion and of the transient and standing eddies superimposed upon it. The evaluation of the energy transformations in this domain usually is less time consuming since integrals can be computed over time-averaged flow conditions.

The original publication by Oort (1964b) contains further details on the definition of the energy terms and the transformation terms in these three domains. Oort found systematic departures between the three averaging methods (in Figs. 3.31 and 3.32, only two methods are represented because of insufficient data in the time domain). Mean kinetic and available potential energies in the space and time domains will be larger than those in the mixed space–time domain. The eddy energies behave in the opposite sense. Also, the transformations are different in each domain, as has been borne out already by the results by Starr (1953, 1959a) mentioned at the beginning of this chapter. Figures 3.31 and 3.32 show that $\langle K_Z, A_Z \rangle$ and G_E even reverse their sign in different averaging procedures.

Reiter (1969b) formally derived expressions for the kinetic energy involving vertical, longitudinal, and time domains. The kinetic energy of the u component in such an expression reads

$$\begin{aligned}
 [u^2]_{(p,\lambda,t)} = & [u]_{(p,\lambda,t)}^2 + [[(u)_p]_{(\lambda,t)}^2]_{(p)} + [[[u]_{(p)}]_{(\lambda)}]_{(t)}^2]_{(\lambda)} \\
 & + [[(u)_{(p,\lambda)}]_{(t)}^2]_{(p,\lambda)} + [[(u)_{(p,\lambda)}]_{(t)}^2]_{(t)} \\
 & + [[[u]_{(p)}]_{(\lambda)}]_{(p,t)}^2 + [[(u)_{(p)}]_{(\lambda,t)}^2]_{(\lambda,t)} \\
 & + [(u)_{(p,\lambda,t)}^2]_{(p,\lambda,t)} \tag{3.72}
 \end{aligned}$$

An analogous term can be written for $[v^2]_{(p,\lambda,t)}$. The total kinetic energy in the vertical space–time domain can be obtained by adding this term to Eq. 3.72. The first term on the right side of Eq. 3.72 stands for the mean kinetic energy in this mixed domain. Terms two, four, six, and eight contain effects of shear flow kinetic energy, and terms one, three, five, and seven deal with the kinetic energy of the barotropic flow. Terms two, three, and four deal with standing eddies, and terms five, six, seven, and eight deal with transient eddies. Attempts are presently being made to evaluate all terms listed in Eq. 3.72 from actual data.

Oort's derivations were used by Holopainen (1965), who computed the total flux of energy (sensible heat plus potential energy), making a comparison in the space domain between mean meridional transports and zonal eddy transports after Mintz (1955a) on the one hand and in the mixed space–time domain between mean

meridional, standing eddy, and transient eddy fluxes [the latter after Peixoto, (1960)] on the other hand. His computations are based on data reported by Goldie, Moore, and Austin, 1957; Heastie and Stephenson, 1960; Jacobs, 1958; Hennig, 1958; London, 1957; Crutcher, 1959, 1961; and Mintz and Lang, 1955. Results are shown in Fig. 3.33.

The mean meridional fluxes are in good agreement with earlier results on energy generation (Vuorela, 1957; Palmén, Riehl, and Vuorela, 1958). According to these authors, kinetic energy is produced in the Hadley cell at a rate of 30×10^{10} kilojoules/sec during winter and is consumed in the Ferrel cell at -11×10^{10} kilojoules/sec. The importance of the Hadley cell in maintaining the kinetic energy in the tropics as well as in the subtropical jet stream is thus confirmed (Palmén, 1959). These numerical estimates are slightly higher than those obtained earlier by Pisharoty (1955). The net generation of kinetic energy by mean meridional circulations, neglecting the Arctic direct cell, would thus amount to 19×10^{10} kilojoules/sec during winter. This represents almost 20% of the total kinetic-energy production during that season ($< 100 \times 10^{10}$ kilojoules/sec, according to Palmén, 1960).

As shown in Fig. 3.33, in the eddy fluxes the effects of transient eddies seem to dominate at all latitudes. In this diagram all forms of eddy transports are assumed to be negligible near the equator. This contradicts Tucker's (1965a) findings; he computed considerable cross-equatorial transport of momentum by standing eddies (see p. 158).

As shown in Chap. 1, the choice of a geographic or a curvilinear coordinate system may have a decisive influence on the sense of the mean meridional circulation around a jet-stream system, i.e., whether the transformation $\langle A, K \rangle$ will be negative or positive. We have to conclude from the foregoing that further refinement in the averaging procedures results in an even wider range of possibilities of energy transformations that the atmosphere has to offer. Each averaging process stresses a certain combination of mean and eddy flow conditions and thus will yield certain magnitudes and directions of transformations between these modes of energy. They may change if another way of averaging is adopted which divides the total energy differently between eddy and mean contributions.

Again we must stress what has been said before: The general circulation must be maintained by certain generation terms (adiabatic effects and import of energy from other layers) against dissipation effects. The achievement of a climatic balance will necessitate certain transport processes and energy transformations. The relative magnitude of such processes depends on the season and on the nature of the atmospheric flow patterns. It also depends on our avenue of approach, the choice of coordinate systems and of filtering techniques, which hold certain types of eddies in higher regard than others. These subjectivities, inherent in the methods of approach, however, permit us to view the problem of the general circulation from many different angles. The composite picture, although not yet firmly established because of the limited number of available comparative studies, will yield an insight into the mechanics of the general circulation of the atmosphere.

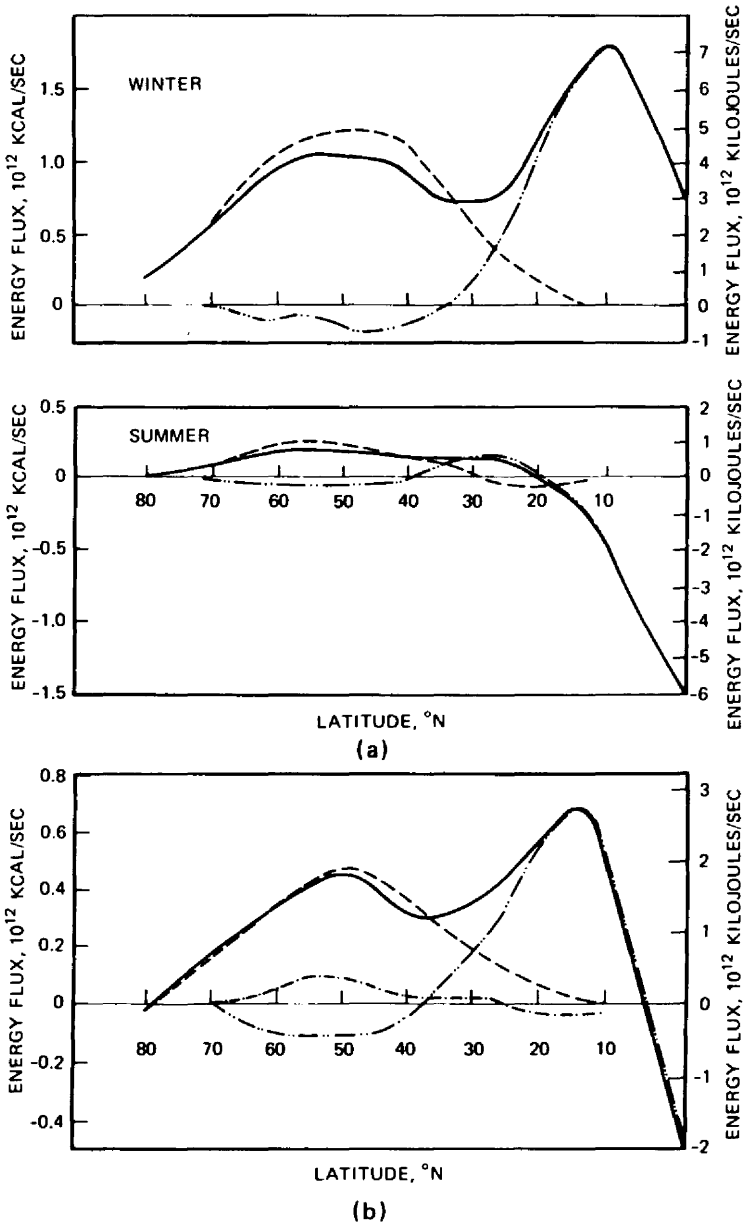


Fig. 3.33 Tentative model of the mean poleward flux of energy (sensible heat plus potential energy) in the atmosphere over the northern hemisphere (a) in the space domain in winter (December-February) and in summer (June-August) (—, total flux. - · - ·, flux associated with the mean meridional circulations. - - - -, flux associated with the zonal eddies) (Mintz, 1955a) and (b) in the time domain [—, total flux. - · - ·, flux associated with the mean meridional circulations. - - - -, flux associated with the transient eddies (Peixoto, 1960); - · - ·, flux associated with the standing zonal eddies (Holopainen, 1965)]. [From E. O. Holopainen, *Tellus*, 17(3): 288 (1965).]

In view of the fact that relatively long periods of time, such as January and February of 1963, may show an "abnormal" behavior in the energy transformations that maintain the general circulation, it may not be quite appropriate to even talk about "normal" and "abnormal" circulations. Wiin-Nielsen (1965) pointed out that the atmosphere can maintain a climatic balance between sources and sinks of energy by more than just one typical energy cycle. Although, from the studies listed in this chapter, it appears that a typical cycle seems to be preferred by the energy-transformation processes, other cycles, such as the one that occurred during January 1963, may be just as efficient, but less frequent, in driving the general circulation. After considerably more studies on this problem have been conducted, we may be able to specify certain frequency distributions of energy cycles and of magnitudes of energy transformations within these cycles for different seasons. Such an approach would provide us with something like a "synoptic climatology" of atmospheric energetics.

As in turbulence theory, the length of the time period over which the energy terms and the transformation terms are integrated will present a certain amount of problems. Too long time averages will tend to yield a bias in the net results in favor of the "normal" or "typical" energy cycles. Interspersed periods of "abnormal" atmospheric behavior will result in a reduction of the magnitudes of the "normal" energy conversions. Too short a period of averaging may lend undue importance to the synoptic noise in the data that may be produced by one or two prevalent synoptic-scale weather systems in the hemisphere under consideration. I am not aware of any systematic studies on the effects of the length of the time period of averaging on the resulting large-scale energy-conversion processes in the atmosphere.

The different, yet important, aspects of the northern and southern hemispheres and the possible linkage between the two hemispheres can only be considered in a preliminary way because of insufficient data from vast regions of the globe (see p. 150). The proposed Global Atmospheric Research Program may remedy these shortcomings (see reports by ICSU/IUGG Committee, 1967, World Meteorological Organization, 1967). A global constant-level balloon sounding system may make it necessary to define fluctuations of wind and of other atmospheric parameters in a quasi-Lagrangian coordinate system. Constant-level or constant-density balloon trajectories only approximate actual air motions. The vertical component of flow is suppressed, and thus a truly Lagrangian coordinate system flowing with the air parcels is not realized. Conversions between an Eulerian and a quasi-Lagrangian frame of reference for the various fluctuations entering the energy transformation and transport terms of large-scale atmospheric motions open an interesting field of investigation.

Vertical Distributions of Energy Fluxes and Conversions

So far we have considered energy-conversion processes integrated over the vertical depth of the atmosphere. Such studies yielded valuable information on the maintenance of the general circulation during specific periods of time. It would be

equally valuable to know which atmospheric layers are the main contributors to these energy-transformation and energy-transport processes. Several investigations of this problem area gave important results.

Figure 3.34 shows the distributions of A_Z , A_E , K_Z , and K_E as functions of pressure. As should be expected, the kinetic energy per unit mass (in this diagram expressed per centibar layer of the atmosphere) is largest at the jet-stream level. However, even per unit volume, the kinetic energy of the jet stream exceeds that of the lower troposphere and of the middle stratosphere (see Table 3.9). In Table 3.9 the quantity $\rho(\Delta z)^2$ gives a measure of the zonal (geostrophic) kinetic energy.

The available potential energy of both the zonal and eddy structures of the atmosphere appears to be largest in the upper troposphere below jet-stream level (see Fig. 3.34).

Kao and Hurley (1962) and Kao and Taylor (1964) also demonstrated the dominant role of the upper tropospheric jet-stream layer in harboring maximum amounts of kinetic energy per unit of volume. From their studies, it is evident that the mean jet-stream positions around the hemisphere coincide with the position of the maximums of mean kinetic energy. Zones of maximum eddy kinetic energy are found poleward of the mean jet positions, with a tendency of the maximums of K_E to be located to the left, ahead of, and slightly below the level of the maximums of K_Z (in the northern hemisphere) (see also Kao and Farr, 1966). Reiter (1963c) has attributed this characteristic distribution to the fact that horizontal shears are asymmetrically distributed about the jet axis. They are stronger on the cyclonic than on the anticyclonic side of the jet, and they are specifically dominant in the stable region underneath the jet core. Latitudinal shifts of the jet stream, therefore, will cause greater variability of wind speeds, hence larger values of K_E , on the cyclonic side of the mean jet axis than on the anticyclonic side. For the same reasons, there also is a tendency for the maximum of K_Z to be close to the southern boundary of the latitude belt within which the jet streams shift their location from day to day (Davis, 1951). The orographic control over the position of the three maximums of K_Z found in the northern hemisphere (Fig. 3.35) especially during winter makes strong jet winds a quasi-permanent feature east of the Himalayas and of the Rocky Mountains. Farther east from these two maximums of K_Z , the variability in wind speeds increases and causes the eastward shift of the maximums of K_E noticed by Kao and Hurley (1962).

In Fig. 3.36 the total production of zonal kinetic energy in the vertically integrated atmosphere is compared with the production at the 300- and the 200-mb levels (Starr, 1953). From this diagram the important role of the jet stream in maintaining the zonal circulation becomes evident: The atmospheric layers near jet-stream level are responsible for the bulk of the energy conversion into mean kinetic energy.

Julian and Labitzke (1965) studied the vertical distribution of the energy-conversion terms in more detail for two days during and after the breakdown of the polar vortex (Jan. 17 and 22 and Feb. 16 and 21, 1963). Because of the abnormal behavior of the atmospheric energetics during these periods, the results might not

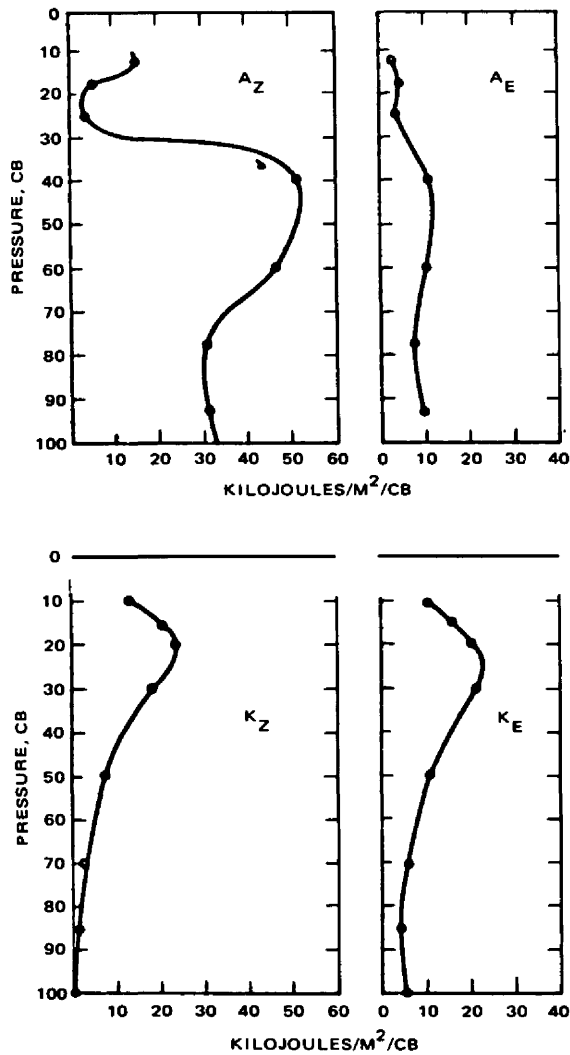


Fig. 3.34 Vertical profiles of the annual averages of A_Z , A_E , K_Z , and K_E as functions of pressure. [From A. Wiin-Nielsen, *Tellus*, 19(4): 543 (1967).]

necessarily be typical, especially not the conversion (K_E , K_Z) in the troposphere (see Fig. 3.20).

Computational results are shown in Fig. 3.37. This figure indicates that three atmospheric regions with typical behavior may be delineated: the troposphere, the tropopause region and lower stratosphere, and the middle stratosphere (pressure <50 mb). The two days in February, characteristic of the transition season in the middle stratosphere, show energy transformations completely different from those

Table 3.9

**KINETIC ENERGY (PER UNIT OF VOLUME) OF THE MEAN
ZONAL FLOW FOR JANUARY BETWEEN CATANIA AND TROMSO***

Isobaric surface, mb	1000	500	225	96	41
Air density (ρ), kg/m ³	1.250	0.738	0.360	0.165	0.065
Δz , dynamic decameters	8	31	50	62	71
Δz^2	64	961	2500	3844	5041
$\rho(\Delta z)^2$	80	709	900	634	328

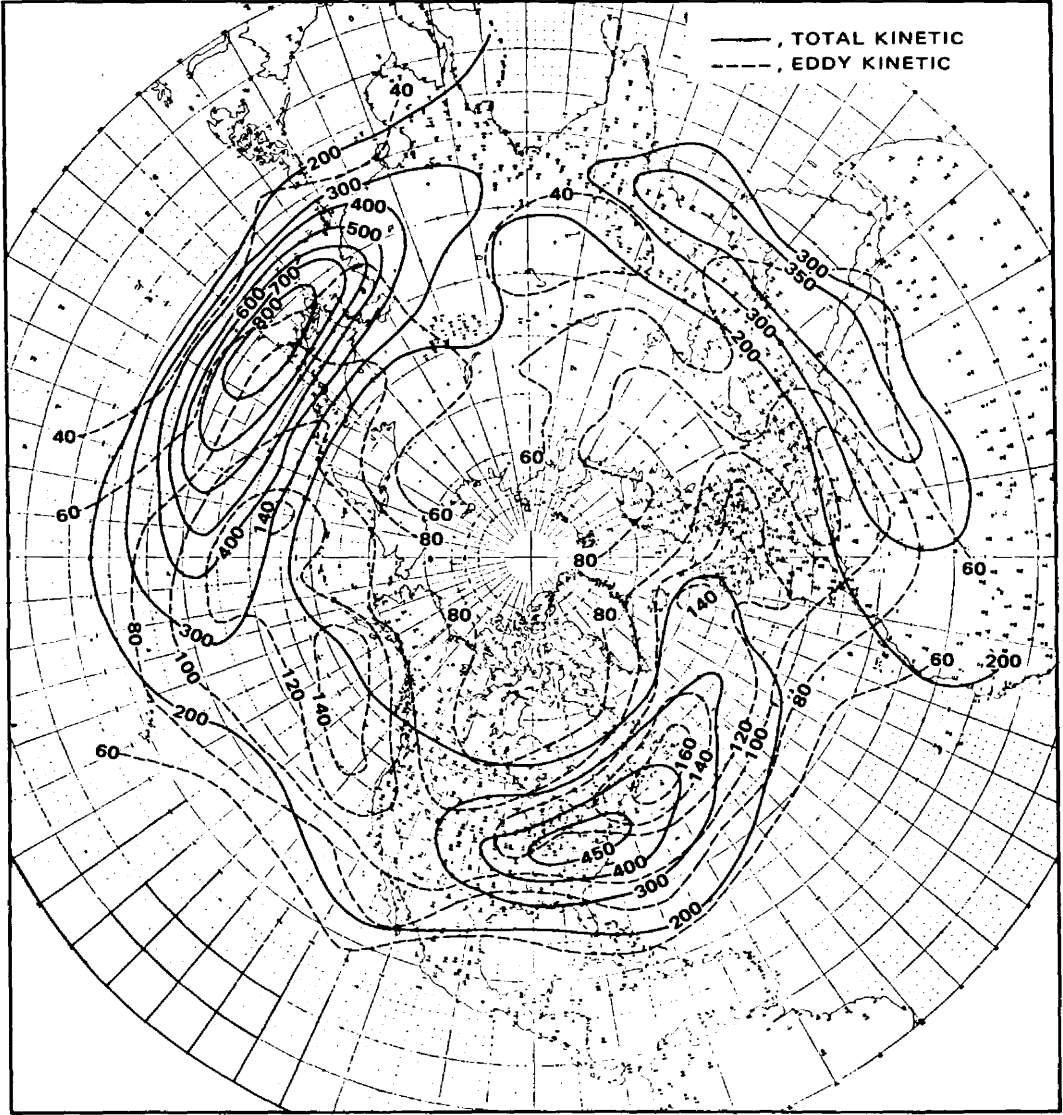
*Adapted from Scherhag (1948).

typical for the January polar-night vortex. The conversion term $\langle K_E, K_Z \rangle$ reveals a certain importance of the jet-stream region, but not as much as is evident from the computations by Starr (1953) (Fig. 3.36). Furthermore, the negative values of $\langle K_E, K_Z \rangle$ in the troposphere, obtained for the longer period average shown in Fig. 3.20, are not evident from Fig. 3.37. The tropospheric average of $\langle K_E, K_Z \rangle$ for the two days in January on which this diagram is based would yield a positive value. This apparent discrepancy may be resolved by means of Fig. 3.38, taken from a study by Wiin-Nielsen, Brown, and Drake (1964). As shown in this figure, Jan. 17, 1963, lay in a brief period of positive energy conversion $\langle K_E, K_Z \rangle$, whereas January 22 gave net results for this term close to zero. [Brown (1967) has shown that when taking the lateral and vertical boundary terms $B(K_Z)$ into account, which have been neglected by Wiin-Nielsen, Brown, and Drake (1964), slight modifications of the values obtained by Wiin-Nielsen, Brown, and Drake will be necessary.]

This brings out again the fact mentioned earlier, that all terms entering the energy equations (see Table 3.1) are functions not only of time and season but also of the length of the time period over which the averaging process is applied. The call for a systematic study of this problem is reemphasized by the apparent discrepancies reported here.

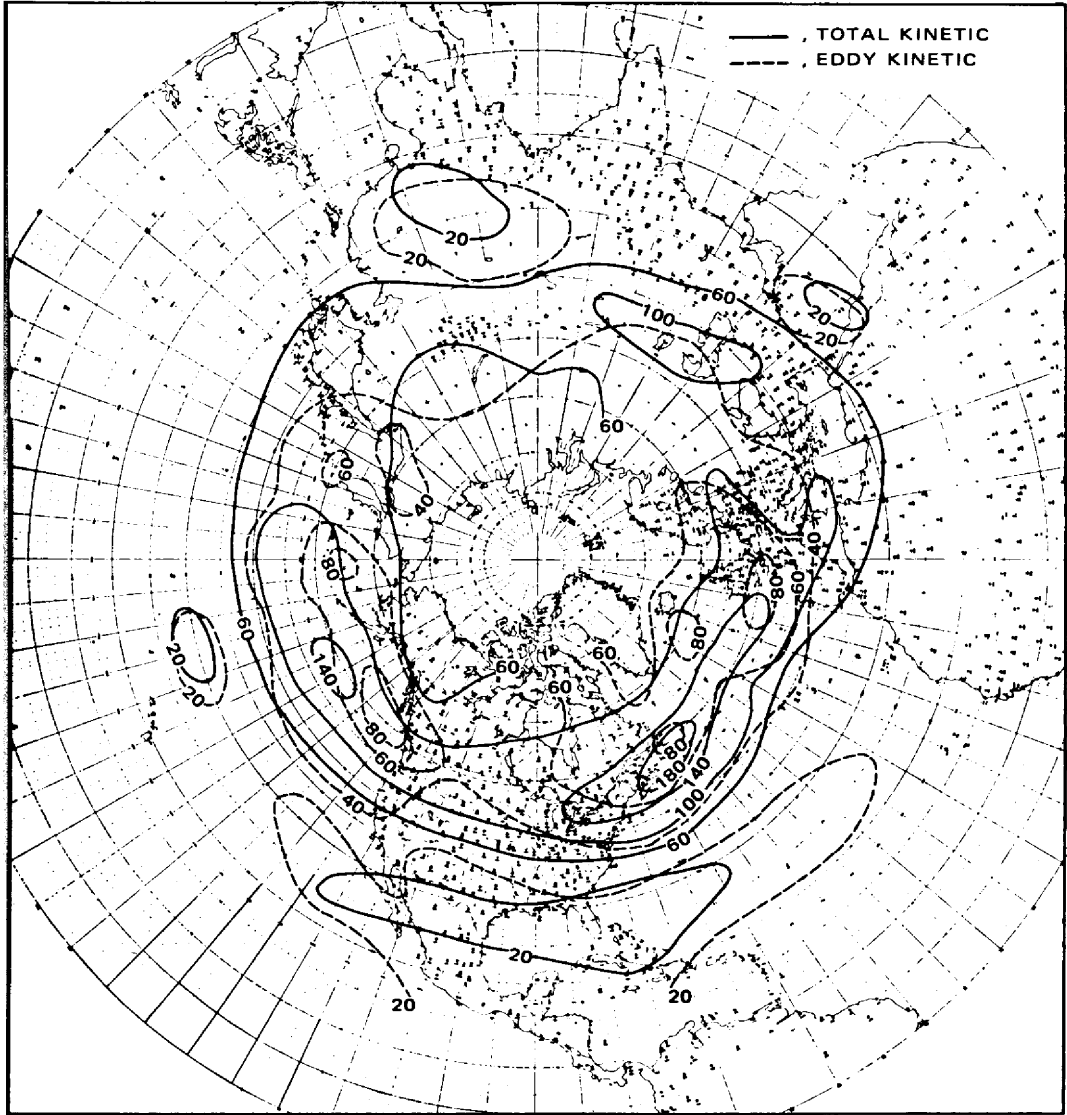
The exclusion of the tropospheric Hadley cell with direct circulation from the data shown in Fig. 3.37 yields positive results for $\langle K_Z, A_Z \rangle$ for the two days in January, i.e., a net indirect meridional circulation that is particularly strong in the middle stratosphere. This indirect cell collapsed by late February 1963, and essentially no conversion by meridional circulation was present then.

The conversions $\langle A_Z, A_E \rangle$ and $\langle A_E, K_E \rangle$, as shown in Fig. 3.37, show large values in the upper and middle troposphere before and after the breakdown of the stratospheric polar vortex (see also Vernekar, 1967). This is the same region of the atmosphere in which, according to Fig. 3.34, both A_Z and A_E attain maximum values. The maximums of K_Z and K_E , however, appear at a slightly higher level near the tropopause. This is not surprising because the wind maximums, by virtue of the



(a)

Fig. 3.35 (See facing page for legend.)



(b)

Fig. 3.35 Distribution of mean total (solid lines) and eddy kinetic energies (dashed lines), (kg/m/sec^2) 300 mb. (a) January. (b) July. [From S.-K. Kao and W. P. Hurley, *Journal of Geophysical Research*, 67(11): 4235; 4236 (1962).]

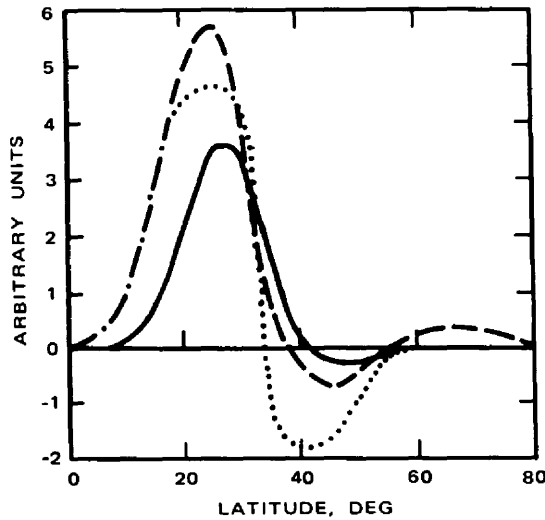


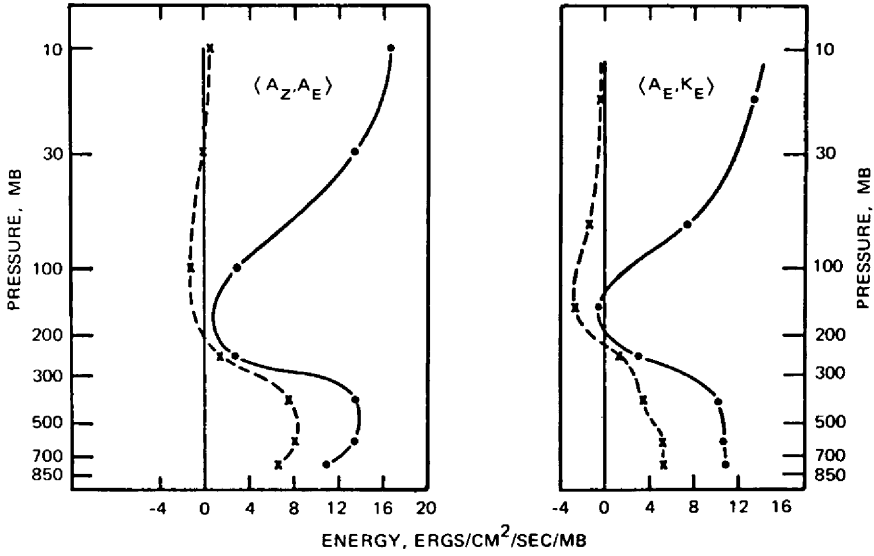
Fig. 3.36 Production of zonal kinetic energy using mean wind and total transport (full curve), 300-mb wind and transport (dashed curve), and 200-mb wind and transport (dotted curve) (in arbitrary units). [From V. P. Starr, *Tellus*, 5(4): 495 (1953).]

thermal-wind equation, are associated with the horizontal temperature gradients, which give a measure of the available potential energy. The position of maximums of K_Z and K_E , therefore, will be determined by the vertically integrated horizontal temperature gradients in the atmosphere underneath the level at which these maximums occur. Positive conversion values (A_E , K_E), according to Reed, Wolfe, and Nishimoto (1963), can be caused by unstable barocline waves similar to those considered theoretically by Charney (1947), Kuo (1952), Phillips (1954, 1956), and Smagorinsky (1963).

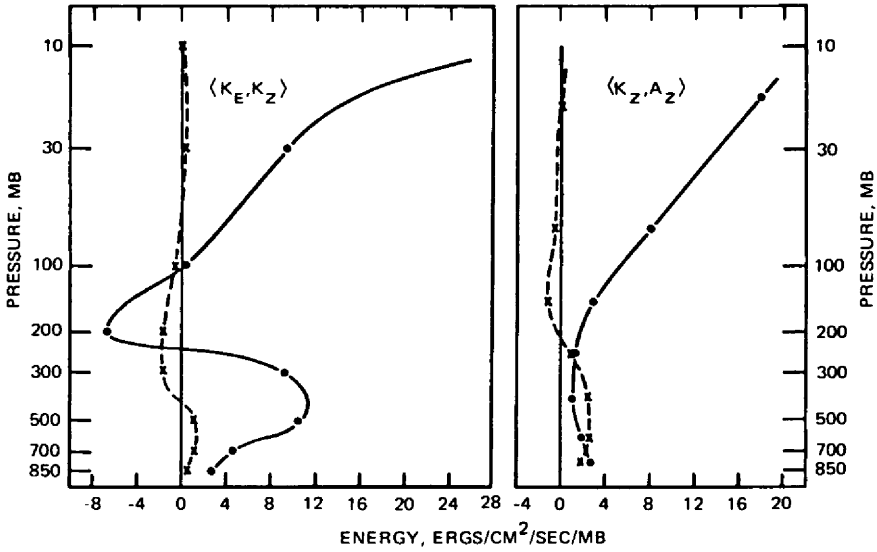
Kung (1966a) finds maximum generation of K_E by pressure forces to be strongest near the jet-stream level. A secondary maximum exists in the planetary boundary layer, where large temperature contrasts and strong ageostrophic components of motion are found.

Figure 3.38 shows that short-term variations in the energy-conversion processes play an important role in characterizing atmospheric energetics. There are seasonal differences, as well as differences between individual years, to consider. This is brought out clearly by Fig. 3.39, which also contains monthly mean values of the conversions. As expected, maximum conversion rates (A_Z , A_E) are realized during the winter months when the mean meridional temperature gradient in troposphere and stratosphere is largest and causes dynamically unstable flow patterns to develop. Chapter 4 will show that the differences in atmospheric energetics between different years are also reflected in the wave-number domain.

Wiin-Nielsen (1967) summarized the seasonal and pressure dependence of the various modes of energy and their transformations for the period February 1963 to



(a)



(b)

Fig. 3.37 Variation with the logarithm of pressure of energy-transformation terms (ergs/cm²/sec/mb) as indicated for two time periods. The solid line is representative of the warming period, January 17 and 22, and the dashed line, the postwarming period, February 16 and 21. [From P. R. Julian and K. B. Labitzke, *Journal of the Atmospheric Sciences*, 22(6): 604; 605 (1965).]

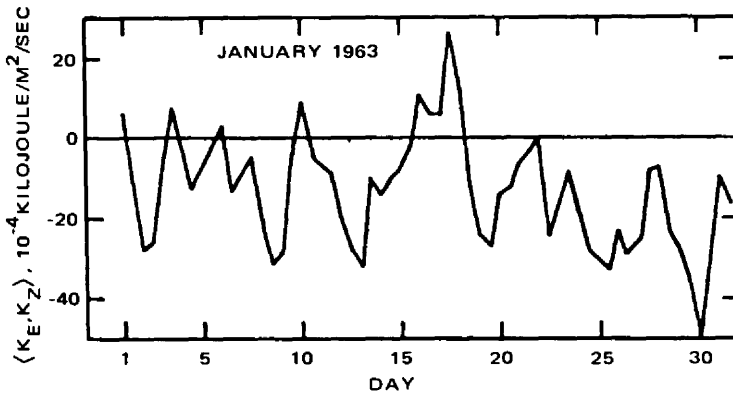


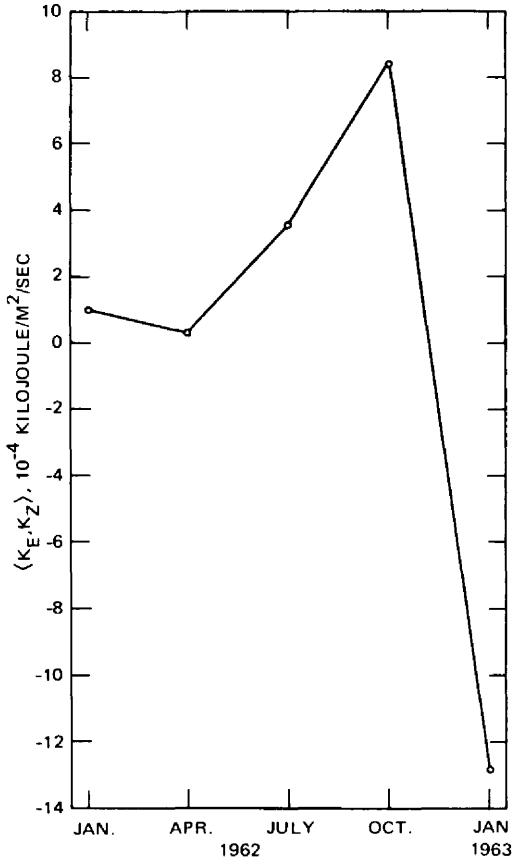
Fig. 3.38 Variation of the daily values of the total energy exchange, $\langle K_E, K_Z \rangle$, as a function of time for January 1963. (Adapted from Wiin-Nielsen, Brown, and M. Drake, 1964.)

January 1964. Results are shown in Figs. 3.40 and 3.41 (see also Fig. 3.34). Noteworthy are the maximums of K_S and of $\langle K_S, K_M \rangle$ in the lower troposphere, as well as at and above the jet-stream level where the main baroclinic processes take place. All modes of energy and of energy conversion with the exception of $\langle K_E, K_Z \rangle$ reveal maximums during the winter season. The $\langle K_E, K_Z \rangle$ appears to be governed mainly by the aspects of atmospheric flow patterns dominating the general circulation within individual months rather than by seasonal effects. The vertical profile of $\langle A_Z, A_E \rangle$ shown in Fig. 3.41 agrees well with the two-day samples given in Fig. 3.37. The annual mean profile of $\langle K_E, K_Z \rangle$, however, reveals marked differences from the profile obtained for the short time period.

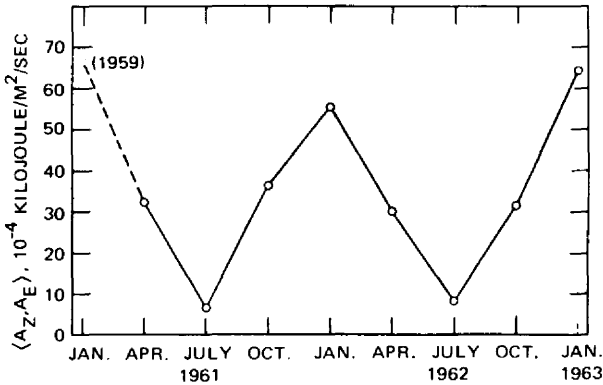
The Heat Budget and the Generation of Available Potential Energy

The eddy transport of sensible heat, produced by a correlation in the departures of v and T from mean values, has been considered by Priestley (1949), White (1954), and later in more detail by Wiin-Nielsen, Brown, and Drake (1963, 1964) (see also Wiin-Nielsen and Vernekar, 1967). There are, again, large seasonal differences, as has to be expected (Fig. 3.42). The largest values for heat transport occur during winter, when largest meridional temperature gradients prevail. The maximum of transport occurs north of the Hadley cell in the region in which the polar front is located (see also Haines and Winston, 1963). The vertical distribution of sensible heat transport will be discussed in Chap. 4. Maximum transport values are found in the lower half of the troposphere, with the exception of July 1962. In the upper troposphere, where the meridional temperature gradient decreases toward the isopycnic jet-stream level, the strong eddy motions $(v)_{(\lambda, t)}$, produce, at best, a small secondary maximum.

According to Haines and Winston (1963), the poleward eddy transport of heat builds up rapidly between August and November and declines less rapidly from



(a)



(b)

Fig. 3.39 Variation of the monthly averages of the total energy exchanges $\langle K_E, K_Z \rangle$ from January 1962 to January 1963 (a) and of the maximum conversion rates $\langle A_Z, A_E \rangle$ from January 1961 to January 1963 (b). [From A. Wiin-Nielsen, J. A. Brown, and M. Drake, *Tellus*, 16(2): 175; 177 (1964).]

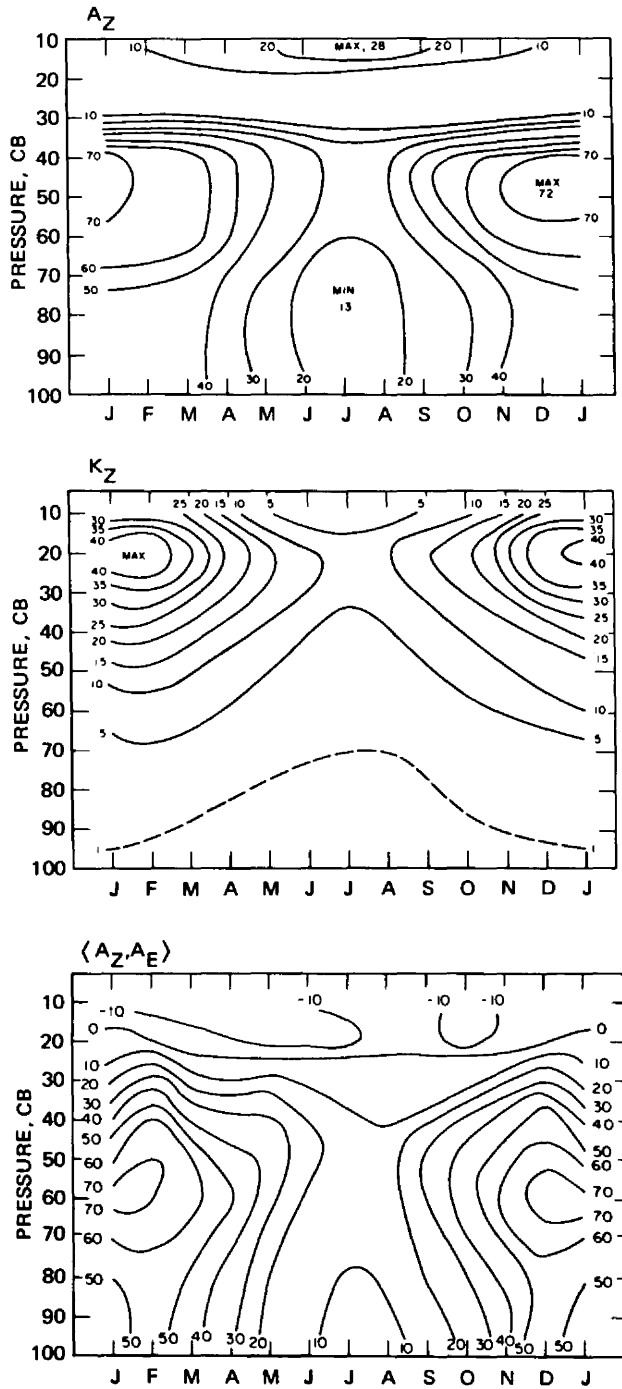


Fig. 3.40 (See page 112 for legend.)

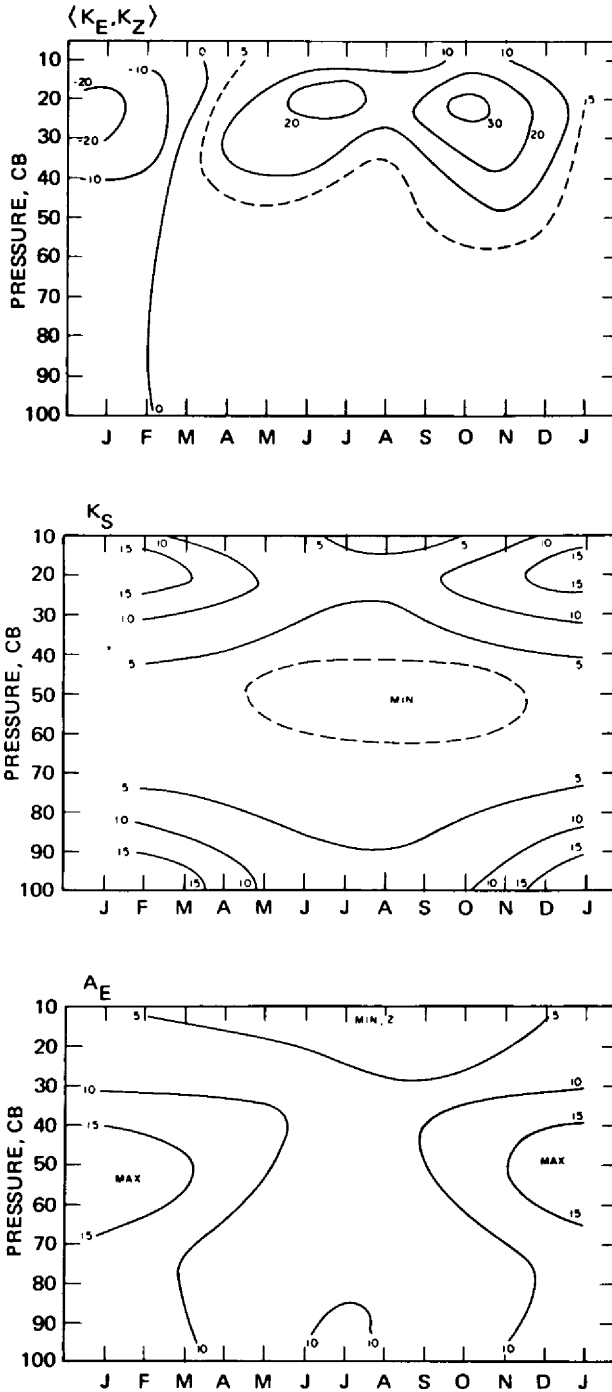


Fig. 3.40 (Continued) (See page 112 for legend.)

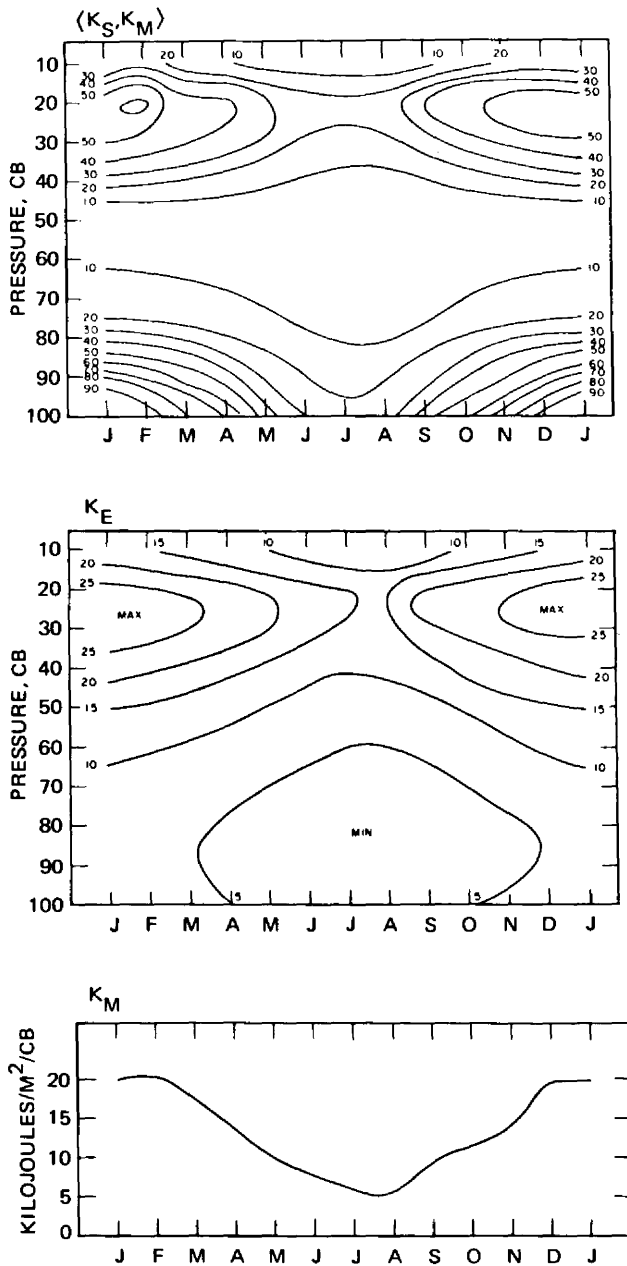


Fig. 3.40 Energies (kilojoules/m²/cb) and energy conversions (10^{-6} kilojoule/m²/sec/cb) as functions of pressure and time of the year (February 1963 to January 1964). [From A. Wiin-Nielsen, *Tellus*, 19(4): 541-544 (1967).]

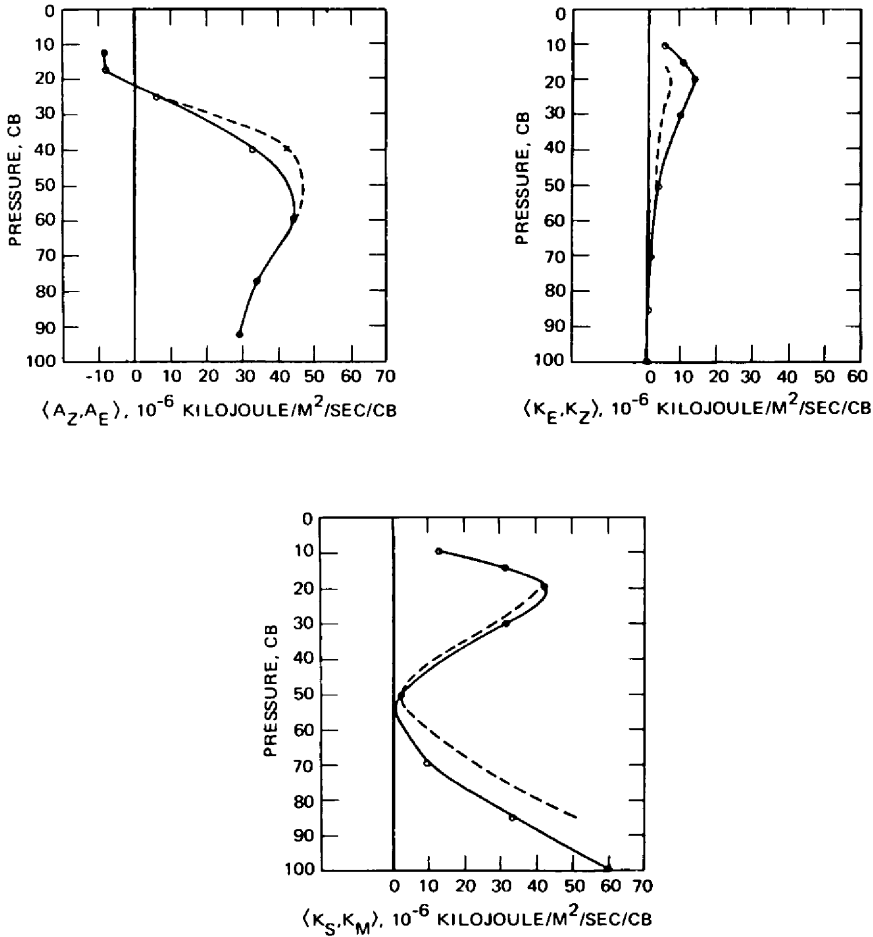


Fig. 3.41 Vertical profiles of the annual mean energy conversions for the periods February 1963 to January 1964 (solid lines) and for the months of January, April, July, and October 1962 (dashed lines). [From A. Wiin-Nielsen, *Tellus*, 19(4): 545 (1967).]

February to June. The longitudinal distribution of poleward heat transport at 45°N is shown in Fig. 3.43. This figure reveals three major regions in which such transports occur, the most outstanding one being associated with the southward movement of cold air to the rear of the East Asian trough. Wiin-Nielsen and Steinberg (1967) showed that these horizontal transport processes in the atmosphere tend to maintain the observed tropospheric temperature variance north of 20°N.

Figure 3.43 gives an indication of the effect of standing eddies on the poleward transport of heat (see also Winston, 1961). With the use of the notation of Eqs. 2.5 and 2.6, this effect is described by a term $[[[T]_{(t)}]_{(\lambda)}([v]_{(t)})_{(\lambda)}]_{(\lambda)}$. Transient

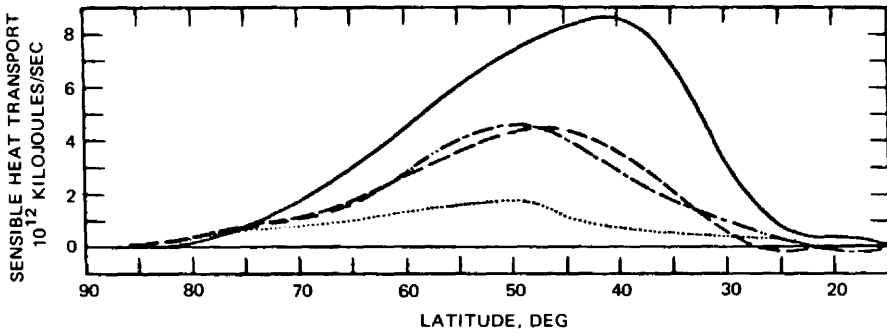


Fig. 3.42 Total northward transport of sensible heat across a latitude circle as a function of latitude. Solid curve for January 1963, dashed curve for April 1962, dotted curve for July 1962, and dashed-dotted curve for October 1962. [From A. Wiin-Nielsen, J. A. Brown, and M. Drake, *Tellus*, 16(2): 169 (1964).]

eddy transport of heat, however, depends on a term of the form $[(T)_{(t)}(v)_{(t)}]_{(t,\lambda)}$. Peixoto (1960) and Starr and Wallace (1964) have shown that transient eddy transports are even more important than standing eddy transports in middle latitudes. In low latitudes standing eddy transports appear to dominate over transient eddy processes. This is evident from Tables 3.10 and 3.11. As shown in these tables and in Table 3.12, the eddy flux of heat in tropical regions is countergradient, especially near the 500-mb level. The negative signs in the eddy transports indicate a heat flux that is directed southward, i.e., with the exception of the lowest tropospheric levels, against the mean, albeit small, temperature gradients.

Estimates of heat sources and sinks and their distribution around the hemisphere have been made by Jacobs (1949) (see also Fritz, 1958) for ocean areas of the northern hemisphere and by Aubert and Winston (1951) for both oceanic and continental regions. More recent data are available by Budyko and Kondratiev (1964) on a global basis. According to the study by Aubert and Winston (1951), large monthly variations, as well as variations between the same months of different years, can be expected in the strength and distribution of sources and sinks. A study by Dickson (1964) reveals the complexity of the problem. Further results have been obtained by Wiin-Nielsen (1959) and by Derome (1966). Figure 3.44 gives the mean relative topography of the layer between 1000 and 100 mb, i.e., the distribution of warm and cold regions in the atmosphere together with the heating computed from a two-parameter atmospheric model (see also Eliassen, 1956), as functions of longitude for the month of January. The importance of wave number 2, produced by the cold Siberian and Canadian trough regions, is clearly evident from this diagram. Main heating takes place near the east coast of Asia and of America (for mean zonal heat budgets over the oceans, see Albrecht, 1961).

More recent computations by Clapp (1961) confirm these results. Since the field of heating is out of phase with that of temperature, one may already conclude qualitatively that planetary waves are strongly influenced by the generation or

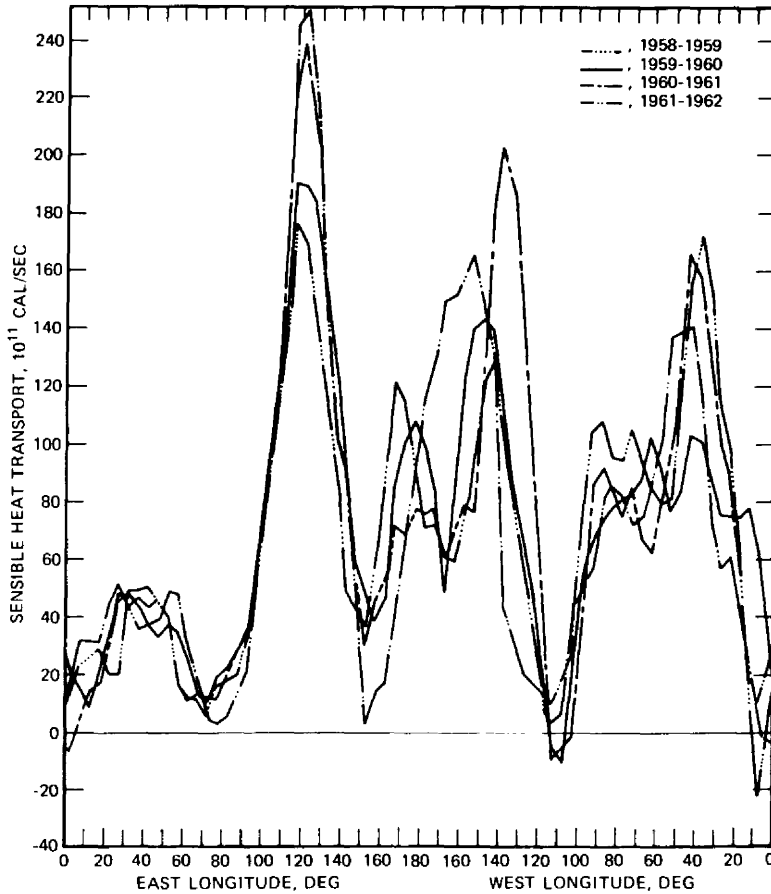


Fig. 3.43 Averages for four consecutive cold seasons (October–March) of contributions in each 5° longitude zone to poleward sensible heat transport across latitude 45°N. [From D. A. Haines and J. S. Winston, *Monthly Weather Review*, 91(7): 325 (1963).]

dissipation of eddy available potential energy. The phase relation between heating and temperature field is rather critical in determining whether A_E will be generated or dissipated. Errors in the estimates of latent-heat release can cause erroneous phase shifts between heating waves and temperature waves (Clapp and Winninghoff, 1963). In a theoretical model of planetary flow, Döös (1962) found the position of the main heat sources to be located about 30° to the west of the temperature maximums of the underlying surface.

A numerical model of the earth's surface heat budget developed by Saltzman (1967) accounts well for the observed surface temperatures at 45° latitude (Fig. 3.45). The effects of various modes of heat transfer on the heat budget are shown in Fig. 3.46 for January and July. The numbers in these diagrams refer to: (1) short-wave

Table 3.10
ZONALLY AVERAGED VALUES OF THE MEAN MERIDIONAL TRANSIENT EDDY
TRANSPORT OF HEAT ($^{\circ}\text{K m/sec}$) FOR YEARLY AND
SEASONAL DATA AT SPECIFIED LATITUDES DURING 1950*

Pressure level, mb	Latitude, degrees								
	70	60	50	45	40	30	20	10	0
Yearly Data									
100	+6.08	+8.82	+6.93	+4.23	+1.89	+1.89	+1.39	-0.87	-0.67
200	+2.49	+4.49	+5.99	+6.25	+5.65	+3.37	-0.62	-1.11	-0.25
300	+0.96	-0.47	-0.36	+1.79	+2.05	+1.75	+0.72	-0.27	-1.04
500	+7.33	+7.95	+6.59	+4.59	+2.54	+0.16	-0.59	-0.74	-0.76
700	+9.71	+11.34	+10.48	+7.79	+6.69	+2.39	+0.48	-0.46	-0.46
850	+9.99	+15.60	+15.94	+13.57	+10.79	+4.00	+1.09	-0.01	-0.49
1000	+2.20	+4.58	+6.82	+7.83	+7.26	+4.29	+1.79	+0.46	-0.35
Summer Data									
100	+0.71	+1.64	+2.52	+1.95	+0.39	-0.20	+0.69	-0.18	-0.11
200	+4.91	+5.56	+7.17	+7.74	+7.52	+3.15	-1.34	-0.60	-0.88
300	+5.55	+3.95	+1.78	+2.35	+2.87	+2.29	-0.26	-0.54	-0.62
500	+6.19	+5.88	+5.28	+3.86	+2.54	-0.73	-0.52	-0.22	-0.34
700	+5.45	+8.84	+7.61	+5.48	+3.78	+0.49	-0.68	-0.52	-0.19
850	+9.11	+12.76	+11.69	+9.02	+6.16	+1.80	-0.29	-0.90	-0.63
1000	+2.56	+4.93	+4.78	+4.21	+3.70	+1.66	+0.56	-0.12	-0.39
Winter Data									
100	+2.90	+8.27	+9.52	+7.25	+6.32	+2.89	-0.89	-2.49	-0.87
200	-0.39	+2.67	+4.53	+6.07	+6.32	+2.46	-1.21	-1.89	-1.11
300	-1.35	+0.22	+2.29	+3.32	+4.14	+2.44	+1.08	-0.56	-1.58
500	+5.85	+6.35	+6.18	+5.06	+3.39	-0.25	-1.18	-1.28	-0.75
700	+9.28	+14.44	+13.56	+10.62	+7.03	+3.76	+0.32	-0.50	-1.12
850	+8.03	+18.00	+18.50	+15.93	+10.86	+5.50	+1.56	-0.12	-0.95
1000	+4.85	+4.90	+6.94	+7.47	+6.40	+3.18	+1.50	+0.32	-0.46

*From V. P. Starr and J. M. Wallace, *Pure and Applied Geophysics*, 58: 142 (1964).

solar radiation; (2) effective long-wave radiation; (3) conduction and convection of heat from the atmosphere; (4) water-phase transformations at the surface; and (5) conduction and convection of heat from below [for references and recent measurements of the conduction and convection of heat from below, see Deardorff (1967)]. The effects of heat addition due to hydrometeors, viscous dissipation, and organic chemical processes have been neglected in this numerical model. Details and references are given in the original paper by Saltzman (1967). A theoretical treatment of the surface heat budget has also been given by Bernard (1962). For measurement results in Sweden, see Högström (1968).

Table 3.11

**ZONALLY AVERAGED VALUES OF THE MEAN MERIDIONAL STANDING EDDY
TRANSPORT OF HEAT ($^{\circ}\text{K m/sec}$) FOR THE WINTER
AT SPECIFIED LATITUDES***

Pressure level, mb	Latitude, degrees							
	70	60	50	45	40	30	20	10
100	-0.74	+0.40	+0.58	+0.60	+0.61	+0.77	-0.30	-0.20
200	-1.48	+0.79	+1.17	+1.20	+1.21	+1.54	-0.61	-0.37
300	-0.13	+5.53	+3.35	+0.20	+0.14	+0.71	-0.65	-1.12
500	-0.53	+6.94	+5.71	+3.37	+1.56	-0.44	-0.62	-0.47
700	+4.16	+5.87	+4.01	+2.24	+1.46	-0.23	+0.05	-0.22
850	+1.68	+0.62	+3.81	+2.05	+0.95	+0.24	-0.72	+0.50
1000	+5.76	+6.49	+2.31	+1.43	+0.15	-0.35	+0.43	+6.43

*From V. P. Starr and J. M. Wallace, *Pure and Applied Geophysics*, **58**: 142 (1964).

The distribution of heat sources and sinks around the hemisphere, shown previously, together with the occurrence of quasi-stationary planetary waves, especially in the domain of low wave numbers (see Chap. 4), suggests that different geographic regions may have characteristic energy budgets of their own which may change from year to year. Such changes are, for instance, indicated by sea surface temperature anomalies and by the interannual variability of snow cover (Namias, 1960, 1969). Such regional studies are not at all plentiful, but they would contribute to a better understanding of the mechanisms that govern the general circulation. Riehl and Malkus (1957) studied the heat balance of the trade winds northeast of Hawaii. They arrived at the important conclusion that the trades export both sensible and latent heat. More recently, Hastenrath (1966) attempted an estimate of the energy budget of the Caribbean area and of the Gulf of Mexico. He found, for instance, that the Caribbean imports latent heat and exports sensible heat during summer (for further details, see the original paper) [see also Ichiye and Zipser (1967) for a case study in the gulf-stream region off the United States east coast and Ninomiya (1968) for a study over the sea of Japan].

From the distribution of heat sources and sinks, Wiin-Nielsen and Brown (1962) and Brown (1964) estimated the generation of available potential energy. The zonal averages of mean monthly heating in the middle and lower troposphere and the monthly averages of the meridional heat flux are summarized in Figs. 3.47 and 3.48, respectively (see also earlier computations by White, 1951a). Seasonal differences, as well as differences between the same months of individual years, are clearly evident. As mentioned previously, January 1963 departs from other years, especially in the magnitude of the meridional heat flux in middle latitudes. In the generation of zonal

Table 3.12

**ZONALLY AVERAGED VALUES OF THE MEAN TEMPERATURE (°K)
FOR YEARLY AND SEASONAL DATA AT SPECIFIED LATITUDES***

Pressure level, mb	Latitude, degrees								
	70	60	50	45	40	30	20	10	0
Yearly Data									
100	226.5	222.6	218.6	215.4	211.7	205.1	200.3	196.3	194.0
200	225.3	222.7	220.6	219.3	218.0	216.8	218.9	219.6	220.6
300	223.6	223.8	227.1	229.9	232.4	236.5	239.2	241.3	242.0
500	243.5	247.3	252.2	255.0	257.7	262.3	265.5	267.3	269.5
700	257.8	261.9	266.8	270.0	273.1	277.9	280.6	281.6	282.6
850	263.7	268.2	273.8	277.1	280.4	285.9	289.3	290.8	291.1
1000	265.5	272.0	279.0	282.1	285.9	293.3	298.2	299.2	296.1
Summer Data									
100	228.9	224.7	218.8	215.3	212.2	206.0	201.6	197.4	194.5
200	226.7	224.4	222.1	220.3	219.5	219.0	218.9	218.8	213.3
300	226.0	227.5	231.1	233.4	235.7	238.9	240.8	242.0	241.4
500	247.9	252.3	256.6	259.2	261.6	264.7	266.5	267.6	269.0
700	262.1	266.9	272.0	274.4	277.1	280.4	282.3	282.0	281.3
850	269.2	274.3	279.5	282.3	285.3	289.7	291.8	291.3	289.4
1000	272.2	278.9	285.1	288.2	291.1	296.3	300.4	299.8	295.7
Winter Data									
100	220.5	220.9	218.5	215.6	211.5	203.8	198.7	194.9	192.7
200	220.4	220.0	218.0	217.0	215.8	216.6	218.9	220.9	221.4
300	216.7	219.6	223.6	226.1	228.7	234.2	238.1	240.8	242.7
500	237.9	241.4	246.8	250.1	253.3	260.1	264.4	267.1	268.8
700	251.5	255.8	261.5	265.2	268.8	275.1	279.3	281.3	282.3
850	256.9	261.2	268.2	271.9	275.9	282.9	287.1	290.3	291.7
1000	254.2	261.2	271.4	276.4	281.5	290.5	295.8	299.6	300.0

*From V. P. Starr and J. M. Wallace, *Pure and Applied Geophysics*, 58: 143 (1964).

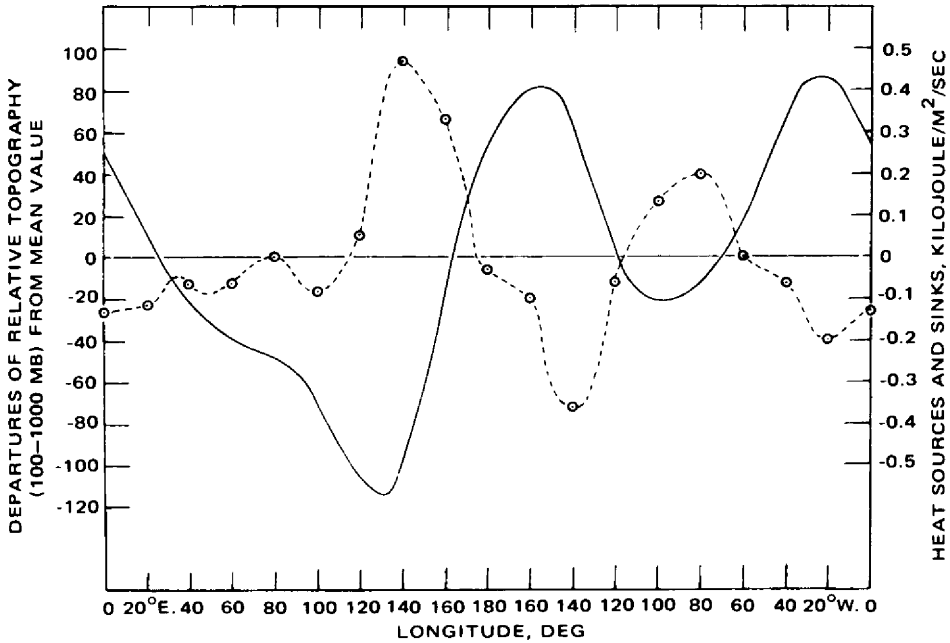


Fig. 3.44 The solid curve is the profile of the mean relative topography along 50°N for the normal maps of January given as departures from the mean value (left scale). The dashed curve gives the latitudinal distribution of heat sources and sinks computed from the same normal maps (right scale). [From A. Wiin-Nielsen, *Monthly Weather Review*, 87(9): 329 (1959).]

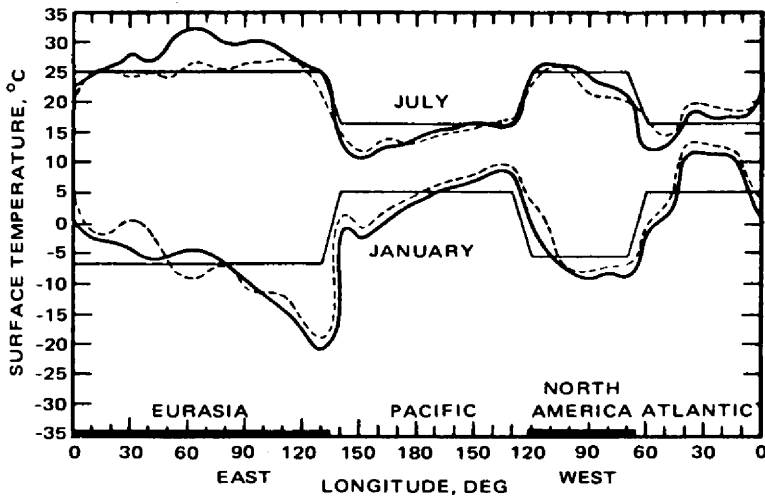
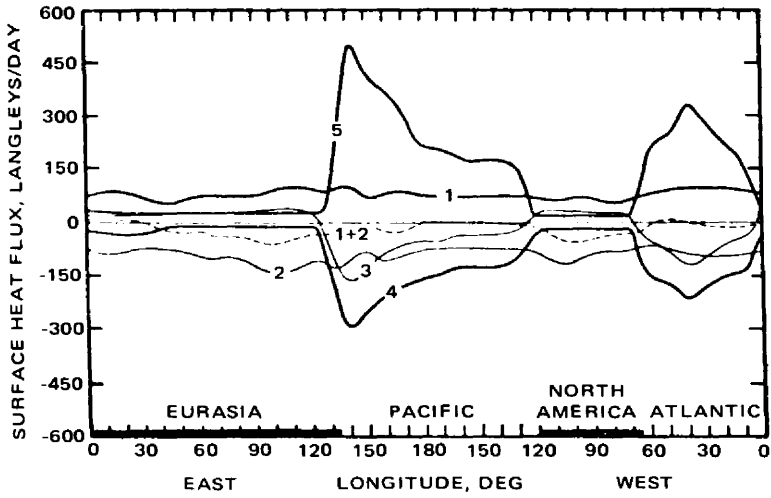
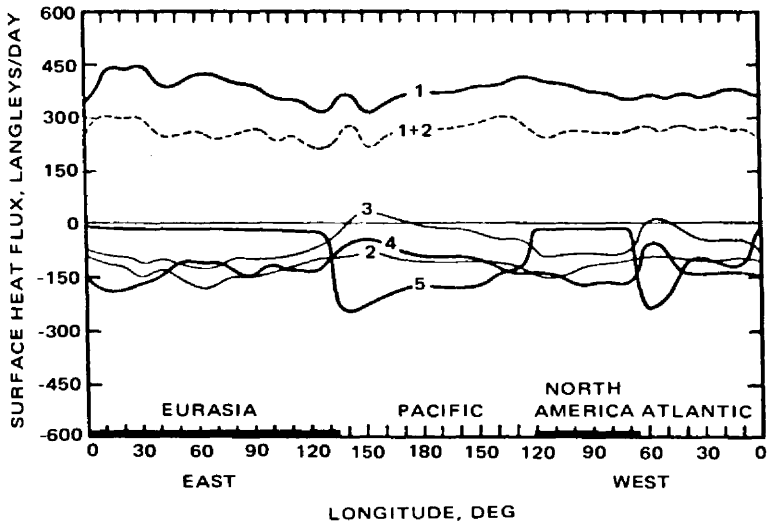


Fig. 3.45 Theoretical distribution of surface temperature around 45°N latitude for January and July (heavy solid curves). Observed distribution shown by dashed curves. Theoretical values for zonal-average values of atmosphere-ocean variables shown by thin curves. [From B. Saltzman, *Tellus*, 19(2): 227 (1967).]



(a)



(b)

Fig. 3.46 Theoretical components of the surface heat balance, $H^{(n)}$ [for explanation of numbers (1 to 5) see text]. (a) January. (b) July. [From B. Saltzman, *Tellus*, 19(2): 227 (1967).]

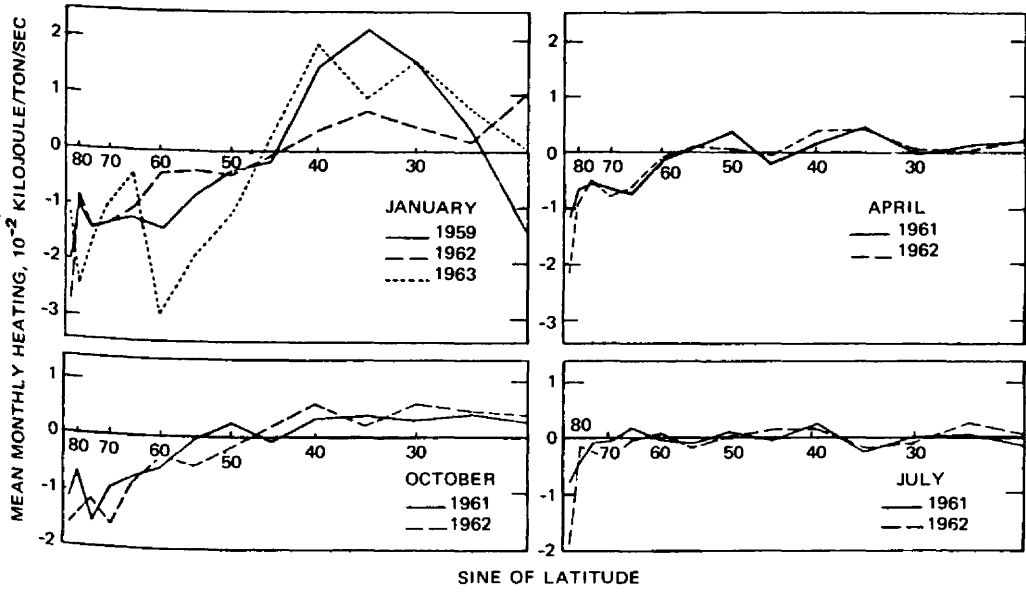


Fig. 3.47 Zonal averages of the mean monthly heating for the 400- to 800-mb layer vs. the sine of latitude. [From J. A. Brown, Jr., *Tellus*, 16(3): 378 (1964).]

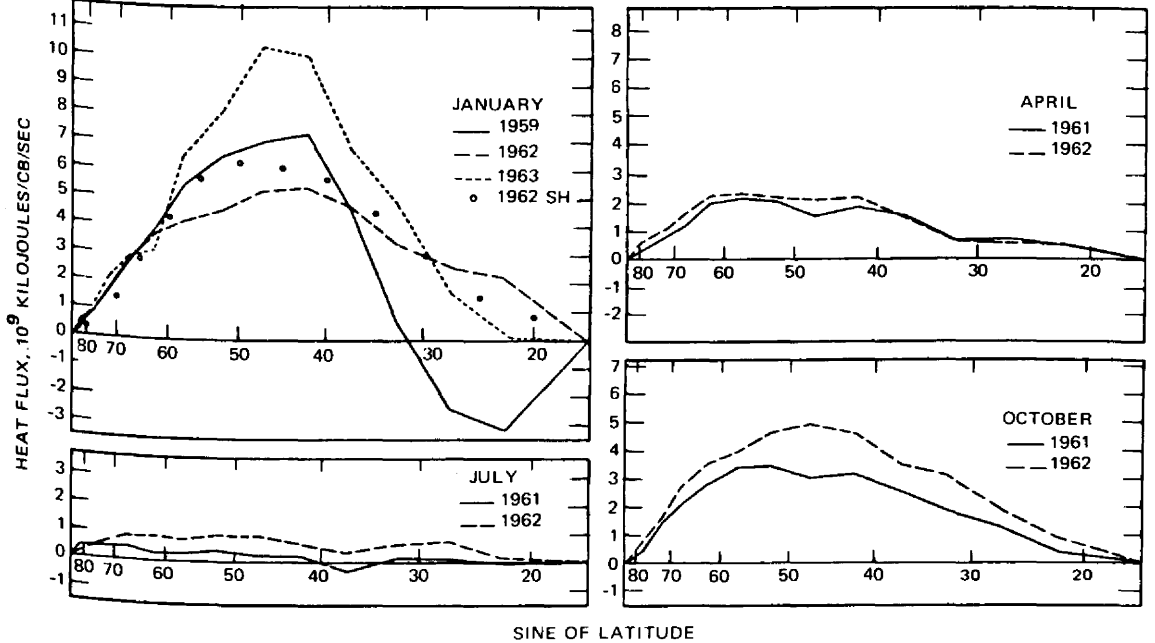


Fig. 3.48 Monthly averages of the meridional heat flux vs. the sine of the latitude. The circles (upper left) represent the sensible heat-flux values obtained by Wiin-Nielsen, Brown, and Drake (1963) for January 1962. [From J. A. Brown, Jr., *Tellus*, 16(3): 379 (1964).]

and eddy available potential energy (Fig. 3.49), there are no striking interannual differences; however, marked seasonal variations are evident. The value of G_Z is positive throughout the year, indicating a warming of air masses at low latitudes and a cooling at high latitudes.

As shown in Fig. 3.50, the outgoing long-wave radiation as measured by satellite (Sabatini and Suomi, 1962; Winston and Rao, 1962, 1963; Raschke, 1965a, 1965b, 1966; Smith, Horn, and Johnson, 1966; Winston, 1967a, 1967b, 1968; Kuhn, 1968) contributes negatively toward the heat budget in middle latitudes where a strong northward gradient of outgoing radiation is observed. This is to be expected since warm air masses radiate more strongly than cold ones. Furthermore, middle and high clouds frequently present at jet-stream latitudes inhibit outgoing radiation but increase the albedo in the visible spectrum range (for satellite measurements, see Arking and Levine, 1967), whereas subtropical latitudes with subsidence and little cloudiness reveal less of a "greenhouse effect" in the infrared (Weinstein and Suomi, 1961; Clapp, 1962; Fritz and Winston, 1962; Fritz, 1963; Kuhn, 1963; Rao and Winston, 1963; Hawkins, 1964; Valovcin, 1968). Thus outgoing long-wave radiation reveals a good inverse correlation with cloudiness-producing vertical motion (Shenk, 1963; Davis, 1965; Bradford et al., 1965; Huang, Panofsky, and Schwalb, 1967; Johnson and Shen, 1968) (Fig. 3.51) and an inverse correlation with albedo (Adem, 1967; Winston, 1967b). Global distributions of cloudiness may be inferred from studies by Clapp (1964), who compiled satellite nephanalyses for the period March 1962 through February 1963 and compared them with conventional data sources. Merritt (1967) analyzed satellite-observed cloud distributions in the tropical and subtropical regions of the northern hemisphere. Sherr et al. (1968) also compiled global cloud statistics.

Such an inverse correlation of outgoing infrared radiation with cloudiness may be the reason why Suomi and Shen (1963) and Shen (1963) found a positive contribution of infrared radiation toward G_E of $+0.583$ watt/m² and $+0.260$ watt/m², respectively, using Explorer VII data. This means that along the same latitude circle warm air is cooled less strongly by outgoing infrared radiation than is cold air (see also Allison and Warnecke, 1966; Raethjen, 1966).

The contribution of outgoing infrared radiation toward G_E seems to be slightly negative from long planetary-scale waves and positive for shorter synoptic-scale waves (Corcoran and Horn, 1965). The mean value, according to their computation, is $+0.055$ watt/m² ($\approx +0.2$ watt/m² by smaller synoptic-scale eddies, -0.1 watt/m² by largest scale eddies). The effect, again, is dominated by the cloud distribution.

Shen (1963) and Johnson (1967) found the zonal generation, G_Z , by outgoing infrared radiation to be negative in a pressure coordinate system (-1.75 watts/m² and -1.92 watts/m², respectively). In isentropic coordinates, however, G_Z is positive ($+1.61$ watts/sec) (Johnson, 1967; Dutton and Johnson, 1967). This is so because the mean slope of isentropic surfaces retains the effect of net heating at high pressure (in low latitudes) and net cooling at low pressure (in high latitudes).

The rate of absorption of solar radiation in the atmosphere is higher in moist (warm) air than in dry (cold) air and hence should also contribute positively toward G_Z and G_E (see, for example, Katayama, 1966). According to Korb and Möller

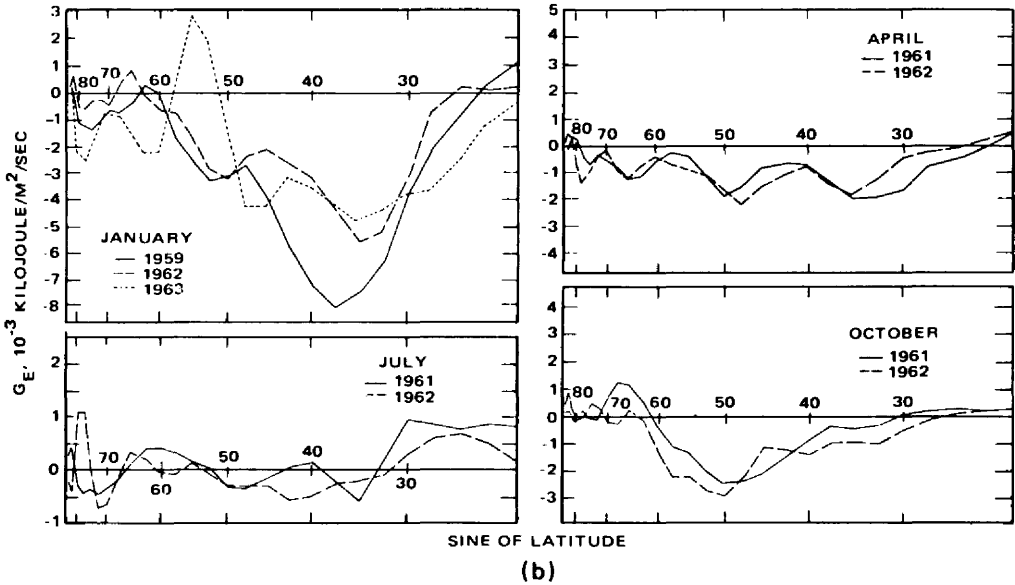
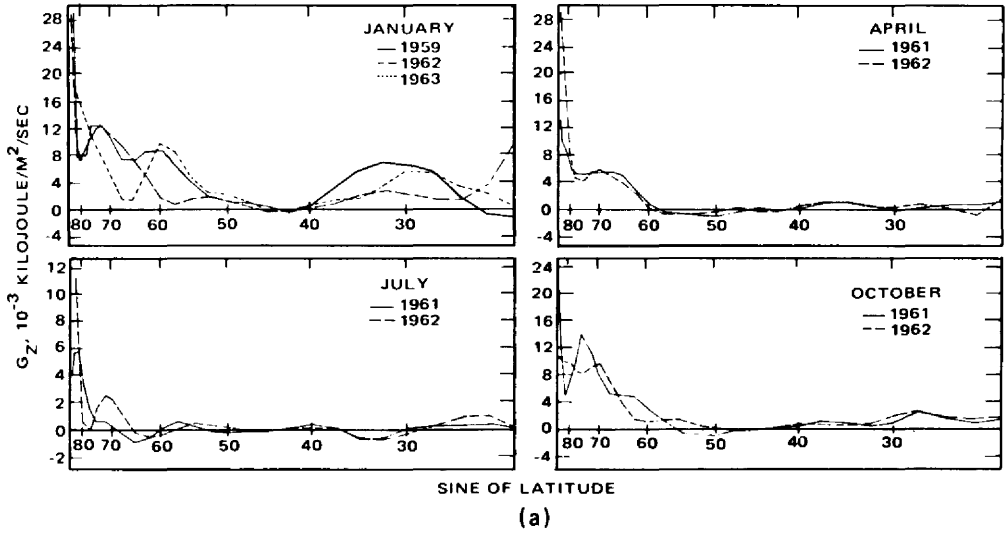


Fig. 3.49 Monthly mean of G_Z (a) and of G_E (b) for the 1000- to 200-mb layer vs. the sine of latitude. [From J. A. Brown, Jr., *Tellus*, 16(3): 380; 381 (1964).]

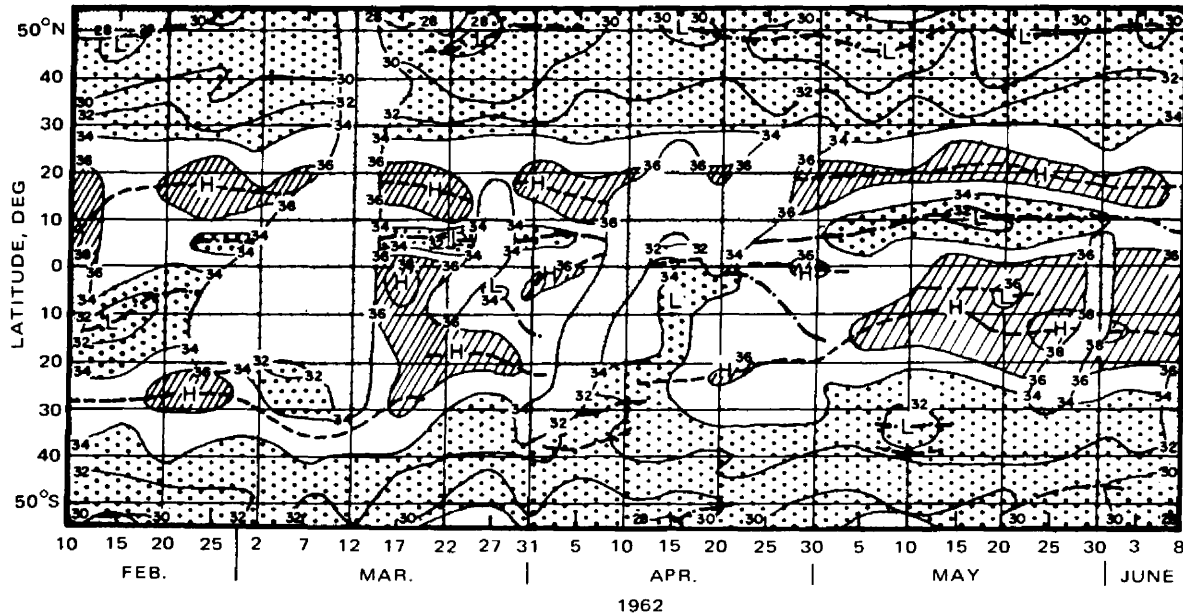


Fig. 3.50 Time-latitude chart of five-day mean outgoing long-wave radiation (10^{-2} langley/min) averaged over the Pacific sector ($120^{\circ}\text{E}-125^{\circ}\text{W}$). Hatching indicates values greater than 0.36 langley/min; heavy stippling, values less than 0.34 langley/min; and light stippling, insufficient data for useful analysis. ---, latitudinal maximum of radiation. -.-, latitudinal minimum of radiation. These are so indicated only if a maximum or minimum has definite continuity for at least two consecutive five-day periods. H and L refer to maximums and minimums, respectively, in both latitude and time. [From J. S. Winston, *Journal of Applied Meteorology*, 6(3): 454 (1967).]

(1962), the rate of absorption in warm moist air may be twice as high as that in cold dry air. In the warm moist air, it is enhanced by the presence of clouds. However, heat absorption by the ground is less in moist and cloudy regions than in dry ones (Hanson, Haar, and Suomi, 1967). The heat absorption by the ground enters the heat budget of the earth's surface.

As shown in Fig. 3.49, minimum values of G_Z appear near jet-stream latitudes slightly north of 40°N during January. For a limited region over the eastern United States and the Caribbean Sea, Johnson (1967) found even negative values of G_Z by infrared radiation prevailing during December 1960 and January 1961 (-1.92 watts/ m^2). His data were obtained from radiometersonde flights.

Wiin-Nielsen (1967) also estimated the total generation of available potential energy from the balance requirements of the energy equations. If he allows for frictional dissipation not only in the boundary layer but also in the free atmosphere as Kung (1966a) does, his estimates of G appear to be too large (71.6×10^{-4} kilojoules/ m^2 /sec vs. 21×10^{-4} kilojoules/ m^2 /sec if all dissipation took place in the surface boundary layer only).

As shown in Fig. 3.49, eddy available potential energy is dissipated by diabatic processes ($G_E < 0$) except for July, when mean values appear to lie close to zero. Maximum dissipation occurs during January at latitudes between 30°N and 50°N . This is the region in which frequent cold outbreaks occur, especially in the quasi-permanent troughs to the lee of the Rocky Mountains and the Himalayas. The cold air flowing south is heated rapidly. Warm air intrusions toward the north, which are subject to cooling, will have a similar effect on G_E in the same latitude belt (for a case study, see Houghton, 1962). This conclusion is corroborated by Johnson (1967) (see also Dutton and Johnson, 1967; Johnson, 1965, 1966), who utilized radiometersonde data over the eastern United States and the Caribbean Sea. During December 1960 and January 1961, infrared radiation produced a sink of available potential energy over the area under consideration [-0.13 watt/ m^2 was attributed to transient eddies and -0.08 watt/ m^2 to stationary eddies. These values are smaller than the one of -1.92 watts/ m^2 for the destruction of zonal available potential energy quoted before from the study by Johnson (1967)]. Large interdiurnal variations and the intermittent occurrence of positive values of G_E as well as of G_Z , especially in the lower troposphere, indicate the importance of the varying distribution of water vapor and cloudiness.

The satellite measurements by TIROS IV, shown in Fig. 3.50, agree with these conclusions. Figure 3.51 shows that south-north gradients of outgoing long-wave radiation correlate well with anticyclonic shears in the lower troposphere (850 to 500 mb). This means that in eddy-flow processes and in cloudiness associated with jet streams the portion of G_Z attributable to outgoing long-wave radiation is negative and, at least to a certain extent, proportional to the intensity of the jet, i.e., to the baroclinicity and to the horizontal temperature gradient with which the jet is associated.

The total (extraterrestrial) radiation balance for the top of the atmosphere, which is composed of reflected short-wave radiation and emitted long-wave radiation (as

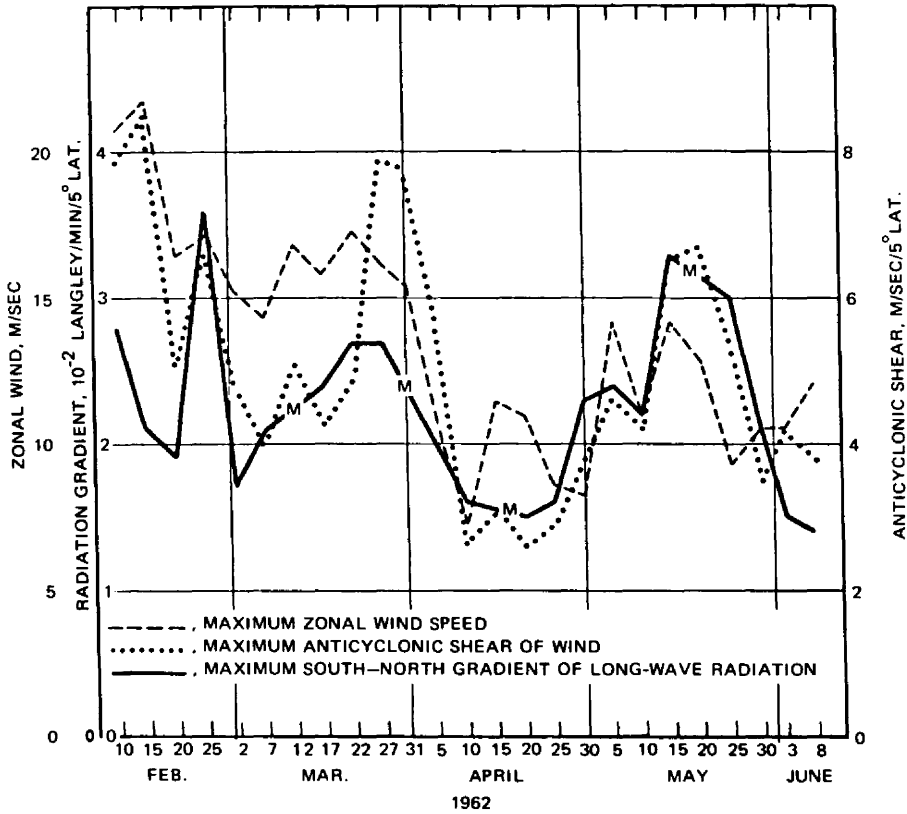


Fig. 3.51 Maximum value of south-north gradient of outgoing long-wave radiation in each five-day period between 17.5°N and 52.5°N as compared with maximums in 850- to 500-mb zonal wind speed and anticyclonic shear of the zonal wind between 20°N and 60°N . Five-day periods when maximums in radiation gradient could not be determined because of insufficient data are indicated by M. [From J. A. Winston, *Journal of Applied Meteorology*, 6(3): 457 (1967).]

measured, for instance, by NIMBUS II), reveals a highly interesting difference between the summer (northern) and winter (southern) hemispheres (Möller, 1967; Raschke, Möller, and Bandeen, 1968). In the winter hemisphere the main contribution of the radiation balance seems to be a positive generation, G_Z . Over the summer hemisphere, however, no uniform gradient of the radiation balance from pole to equator can be recognized (Fig. 3.52) (see also Ashbel, Eviatar, and Doron, 1961). It appears, therefore, that effects of G_E are dominant during the summer season. Möller (1967) points out that measured values of the reflected short-wave radiation are, on the average, lower by a factor of 1.5 than those computed by London (1957).

The seasonal variations of G_Z and G_E have been summarized by Brown (1964) in Fig. 3.53. The total of $G_Z + G_E$, also shown in this diagram, constitutes the net diabatic effect that drives and maintains the general circulation of the atmosphere. The



Fig. 3.52 The extraterrestrial radiation budget in a two-week period from July 2 to 15, 1966, from measurements of the reflected solar radiation and the emitted infrared radiation made by NIMBUS II (cal/cm²/min) (Raschke, Möller, and Bandeen, 1968).

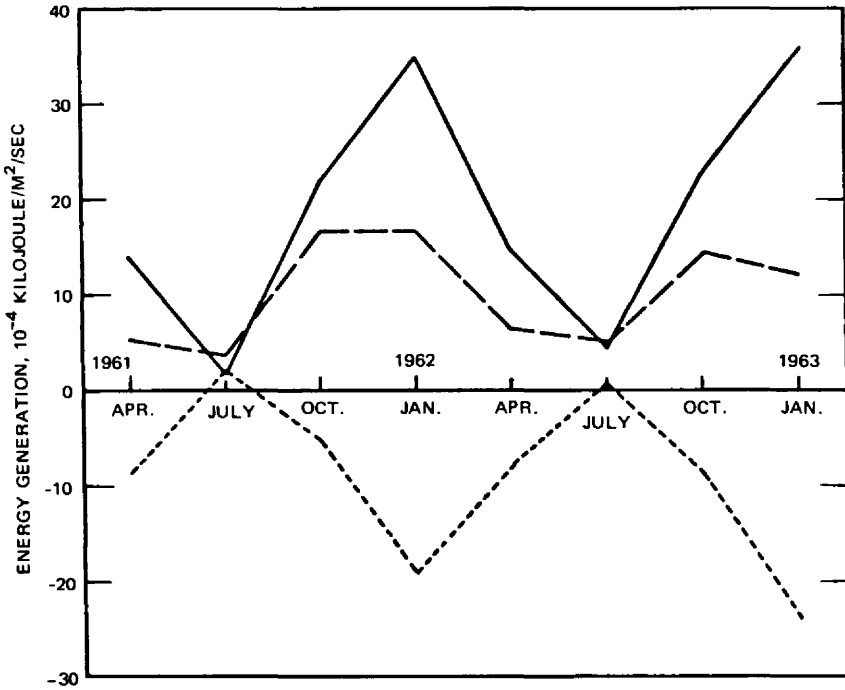


Fig. 3.53 Monthly averages of G_Z (solid line), G_E (small dashed line), and $G_Z + G_E$ (large dashed line) vs. time. [From J. A. Brown, Jr., *Tellus*, 16(3): 385 (1964).]

contribution from G_E toward this net effect is negative except for July (see also Fig. 3.49). The monthly averages of G_Z are positive throughout the year. Since these data were compiled from daily 500- to 850-mb thickness and heating fields, they incorporate the total heat budget of the atmosphere, including the release of latent heat. During July G_Z reaches a minimum. The values of G_E during this month, therefore, will constitute a sizeable fraction of the total diabatic effects ($G_Z + G_E$), thus confirming the conclusions reached by Möller (1967) and Raschke, Möller, and Bandeden (1968) and shown in Fig. 3.52 (see also Haar and Suomi, 1969).

In Fig. 3.54 the annual average of diabatic heating computed by Brown (1964) is compared with results by other authors. Brown assumed the net heating between pole and equator to be zero. However, south of 20°N he used values obtained by Smagorinsky (1963) and inferred from London's (1957) radiation balance and Budyko's (1956) heat balance of the earth (see also Budyko and Kondratiev, 1964). Houghton's (1954) results, shown in this diagram, represent the annual mean of the net radiational heating at the tropopause, whereas London's values refer to the radiation balance at the top of the atmosphere. The profiles by Brown and Smagorinsky given in Fig. 3.54 include both latent and sensible heat exchanges at the

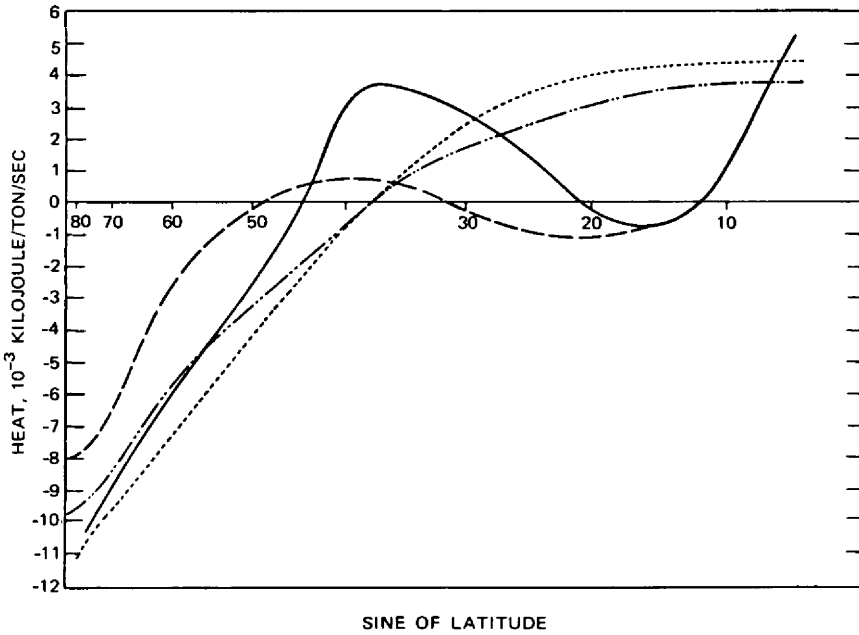


Fig. 3.54 Adjusted mean diabatic heating computed by Brown (1964) (solid line), Houghton (1954) (small dashed line), London (1957) (dash-dotted line), and Smagorinsky (1963) (large dashed line) vs. sine of latitude. [From J. A. Brown, Jr., *Tellus*, 16(3): 385 (1964).]

earth's surface. Additional data on the atmospheric heat balance not reproduced here have been published by Berliand (1956) (see Holopainen, 1965); Davis, 1963; Asakura and Katayama, 1964; and Möller, 1960. Möller found especially the values of outgoing long-wave radiation to be lower than the estimates by Houghton (1954) but in close agreement with the results obtained by London (1957).

Differences between Brown's results and Smagorinsky's model may in part be caused by the choice of the time period from which the observational data were taken and by the assumption that the heating computed by Brown was representative for the entire atmosphere. This latter assumption may not be quite justified. An investigation by Davis (1963), for instance, revealed that the layer between 1000 and 500 mb may show a net heating between 20°N and 60°N, whereas the layer between 1000 and 25 mb reveals a loss of heat energy at all latitudes.

Net heating or cooling rates for the stratosphere are difficult to estimate (see, for example, Kennedy, 1964). They depend critically on the assumptions of moisture distribution above the tropopause. From model calculations, Jurica (1966) infers that a moist stratosphere (with a constant 5% relative humidity) would show a layer of heating during January approximately 25 to 50 mb below the tropical troposphere (near 100 mb). However, a dry stratosphere shows no such layer. A decrease with

altitude of net radiative flux below the tropopause, found by Riehl (1962a) over the Caribbean and by Kuhn and Suomi (1960) over the United States, would indicate such a warming zone produced by vertical radiative flux convergence. At higher levels, near 25 mb, radiative cooling rates computed by Jurica (1966) may vary between 0 and 1°C per day, depending on dry or moist assumptions for the stratosphere.

Vertical Heat Transports

The vertical mean and eddy transports of latent and sensible heat, averaged for October 1961, have been discussed by Berggren and Nyberg (1967) for the region north of 30°N. The latent heat transport through the 700-mb surface

$$F_M = -\frac{L}{g} [(\omega)_{(t,\lambda)}(S)_{(t,\lambda)}]_{(t,\lambda)} \quad (3.73)$$

and the sensible heat transport through the same pressure level

$$F_T = -\frac{c_p}{g} [(\omega)_{(t,\lambda)}(T)_{(t,\lambda)}]_{(t,\lambda)} \quad (3.74)$$

where S is the mixing ratio of water vapor and L is the latent heat of evaporation, are plotted in Fig. 3.55. The values of F_T obtained by Berggren and Nyberg agree well with the results obtained earlier by White and Saltzman (1956), Wiin-Nielsen (1959), and Saltzman and Fleisher (1960a, 1961). As shown in this figure, the vertical transport of latent heat has nearly as strong a warming effect on the atmosphere above 700 mb as the transport of sensible heat. The total heat transport is equivalent to a 24-hr warming of the layer 700 to 300 mb at 85°N of 0.4°C and of the layer 700 to 200 mb at 50°N of 2.3°C. The vertical transport of heat thus appears to be at least of the same order of magnitude as the horizontal transport (Nyberg, Duvedal, and Fryklund, 1954; Shaw, 1966). The total vertical heat transport through the 700-mb surface, according to Berggren and Nyberg (1967), in itself would be large enough to compensate for the net radiational heat loss in the middle and upper troposphere (as computed, for instance, by Davis, 1963; London, 1957; Möller, 1951a; and Karsten et al., 1959) except at low latitudes. This leads Berggren and Nyberg to the conclusion that the vertical heat transport "by small-scale convective processes in cumulus and cumulonimbus is of little significance compared to the vertical transport by large-scale eddies associated with cyclones and anticyclones in middle and high latitudes, at least in layers above the level of a few kilometers."

Shaw (1966) also reaches the conclusion that transient eddies play an important role in the heat transport by considering mean and eddy terms in the thermodynamic equation. However, as has been pointed out by many authors, convective heat transport in "hot towers" seems to be dominant in tropical regions. According to

Rosenthal (1967), even in the subtropical oceanic regions, organized convection and the release of latent heat therefrom may be a driving agent for large-scale disturbances. The statistics by Berggren and Nyberg apply to extratropical latitudes where organized vertical motions along inclined isentropic surfaces are characteristic for cyclone eddies.

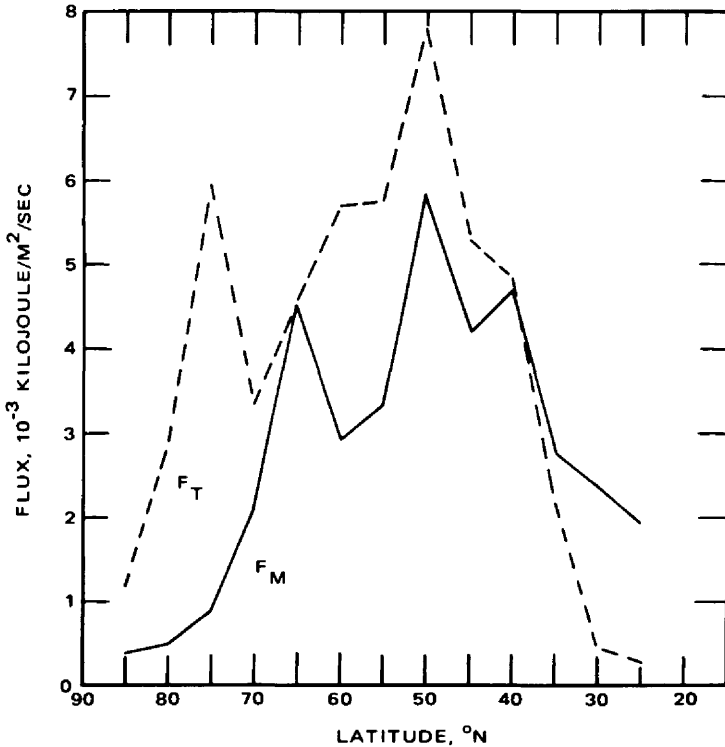


Fig. 3.55 Latitudinal mean values for mean meridional flux (F_M) and total flux (F_T), respectively, for October 1961. [From K. Berggren and A. Nyberg, *Tellus*, 19(1): 20 (1967).]

In the tropics, however, the atmosphere is nearly barotropic, and the vertical transport of latent and sensible heat apparently is more efficiently accomplished by the smaller scale eddy processes of convection. It should be recognized, however, that even in the tropics small-scale convective activity and associated vertical transports of sensible and latent heat may vary considerably with the synoptic conditions. In general, more heat is transferred from the ocean to the atmosphere during disturbed periods than during undisturbed periods. Over limited regions of the disturbance, the heat transfer can increase by an order of magnitude. The average transfer integrated over the area of the disturbance may be twice as large as that over the undisturbed area (see Table 3.13, Garstang, 1967).

More recently, Palmén (1966b) estimated the atmospheric heat budget in extratropical regions by layers, using the balance equation for a belt of latitude with the area A

$$R_a + Q_s + LP + \frac{W_{\phi_n} - W_{\phi_{(n+1)}}}{A} = 0 \quad (3.75)$$

where R_a = radiation effect [Mean values of this quantity obtained by London (1957) have been used in Palmén's study.]

Q_s = turbulent heat flux from the earth's surface (Since this quantity is difficult to estimate from observations, it has been determined as a residual from Eq. 3.75.)

L = latent heat of condensation

P = rate of precipitation [taken from data by Möller (1951a) but modified somewhat for the tropics to fit the estimates by Meinardus (1934)]

W_{ϕ_n} = heat flux through the latitude boundary ϕ_n

$$W_{\phi_n} = \frac{2\pi a \cos \phi}{g} \left\{ \int_0^{p_0} (c_p [T]_{(\lambda,t)} + [\Phi]_{(\lambda,t)} + [K]_{(\lambda,t)}) [v]_{(\lambda,t)} dp \right. \\ \left. + \int_0^{p_0} (c_p [(T)_{(\lambda,t)}(v)_{(\lambda,t)}]_{(\lambda,t)} + [(\Phi)_{(\lambda,t)}(v)_{(\lambda,t)}]_{(\lambda,t)} \right. \\ \left. + [(K)_{(\lambda,t)}(v)_{(\lambda,t)}]_{(\lambda,t)} dp \right\} \quad (3.76)$$

where Φ is the geopotential and K is the kinetic energy. Palmén used Holopainen's (1965) computations in estimating this term. Results are shown in Fig. 3.56. Horizontal (based on data by Mintz, 1954) and vertical arrows indicate fluxes of sensible heat. The lower troposphere shows the largest values in all these terms. Figure 3.57 shows the computed heat budget for tropical and extratropical regions. The conclusions by Berggren and Nyberg (1967) on the importance of vertical large-scale eddy transports quoted previously are essentially corroborated by Palmén's study. Q_s , computed as a residual of Eq. 3.75, turns out to be larger than the results by Budyko (1963). This may be due to a slight overestimate of radiational cooling, R_a . However, Budyko's values possibly may be too small, especially during the winter season when Q_s is large in oceanic regions (Petterssen, Bradbury, and Pedersen, 1962).

According to Palmén, the physical nature of the vertical heat flux is essentially different from that of the horizontal flux. The horizontal heat flux is mainly accomplished by large synoptic-scale eddies, whereas a wide-spectrum range of eddies of different scale has to be considered in the vertical heat flux. Treatment of the synoptic-scale vertical eddy transports, therefore, would not give a complete picture of vertical heat flux, especially not in tropical regions with their strong, but small-scale, cumulus convection.

The turbulent heat flux from the earth's surface, Q_s , in the lowest layers of the atmosphere is almost entirely a result of small-scale turbulence by which sensible heat

Table 3.13

HEAT TRANSPORT FROM THE OCEAN TO THE ATMOSPHERE
(cal/cm²/day) UNDER VARYING SYNOPTIC CONDITIONS*

	Q _e		Q _s		Q		Bowen ratio†	
	1957	1963	1957	1963	1957	1963	1957	1963
Undisturbed trades	265.2	371.8	3.1	14.0	268.3	385.8	0.012	0.038
Disturbed modes	309.4	396.2	24.0	28.5	333.4	424.7	0.078	0.071
Weak and moderate trades	254.2	326.0	3.0	14.4	257.2	340.4	0.012	0.044
Moderately disturbed modes	492.8	408.2	35.1	31.2	527.9	439.4	0.071	0.076

*From M. Garstang, *Tellus*, 19(3): 496 (1967).

†Defined as R = Q_s/Q_e.

is carried upward. The same holds for the transport of latent heat measured by evaporation from the ground. This turbulent transport in the lower atmosphere is directed upward in spite of the stable stratification that prevails on the average. The importance of this heat flux by "convective turbulence" has been stressed by Ertel (1942), Priestley and Swinback (1947), and Priestley and Sheppard (1952). Deardorff (1966) also points out that the upward eddy flux of heat in the lower atmosphere is directed against the mean gradient. Thus it does not correspond to the Fickian diffusion equations, which assume a proportionality of the transport to the gradient of the quantity to be transported. Such flux is to be expected if the triple correlation term

$$-\frac{\partial}{\partial z} \frac{[(\omega)_{(x)}(\theta)_{(x)}^2]_{(x)}}{2}$$

is positive and exceeds the effect of temperature changes caused by diabatic effects.

In the lower stratosphere we also find non-Fickian transport processes of heat (and of ozone) operating in a meridional direction. These processes are directed against the mean gradients of these atmospheric properties and thus have to be accomplished by eddies. Reed and German (1965) incorporated these conclusions into a large-scale diffusion model which yielded reasonable results for tungsten, ¹⁸⁵W, transports (see Part 2 of this review, *Chemical Tracers*).

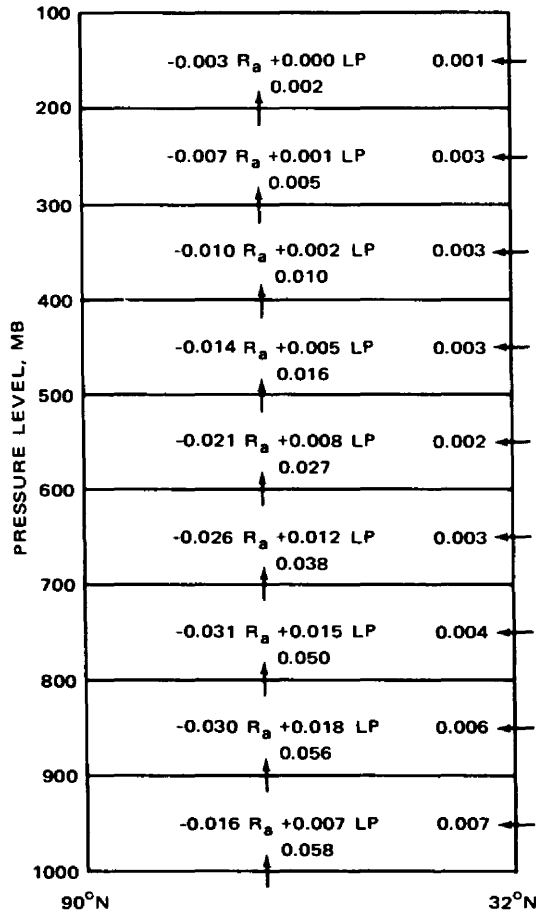


Fig. 3.56 Mean energy budget of standard isobaric layers in the cap north of 32°N . Arrows show horizontal and vertical flux of sensible heat (langley/min). R and LP represent radiation and latent-heat effects, respectively. [From E. Palmén, *Tellus*, 18(4): 841 (1966).]

With increasing distance from the ground, the effect of convective turbulence decreases, and the synoptic-scale eddy transport provides most of the heat flux. Even though during winter convective clouds appear over large regions, most of them do not reach very high altitudes (Petterssen, Bradbury, and Pedersen, 1962). In the upper clear regions of the atmosphere, small-scale turbulence tends to transport heat downward because of the prevailing stability of the atmosphere. Conditions thus described have been estimated numerically by Palmén (1966b) (Fig. 3.58).

From the vertical heat flux caused by large-scale disturbances, Palmén estimates the rate of generation of kinetic energy to be about 5.5 watts/m^2 . This comes close to the amount of frictional dissipation of kinetic energy in the troposphere, estimated by

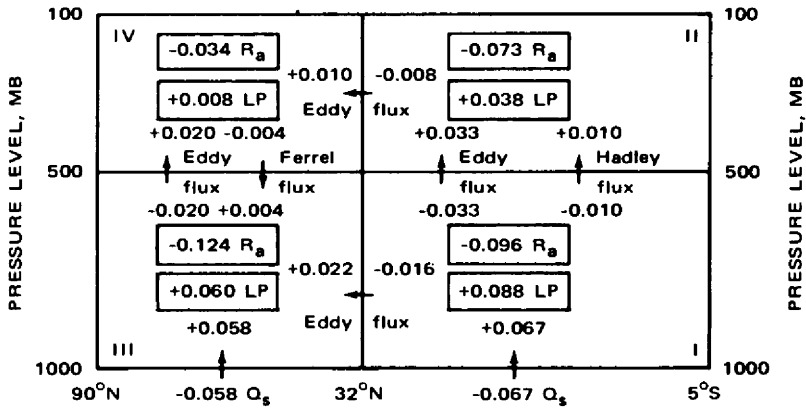


Fig. 3.57 Tentative energy budget of the region 5°S–90°N in winter and vertical energy fluxes through the 500-mb surface (langley/min). [From E. Palmén, *Tellus*, 18(4): 840 (1966).]

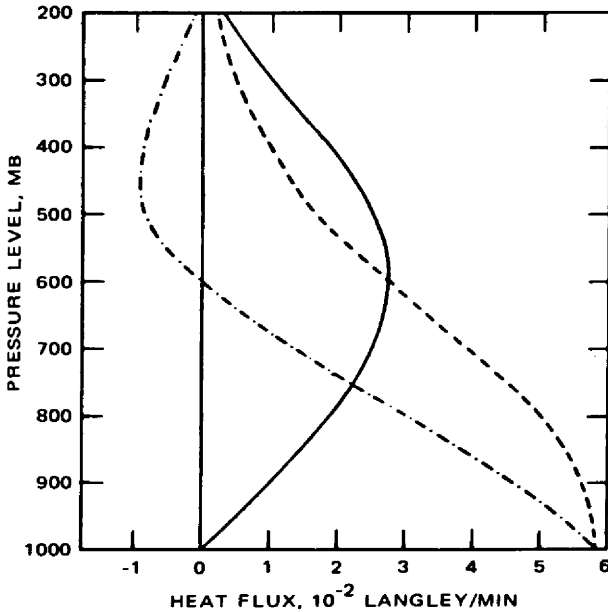


Fig. 3.58 Separation between small-scale vertical heat flux (dash-dotted curve) and synoptic-scale vertical heat flux (solid curve). The dashed curve represents the mean total flux derived from Fig. 3.56. [From E. Palmén, *Tellus*, 18(4): 842 (1966).]

Brunt (1934) to be 5 watts/m². However, since there also is kinetic-energy advection across the lateral boundary of the region under consideration, Brunt's value of dissipation appears to be too low (see p. 141).

The Flux of Water Vapor

The importance of water-vapor transports in maintaining the general circulation has been stressed by a number of authors (e.g., Starr, 1951b; White, 1951b; Benton and Estoque, 1954; Sutcliffe, 1956; Hutchings, 1957, 1961; Peixoto, 1958, 1959; Starr and Peixoto, 1958, 1960, 1964; Lufkin, 1959). Schmitz (1963) developed a system of equations governing the transport of water in solid, liquid, and vapor form. (For details consult the original paper.) Unfortunately, the quality of upper-air humidity measurements taken on a routine basis leaves something to be desired, and thus divergent results in some of the investigations will have to be expected.

Boogaard (1964) studied the horizontal mean and eddy transport of water vapor for Dec. 12, 1957, between the equator and 40°N. He considered

$$[qv]_{(\lambda)} = [q]_{(\lambda)} [v]_{(\lambda)} + [(q)_{(\lambda)}(v)_{(\lambda)}]_{(\lambda)} \quad (3.77)$$

where q is the specific humidity. Results are shown in Fig. 3.59. These diagrams are to be compared with Fig. 2.5, which contains the mean meridional mass circulation for this particular day. The centers of total flux lie close to the 900-mb level, in agreement with earlier studies by Benton and Estoque (1954) and recent results by Rasmusson (1967, 1968) and Barry (1967) over the North American continent, by Hutchings (1957, 1961) over England and Australia, by Flohn, Henning, and Korff (1965) over North Africa, and by Drozdov and Grigor'eva (1965) over the USSR. Above the 500-mb level, the water-vapor flux is very weak. South of approximately 25°N, according to Boogaard (1964), the equatorward transport in the mean meridional Hadley cell prevails. The lower limb of the indirect Ferrel cell transport only little vapor northward. The bulk of the poleward flux in temperate latitudes is provided by eddies. (For details of this transport in the wave-number space, see Chap. 4.) This also becomes evident from studies by Starr, Peixoto, and Livadas (1958) for the year 1950, by Barnes (1965), and by Peixoto and Crisi (1965) for the IGY period; results by Peixoto and Crisi are shown in Fig. 3.60. (In this figure N indicates north winds, i.e., southward transport.)

Zonally integrated profiles of water-vapor flux (northward flux greater than zero) are shown in Fig. 3.61 for Dec. 12, 1957. The lower part of this figure contains estimates of the divergence and convergence of water vapor [zonally averaged evaporation $[E]_{(\lambda)}$ minus zonally averaged precipitation $[P]_{(\lambda)}$] for the same day. Three zones can be distinguished: From 0°N to 10°N precipitation exceeds evaporation. This is the region of the equatorial trough zone with abundant rains. In the prevailing anticyclonic regime between 10°N and 35°N, evaporation exceeds precipitation. North of 35°N precipitation prevails in eddy disturbances underneath the subtropical and polar-front jet streams. The results obtained by Boogaard (1964) fit reasonably well to those obtained by other authors (e.g., Jacobs, 1950; Möller, 1951a; Peixoto, 1958) in latitudes dominated by the Hadley cell. The water-vapor content of the troposphere seemed to have been slightly higher on Dec. 12, 1957, than

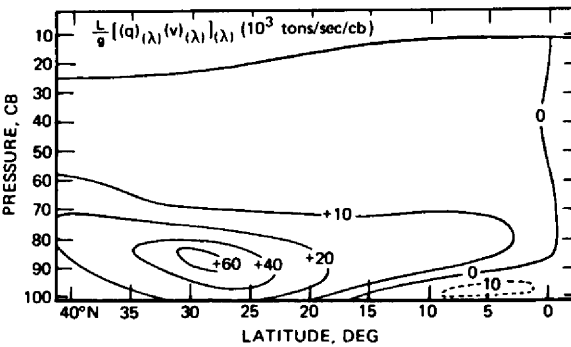
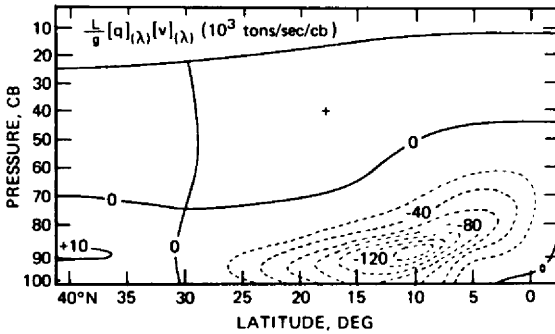
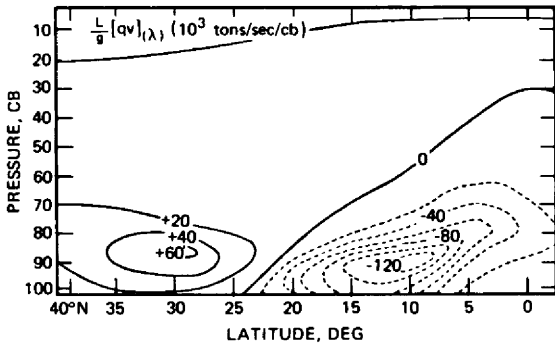
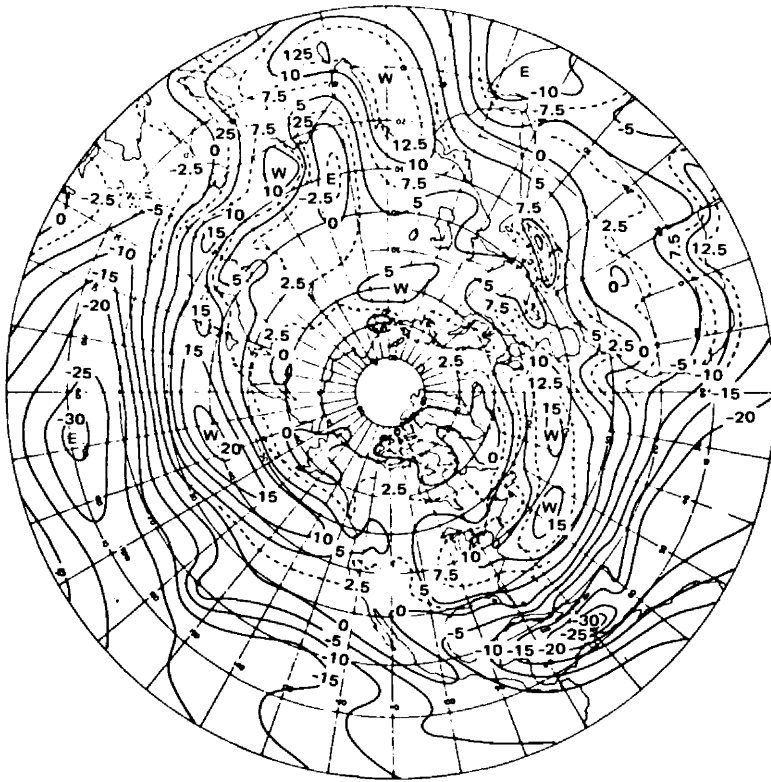


Fig. 3.59 Total water-vapor flux (a), flux accomplished by the mean circulation (b), and eddy flux (c) across latitude circles, for Dec. 12, 1957 (northward fluxes greater than zero). (Adapted from Boogaard, 1964.)



(a)

Fig. 3.60 (See facing page for legend.)

on other occasions (Peixoto, 1958; Bannon and Steele, 1960). Thus the flux values given in Figs. 3.59 and 3.60 probably are slightly higher than normal.

Results obtained by Vuorela and Tuominen (1964) for the summer seasons (June–August) of 1948 to 1953 agree well with those reported above if one considers the northward shift of the intertropical convergence zone and of the Hadley cell during that season. The water-vapor flux caused by mean meridional motions and by transient eddies, according to Vuorela and Tuominen, is given in Table 3.14. It should be compared with the pattern shown in Fig. 3.59. Differences between precipitation and evaporation obtained from the divergence of water-vapor flux are given in Table 3.15. They may be compared with the values obtained by Boogaard and shown in Fig. 3.61 (note the difference in units).

More recent estimates on water-vapor flux and its divergence, broken down into mean, standing eddy, and transient eddy contributions, have been made by Adem (1968). From this study it also appears that there are large differences from year to



Fig. 3.60 (a) Vertically integrated mean total zonal water-vapor flux, $[Q_\lambda](\lambda)$, and (b) mean total meridional water-vapor flux, $[Q_\phi](\lambda)$ (10^2 g/cm/sec). E, easterlies, W, westerlies. N, north winds, S, south winds (Peixoto and Crisi, 1965).

year in the quantity, “evaporation minus precipitation.” These differences may be as large as the mean values of this quantity.

The vertical flux of moisture in the lower and middle troposphere is strongly influenced by “hot tower convection,” similar to the “convective turbulence” that transports heat as discussed in the preceding chapter. Auer and Marwitz (1968), for instance, estimate that an average of 2.1×10^9 g/sec of moisture flows into a hail-producing convective cell of middle latitudes. Although a large fraction of this moisture is rained out, there still is enough left to be transported out of the region by horizontal flow processes.

Large eddies, such as hurricanes and typhoons, play an important role in the vertical transport of moisture (see, for example, Hawkins and Rubsam, 1968). The release of latent heat in such disturbances affects in an important way the generation of available potential energy (Anthes and Johnson, 1968).

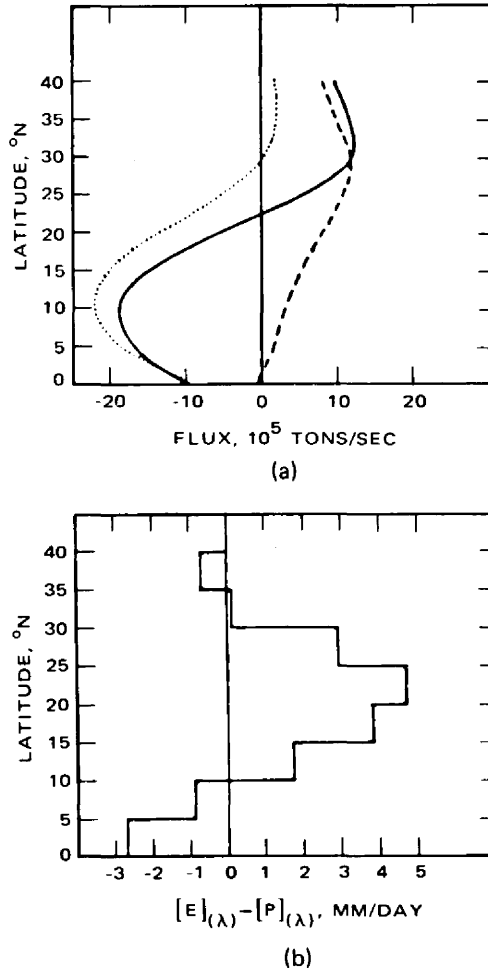


Fig. 3.61 (a) Latitudinal profiles of the pressure-integrated total (full line), mean meridional (dotted line), and eddy (dashed line) fluxes of water vapor and (b) the zonally averaged divergence and convergence of water vapor in belts of five-degree latitude expressed as $[E]_{(\lambda)} - [P]_{(\lambda)}$. [From H. M. E. Van de Boogaard, *Tellus*, 16(1): 50 (1964).]

The Dissipation of Kinetic Energy

As shown in Fig. 3.1 and Eqs. 3.43 and 3.48, the net generation of potential energy by radiative and other diabatic processes must be balanced by frictional dissipation of eddy and mean kinetic energy. The transformations of energies computed for a frictionless adiabatic and quasi-geostrophic model atmosphere

Table 3.14
FLUX OF WATER VAPOR (10^5 tons/sec) ACROSS DIFFERENT
LATITUDE CIRCLES CAUSED BY MEAN MERIDIONAL WIND (Q) AND BY
TRANSIENT WAVES (Q_t) DURING SUMMER OF THE NORTHERN HEMISPHERE*

	Latitude, °N									
	45	40	35	30	25	20	15	10	5	0
Q	1.3	-0.3	-2.5	-3.3	-3.8	-0.8	0.6	4.3	18.0	25.6
Q_t (Peixoto, 1958)	3.8	3.3	2.6	2.0	2.0	1.9	1.7	1.4	0.5	-0.3
Q + Q_t	5.1	3.0	0.1	-1.3	-1.8	1.1	2.3	5.7	18.5	25.3
Flux divergence	2.1	2.9	1.4	0.5	-2.9	-1.2	-3.4	-12.8	-6.8	

*Adapted from Vuorela and Tuominen (1964).

Table 3.15
AVERAGE PRECIPITATION AND EVAPORATION AND THEIR
DIFFERENCES* (mm/three months)

	Latitude, °N									
	45	40	35	30	25	20	15	10	5	0
P-E†	-118	-136	-58	-17	113	43	122	457	240	
Starr et al. ‡	-29	-75	-76	68	126					
P§	178	162	164	228	218	260	388	525	312	
E¶	296	298	222	245	105	217	266	68	72	

*Adapted from Vuorela and Tuominen (1964).

†Computed from the divergence of water-vapor flux caused by mean meridional wind and by transient waves.

‡Computed from the divergence of the entire water-vapor flux, according to Starr, Peixoto, and Livadas (1958).

§ Average precipitation according to Möller (1951b).

¶Computed average evaporation.

(Wiin-Nielsen, 1959; Saltzman and Fleisher, 1960b), therefore, will yield only approximate results.

Brunt (1926, 1934) estimated that the dissipation rate of total kinetic energy was 3 watts/m^2 ($1 \text{ watt} = 10^7 \text{ g-cm}^2/\text{sec}^3 = 10^7 \text{ ergs/sec} = 1 \text{ joule/sec}$) in the lowest kilometer of the atmosphere, and 2 watts/m^2 in the layer 1 to 10 km. The total dissipation in the troposphere thus would be 5 watts/m^2 (see also Pisharoty, 1955). Ball (1961) compared the rate of dissipation per unit mass, ϵ , (cm^2/sec^3) obtained by various authors. From the sparse observations, it appears that there is approximately

one order of magnitude decrease of ϵ between the 1- and 10-km levels (Wilkins, 1960). In general, at low levels (<150 m) the proportionality seems to be satisfied

$$\epsilon \propto [u]_{(t)}^3$$

where $[u]_{(t)}$ is the mean wind speed.

Palmén (1959) also found for tropical and subtropical regions that the frictional dissipation in the free atmosphere (1 to 12 km) was slightly less than that in the friction layer (0 to 1 km). Assuming a constant value of the eddy viscosity $\mu = 100$ g-cm/sec, he obtained from the vertical shear of the mean zonal wind in the layer 1 to 12 km a maximum value of dissipation of 8×10^{-4} kilojoule/m²/sec (0.8 watt/m²) near 30°N, the northern boundary of the region under consideration. In the whole belt 0°N to 30°N, the dissipation in the free atmosphere was computed to be 4×10^{10} kilojoules/sec (4×10^{13} watts).

Holopainen (1963) computed the dissipation of kinetic energy over the British Isles during two periods in January 1954. The total rate of dissipation in the troposphere was 10 watts/m², of which 4 watts/m² were dissipated below 900 mb. A second maximum of dissipation was found slightly below jet-stream level (Fig. 3.62). According to Hare (1965), frictional dissipation at levels above 20 km is dynamically unimportant. This is also suggested by Sawyer (1961), who comments on the long-lived nature of mesoscale wind oscillations.

The seasonal variation on the frictional dissipation in the surface boundary layer, D_b , was estimated by Wiin-Nielsen (1967) for the period February 1963 to January 1964. Results are shown in Table 3.16. Estimates were obtained by using the method derived by Lettau (1962) and Kung (1963), whereby

$$D_b = \rho C_g V_{g,o}^3 \quad (3.78)$$

where ρ is the air density, C_g is the geostrophic drag coefficient (taken from Kung, 1963), and $V_{g,o}$ is the geostrophic wind in the atmospheric boundary layer. Values given in Table 3.16 agree in magnitude with the results obtained by Palmén and Holopainen.

Whereas Wiin-Nielsen's data were collected on a hemispheric basis, Kung (1966a) reports on results obtained over the North American continent (Table 3.17). It has been pointed out in Chap. 2 that oceanic surface stresses are of the same magnitude as continental ones (see Kung, 1968). His values of D_b agree well with those given by Wiin-Nielsen. In addition, Kung obtained values for the frictional dissipation in the free atmosphere, D_f . Both modes of dissipation are also computed for the mean flow, $[D]_{(p)}$, and the shear flow, $(D)_{(p)}$. Gross results are summarized in Table 3.18.

Holopainen's (1963) findings of a relatively large dissipation in the free atmosphere are corroborated by Kung's (1966a, 1966b, 1967) data. It is interesting to note that the boundary layer contributes only little to the mean-flow dissipation unless the latter is small itself (see Table 3.17). Most of the mean flow appears to be dissipated in the free atmosphere. On the average, the shear flow is dissipated equally

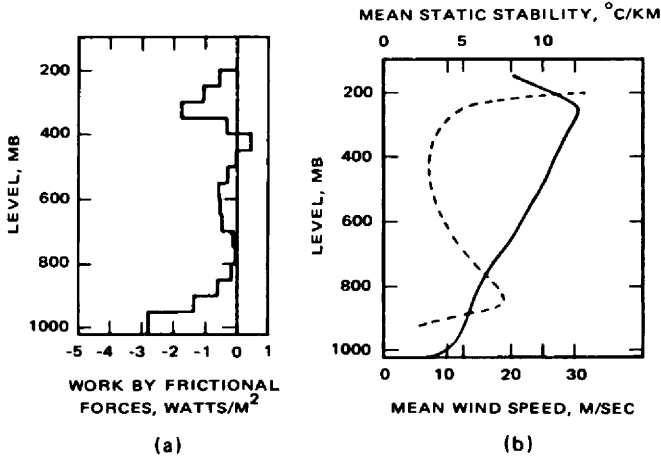


Fig. 3.62 (a) Mean work done by frictional forces in different layers (watts/m²). (b) Mean wind speed (heavy line) (m/sec) and the mean static stability (dashed line) (°C/km). [From E. O. Holopainen, *Tellus*, 15(1): 29 (1963).]

Table 3.16

DISSIPATION IN THE SURFACE BOUNDARY LAYER (D_b)*

Month	$\rho, 10^{-3} \text{ ton/m}^3$	$10^3 C_g$	$V_{g,o}^3, \text{ m}^3/\text{sec}^3$	$D_b, 10^{-4} \text{ kilojoule/m}^2/\text{sec}$
January	1.268	0.878	2335	25.99
February	1.262	0.900	2127	24.14
March	1.246	0.928	1617	18.60
April	1.226	0.940	1293	14.91
May	1.205	0.990	1153	13.77
June	1.191	1.050	1209	15.13
July	1.185	1.090	1002	12.95
August	1.191	1.068	1170	14.89
September	1.207	1.010	1864	22.72
October	1.228	0.984	2098	25.34
November	1.248	0.946	2484	29.62
December	1.263	0.916	2949	34.10

*From A. Wiin-Nielsen, *Tellus*, 19(4): 552 (1967).

in the boundary layer and in the free atmosphere. Only when $[D]_{(p)}$ is significantly larger than $(D)_{(p)}$, as in February and May 1962, does the major dissipation of $(D)_{(p)}$ occur in the boundary layer as $(D_b)_{(p)}$.

By comparing data taken over North America at 00 and 12 GMT, Kung (1967) found a significant diurnal variation in dissipation, especially pronounced during

Table 3.17
TOTAL AND PARTITIONED KINETIC-ENERGY DISSIPATION
 (watts/m²)*

	January 1963	February 1962	March 1962	May 1962	July 1962	August 1962	Grand mean
D	7.53	4.35	4.87	7.21	6.58	7.71	6.38
D _b	2.41	1.90	1.90	2.07	1.50	1.41	1.87
D _f	5.12	2.45	2.97	5.14	5.08	6.30	4.51
[D] _(p)	3.51	4.49	1.95	6.69	0.19	1.83	3.11
(D) _(p)	4.02	-0.14	2.92	0.52	6.39	5.88	3.27
[D _b] _(p)	0.64	0.05	-0.41	0.23	0.29	0.01	0.14
[D _f] _(p)	2.87	4.44	2.36	6.46	-0.10	1.82	2.97
(D _b) _(p)	1.77	1.85	2.31	1.84	1.21	1.40	1.73
(D _f) _(p)	2.25	-1.99	0.61	-1.32	5.18	4.48	1.54
D _b /D, %	32.0	43.7	39.0	28.7	22.8	18.3	29.3

*From E. C. Kung, *Monthly Weather Review*, 94(2): 73 (1966).

Table 3.18
DISSIPATION OF KINETIC ENERGY
 (watts/m²)*

D _{total} , †	[D] _(p) , †	(D) _(p) , †
6.38	3.11	3.27
D _b	[D _b] _(p)	(D _b) _(p)
1.87	0.14	1.73
D _f	[D _f] _(p)	(D _f) _(p)
4.51	2.97	1.54

*From E. C. Kung, *Monthly Weather Review*, 94(2): 74 (1966).

†b, boundary layer; f, free atmosphere.

summer, with values at 00 GMT being consistently larger than at 12 GMT. This holds for the lower troposphere as well as for jet-stream levels.

Quasi-Periodicities of the General Circulation

The discovery of the biennial or 26-month oscillation of stratospheric winds over the equator prompted a search for additional parameters describing the general circulation of the atmosphere that might exhibit a similar periodicity (for summaries, see Wallace, 1966; Reed, 1966a, 1966b; for an analysis of observed periods, see Angell, Korshover, and Carpenter, 1966). Labitzke (1965a, 1965b) noted a peculiar biennial change in the characteristics of stratospheric motion patterns which was by no means confined to equatorial regions: Stratospheric high-pressure regions in the belt of the polar westerlies revealed a tendency to move either eastward or westward in successive years (Fig. 3.63). Williams and Miers (1968) established a retrogression of the Aleutian High during the 1967–1968 winter, in agreement with the observations during even-numbered years, as shown in Fig. 3.63. Shen, Nicholas, and Belmont (1968) noted an eastward progression of the 1963 stratospheric warming in the southern hemisphere from TIROS VII 15- μ radiation data. Even though this agrees with Fig. 3.63, it is not enough evidence of a parallel behavior of the two hemispheres. Hirota (1968) showed that the phase velocities of long planetary waves in the upper stratosphere do not necessarily behave uniformly but may reverse during the same season. Laby, Sparrow, and Unthank (1964) and Sparrow and Unthank (1964) noted a biennial oscillation in winds as far away from the equator as 50°S between 70,000 and 100,000 ft (see also Tucker and Hopwood, 1968). Angell and Korshover (1962, 1963, 1964) and Shah and Godson (1966) noted such quasi-periodicities in the northern hemisphere in temperate and even in polar latitudes. According to Landsberg et al. (1963), there seems to be a biennial oscillation also in surface temperatures (see also Bjerknæs, 1967, for anomalous equatorial sea temperatures and the associated response of the index in the westerlies of temperate latitudes). Böhme (1967) comments on a 26-month periodicity of zonal flow over Europe and Brier (1969) on a quasibiennial periodicity in the sea-level zonal index for the northern hemisphere. Belmont and Dartt (1968) note a longitudinal dependence of the oscillation.

The abnormal behavior of January 1963, especially in the energy-transport terms, has already been commented on and will be described further in Chap. 4. This month was, according to Labitzke, representative of an eastward progression of stratospheric warming regions (Fig. 3.63).

From such preliminary evidence it seemed encouraging to investigate the transport characteristics of the stratospheric circulation in extratropical latitudes for possible periodicities, even though recent indications suggest a temporary breakdown or at least a significant phase shift in such oscillations after 1965. Such evidence comes especially from ozone data (Dyer and Hicks, 1965; Tucker, 1967; London, 1967) (see Part 2). In the southern hemisphere this temporary breakdown of the biennial variation may already have occurred in 1963 (Kulkarni, 1966; see also Ramanadham, 1965; Dütsch,

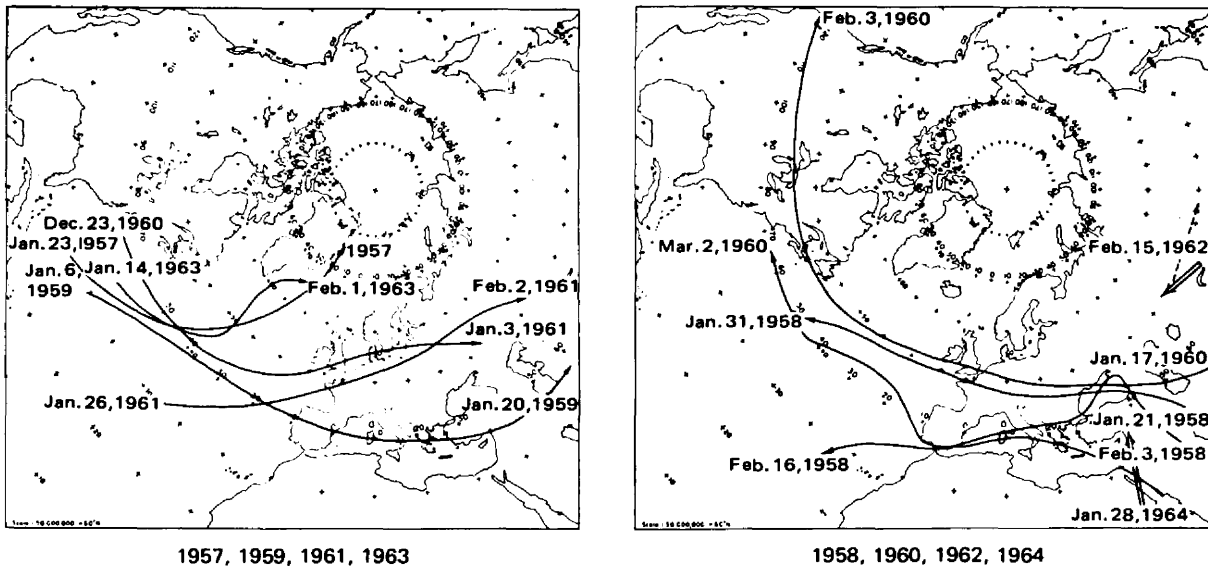


Fig. 3.63 Movements of high-pressure regions for dates indicated at the 10-mb level during stratospheric warming periods. [From K. Labitzke, *Journal of Applied Meteorology*, 4(1): 93 (1965).]

1966; and Wallace, 1967). From the long series of ozone observations at Arosa, Switzerland, no biennial variation is indicated before 1952 (Wallace and Newell, 1966; Ramanadham, 1965).

Tucker (1964) found that the divergence of eddy transport of momentum, $(\partial/\partial y)[(v)_{(\lambda,t)}(u)_{(\lambda,t)}]_{(\lambda,t)}$, reveals a 26-month periodicity similar to that of the zonal wind, $[u]_{(\lambda,t)}$. (The averaging period, t , is one month in Tucker's computations.) In a second study Tucker (1965b) noted a phase difference between the oscillations of the divergence of the horizontal eddy momentum flux and those of the mean zonal wind of approximately $\pi/2$ (or 6.5 months), with the divergence wave preceding the zonal wind wave. Stations close to the equator reveal the periodicity in momentum-flux divergence much less distinctly than stations at some distance from the equator. This probably is the reason why Rogers (1962) did not detect such a periodic oscillation in the flux itself (see Reed, 1963a). From a case presented by Riehl and Higgs (1960), Reed (1963a) concludes that eddy fluxes are dominant in producing momentum transports in equatorial regions.

A more recent study by Wallace and Newell (1966) (see also Wallace, 1966) confirms these results: A biennial oscillation in eddy momentum transport and in the latitudinal divergence in this transport appears above the 30-mb level in the tropics and above the 50-mb level in higher latitudes. There is no evidence of such an oscillation below the 30-mb level in the tropics. The oscillation in the momentum transport appears to be synchronous at all levels and at all latitudes; its amplitude, however, increases with latitude, as noted by Tucker.

According to Wallace and Newell (1966), the heat transport by transient eddies reveals a similar biennial variation. The oscillation seems to be dominated by the winter months, with Januaries of even-numbered years showing the larger eddy-flux values, as is the case for momentum transport. (The dominating role of winter months has been confirmed by Shapiro (1964) for surface-pressure variances, which also exhibit a weak biennial variation.) The biennial component of the flux appears to be countergradient since the winters with larger poleward heat fluxes are characterized by colder than normal temperatures in the 20- to 50-mb regions at the equator and by warmer than normal temperatures at the same levels in the subtropics. The year-to-year differences of eddy-heat-flux divergence could account for a heating rate of 0.02°C per day at 20 mb, which is the same order of magnitude as the radiative heating rates assumed by Reed (1964) but smaller than the radiative heating computed by Kennedy (1964).

This countergradient eddy heat flux produced by the biennial oscillation is at odds with the assumptions made by Reed (1964) (see also Staley, 1965; Tucker and Staley, 1965) in deriving a model for this periodicity. The mean meridional circulations computed by Reed, therefore, may be subject to revisions.

The periodicity in eddy momentum flux observed by Wallace and Newell (1966) above 30 mb is capable of producing the observed changes in zonal winds. Thus the latter are strongly affected by eddy-transport processes. Below 30 mb mean meridional circulations are likely to play a dominant role in the biennial oscillation (Tucker, 1964, 1965b; Reed, 1964). The biennial ozone variations (see, e.g., Shah, 1967) at

middle latitudes concur with the fluctuations in eddy transport, yielding large amounts of ozone after winters with large eddy transports of heat and momentum. This conforms to the statement by Newell (1964a, 1964b) that eddy transports are mainly responsible for the high ozone concentrations at middle and high latitudes during the late winter and spring months.

Wallace (1966, 1967a) points out that the long-period variations of the mean zonal flow are geostrophic to well within 1 km of the equator. [Geostrophic flow conditions at the equator may be derived by differentiating the zonal geostrophic wind equation with respect to y (Hollmann, 1955; see also Fortak, 1957; Vitek, 1962; Vitek and Vitkova, 1962; Reiter, 1963b).] This means that wind and temperature fluctuations are coupled by the geostrophic thermal-wind equation (see LaCruz, 1962). Wallace suggests that changes in the zonal wind field cause vertical motions, which, in turn, produce the observed temperature fluctuations. Radiative processes could not explain the observed wind variations (Wallace, 1967b; Wallace and Holton, 1968) and actually would play a dissipative role in the biennial oscillation. Maeda (1967) suspects that the effect of 26-month temperature variations on cosmic-ray intensity should be detectable at the earth's surface. Spectrum analysis of ion-chamber data taken at Cheltenham and Huancayo actually shows a small peak at a period of 26 months.

As will be pointed out in Part 2 of this review, *Chemical Tracers*, the "trapping" of waves that transport westerly momentum upward in the tropics (see, for example, Wallace and Kousky, 1968; Maruyama, 1968a, 1968b) may be a plausible cause for the biennial wind oscillation.

Miller, Teweles, and Woolf (1967a) and Miller, Woolf, and Teweles (1967b), using a 10-year period (1955–1964), found a quasi-biennial periodicity in the angular momentum transport at 500 mb. Maximum northward flux by wave number 1 (equivalent to the eccentricity of the polar vortex) occurred in odd-numbered years at 42.5°N latitude. Transport by wave number 2 revealed a similar periodicity but was out of phase with wave number 1. Wave number 3 contained more short-term variability but, in general, agreed in phase with wave number 1 at high and middle latitudes. The higher wave numbers, as well as the zonal wind component, do not reveal a regular periodicity. The phase shift in the biennial fluctuations between wave number 1 and wave number 2 may be a clue to the fact that Wallace and Newell (1966) found no periodicities in the total angular momentum flux below 50 mb.

According to Saltzman and Teweles (1964), wave number 2 at 500 mb is important in converting available potential energy into kinetic energy. This prompted Miller et al. (1967a, 1967b) to conclude that the quasi-biennial oscillation might be "directly influenced by the continent–ocean structure and its related thermal effect."

Recently, Smith (1968) has shown the existence of a biennial variation in the frequency of occurrence of intense sporadic E-layers in the ionosphere at several northern hemisphere stations (Kokubunji in Fig. 3.64). Sporadic E-layers occur near the 110-km level in the thermosphere (see Part 2). Peak frequencies of observation are encountered during summer (June and July in the northern hemisphere), with a small secondary maximum during winter. Very intense sporadic E-layers are observed from approximately 2 hr after sunrise to approximately 2 hr after sunset. The interannual

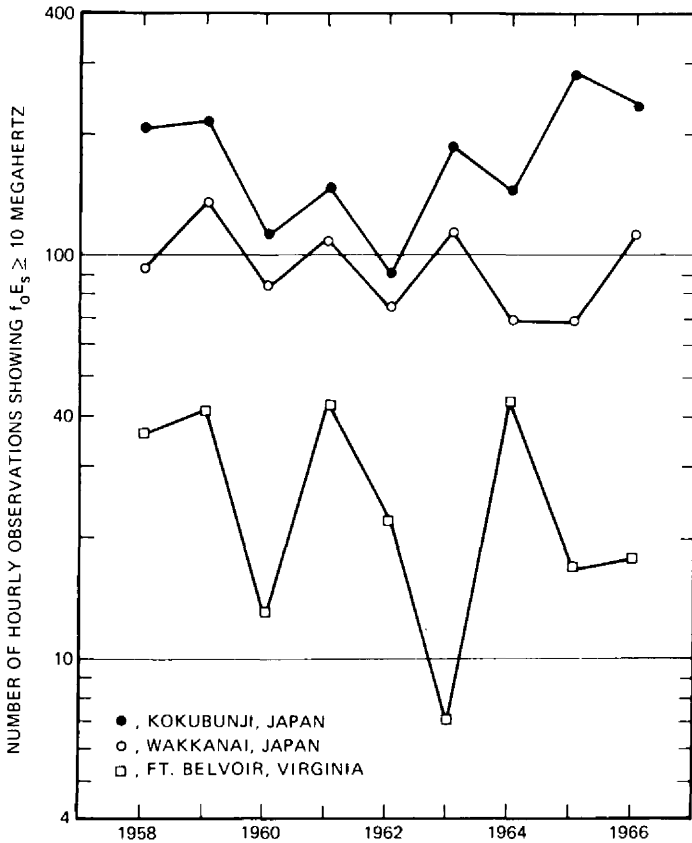


Fig. 3.64 Year-to-year variation of intense sporadic E-layers ($f_0E_s \geq 10$ megahertz) for three northern hemisphere ionosonde stations. The critical frequency is indicated by f_0 (Smith, 1968).

variations of sporadic E-layers, shown in Fig. 3.64, would suggest that, in addition to diurnal and seasonal variations, which are obviously coupled with solar radiation processes and with the photochemistry of the upper atmosphere, this phenomenon is influenced to a certain degree by atmospheric circulation and transport processes. The extent to which the ionospheric variations found by Smith may actually be linked to interannual variations of transport processes studied by Wallace (1966) and Wallace and Newell (1966) will yet have to be explored.

Quasi-periods of a duration longer than 26 months have been discussed elsewhere in climatological literature. Namias (1969) points out a possible correlation of such "slow trends" in the general circulation with long-lived sea-surface temperature anomalies (see also Bjerknes, 1967). It would exceed the scope of this review to present more details of these yet little-understood long-term variations.

Differences Between Hemispheres

In the foregoing, conditions on the northern hemisphere have been considered exclusively. The data for the southern hemisphere are too sparse to permit energy-transfer and energy-conversion calculations similar to those outlined previously. Therefore the results of mean meridional and eddy circulation aspects available so far have to be regarded as preliminary in nature. Only mean meridional profiles of zonal winds can be considered reliable for certain sectors (Schwerdtfeger and Martin, 1964; Sparrow, 1965).

Obasi (1963a) computed the fluxes of angular momentum by transient eddies, by standing eddies, and by the mean meridional circulation for summer and winter 1958 (IGY) in the southern hemisphere (Fig. 3.65). His results confirm the overwhelming importance of transient eddy processes in the poleward flux of momentum. Except for a slightly higher equatorward flux at high latitudes, his results agree well with those obtained by Holopainen (1967) (Figs. 2.3 and 2.4). As shown in Fig. 3.65, standing eddies seem to be mainly responsible for the transequatorial flux of momentum, at least during the summer season when the monsoon circulation prevails over the Indian Ocean. More details about this flux will be given in the following chapter.

The rate of conversion of eddy kinetic to zonal kinetic energy, according to Obasi (1963b), appears to be almost twice as large in the southern hemisphere as in the northern hemisphere. This is confirmed by Gilman (1965), who computes a conversion $\langle K_E, K_Z \rangle$ for the southern hemisphere of 9.63×10^{20} ergs/sec in winter and 9.72×10^{20} ergs/sec in summer. These values can be compared to the results by Saltzman and Fleisher (1960a) reported in Table 3.2. In this conversion process, again the transient eddies play a dominant role in the southern hemisphere. According to Obasi (1965), the average annual conversion of transient eddy kinetic energy into zonal kinetic energy in the southern hemisphere in 1958 was 9.63×10^{20} ergs/sec when the transformation equation was integrated by levels (method A). An equivalent value for the northern hemisphere is 4.84×10^{20} ergs/sec (from data published by Buch, 1954). The use of vertically averaged momentum flux and vertically averaged shear of the relative angular velocity (method B) changes these results only slightly. Even the assumption that 500-mb data alone are representative for the whole atmosphere (method C) brings out approximately the same ratio of energy conversion between the northern and southern hemispheres (see also Table 3.3).

The energy conversion between standing eddies and mean zonal flow in the southern hemisphere yielded -0.25 , -0.22 , and -0.89×10^{20} ergs/sec after methods A, B, and C (Obasi, 1965). Equivalent values obtained by these three methods for the northern hemisphere are 0.88 , 0.80 , and 1.02×10^{20} ergs/sec, respectively. Thus, in the southern hemisphere the standing eddies tend to withdraw kinetic energy from the mean zonal flow but at an insignificant rate. In the northern hemisphere these eddies supply a significant amount of energy to the zonal motions. It appears, therefore, that the orography and land-sea distribution in the northern hemisphere has a well-recognizable effect on the energetics of the atmosphere, which is lacking to a large degree in the southern hemisphere.

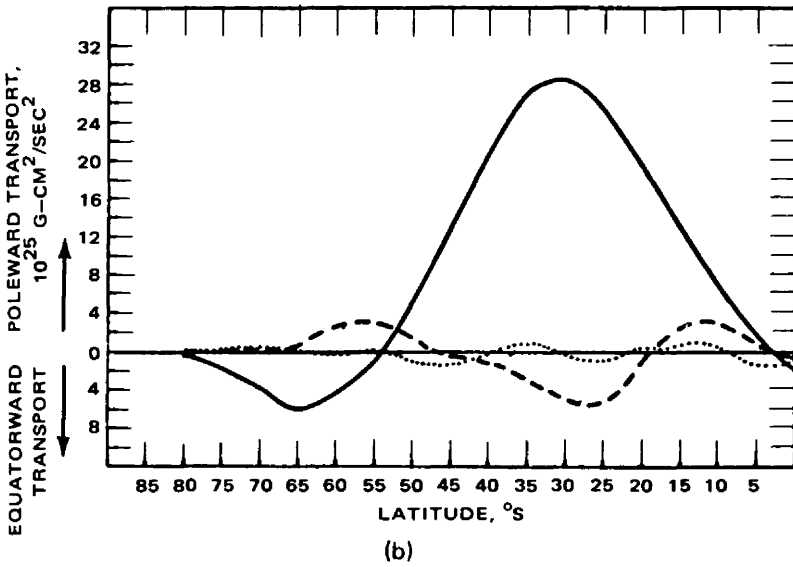
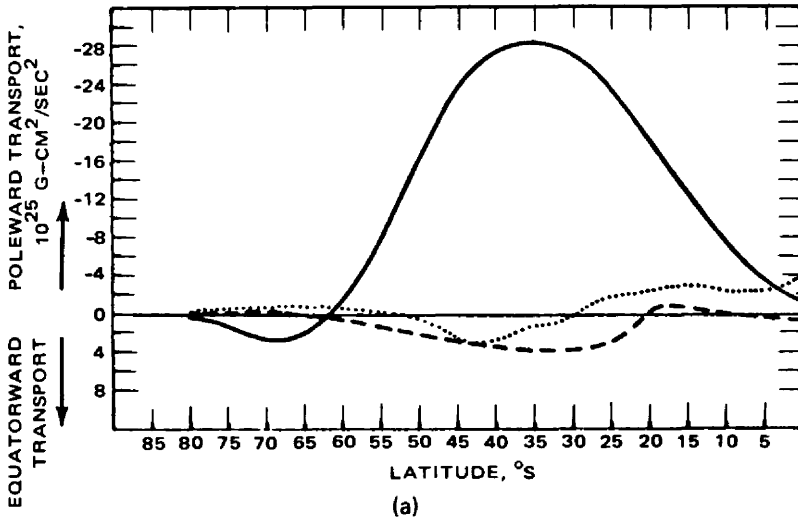


Fig. 3.65 Vertically integrated mean relative angular momentum flux (10^{25} g-cm²/sec²) across various latitudes of the southern hemisphere. (a) In summer 1958. (b) In winter 1958. The full curve is flux caused by the transient eddies, the dashed curve is flux caused by mean meridional motion, and the dotted curve is flux caused by the standing eddies. [From G. O. P. Obasi, *Journal of the Atmospheric Sciences*, 20(6): 521 (1963).]

Obasi (1965) estimated that the atmosphere of the southern hemisphere would assume a state of solid rotation within two and one-half weeks after the supply of energy by eddies ceased. Equivalent estimates by Starr (1953) for the northern hemisphere yielded a decay time into solid rotation of two weeks. Obasi's estimates for the southern hemisphere may be subject to revision in the light of the data of Hellerman (1967), who finds considerably higher zonal surface stresses than those given by Obasi.

Seasonal differences of the relative angular velocity in the southern hemisphere are shown in Fig. 3.66. These velocities are larger in the southern hemisphere than in the northern hemisphere during the same seasons, in agreement with the larger mean tropospheric temperature difference between equator and pole in the southern hemisphere (see Fig. 3.67) (Doberitz, Flohn, and Schütte, 1967; see also Theon and Horvath, 1968). One should expect the flux of momentum by transient eddies to be directed away from the jet-stream latitudes with peak zonal wind velocities. This is borne out by a comparison of Figs. 3.65 and 3.66.

Figure 3.68 shows the seasonal variations in the production of zonal kinetic energy by transient eddies (after method B). We have seen from Wiin-Nielsen's computations (Fig. 3.39) that large seasonal and interannual variations of this transformation quantity can occur in the northern hemisphere. It is difficult to say, therefore, how representative for mean conditions the values obtained by Obasi (1965) (Fig. 3.66) really are. We are led to believe, however, that flow patterns in the southern hemisphere are less subject to drastic changes than those in the northern hemisphere.

Energy-transfer calculations in the stratosphere of the southern hemisphere, especially during the breakdown of the circumpolar vortex, have not yet achieved a satisfactory degree of reliability because of the sparsity of data. Although Phillpot (1964) and Labitzke and Loon (1965) have detected "minor" warming periods (terminology according to CIG-IQSY Committee, 1963) in midwinter in the antarctic stratosphere, "major" warming epochs, in which the normal winter stratospheric polar vortex collapses completely and the circulation reverses, have not yet been found in the southern hemisphere during midwinter (Godson, 1963; Maenhout and Miegheem, 1964; Miegheem, 1966; Julian, 1967; Belmont, Nicholas, and Shen, 1968). This might suggest that degrees of stability in the southern polar vortex differ from those in the northern polar vortex (Mahlman, 1966) and that various mean and eddy transport terms are of different importance in the two hemispheres. Schwerdtfeger (1960, 1962, 1963, 1967) holds the superposition of the annual and semiannual wave in meridional temperature gradients (hence in the intensity of the circumpolar vortex) observed in the southern hemisphere responsible for the vortex breakdown in September (see also Loon, 1967). The temperature curve for the south pole (S) in Fig. 3.67 indicates such a double-wave structure.

The establishment of the circumpolar vortex in fall seems to proceed in quite a regular fashion in both hemispheres. This would indicate a control of the initial establishment of the vortex by radiative processes rather than by eddy transport processes (Finger and Woolf, 1967).

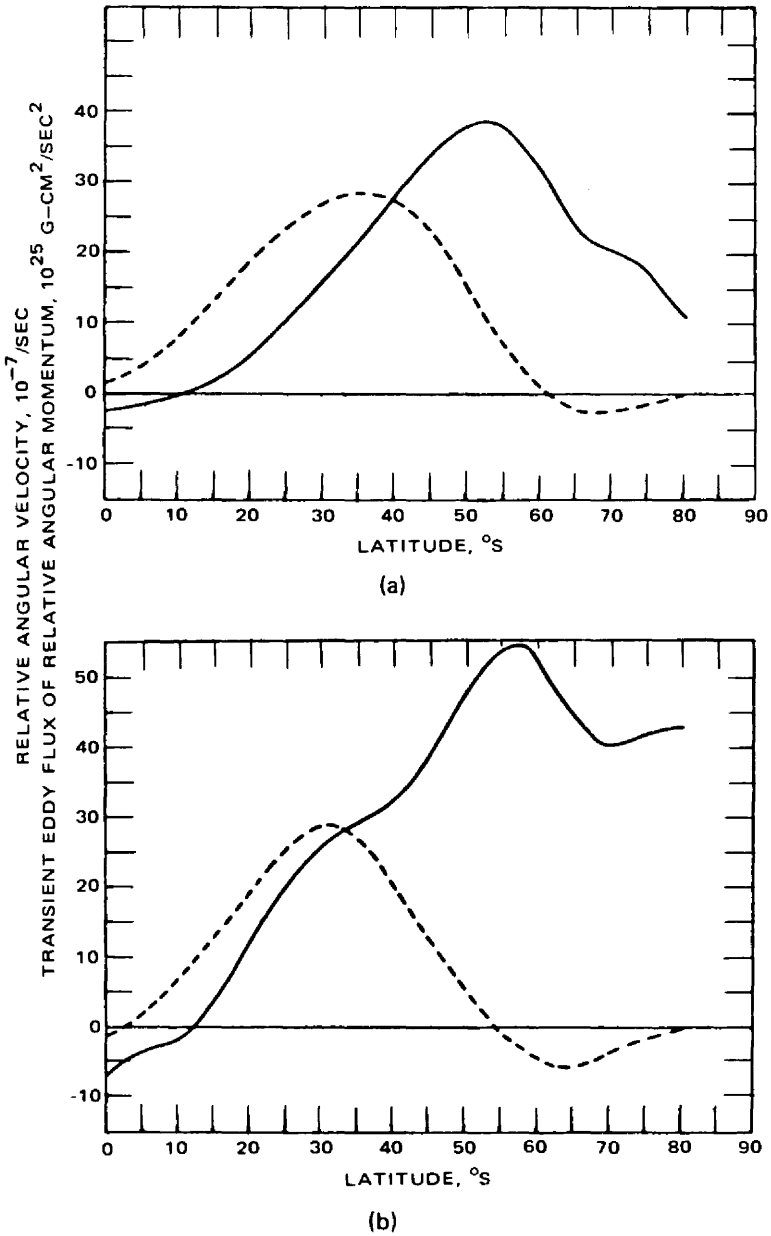


Fig. 3.66 Seasonal differences of the relative angular velocity in the southern hemisphere. (a) Summer 1958. (b) Winter 1958. The full curve gives the relative angular velocity ($10^{-7}/\text{sec}$) as function of latitude and the dashed curve gives the transient eddy flux of relative angular momentum ($10^{25} \text{ g-cm}^2/\text{sec}^2$). [From G. O. P. Obasi, *Tellus*, 17(1): 103; 104 (1965).]

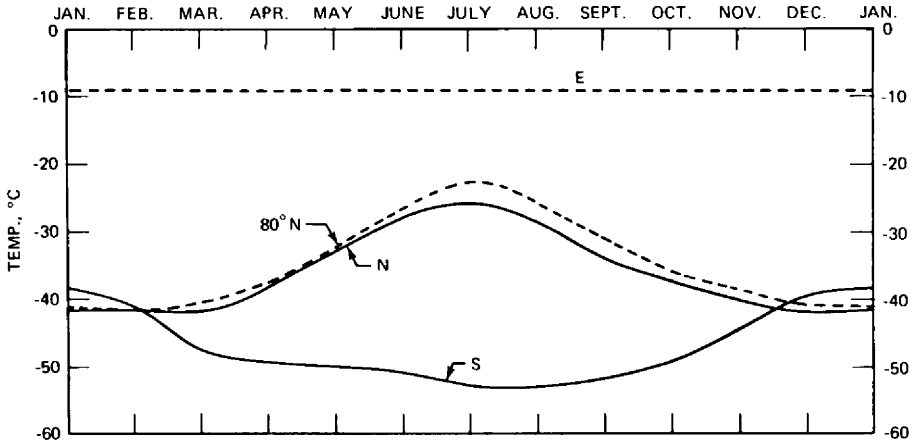


Fig. 3.67 Average temperature of the layer 300 to 700 mb at the equator (E), at 80°N (seven stations), at the North Pole (N), and at the South Pole (S) as a function of the month of the year. [From R. Doberitz, H. Flohn, and K. Schütte, *Bonner Meteorologisches Abhandlungen*, No. 7, (1967).]

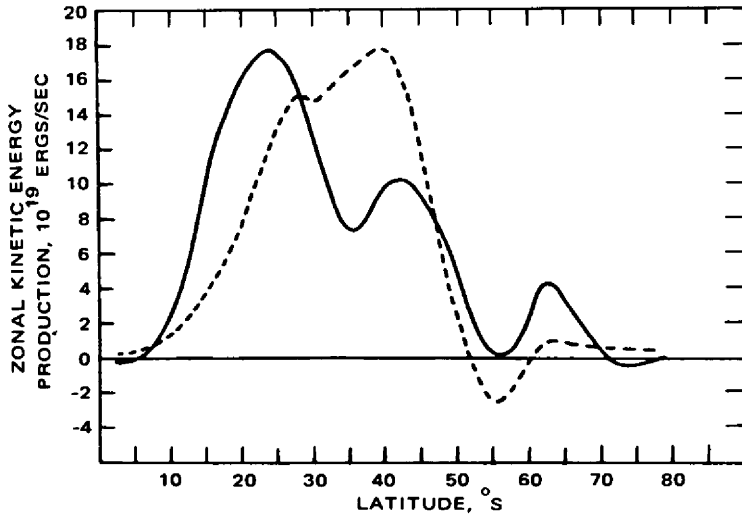


Fig. 3.68 Production of zonal kinetic energy (10^{19} ergs/sec) using mean wind and transient eddy transport of relative angular momentum. The full curve represents the situation in winter, and the dashed curve represents the summer condition. [From G. O. P. Obasi, *Tellus*, 17(1): 104 (1965).]

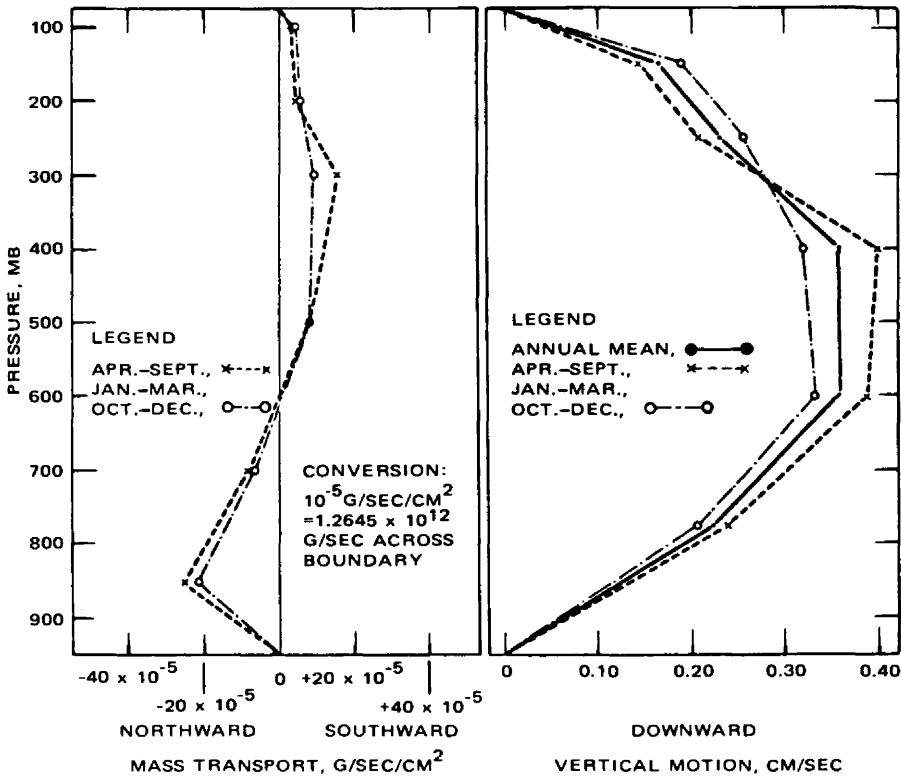
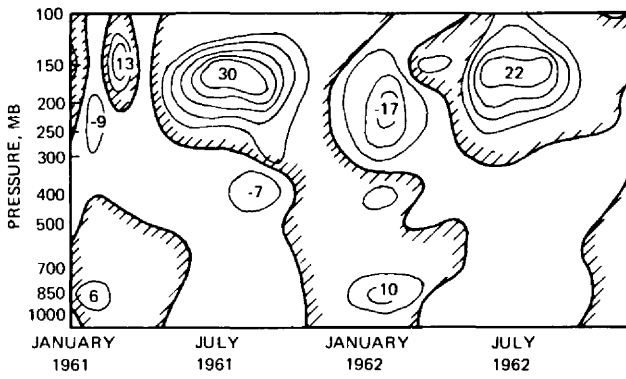


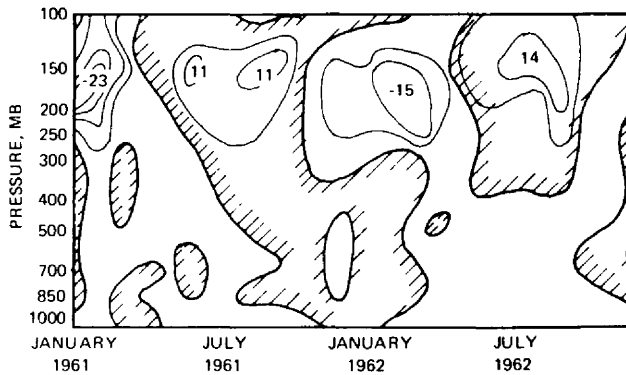
Fig. 3.69 Mean mass transports and vertical motions in the antarctic atmosphere, 1958. [From M. J. Rubin and W. S. Weyant, *Monthly Weather Review*, 91(10-12): 489 (1963).]

Heat and mass budget calculations for the antarctic atmosphere during the IGY period (Rubin and Weyant, 1963; Rubin, 1964) suggest a downward motion over Antarctica between 950 and 75 mb, with a maximum at 500 mb (Fig. 3.69). This would corroborate the circulation model proposed by Wexler, Moreland, and Weyant (1960) to account for the antarctic surface ozone observations (see Part 2). Observational evidence is not yet detailed enough to ascertain the presence or absence of a two-cell structure of vertical motions in the stratosphere as it is found in the northern hemisphere. The vertical velocities shown in Fig. 3.69 and the ozone observations made in Antarctica (see Part 2), however, would speak in favor of a one-cell model of stratospheric circulation in the southern hemisphere during winter, with rising motions in equatorial latitudes and sinking motions over the pole. If this were the case, it would not appear appropriate to substitute northern hemispheric data in the observational gaps of the southern hemisphere as, for instance, attempted by Webb (1964).

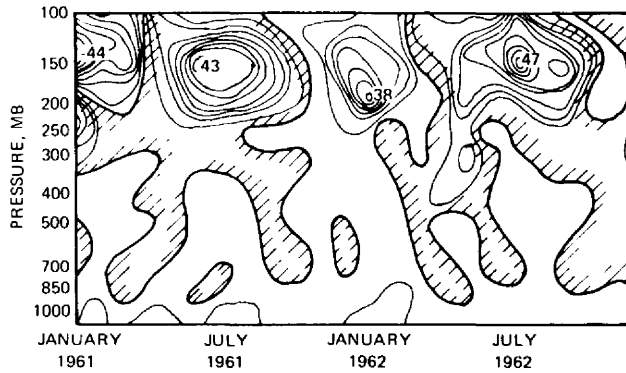
From the calculations by Rubin and Weyant (1963) (see also Rubin, 1964), the net gain of heat during the spring warming period in the layer 75 to 150 mb in the



(a)



(b)



(c)

Fig. 3.70 Momentum flux (m^2/sec^2) across equator according to Eq. 3.79. (a) By mean meridional circulation. (b) By local (transient) eddies. (c) By standing eddies. Northward flux positive (shaded areas). [From G. B. Tucker, *Quarterly Journal of the Royal Meteorological Society*, 91(338): 147 (1965).]

Table 3.19
MASS CIRCULATION ACROSS THE EQUATOR
 (10^{12} g/sec)*

Reference	Season	Amount	Direction of flow
Rao (1964)	January	215	Southward at low levels
Tucker (1965a)	January	270	Southward at low levels
Palmén and Vuorela (1963)	December–February	80	Southward at low levels
Defant and Boogaard (1963)	Dec. 12, 1957	62	Southward at low levels
Rao (1964)	July	190	Northward at low levels
Tucker (1965a)	July	150	Northward at low levels
Vuorela and Tuominen (1964)	June–August	180	Northward at low levels

*Adapted from Palmén (1966a).

Table 3.20
**ESTIMATE OF SOURCES AND OF CROSS-EQUATORIAL
 FLUXES OF ANGULAR MOMENTUM (10^{26} g-cm²/sec²)***

	January	April	July	October
Flux of angular momentum (+ northward, –southward)	–0.5	–0.1	+0.7	+0.4
Northern hemisphere source†	3.8	3.5	1.2	2.3
Southern hemisphere source†	3.4	3.6	4.1	3.4
Difference (northern – southern hemisphere)	–0.4	+0.1	+2.9	+1.1

*From G. B. Tucker, *Quarterly Journal of the Royal Meteorological Society*, **91**(388): 146 (1965).

†Data by Priestley (1951) have been modified to refer to the geographic equator as the dividing line between the two hemispheres.

somewhat in disagreement with the results obtained by Holopainen (1965), whereby eddy processes become virtually nil near the equator (see Fig. 3.33). The fact that the tropical easterly jet stream can be explained from eddy-transport processes (Reiter, 1967, 1969a) would speak in favor of Tucker's results, at least in a qualitative way. The standing eddy flux is mainly the result of the high-level monsoon flow pattern over the Indian Ocean and over the West Pacific area. The atmospheric level at which the tropical easterly jet stream occurs (about 150 mb; Koteswaram, 1958) thus appears to be of significance in interhemispheric mass and momentum exchange (see also Berson and Troup, 1961).

According to Tucker's study, during January, July, and October the momentum flux across the equator is more than 10% of the total westerly momentum source in the northern hemisphere (Table 3.20). Therefore neither of the two hemispheres should be treated in isolation by general-circulation models.

Palmén (1966a) suggests that the estimates by Rao (1964) and Tucker (1965a) of cross-equatorial mass transfer for winter are too high. Since the thermal equator in the northern hemisphere is closer to the equator in winter than in summer (Riehl, 1954), one should expect the transequatorial mass circulation to be weaker in January than in July. This conclusion is confirmed by Defant and Boogaard (1963), Palmén and Vuorela (1963), and Vuorela and Tuominen (1964) (see Table 3.19). The excessive estimates by Rao and Tucker may have been caused by their peculiar choice of key stations in their investigations.

According to the computations by Palmén, Vuorela, and Tuominen, during winter the mean meridional circulation transports 175×10^{12} g/sec across latitude 5°N in the troposphere, with northerly winds at low levels. During summer the transport is 140×10^{12} g/sec at 5°N , with southerly winds at low levels. In the annual mean there is no net flow across the mean meteorological equator at 4°N to 5°N , as should be expected. The computations by Rao (1964) and Tucker (1965a), however, would place the mean meteorological equator somewhere to the south of the geographic equator, in contradiction to meteorological observations.

4 SPECTRAL CONSIDERATIONS OF EDDY TRANSPORTS

GENERAL REMARKS

When dealing with large-scale flow phenomena, a simple approach in arriving at a spectrum of eddy motions would be to perform a Fourier analysis of the hemispheric flow pattern around a certain latitude belt. The amplitude thus computed for each wave mode may be considered as a good indicator of the energy of perturbation motion for a particular wave number. One has to be careful, however, in the interpretation of results. "Tilting" troughs, for instance, which are frequently observed in the hemispheric wave pattern, by virtue of their asymmetry, lead to contributions in wave numbers harmonic to the basic wave number. Thus a system of three equally spaced asymmetric waves will yield an energy contribution to wave number 6 as well, even though the synoptic pattern may not show such shorter waves. If waves are irregularly spaced, again a condition that is normally observed on weather maps, perturbation energy will be distributed to adjacent wave numbers as well, even though these waves may not be visible directly in the flow pattern. A numerical analysis technique that would circumvent all these problems has yet to be devised.

These problems can be ignored if a random distribution of eddy sizes is assumed and if no individual wave number dominates. Where and when to draw the border between eddy motions and wave motions is difficult, especially for the free atmosphere. Observations of clear air turbulence, for instance, suggest a transition regime between short gravity waves (wavelength of the order of 10^2 to 10^3 m) on a stable interface or transition layer in the atmosphere and isotropic, random

turbulence. Within this regime it would be difficult to distinguish between undulance and turbulence. Even those waves observed occasionally in thin cloud banks (Reiter and Hayman, 1962; Ludlam, 1967) rarely show a uniform and well-defined wavelength. The presence of a conglomerate of wavelengths and wave numbers, again, would be revealed as more or less "random" distribution of eddy sizes in one-dimensional spectra. A distinction between undulance and turbulence could, however, be made on the basis of isotropy, considering spectra of all three components of motion: Wave motions are anisotropic in their velocity fluctuations.

From this it appears that the distinction between wave motions and eddy motions should be made not so much from computed values of perturbation energy as a function of wave number or from the appearance of a one-dimensional power spectrum of velocity fluctuations but rather from a consideration of the isotropy of these perturbation motions: As long as the statistical characteristics of seemingly random eddy motions are the same along all coordinate directions, true turbulence can be assumed to exist. Strong suppression of the vertical motions as compared to the horizontal components would suggest the presence of (irregular) waves. Even here one may have to avoid pitfalls because organized and strong convective motions may simulate large-scale turbulence as a result of the strong vertical drafts that may be present. However, the existence of organized, not random, cells may make the application of the term "turbulence" questionable.

In spite of the preceding difficulties and if the results are interpreted with caution, spectrum analysis of atmospheric-motion patterns may yield valuable and interesting results far beyond the limited range of applications for which these tools were designed originally.

THEORETICAL BACKGROUND

In the following only large-scale planetary flow patterns will be considered. The energy-transformation processes described in Chap. 3 show that terms of the form of $[(u)_{(\lambda)}^2]_{(\lambda)}$, $[(v)_{(\lambda)}^2]_{(\lambda)}$ and $[(v)_{(\lambda)}(T)_{(\lambda)}]_{(\lambda)}$, $[(u)_{(\lambda)}(v)_{(\lambda)}]_{(\lambda)}$ are involved in the energy-transformation equations. Each of the quantities in parentheses, which constitute deviations from mean values, may be represented as a function of longitude, $f(\lambda)$, which is piecewise differentiable in the interval $(0, 2\pi)$. Saltzman (1957) was the first to propose a systematic treatment of these quantities and of their relation to atmospheric energetics in the wave-number regime (see also Reed, Wolfe, and Nishimoto, 1963; Kao, 1968).

Each of these functions can be written in a Fourier representation

$$f(\lambda) = \sum_{n=-\infty}^{\infty} F(n)e^{in\lambda} \quad (4.1)$$

where the complex coefficients, $F(n)$, are given by

$$F(n) = \frac{1}{2\pi} \int_0^{2\pi} f(\lambda)e^{-in\lambda} d\lambda \quad (4.2)$$

The functions $f(\lambda)$ may represent the following meteorological variables: $u, v, \omega, z, T, h, F_x, F_y$, etc., the latter two being the horizontal components of the frictional force. $F(n)$ is the spectral function of $f(\lambda)$.

For the derivatives of $f(\lambda, \phi, p, t)$, the Fourier transform pairs can be written as

$$\frac{\partial f}{\partial \lambda} = \sum_{n=-\infty}^{\infty} in F(n)e^{in\lambda} \tag{4.3}$$

and

$$\{in F(n)\} = \frac{1}{2\pi} \int_0^{2\pi} \frac{\partial f}{\partial \lambda} e^{-in\lambda} d\lambda \tag{4.4}$$

$$\frac{\partial f}{\partial \xi} = \sum_{n=-\infty}^{\infty} \frac{\partial F(n)}{\partial \xi} e^{in\lambda} \tag{4.5}$$

$$\frac{\partial F(n)}{\partial \xi} = \frac{1}{2\pi} \int_0^{2\pi} \frac{\partial f}{\partial \xi} e^{-in\lambda} d\lambda \tag{4.6}$$

where ξ may be ϕ, p , or t .

In view of the products of deviations from the mean values in the energy-transformation equations, the products of functions $f(\lambda)$ and $g(\lambda)$, whose spectral functions are $F(n)$ and $G(n)$, respectively, will now be considered:

$$\frac{1}{2\pi} \int_0^{2\pi} [f(\lambda) g(\lambda)] e^{-in\lambda} d\lambda = \frac{1}{2\pi} \int_0^{2\pi} f(\lambda) \left[\sum_{m=-\infty}^{\infty} G(m)e^{im\lambda} \right] e^{-in\lambda} d\lambda \tag{4.7}$$

Assuming that $g(\lambda)$ is uniformly convergent so that in Eq. 4.7 the order of summation and integration may be reversed, one arrives at

$$\begin{aligned} \frac{1}{2\pi} \int_0^{2\pi} [f(\lambda) g(\lambda)] e^{-in\lambda} d\lambda &= \sum_{m=-\infty}^{\infty} G(m) \frac{1}{2\pi} \int_0^{2\pi} f(\lambda) e^{-i(n-m)\lambda} d\lambda \\ &= \sum_{m=-\infty}^{\infty} G(m)F(n-m) \end{aligned} \tag{4.8}$$

This multiplication theorem gives the spectral function of the product of two variables. $n = 0$ yields Parseval's theorem

$$\frac{1}{2\pi} \int_0^{2\pi} f(\lambda)g(\lambda)d\lambda = \sum_{m=-\infty}^{\infty} G(m) F(-m) \tag{4.9}$$

where $F(-m)$ is the complex conjugate of $F(m)$. Since

$$F(m) \cdot F(-m) = |F(m)|^2 \quad (4.10)$$

for $f = g$, we obtain

$$\frac{1}{2\pi} \int_0^{2\pi} f^2(\lambda) d\lambda = \sum_{m=-\infty}^{\infty} |F(m)|^2 \quad (4.11)$$

It follows from Eq. 4.2 that $F(0) = [f]_{(\lambda)}$.

These considerations can now be applied to the energy-transformation and energy-transport processes outlined in Chap. 3. Conversions between available potential and eddy kinetic energy were considered in detail by Wiin-Nielsen (1959) and by Saltzman and Fleisher (1960b, 1961). In line with the notation used in Chap. 3 and explained in general terms in Chap. 1, we must distinguish between these averaging processes:

Zonal average of variable x ,

$$[x]_{(\lambda)} = \frac{1}{2\pi} \int_0^{2\pi} x \, d\lambda \quad (4.12)$$

and the departures therefrom,

$$(x)_{(\lambda)} = x - [x]_{(\lambda)}$$

Meridional average of x between latitudes ϕ_1 and ϕ_2 ,

$$[x]_{(\phi)} = \frac{1}{\sin \phi_2 - \sin \phi_1} \int_{\phi_1}^{\phi_2} x \cos \phi \, d\phi \quad (4.13)$$

and the departures therefrom,

$$(x)_{\phi} = x - [x]_{\phi}$$

From Eqs. 4.12 and 4.13, we obtain an area average over a constant pressure surface, $[x]_{(\lambda, \phi)}$, with

$$(x)_{(\lambda, \phi)} = x - [x]_{(\lambda, \phi)} \quad (4.14)$$

Time average over the record length τ ,

$$[x]_{(t)} = \frac{1}{\tau} \int_0^{\tau} x \, dt \quad (4.15)$$

and the departures therefrom,

$$(x)_{(t)} = x - [x]_{(t)}$$

Using these averaging techniques, we can compute spectrum functions for the characteristic terms that enter the energy-transformation equations. For more details of derivation, consult the original papers by Wiin-Nielsen (1959) and by Saltzman and Fleisher (1960b, 1961). A recent paper by Hinich and Clay (1968) pointed out the pitfalls in the application of spectrum computations.

In the foregoing, harmonic analysis of atmospheric variables within a belt of constant latitude has been considered in describing conditions over the whole hemisphere. Eliassen and Machenhauer (1965), on the basis of work by Haurwitz and Craig (1952), Gilchrist (1957), and Ellsaesser (1963), proposed an expansion of the height of a pressure surface into a series of spherical-harmonic components. The basic philosophy of the approach, however, remains the same.

COMPUTATIONAL RESULTS

Meridional and Zonal Kinetic-Energy Spectra

The kinetic energy of meridional motions in the domain of wave numbers has been analyzed by several authors. White and Cooley (1956) found two wave-number bands, centered at wave numbers 4 and 8, dominating the meridional eddy-kinetic-energy distribution during the winter of 1949–1950 at 500 mb and at 40°N. Earlier, Charney (1951) obtained two energy peaks at wave numbers 2,5 and 7,5 for a three-day period in January 1946, also at the 500-mb level and at 45°N. Other investigators (Kubota and Iida, 1954; Syono, Kasahara, and Sekiguchi, 1955; Benton and Kahn, 1958; Henry and Hess, 1958; Kahn, 1962; Miegheem, Defrise, and Isacker, 1959, 1963) arrived at similar results. Shapiro and Ward (1963) pointed out the fallacy of generalizing conclusions from too short a time sample or too narrow a latitude belt because of the large time and space variations that can occur (see also Henry and Hess, 1957). They computed monthly meridional geostrophic kinetic-energy spectra at 500 mb for a seven-year period (1946–1952) at 30°N, 45°N, and 60°N. Considerable seasonal and annual variations in monthly mean meridional kinetic energies are evident from this study. Deland (1964) also found considerable day-to-day fluctuations in amplitudes and phase angles of wave numbers 1 and 2.

Benton and Kahn (1958) computed spectra of the zonal kinetic energy for winter and summer of 1949 at the 300-mb surface. As expected, they found that the kinetic energy of zonal motion dominated over that of meridional motion at low wave numbers. At higher wave numbers, the opposite was true. The preponderance of eddy kinetic energy in the meridional flow component appears to shift to lower wave numbers with increasing latitude (see also Kahn, 1962).

Ogura (1958) and Benton and Kahn (1958) commented on the horizontal isotropy of eddy kinetic energy, drawing their conclusions from the same set of data. As one condition of isotropy, the perturbation kinetic energy can be considered equally partitioned between the two horizontal wind components at all latitudes, i.e.,

$$\frac{[(v)_{(\lambda,t)}^2]_{(\lambda,t)}}{[(u)_{(\lambda,t)}^2]_{(\lambda,t)} + [(v)_{(\lambda,t)}^2]_{(\lambda,t)}} = 0.5 \tag{4.16}$$

Such appears not to be the case in the 1959 sample of data, especially not for small wave numbers (Ogura, 1958) and at high latitudes (Fig. 4.1).

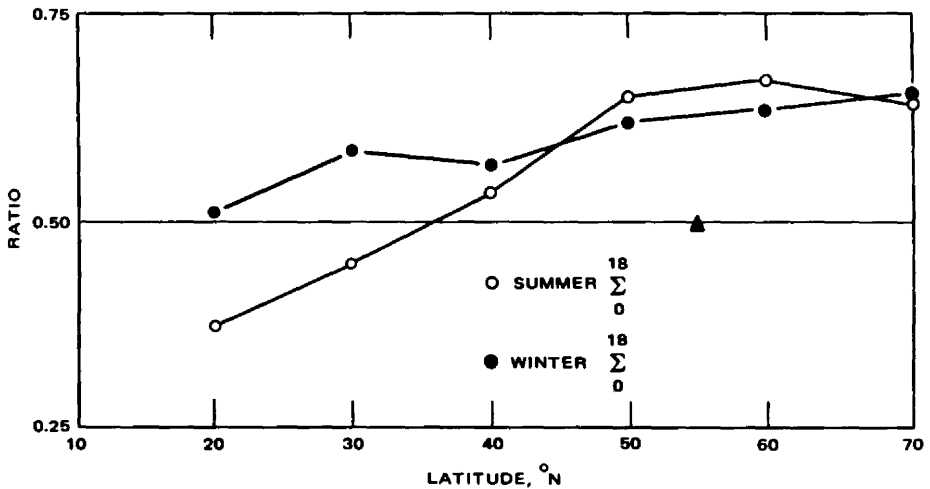


Fig. 4.1 Ratio of perturbation kinetic energy associated with meridional wind to total perturbation kinetic energy. (Triangle shows observation by Henry and Hess, 1958.) [From G. S. Benton and A. B. Kahn, *Journal of Meteorology*, 15(4): 408 (1958).]

Kao (1965) computed Eulerian and Lagrangian autocorrelation coefficients $R(\tau)$ from the wind velocities measured at 300 mb over Salt Lake City, Utah, during the IGY and from Angell's (1960) transosonde data, respectively. By means of the Fourier transformation,

$$F(n) = 4 \int_0^\infty R(\tau) \cos(2\pi n\tau) d\tau \tag{4.17}$$

he obtained the one-dimensional energy spectra of the Eulerian and Lagrangian velocities shown in Fig. 4.2. In Eq. 4.17, n is the frequency (cycles per hour) and τ is the time lag (hours). The kinetic energy of Eulerian velocities seems to be larger than that of the Lagrangian velocities at low frequencies and smaller at high frequencies.

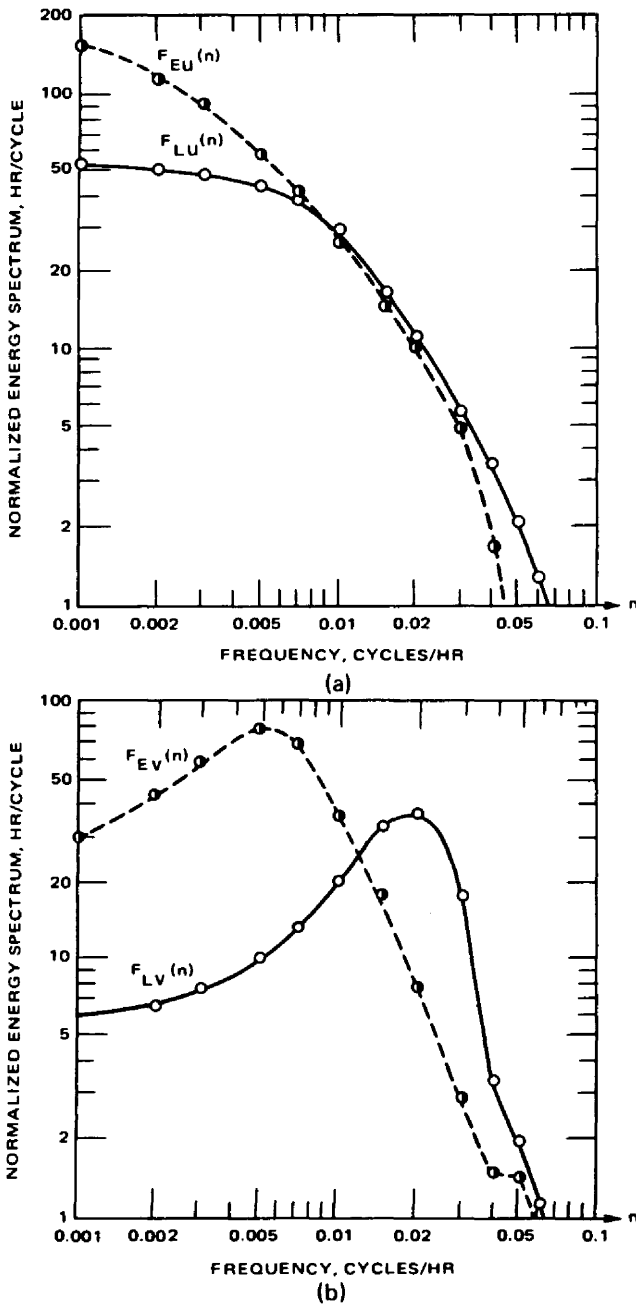


Fig. 4.2 Eulerian and Lagrangian energy spectra of fluctuations in the u component (a) and v component (b). [From S.-K. Kao, *Quarterly Journal of the Royal Meteorological Society*, 91(387): 12 (1965).]

This suggests a frequency-dependent value of β , which correlates the Lagrangian and Eulerian scales of turbulence

$$R_L(y) = R_E(\tau) \quad (\text{for } y = \beta\tau) \quad (4.18)$$

Hay and Pasquill (1959) found $\beta = 4$ to 6 for small-scale turbulence and $\beta = 4$ for mesoscale turbulence. For large-scale eddies, Kao obtained

$$\beta = \left| 1 - \frac{[u]_{(\lambda)} n^2}{2\Omega r \cos^3 \phi} \right| \quad (4.19)$$

where $[u]_{(\lambda)}$ is the mean zonal velocity (meters per second) and n is the wave number of planetary waves measured around the hemisphere (Fig. 4.3) (for a theoretical formulation of the problem, see also Wippermann, Gburčik, and Klug, 1963).

According to Kao, in the frequency range 0.008 to 0.030 cycle/hr, both Lagrangian and Eulerian energy spectra appear to be proportional to the minus second power of frequency (Fig. 4.2). Wiin-Nielsen (1967) found an exponent $b = 2.83$ from the relation

$$\log F(n) = \log a - b \log n \quad (4.20)$$

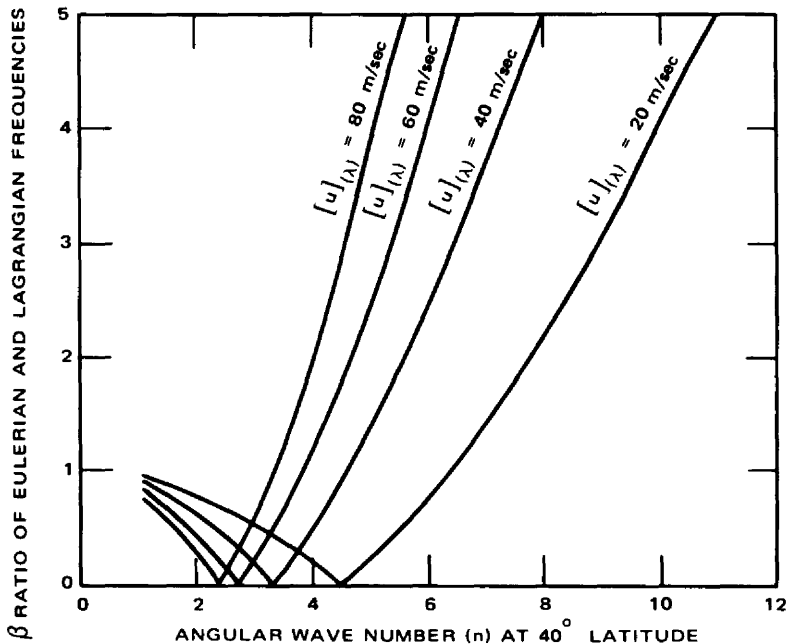


Fig. 4.3 Values of β as function of angular wave number and mean zonal velocity. [From S.-K. Kao, *Quarterly Journal of the Royal Meteorological Society*, 91(387): 16 (1965).]

for the total eddy kinetic energy, K_E , of the whole atmosphere between planetary wave numbers 8 and 15. For the kinetic energy of the mean flow, K_M (for definition, see p. 87), an exponent of -3.22 was found, and for the kinetic energy of the shear flow, K_S (see p. 86), an exponent of -2.17 was found for the same range of wave numbers. (For comparison, the spectral distribution of available potential energy for the whole atmosphere yielded an exponent of -3.21 .) Ogura (1958) found exponents of -3.5 at 70°N , -2.3 at 40°N , and -2.4 at 20°N to satisfy approximately the spectra of u and v components, with the exception of low wave numbers. Similar results were obtained by Barrett (1961). Horn and Bryson (1963) found values of the slope b ranging from 2.3 to 2.9 (smaller in the lower troposphere and larger in the upper troposphere). An average value of b of slightly less than $8/3$ is indicated from their data.

According to the results obtained by Wiin-Nielsen (1967), the slope of the spectrum of the vertically averaged flow, K_M , is steeper than that of the total flow, K_E , and the spectrum of the shear flow, K_S , shows a smaller slope than the spectrum of K_E for eddies $n \geq 8$. This indicates that the vertical-averaging process inherent in K_M removes considerable energy from the smaller eddies with large wave numbers.

In agreement with earlier results by Horn and Bryson (1963), Wiin-Nielsen found an increase of the spectrum slopes of K_E and of A_E with decreasing pressure. This would indicate that there is relatively more energy in the smaller scale eddies in the lower troposphere than in those in the upper troposphere and lower stratosphere. One is tempted to conclude that terrain effects may be reflected in these relatively larger energies at large wave numbers. The use of finite differences (Ogura, 1957) and of smoothing operators involved in numerical map analysis (Shuman, 1957) both tend to decrease the spectrum slope b slightly.

According to the study by Kao (1965), the spectra of the eddy kinetic energy of the v component look considerably different from those of the u component (Fig. 4.2), the former showing a significant peak at intermediate frequencies. To what extent the large shift in the position of this peak between Eulerian and Lagrangian spectra is produced by the geographic bias in the different sources of data has not been ascertained. (One might expect the orographically influenced Salt Lake City region to behave differently in the observed v component than the Pacific Ocean region, from which most of the transsonde data were obtained.) A significant leveling off of the spectra at wave numbers less than 8, however, was also observed by Wiin-Nielsen (1967) (Fig. 4.4) (see also Horn and Bryson, 1963). The shape of the spectrum curve for wave numbers less than 8, shown in this diagram, and representing the total eddy kinetic energy, somehow seems to compromise between the curves F_{Eu} and F_{Ev} computed by Kao and shown in Fig. 4.2. The anisotropy of large-scale motions mentioned previously is again corroborated by the different spectra of the u and v components of flow found by Kao (1965) (Fig. 4.2).

Why the spectra seem to be partitioned at wave number 8 and what causes the respective slopes of the spectra have not been ascertained. Wiin-Nielsen (1967) speculated that the occurrence of maximum baroclinic instability at wave number 6

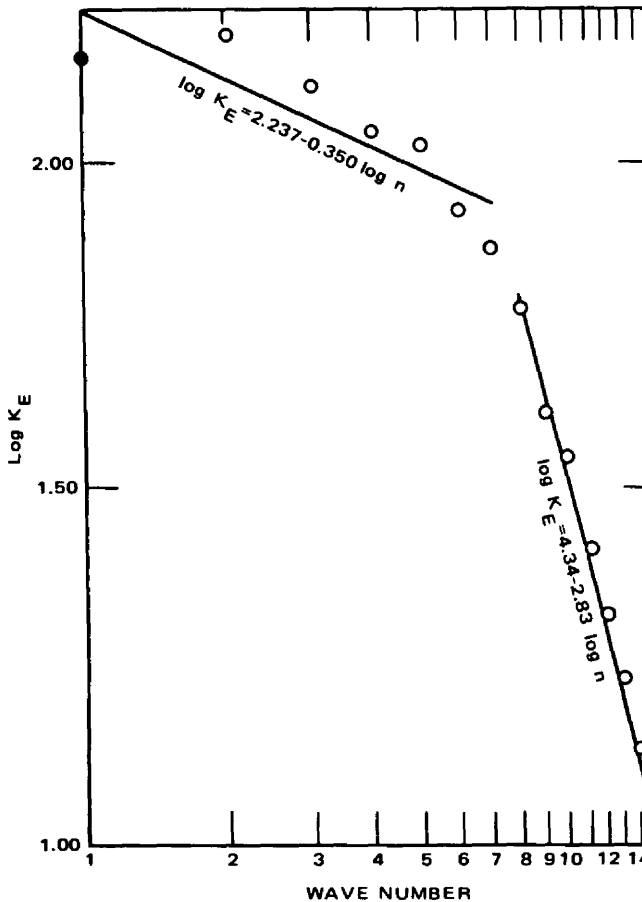


Fig. 4.4 Eddy kinetic energy, K_E , for the total atmosphere as a function of wave number plotted on logarithmic scales. [From A. Wiin-Nielsen, *Tellus*, 19(4): 554 (1967).]

might be related to the shape of the observed spectra. According to a two-level quasi-geostrophic model, waves $n > n_{critical}$ are stable, where

$$n_{critical} = a \cos \phi \frac{f}{p} \sqrt{\frac{2}{\sigma}} \tag{4.21}$$

where a = earth's radius, $p = 500$ mb, and $\sigma = -\alpha(\partial \ln \Theta / \partial p)$ is the static stability. For $\phi = 45^\circ N$, $f = 10^{-4}$ sec, and $\sigma = 2.5$ mts units, one obtains $n_{critical} = 8$. [A critical wavelength beyond which perturbations become unstable has already been noted by Jaw (1946).] Therefore the waves $8 \leq n \leq 15$ should be stable, indicating that in this wave domain there should be no direct conversion of available potential energy into

kinetic energy, just frictional dissipation and nonlinear exchanges of energy between individual wave modes (see p. 184). Thus this part of the large-scale turbulent spectrum can be compared to the equilibrium range of homogeneous turbulence, in which, by analogy, no turbulent energy is generated or dissipated, just redistributed among the various eddy sizes.

Eulerian autocorrelation spectra of the angular momentum over a number of North and Central American stations are available from a study by Chiu and Crutcher (1966). No power laws have been derived in this study, however. Blaes (1961) reports on cospectra of angular momentum transport for several North American stations.

Conversion Between A_E and K_E

Spectra of available potential energy, total potential energy, and entropy have been computed by Dutton and Johnson (1967) for a cross section along 75°W through the northern hemisphere and for the year 1958. These three spectra show striking similarities, especially near their low-frequency end. A rather broad peak in these spectra near a period of 40 days has been identified by these two authors with the index cycle. An average spectral slope of “-2” implies that the amplitude of the pressure fluctuations increases more or less linearly with the period of the disturbance.

Saltzman and Fleisher (1960b) and Wiin-Nielsen (1959) have computed conversion rates between eddy available potential energy (A_E) and eddy kinetic energy (K_E) for February 1959 and January and April 1959, respectively. Even though Saltzman and Fleisher considered the conversion rate (ergs per second) per square centimeter of surface and per millibar of isobaric layers and Wiin-Nielsen computed the conversion rate for the total atmosphere north of 15°N , the computational results agree remarkably well (Figs. 4.5 and 4.6).

Both sets of computations show two main peaks, one near wave number 2 and one near wave numbers 6 and 7, at which relatively large amounts of eddy available potential energy are transformed into eddy kinetic energy. A similar wave-number dependence of energy conversions holds for the mean winter conditions observed during January through March and October through December 1959 (Fig. 4.7) (see also Murakami and Tomatsu, 1965b). Although in these computations no distinction has been made as yet between standing and transient waves, we may argue that wave number 2 corresponds to the two large quasi-stationary troughs of the northern hemisphere, one in the lee of the Rocky Mountains and one east of the Himalayas. From numerical experiments Kasahara (1967) found that during winter orographic and thermal effects (produced by land-sea distribution) cooperated in the generation of planetary waves in the northern hemisphere. The thermal effect appears to dominate during summer and also in the southern hemisphere (see also Döös, 1969). Murakami (1967), on the other hand, finds a considerable mountain effect, especially in wave number 3.

According to Eliassen (1958), waves 1 to 4 are semi-permanent and occur in preferred locations (see Stark, 1965; Barrett, 1961; Rao, 1965). For a harmonic

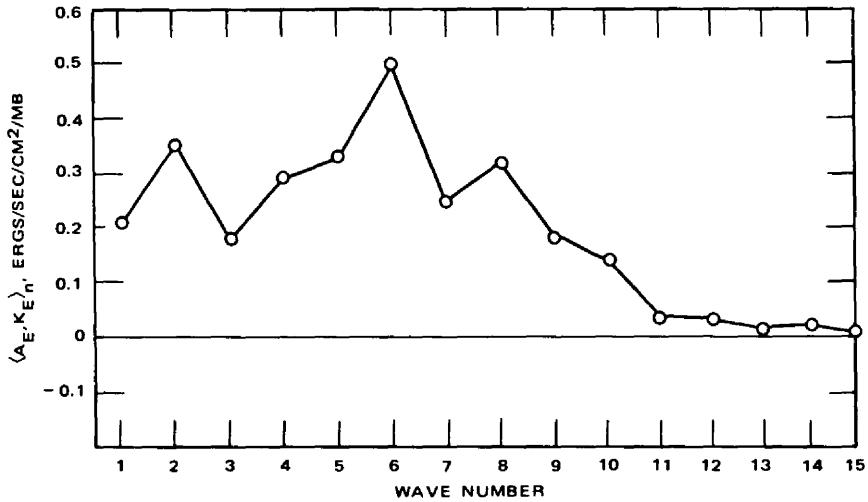


Fig. 4.5 Mean spectral function for rate of conversion from eddy available potential energy to eddy kinetic energy for February 1959. [From B. Saltzman and A. Fleisher, *Journal of Geophysical Research*, 65(4): 1220 (1960).]

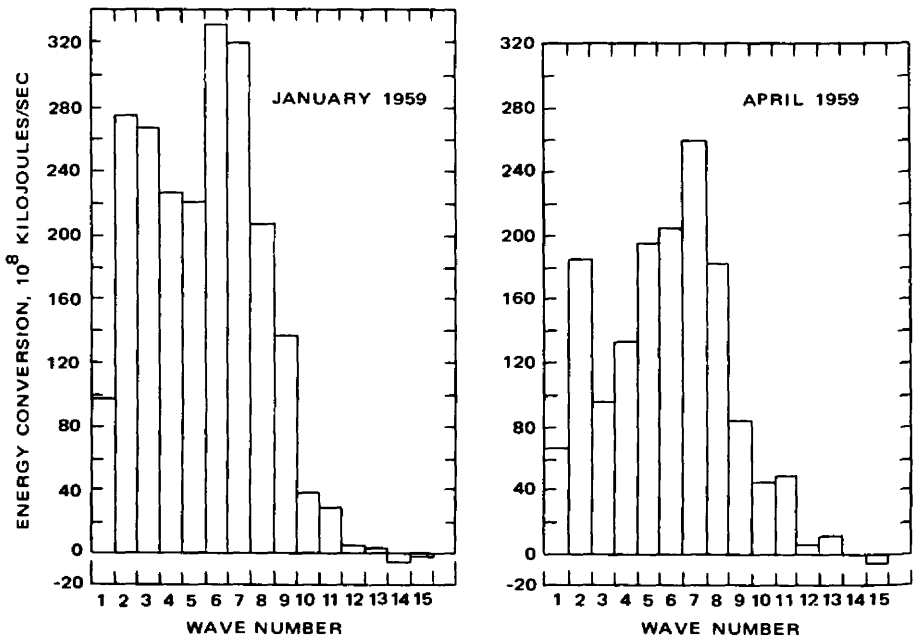


Fig. 4.6 Energy conversion as a function of wave number averaged in time for January 1959 and April 1959. The horizontal coordinate is the number of waves around the hemisphere and the vertical coordinate is energy conversion per unit time north of about 15°N. [From A. Wiin-Nielsen, *Monthly Weather Review*, 87(9): 326; 327 (1959).]

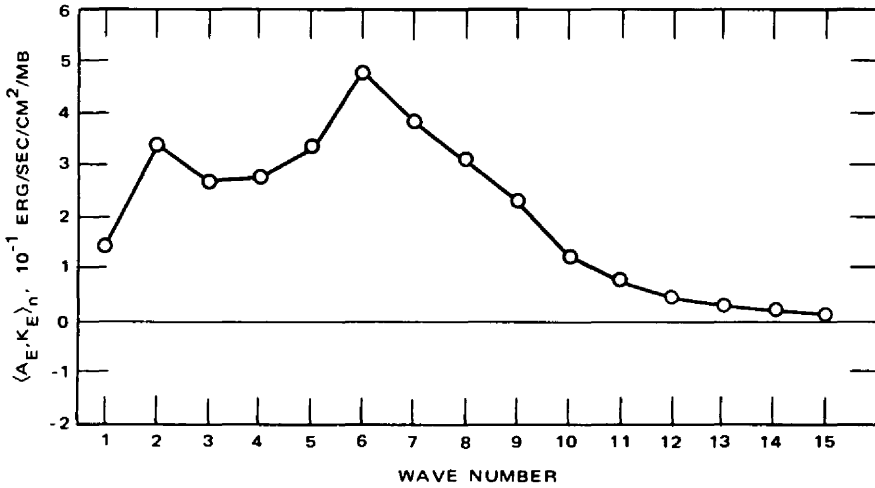


Fig. 4.7 Mean spectral function for the rate of conversion from eddy available potential energy to eddy kinetic energy for the winter half year, 1959. [From B. Saltzman and A. Fleisher, *Journal of Geophysical Research*, 66(7): 2273 (1961).]

analysis of topography, see Peixoto et al. (1964). Higher wave numbers characterize traveling waves. Haney (1961) found these low-number waves to be stationary in middle latitudes (50°N) only and slightly retrograde at high (70°N) and low latitudes (30°N). Wave numbers 6 and 7 correspond roughly to wavelengths of 4700 and 4000 km, respectively, in middle latitudes. They coincide with the most unstable baroclinic waves of migrating (and deepening) cyclones and anticyclones (Eady, 1949; Mieshem, 1955).

The transformation of A_E into K_E will mainly occur in deepening cyclones. Such cyclones, however, reveal a westward tilt of the trough axis with increasing altitude (Fleagle, 1947). It is not surprising, therefore, that Nitta (1967) found from a theoretical 20-level model of the atmosphere an increase in eddy kinetic energy with such a tilt of the trough with altitude. The tilt of the ultralong and long waves appears to be important for eddy-kinetic-energy changes near or above the tropopause, whereas the short-wave tilt influences mainly the lower troposphere.

Wiin-Nielsen (1962) showed that K_E can be decomposed into eddy kinetic energy of the (baroclinic) shear flow and of the (barotropic) mean flow (see Eq. 3.64). The main conversion between these two modes, (K_{SE}, K_{ME}), appears to take place at wave number 7 with wave numbers 6 and 8 following closely in magnitude. There again the conversion is mainly due to the nondivergent part of the flow pattern.

Linear perturbation theory predicts that all waves with a wavelength shorter than 3000 km should be stable in middle latitudes. This agrees well with the rapid cutoff of energy conversion at wave number 10 in Fig. 4.6. This wave number corresponds to a wavelength of approximately 2800 km.

A physical interpretation of the foregoing results may be attempted as follows: A_E is converted into K_E by the sinking of cold air and the rising of warm air in planes

parallel to latitude circles. Such vertical motions take place mainly in deep frontal cyclones of the horizontal dimensions stated previously. The sinking cold air leads to cold outbreaks behind a cold front advancing equatorward, whereas the rising warm air in such cyclones flows poleward along the sloping surface of the warm front.

From climatological data it is well known that cold outbreaks occur very frequently in the lee of the Rocky Mountains over the midwestern plains. They tend to follow the quasi-stationary upper trough, which has been explained by Bolin (1950) as a consequence of flow over the mountains under conservation of potential vorticity. Similar conditions are found to the lee of the Himalayas. It is not surprising, therefore, that wave numbers 2 and 3, which are orographically generated (wave number 3 incorporating the "resonance trough" over Europe, which usually is not as pronounced as the other two), play an important role in the release of A_E .

The A_E converted into K_E is revealed in the form of meandering jet maximums. From synoptic analyses we know that unstable baroclinic waves associated with cyclones are connected with intense jet maximums. Cyclogenetic processes, which obviously occur in the wave-number domain 6 or 7, according to the computations by Wiin-Nielsen and Saltzman and Fleisher, lead to a strong interchange between stratospheric and tropospheric air masses. Again such cyclogenesis is found frequently in the lee of the Rocky Mountains and of the Himalayas. One might argue, therefore, that the large contributions of conversions of A_E into K_E by wave number 2 (Figs. 4.5 to 4.7) are not so much due to releases in the quasi-barotropic stable waves of this spectrum range but are produced by frequent cyclogenesis of horizontal dimensions corresponding to wave number 6 or larger, which occurs in a preferred location to the east of the two large mountain ranges of the northern hemisphere.

The numerical results shown in Figs. 4.5 to 4.7 constitute net conversions of A_E to K_E , based on correlation terms $[(\omega)_{(\lambda)}(T)_{(\lambda)}]_{(\lambda)}$ (see Table 3.1). If confined regions near a jet maximum are considered, transformations of eddy potential energy into kinetic energy even larger than those indicated by the hemispheric zonal-average values may be realized. A study by Palmén (1958), involving the transition of hurricane "Hazel" of October 1954 into an extratropical cyclone, shows, for instance, a release of available potential energy of 26.4×10^{10} kilojoules/sec or 52 watts/m² (Palmén, 1966b) (Fig. 4.8) in the region occupied by the cyclone. This is almost one order of magnitude more than the hemispheric release of A_E of either wave number 6 or 7 during January 1959 (Fig. 4.6). A nearly equivalent amount of kinetic energy is exported from the eastern part of the cyclone region (Fig. 4.9). This export takes place almost exclusively in the jet-stream region. This fact illustrates the dynamic interaction between cyclones and jet streams.

Palmén's (1958) estimate of the generation of K_E of 52 watts/m² holds for an extremely strong cyclone. For an average polar-front cyclone, 20 watts/m² may be a more realistic value of kinetic-energy generation (Palmén and Holopainen, 1962; Danard, 1964; Palmén, 1966b).

Since usually more than one deep cyclone exists in a hemisphere and since each of these cyclones individually may account for more than the mean hemispheric transformation of A_E into K_E , we can conclude that relatively large amounts of K_E

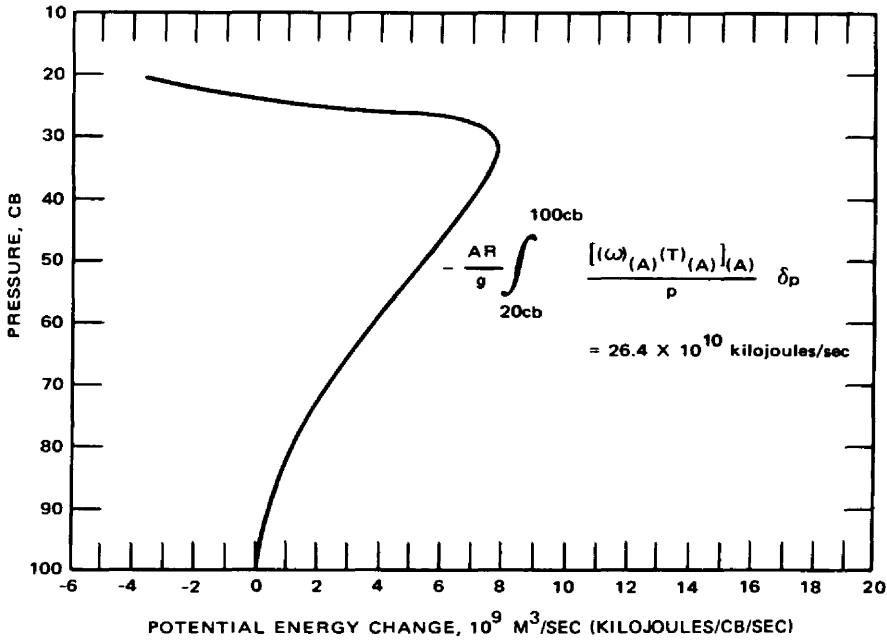


Fig. 4.8 Negative value of the change of available potential energy due to vertical circulations per centibar layer over the whole area of the cyclone. [From E. Palmén, *Tellus*, 10(1): 22 (1958).]

are converted back again into A_E . These amounts are not contained in the statistics by Wiin-Nielsen nor in those by Saltzman and Fleisher. The mechanism of this conversion can be seen from the flow processes in the vicinity of a jet-stream maximum: To the rear of a jet-stream maximum, which is a manifestation of the presence of K_E , a direct circulation is produced by the distribution of convergence and divergence aloft. A_E is released in the circulation and contributes to the strong winds observed in the jet maximum. Downstream from the velocity maximum, however, the divergence and convergence distribution causes an indirect circulation (see Newton, 1954) in which the decelerating air motions lose K_E and gain A_E .

The loss of A_E to the rear and the gain of A_E in front of a jet-stream maximum, expressed by frontolysis and frontogenesis, respectively, cause the jet-stream maximum and its associated frontal zone to move slowly downstream. Here frontolysis and frontogenesis are understood with respect to the migrating jet stream. The air, however, which moves quickly through the jet maximum, undergoes frontogenetic processes as it enters the maximum from the rear and frontolytic processes as it diverges when leaving the maximum in front (Reiter, 1961, 1963b).

A cyclone index developed by Mahlman (1964a, 1964b, 1965), indicating cyclogenesis, shows a good correlation with radioactive fallout at the surface, i.e., with the transport of stratospheric air to the ground. The cyclone intensity, however, depends on the magnitude of the conversions of A_E into K_E and back into A_E and not

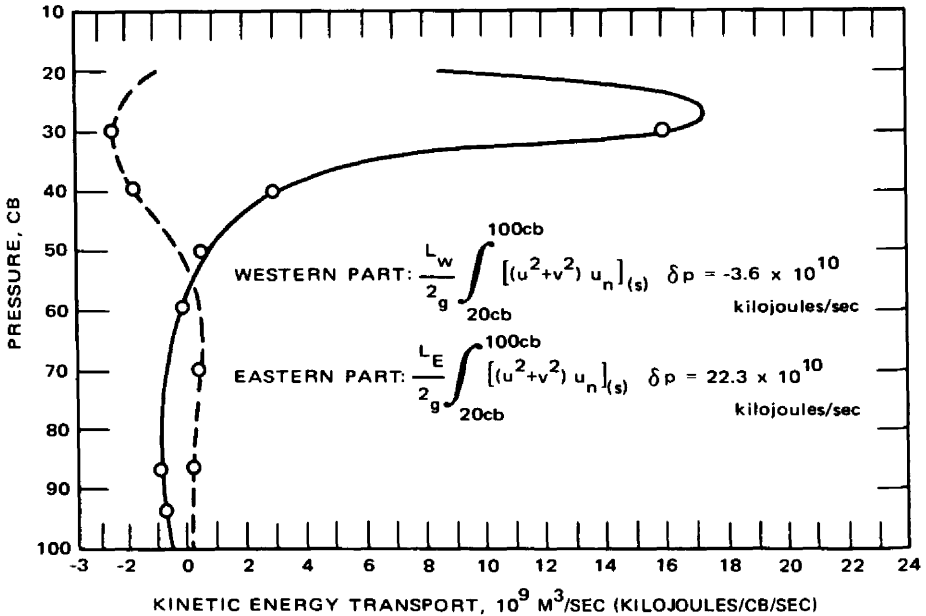


Fig. 4.9 Net export of kinetic energy per centibar layer from the western part of the area of the cyclone (dashed curve) and from the eastern part (solid curve). (u_n is the velocity component normal to the boundary of the area under consideration.) [From E. Palmén, *Tellus*, 10(1): 19 (1958).]

so much on the hemispheric net conversions shown in Figs. 4.5 to 4.7. It would seem, therefore, that these diagrams, although they give valuable information on the maintenance of the general circulation, do not reflect the true amount of large-scale turbulent-mixing processes prevailing in the atmosphere.

To estimate the latter, one would have to compute $\langle A_E, K_E \rangle_{max}$ by counting only the positive contributions to this quantity around the hemisphere before performing the space- and time-averaging operations. $\langle A_E, K_E \rangle_{max} / \langle A_E, K_E \rangle$ should give a measure of the turbulent mixing in the atmosphere that actually goes on while the general circulation is maintained. To my knowledge, no such detailed computations have been made. Palmén (1961) points out, without giving numerical estimates, that, in view of the excessive amounts of A_E converted into K_E within disturbances like hurricane "Hazel," large amounts of K_E have to be converted back into A_E .

Conversion Between K_E and K_Z

The preceding data considered mainly the exchange of energy between A_E and K_E . Saltzman and Fleisher (1960a) also estimated the conversion between eddy and zonal kinetic energy. Such conversion is expressed by $\langle K_E, K_Z \rangle$ in Table 3.1. As shown in this table, this term contains the quantity $(u)_{(\lambda)}(v)_{(\lambda)}$, which is a result of the

presence of large-scale horizontal Reynolds stresses. The two authors computed the expression

$$M(n) = \frac{2\pi a}{g} \int \int [U(n, \phi, p) V(-n, \phi, p) + U(-n, \phi, p) V(n, \phi, p)] \\ \times \cos^2 \phi \frac{\partial}{\partial \phi} \left[\frac{[u(\phi, p)]_{(\lambda)}}{\cos \phi} \right] d\phi dp \quad (4.22)$$

which measures the rate of transfer of kinetic energy between the mean zonal flow and the harmonic components of the eddy flow (see also Lorenz, 1951; Kao, 1954a; Kubota and Iida, 1955; Isacker and Miegheem, 1956; Perry, 1967). It comprises the first integral term of $\langle K_E, K_Z \rangle$ (Table 3.1), which, according to Kuo (1951a) and Starr (1953), is the dominant term (see also work by Reynolds, 1895; Lamb, 1932; Blackadar, 1950; Starr, 1959a). $[u(\phi, p)]_{(\lambda)}$ is the mean zonal wind, which is considered as a function of latitude and pressure. U and V are the complex Fourier coefficients of the zonal and meridional components of wind, respectively. They were computed geostrophically from complex spectra $A(n)$ of contour heights at the 500-mb level (Saltzman, 1958):

$$U(n) = -\frac{g}{fa} \frac{\partial}{\partial \phi} A(n) \\ V(n) = \frac{ing}{fa \cos \phi} A(n) \quad (4.23)$$

where n is the wave number around latitude circles and a is the earth's radius.

In Eq. 4.22, integration was performed over the entire depth of the atmosphere and between 15°N and 80°N latitude. Estimates were made for each day of the year 1951 at 500 mb. Results are shown in Fig. 4.10 and in Table 4.1. For an estimate of the contributions from the unsampled portions of the hemisphere, it was assumed that the integrand faded to zero linearly from 22.5°N to 10°N and from 72.5°N to the pole.

As mentioned in Chap. 3, the computational results indicate a transfer of energy on the average from the eddies to the mean flow.

As shown in Table 4.1, the daily variations of the energy-conversion term $M(n)$, expressed by its standard deviation, are larger than the annual or seasonal mean values. This would imply that during certain limited periods of time even wave numbers that, on the average, contribute heavily toward the maintenance of the mean zonal circulation can draw energy from the zonal flow. This is probably the case during the transition from high index to low index periods, when the zonal westerly polar vortex breaks down into meanders of large-amplitude planetary waves (see Chap. 3).

Estimates of short-term fluctuations of $\langle K_E, K_Z \rangle$ by Wiin-Nielsen, Brown, and Drake (1964) are given in Fig. 3.38. This diagram shows, indeed, such reversals in the

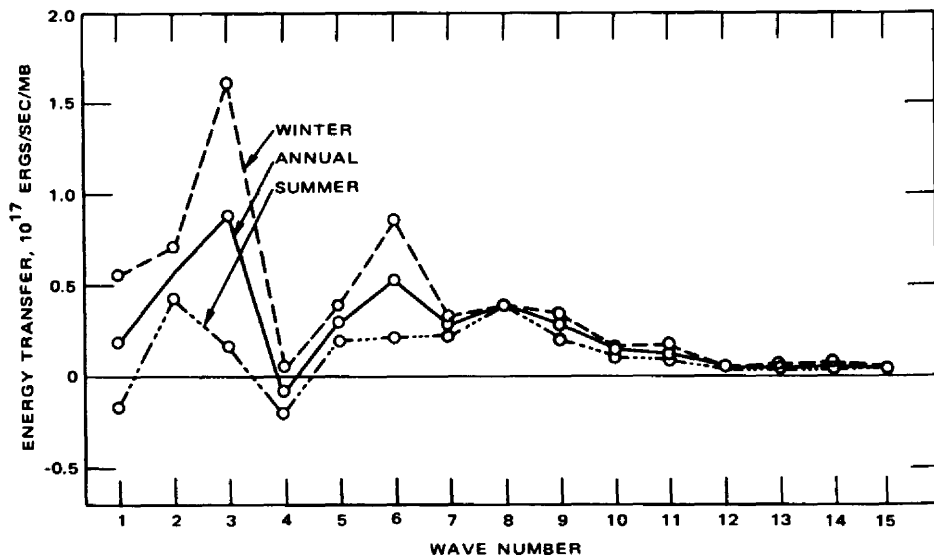


Fig. 4.10 Average values of $M(n)$ for the entire year 1951, for the winter half year (January–March, October–December), and for the summer half year (April–September). A positive value signifies a transfer of kinetic energy from disturbances of wave-number n to the mean zonal current. [From B. Saltzman and A. Fleisher, *Tellus*, 12(1): 110 (1960).]

Table 4.1
STANDARD DEVIATIONS OF THE DAILY VALUES OF $M(n)$ FROM THE AVERAGES SHOWN IN FIG. 4.10 ($\pm 10^{17}$ ERGS/SEC/MB)*†

	Wave number															$\sum_{n=1}^{15} M(n)$
	1	2	3	4	5	6	7	8	9	10	11	12	13	14	15	
Winter	1.54	2.59	2.76	1.90	2.20	2.41	1.63	1.47	0.91	0.79	0.48	0.47	0.34	0.33	0.34	9.10
Summer	0.73	1.22	1.52	1.08	1.02	0.99	1.03	0.92	0.62	0.45	0.41	0.34	0.24	0.30	0.23	3.66
Annual	1.26	2.03	2.33	1.55	1.72	1.87	1.37	1.23	0.78	0.65	0.45	0.41	0.29	0.32	0.29	6.98

*From B. Saltzman and A. Fleisher, *Tellus*, 12(1): 111 (1960).

†The last column gives the standard deviation of the net daily transfer.

sign of $\langle K_E, K_Z \rangle$, as has been suspected from Table 4.1. Moreover, significant differences are shown between seasons and even between the same seasons of different years (see also Chap. 3). Such differences are expressed not only in the total transformation $\langle K_E, K_Z \rangle$ but also in the distribution of this quantity in wave-number space. This is shown in Fig. 4.11. Whereas January 1959 revealed a net positive conversion $\langle K_E, K_Z \rangle$, January 1963 showed an abnormal negative conversion. This has been commented on in detail in Chap. 3. In 1959 during this month, wave numbers 5

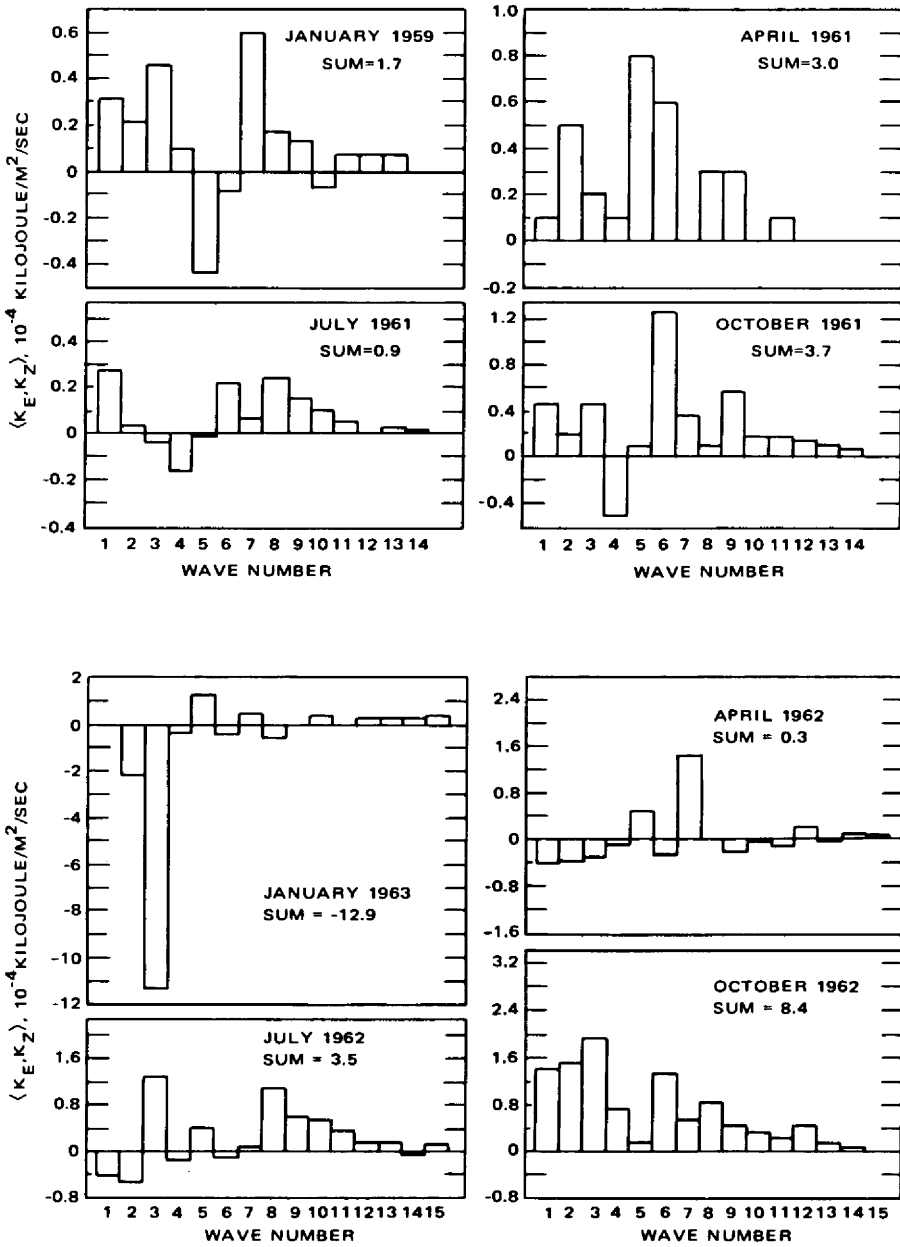


Fig. 4.11 Energy exchange from eddy to zonal kinetic energy as a function of wave number for the months indicated. Upper four diagrams based on 850- and 500-mb data and lower four diagrams on 850-, 700-, 500-, 300-, and 200-mb data. [From A. Wiin-Nielsen, J. A. Brown, and M. Drake, *Tellus*, 16(2): 176; 177 (1964).]

and 7 achieved significant importance in addition to wave numbers 1, 2, and 3. Wave numbers 5 and 6 were the only ones that revealed a negative conversion; this was counterbalanced, however, by the effects of the other wave numbers. In January 1963, on the average of tropospheric conditions, only wave number 3 was of importance, with strong negative values of $\langle K_E, K_Z \rangle$. In Chap. 3 it was mentioned that the atmosphere obviously is at liberty to choose more than one energy cycle in maintaining its general circulation. The factors that prompt this choice remain unexplored so far.

The irregular behavior of wave number 3 during January 1963, indicating the presence of index cycles, is evident from Fig. 4.12.

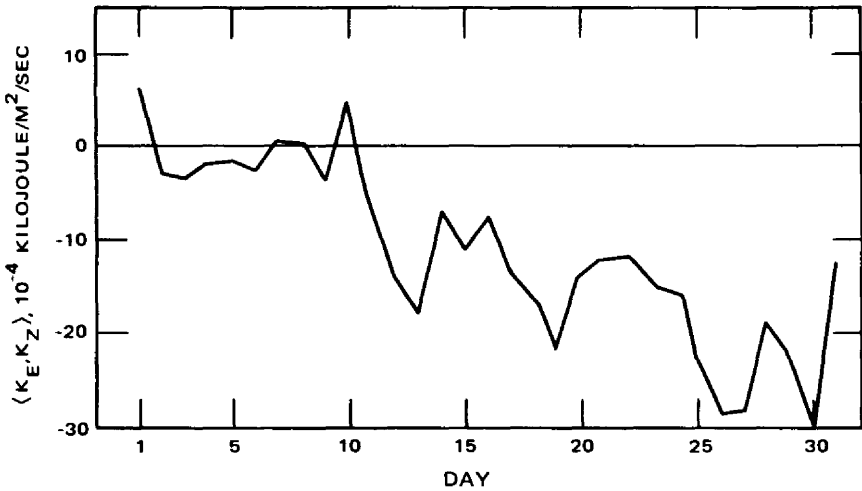


Fig. 4.12 Daily values of the energy exchange $\langle K_E, K_Z \rangle$ for wave number 3 as a function of time for January 1963. [From A. Wiin-Nielsen, J. A. Brown, and M. Drake, *Tellus*, 16(2): 178 (1964).]

For the stratosphere (65-mb level), Julian and Labitzke (1965) computed a predominance of wave numbers 2 and 3 during January 1963 in the conversion terms $\langle K_E, K_Z \rangle$ and $\langle A_E, K_E \rangle$. For the period Jan. 25 to Feb. 9, 1957, Reed, Wolfe, and Nishimoto (1963) found that wave number 2 accounted for most of the positive conversion $\langle K_E, K_Z \rangle$. Maximum values were realized near 50°N latitude. The conversion $\langle A_E, K_E \rangle$, which was positive during the first part of this time period and negative during the second part (see Table 3.4), was also mainly due to wave number 2. The average value over the whole period showed maximum negative values near 50°N latitude and maximum positive values near 70°N . From a case study of January and February 1959, Boville, Wilson, and Hare (1961) also stressed the importance of the long wave perturbations (1 and 2) in stratospheric energetics. In addition, they found waves near wave number 4 to be baroclinic and to contribute in the conversion $\langle A_E, K_E \rangle$.

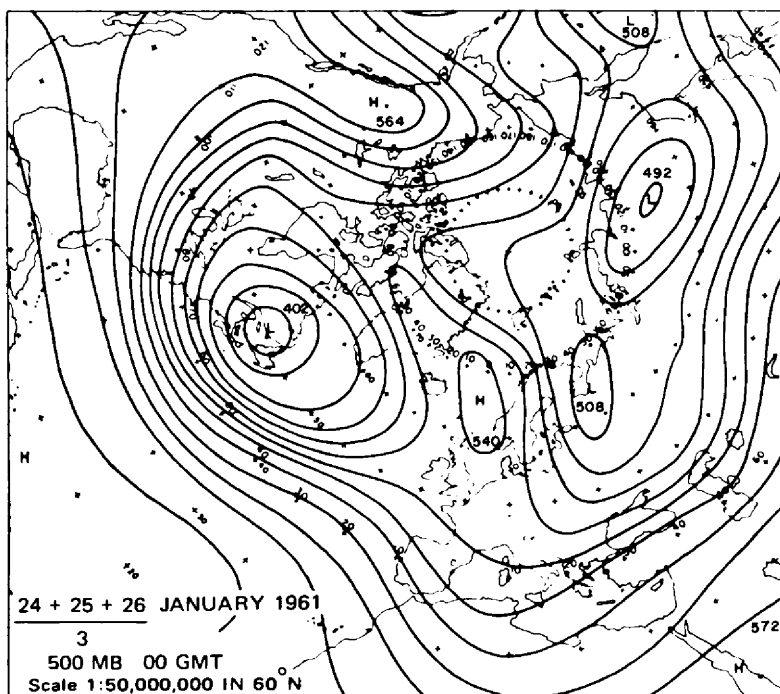
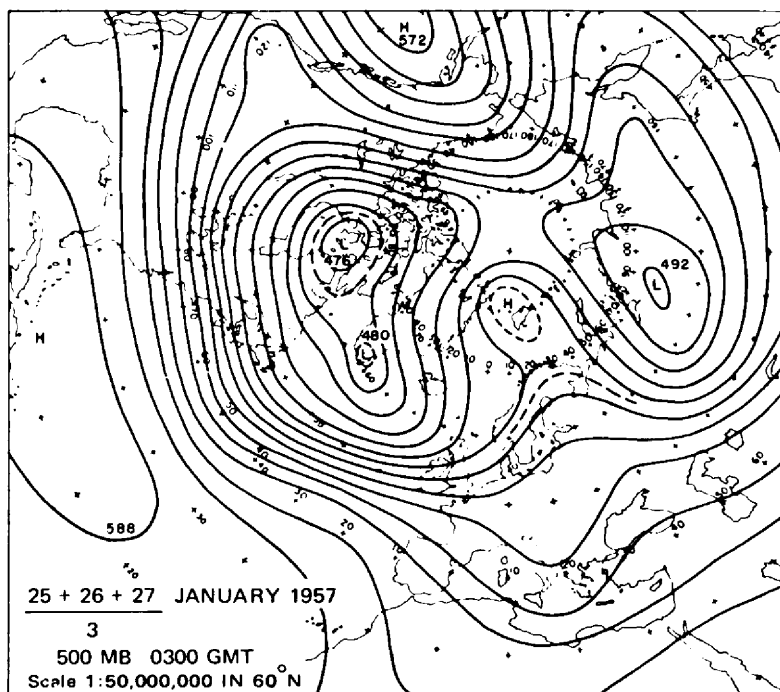


Fig. 4.13 (See page 183 for legend.)

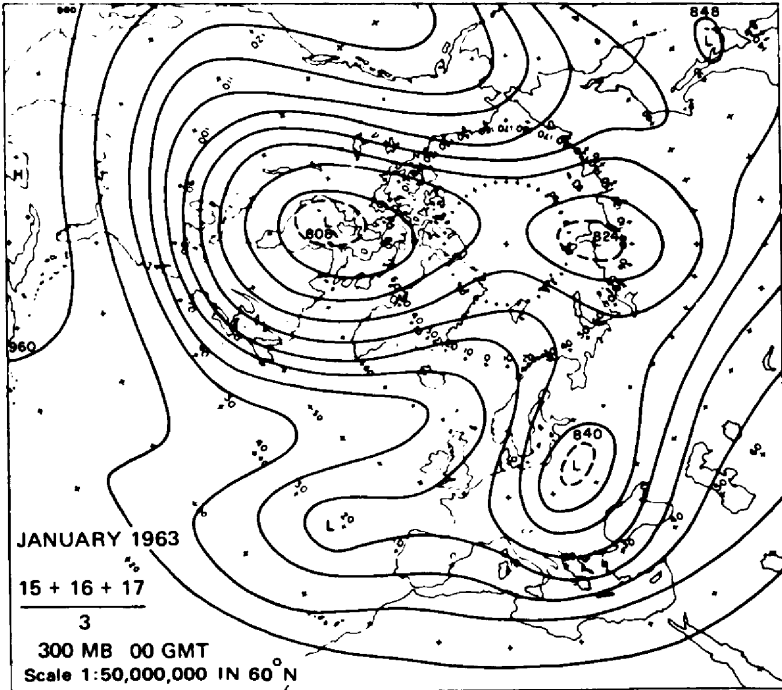
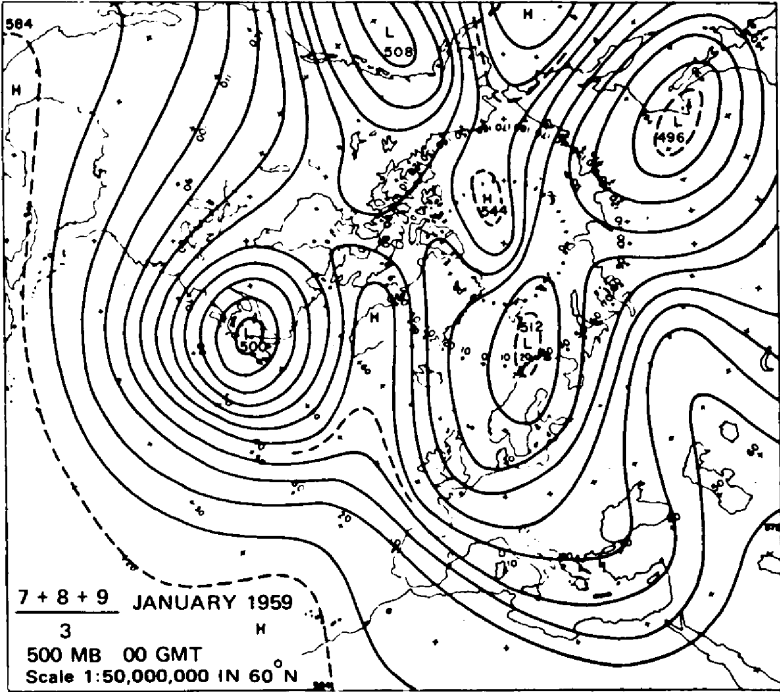


Fig. 4.13 (Continued) (See facing page for legend.)


The different behavior of January 1957, 1959, and 1963 is noteworthy because, according to Labitzke (1965a, 1965b), these three months belong to the same category of stratospheric vortex breakdown in which the movements of anticyclonic vortices at the 10-mb level proceed from west to east (Fig. 3.63). Figure 4.13 shows the significantly different long wave patterns that prevailed in the stratosphere during these January months. During 1957 a two-wave pattern appeared to be quite dominant. Four waves are well established during January 1959. As shown in Fig. 4.11, these waves converted some of their kinetic energy into K_Z of the zonal flow. January 1961 reveals a rather diffuse three- to four-wave pattern. Three waves are more clearly established during January 1963, but, as shown in Fig. 4.11, these waves tend to extract energy from the mean zonal flow.

Teweles (1963b) studied the warming epoch of January 1958, which, according to Labitzke (1965a, 1965b), belonged to the category of westward-drifting stratospheric highs (see Chap. 3). He found an increase of kinetic energy of wave number 1 caused by transfer of K_Z as well as of K_E from other waves. The kinetic energy of wave number 2 also increased during this period, and a large transfer of K_E occurred from this wave to both the zonal kinetic energy, K_Z , and to other waves. He concluded from this that the development of wave number 2 was of baroclinic nature.

Such energy-transfer processes were also brought to light in a recent study by Perry (1967) of the stratospheric warming of January 1963. He constructed the flow diagram shown in Fig. 4.14. This diagram also reveals the coupling that took place between stratosphere and troposphere in the various wave domains. Such coupling was also envisioned by Doperto (1964). His derivations of an in-phase coupling of vertical motions associated with large cyclonic and anticyclonic disturbances in the lower troposphere and upper stratosphere do not agree, however, with statistical results found by Molla and Loisel (1962) and mentioned previously. The arguments by Faust (1960) in favor of no coupling between lower and upper stratosphere have been disproved by the preceding investigations. Muench (1966) found an upward propagation of perturbation energy from the earth's surface into the stratosphere mainly in wave numbers 1 and 2.

In Chap. 3 it has been demonstrated that the kinetic energies K_Z and K_E can be separated into contributions from the vertically averaged mean flow and from the departures from it—the baroclinic shear flow (Eqs. 3.59 to 3.65). Wiin-Nielsen and Drake (1965) have studied these modes of kinetic energy in the wave-number space. Figure 4.15 shows the conversion $\langle K_S, K_M \rangle$ as a function of wave number. Conditions for $n = 0$ conform to $\langle K_{SZ}, K_{MZ} \rangle$, whereas the sum of conversions in the other wave numbers $n = 1, \dots, 15$, yields $\langle K_{SE}, K_{ME} \rangle$.

From Tables 3.5 to 3.8 and Fig. 3.29, no drastic differences between January 1962 and January 1963 could be detected. Only seasonal differences became evident from

 Fig. 4.13 Synoptic situation in the middle troposphere immediately before the stratospheric warmings (geopotential decameters). Contour interval 8 decameters on the 500-mb maps and 16 decameters on the 300-mb map. [From K. Labitzke, *Journal of Applied Meteorology*, 4(1): 92 (1965).]

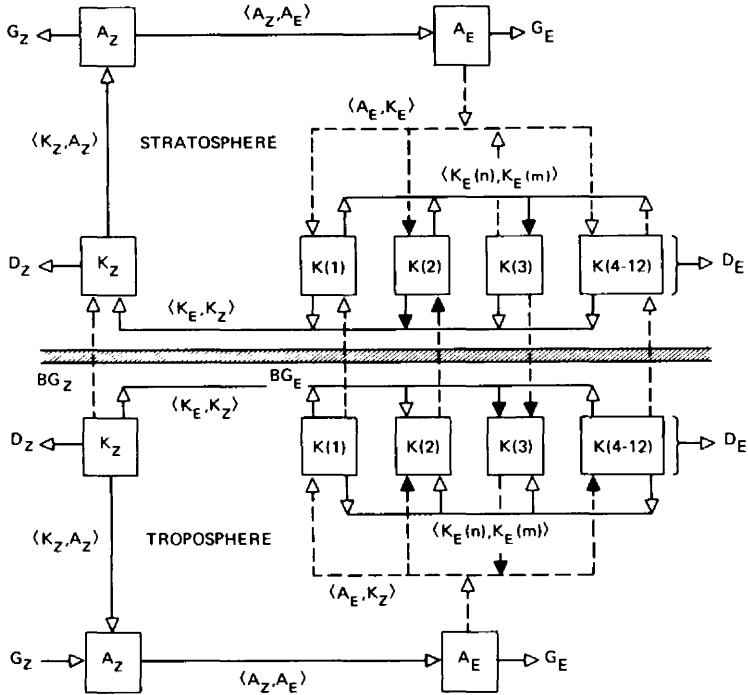


Fig. 4.14 Schematic flow diagram of energy for the stratosphere and troposphere in January 1963. Principal eddy energy processes are indicated by bold arrows. [From J. S. Perry, *Journal of the Atmospheric Sciences*, 24(5): 547 (1967).]

the changing mean magnitudes of kinetic-energy modes and their transformations. Figure 4.15, however, reveals a striking change in the behavior of the general circulation between the months of January 1962 and January 1963. During January 1962, the largest amounts of energy conversion were accomplished by wave numbers 7 and 8, whereas wave numbers 2 and 3 dominated during January 1963. Miller (1969) also points out strong variations from year to year in the energy cycle of individual wave numbers.

The energies K_S and K_M themselves reveal a predominance in $n = 0$ for all months. The eddy contributions show a slight peak at wave numbers 2 and 3 during January 1963. In January 1962, maximum values were found at wave number 1, with steadily decreasing energies contained in higher wave numbers. (Data are not reproduced here. For further details consult the original paper by Wiin-Nielsen and Drake, 1965.)

Energy Exchange Between Wave Numbers

Although the preceding studies are concerned with the transfer of energy between K_E and K_Z , it is also of interest to estimate the energy exchange between eddies of

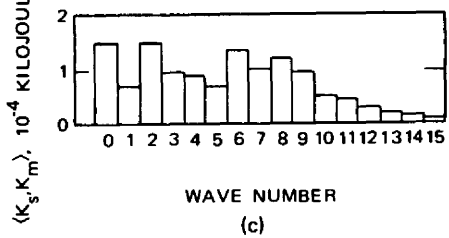
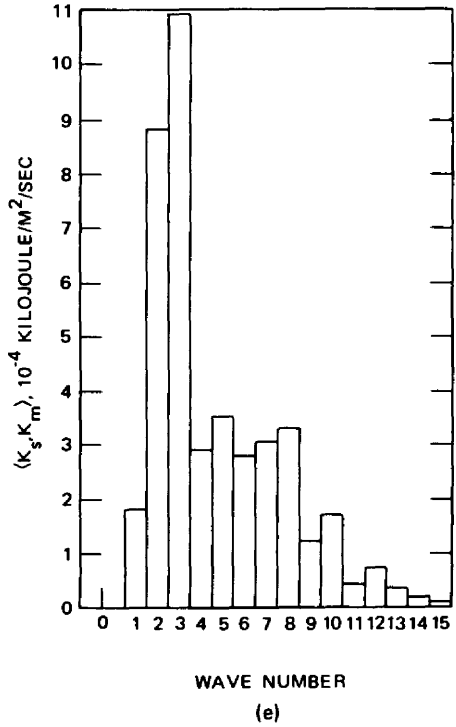
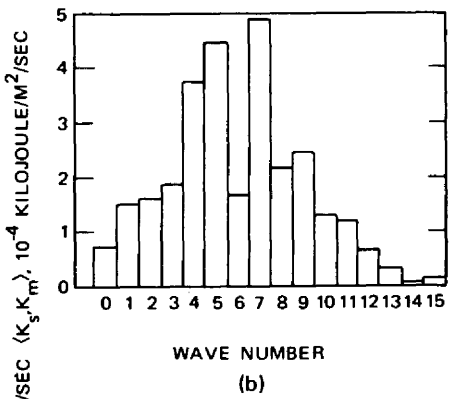
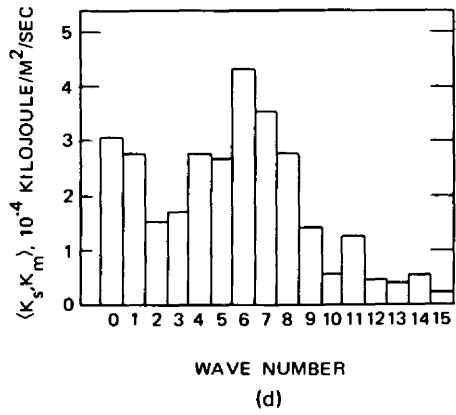
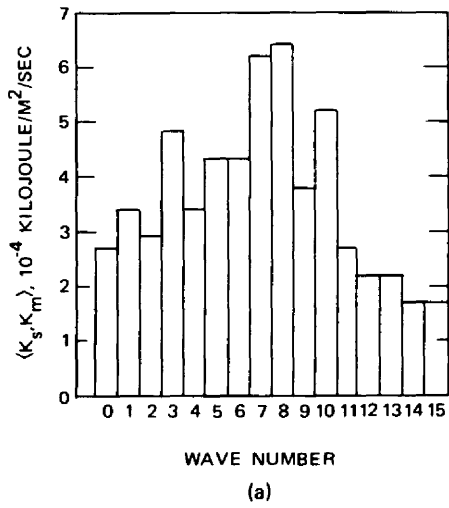


Fig. 4.15 Spectrum of the energy conversion $\langle K_S, K_M \rangle$ in the average for the months indicated as a function of wave number. (a) January 1962. (b) April 1962. (c) July 1962. (d) October 1962. (e) January 1963. [From A. Wiin-Nielsen and M. Drake, *Monthly Weather Review*, 93(2): 86 (1965).]

various wave numbers. Based on Saltzman's (1957) harmonic-analysis scheme, Saltzman and Fleisher (1960c) indicated a method of computing these exchange processes. The rate, $L^*(n)$, at which the existing kinetic energy at wave number n is redistributed among all other wave numbers can be written as

$$L^*(n) = L'(n) + L''(n) \quad (4.24)$$

with the condition

$$\sum_{n=1}^{\infty} L^*(n) = 0 \quad (4.25)$$

This redistribution process is assumed to be independent of all other processes that can alter the total eddy kinetic energy, such as the transfer to or from zonal motion ($n = 0$), viscous dissipation, or conversion of potential energy. This assumption may not always be justified, especially in the lower stratosphere, which receives considerable energy through boundary terms $B\phi_z$ and $B\phi_E$ (Table 3.1) (see also Fig. 4.14). $L'(n)$ denotes the contribution to $L^*(n)$ from large-scale horizontal winds, for which the geostrophic approximation can apply. $L''(n)$ contains the effect of individual pressure changes, dp/dt . If the investigation is restricted to large-scale eddies only (wave numbers 1, . . . 15), $L''(n)$ may be neglected as a first approximation, and Eq. 4.25 can be written as

$$\sum_{n=1}^{15} L^*(n) = \sum_{n=1}^{15} L'(n) = 0 \quad (4.26)$$

For the 500-mb surface, between 22.5°N and 72.5°N, and the year 1951, Saltzman and Fleisher (1960c) obtained the results shown in Fig. 4.16. As shown in this figure, the cyclone waves (wave numbers 6 to 10) appear to feed the long waves as well as the shorter waves by redistribution of their kinetic energy (see also Fjørtoft, 1953, Paulin, 1968). All three ranges of wave numbers, in turn, provide energy to the mean zonal flow ($n = 0$) according to Saltzman and Fleisher. Saltzman, Gottuso, and Fleisher (1961) found that energy transfers between the eddies and the mean zonal current are more effective at low latitudes, whereas at higher latitudes processes involving interactions between eddies seem to prevail (see also Murakami and Tomatsu, 1964, 1965b). (For more details, especially on computational schemes, consult the original papers.) Holopainen (1966) found, furthermore, that the stationary eddies tend to feed the transient ones, especially in subtropical and middle latitudes. This is in agreement with the concept that traveling disturbances frequently develop out of (orographically generated) stationary long-wave troughs.

From a study by Saltzman and Teweles (1964) of a nine-year period of data, all waves (2 to 15) appear to support $n = 0$ and 1, i.e., the asymmetric polar vortex. Wave numbers 2 and 5 to 10 are sources of kinetic energy; the other waves are sinks (Fig. 4.17). Thus at wave number 2 there appears to be a forced generation of kinetic energy on the scale of the land-sea distribution or of the large orographic barriers of the northern hemisphere, or both (see also M. S. Rao, 1965).

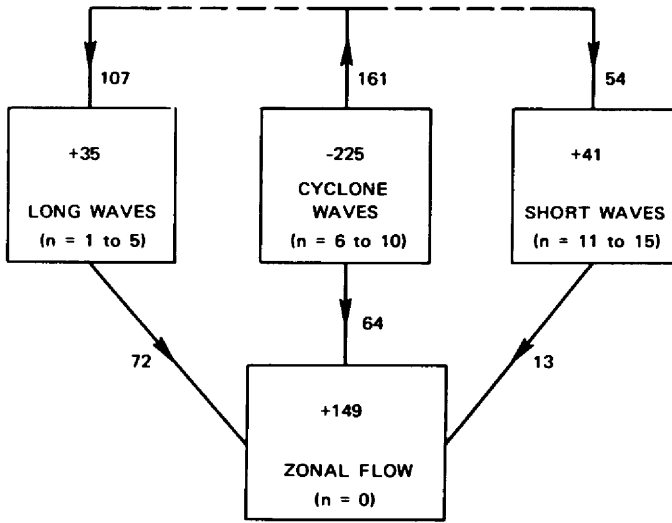


Fig. 4.16 Estimate of the mean rate of kinetic-energy exchange (10^{-3} erg/sec/cm²/mb) among long waves, cyclone waves, and shorter waves and between these waves and the zonal current. Computations are based on 500-mb geostrophic measurements for the year 1951. [From B. Saltzman and A. Fleisher, *Tellus*, 12(4): 376 (1960).]

From special harmonic analyses, Eliassen and Machenhauer (1965) (see also Merilees, 1968) found that the main transfer from longitudinal waves was to the zonal current (0,3) [the first number is the longitudinal wave number (0 indicating the zonal current) and the second number is the latitudinal wave number for the northern hemisphere], whereas at (0,5) and (0,7) the zonal current, on the average, contributed slightly to the longitudinal waves. Deland (1965a, 1965b, 1965c) also computed spherical harmonic waves. He showed that the speed of transient waves depended on the latitudinal wave number. Merilees (1966) found rapidly retrogressive spherical waves at 500 mb in the northern hemisphere (see also Deland and Johnson, 1968, and Deland and Lin, 1967).

Orthogonal polynomials, such as Tchebychev polynomials, have been used by various authors to describe the distribution of atmospheric parameters on a surface (Friedman, 1955; Malone, 1956; Cehak, 1962). To my knowledge such treatment has not been extended to incorporate energy transports or conversions.

Transport of Momentum and Heat

The vertical distribution of momentum in the wave-number space is shown in Fig. 4.18 (see also Wiin-Nielsen, 1965b). As mentioned previously, most of the momentum transport occurs at jet-stream level. During the months of April and July, the transport in wave numbers $n \geq 5$ exceeds that in low wave numbers. During October and

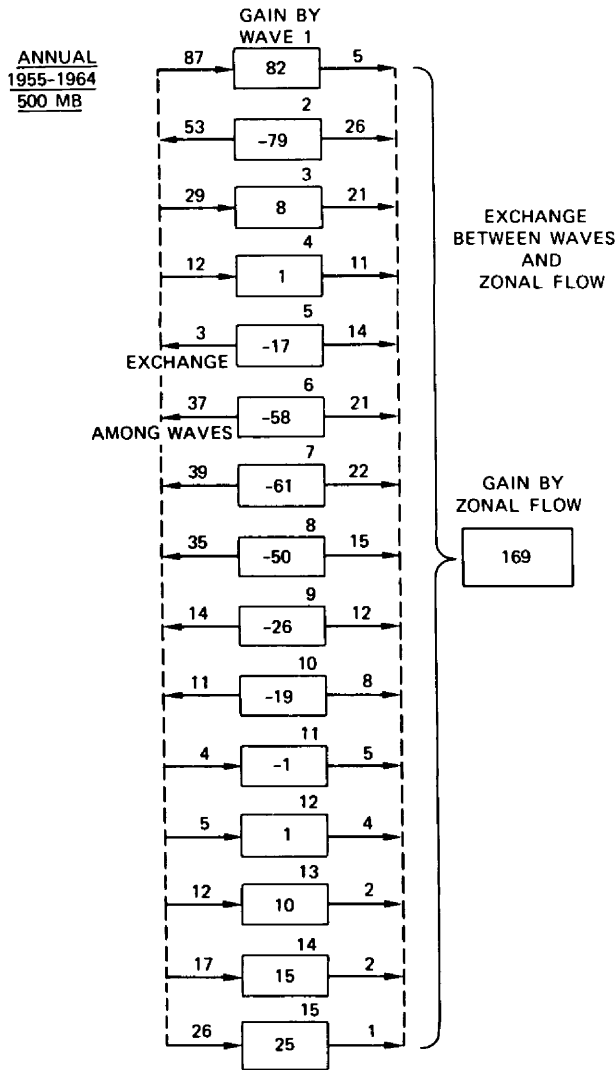


Fig. 4.17 Annual means of L (see Eq. 4.26) and M (see Eq. 4.22) (10^{-3} erg/cm²/sec/mb) represented in the form of a budget. L values are in the first open column and M values in the second open column with the plus sign shown by an arrow pointing toward the right. The net gain of kinetic energy by individual waves, $[L(n)-M(n)]$, and by the zonal flow, $\sum_{n=1}^{15} M(n)$, is shown by the figures in boxes. A negative value in a box represents an exported quantity of kinetic energy which, it is assumed, was generated within the given wave number principally by conversion from available potential energy and which is in excess of any amount consumed by friction. [From B. Saltzman and S. Teweles, *Tellus*, 16(4): 434 (1964).]

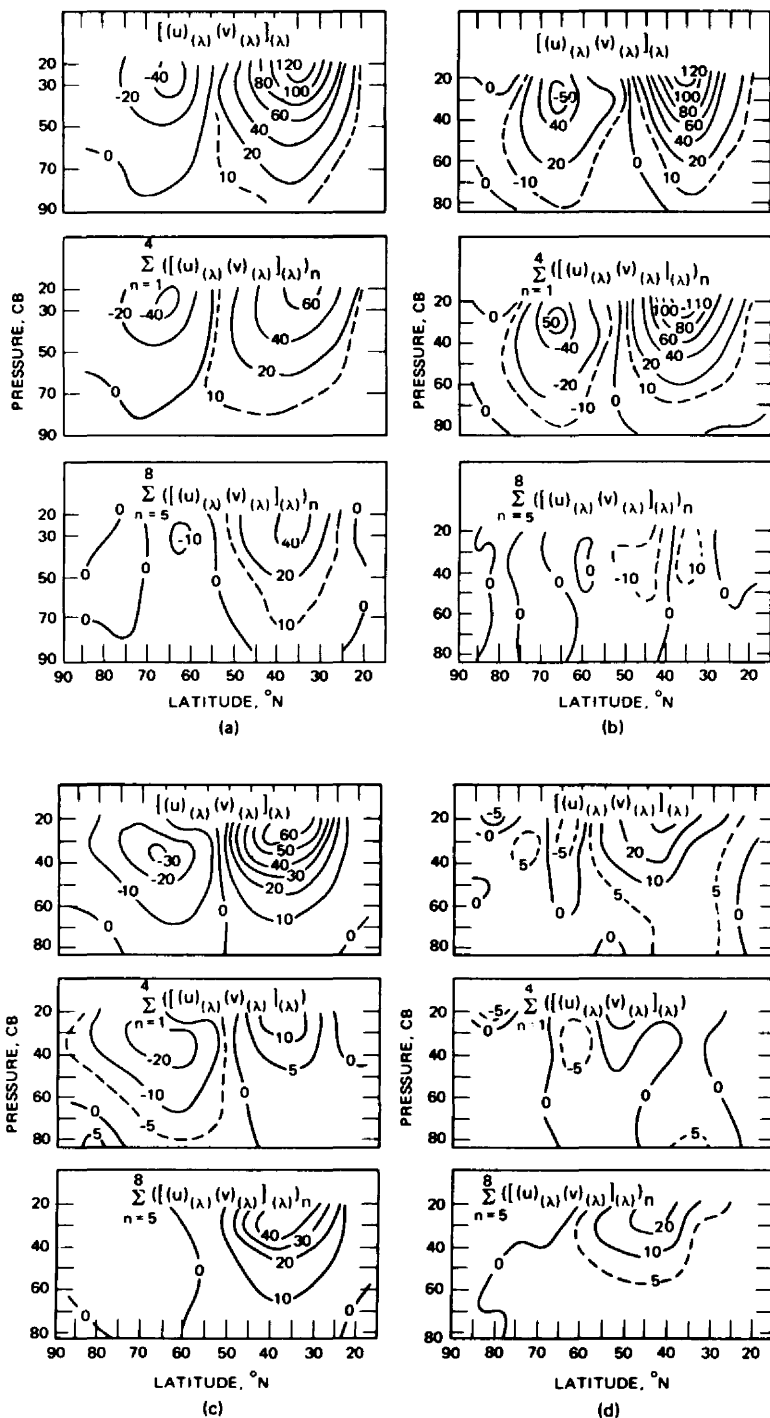


Fig. 4.18 (See page 190 for legend.)

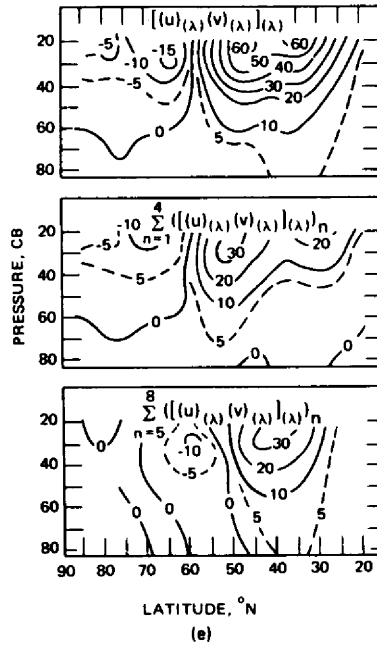


Fig. 4.18 Transport of relative momentum (m^2/sec^2) as a function of latitude and pressure. (a) January 1962. (b) January 1963. (c) April 1962. (d) July 1962. (e) October 1962. The upper part of each figure shows the total momentum transport, the middle part gives the momentum transport by waves with wave numbers 1 to 4, and the lower part shows the momentum transport by waves with wave numbers 5 to 8. [From A. Wiin-Nielsen, J. A. Brown, and M. Drake, *Tellus*, 15(3): 271 (1963); 16(2): 172, 173, 174 (1964).]

especially during January, transport by long planetary waves (1 to 4) prevails (see also Henry and Hess, 1958). Again, January 1962 and 1963 differ significantly from each other. January 1963 transports almost the entire amount of momentum in wave number 3, whereas January 1962 relies heavily on shorter waves ($n = 5, 6, 7,$ and 8).

Miller, Teweles, and Woolf (1967) studied the average conditions of the transport of relative angular momentum for the 10-year period, Apr. 1, 1955, to Mar. 31, 1965. Results are shown in Fig. 4.19 for wave numbers 1, 2, 3, and 6 and for the total transport accomplished by wave numbers 1 to 10. From this diagram it is evident that wave number 2 tends to transport momentum equatorward, especially during January. This southward transport extends over a considerable latitude belt. Wave number 3 appears to carry the bulk of northward transport in midlatitudes. Wave numbers 6 to 10 accomplish most of the northward transport during summer at the latitudes of the summertime tropospheric jet stream.

The main transport of sensible heat occurs in the lower troposphere (see Chap. 3). Similar to the momentum transport, the months of April and July 1962 favor

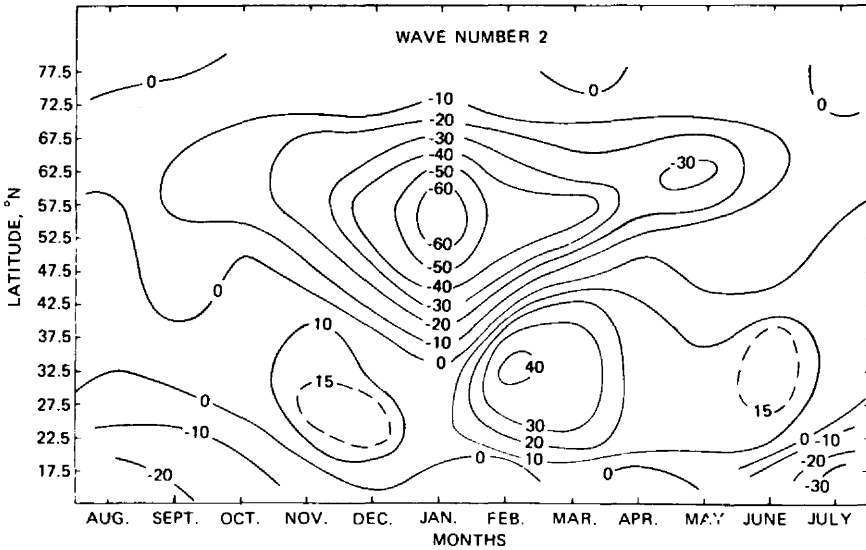
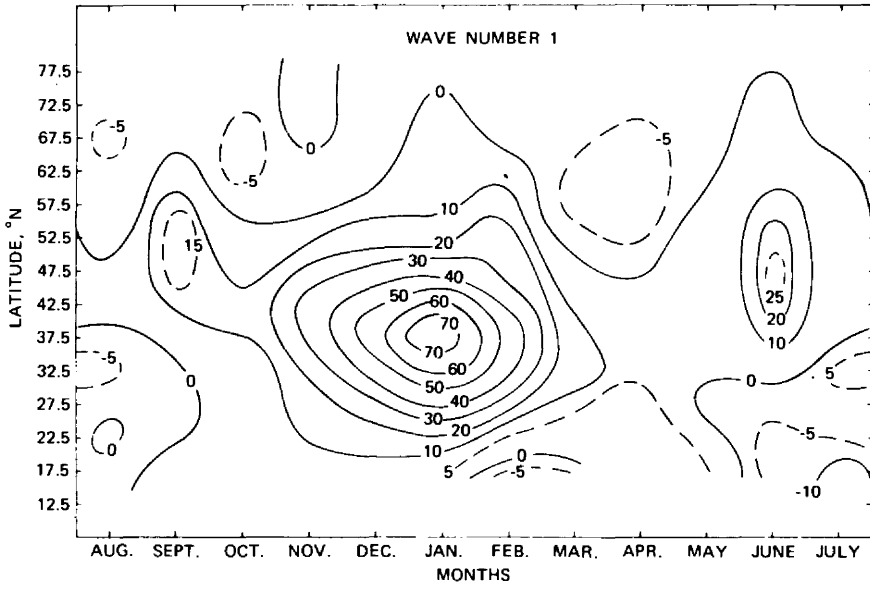


Fig. 4.19 (See page 193 for legend.)

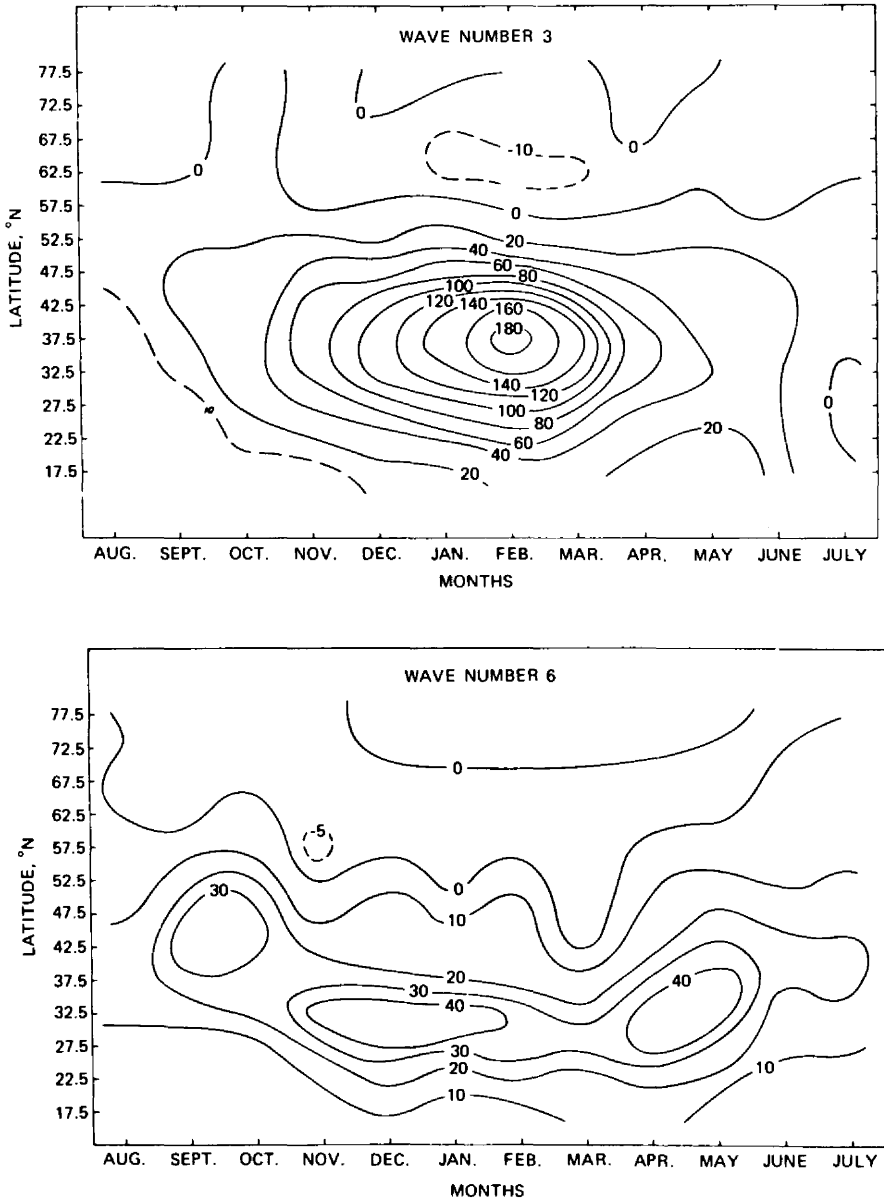


Fig. 4.19 (Continued) (See facing page for legend.)

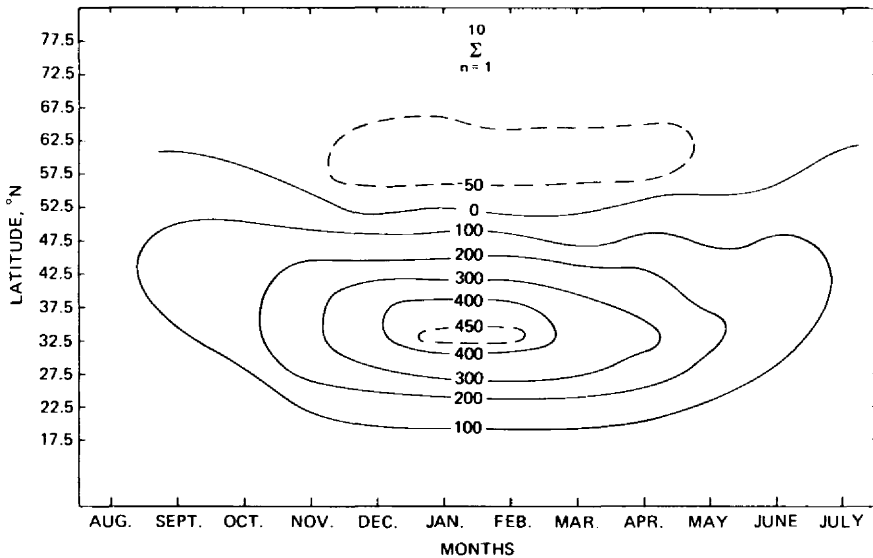


Fig. 4.19 Ten-year average of relative angular momentum transport (10^{21} ergs/mb) by wave numbers as indicated as a function of latitude and month. [From A. J. Miller, S. Teweles, and H. M. Woolf, *Monthly Weather Review*, 95(7): 430; 431; 432; 434; 438 (1967).]

heat transport by wave numbers 5 to 8 (Fig. 4.20). October 1962 shows almost equal magnitudes of transport in wave numbers 1 to 4 and 5 to 8. Both January 1962 and 1963 favor the longer wave domains. The differences in heat transport between these two months are relatively small in contrast to the momentum transports shown in Fig. 4.18. From this we can conclude that mainly the transport processes in the upper troposphere and in the stratosphere are affected by drastic changes in the atmospheric energy cycle, such as expressed by a reversal in sign of $\langle K_E, K_Z \rangle$, and not so much by the processes in the lower troposphere, which are responsible for the bulk of sensible heat transport. Jet-stream configurations and transport processes associated therewith appear to be most critically affected by the particular choice of the energy cycle that maintains the general circulation during a given month or season. Anything that would help in understanding the reasons behind such a choice would mean a dramatic step forward in long-range weather prediction.

The latitudinal differences in the importance of various wave numbers in transporting momentum and heat are shown in Fig. 4.21 for January 1962. The results are in general agreement with those obtained by Mintz (1951) for January 1949. A shift of emphasis in relative transport magnitudes to smaller wave numbers with increasing latitude, because of the shorter circumference of the earth, is not generally indicated in Wiin-Nielsen's data. Results obtained by Miller, Teweles, and Woolf (1967) agree with this conclusion (see Fig. 4.19).

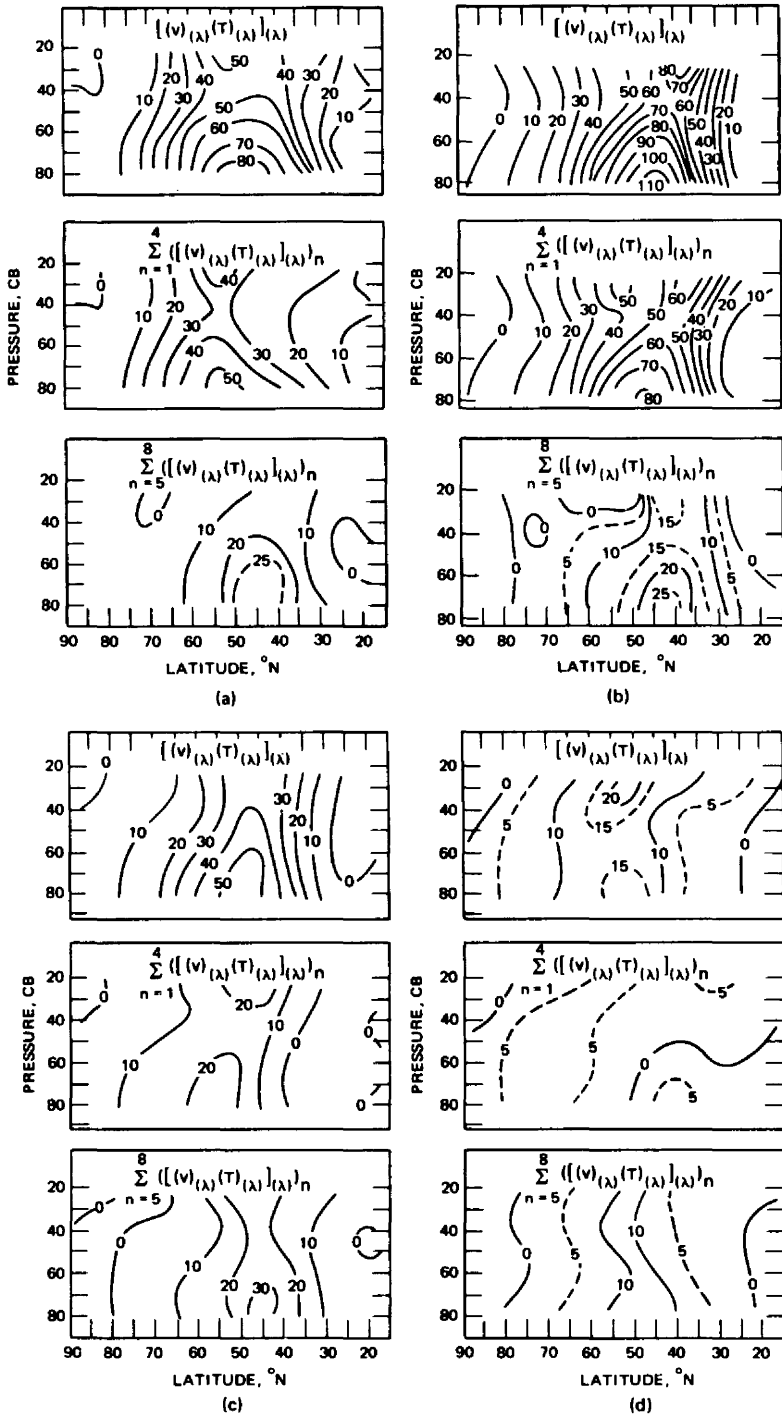


Fig. 4.20 (See facing page for legend.)

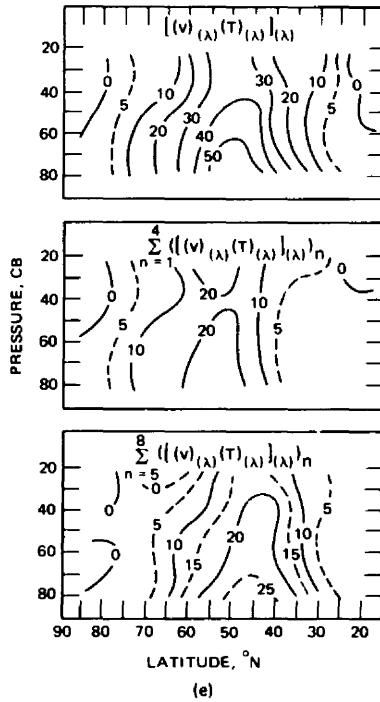


Fig. 4.20 The transport of sensible heat (kilojoule/sec/cb) as a function of latitude and pressure. (a) January 1962. (b) January 1963. (c) April 1962. (d) July 1962. (e) October 1962. The upper part of each figure shows the total heat transport, the middle part gives the heat transport by the waves with wave numbers 1 to 4, and the lower part shows the heat transport by waves with wave numbers 5 to 8. [From A. Wiin-Nielsen, J. A. Brown, and M. Drake, *Tellus*, 15(3): 266, 267 (1963); 16(3): 169, 170, 171 (1964).]

Energy Generation and Dissipation

The generation and dissipation of eddy available potential energy in the wave-number space, $G_E(n)$, has been dealt with in detail by Brown (1964). Results for various months are shown in Fig. 4.22. The dashed lines in each of the diagrams indicate the standard deviations of the daily average contributions to $G_E(n)$. As mentioned in Chap. 3, diabatic effects on the average tend to dissipate available potential energy ($G_E < 0$) except for July. The strongest dissipation is found in the long planetary waves. This is also corroborated by TIROS IV radiation data (Winston, 1967a; see also Chap. 3). However, as can be seen from the magnitudes of the standard deviations, there are periods interspersed throughout the year when $G_E(n)$ is greater than zero, i.e., when eddy available potential energy is generated by diabatic effects. One such way of generating A_E would be by precipitation processes and by release of latent heat in warm air masses.

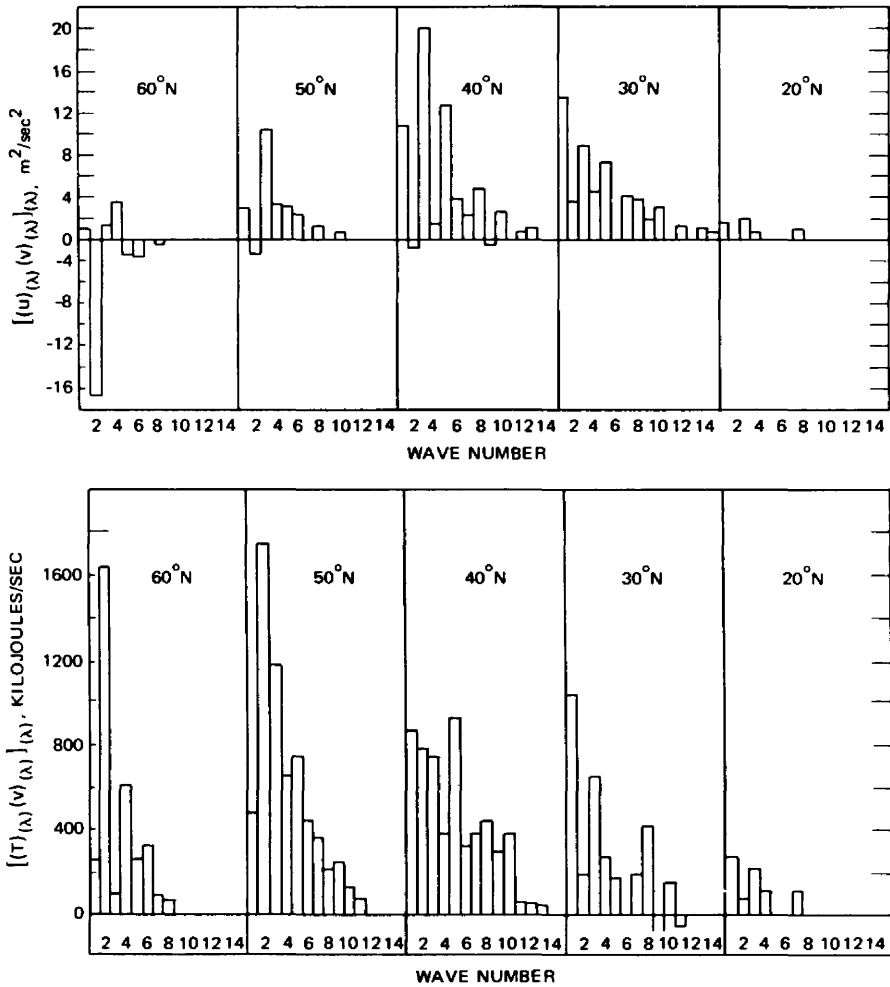


Fig. 4.21 Momentum transport averaged with respect to pressure (upper diagrams) and total transport of heat across latitude circles (lower diagrams) as functions of the wave number for selected latitudes. Averaged values for the month of January 1962. [From A. Wiin-Nielsen, J. A. Brown, and M. Drake, *Tellus*, 15(3): 268; 272 (1963).]

Interannual changes, as discussed previously, especially with respect to January 1963, also occur in the distribution of G_E over the various wave numbers.

Frictional and terrain effects (see Cressman, 1959) based on drag coefficients computed by Cressman (1960) are incorporated in Brown's data. Comparisons with an earlier frictionless model (Wiin-Nielsen and Brown, 1962) reveal that friction and mountains tend to reduce the values of $G_E(n)$, especially for wave number 2 (see top of Fig. 4.22). Smallest reductions occur at wave numbers 1 and 5.

Water-Vapor Transport

Peixoto and Saltzman (1958) computed the eddy water-vapor transport over the northern hemisphere for the year 1950 in the wave-number domain. In the spectra of mean water-vapor distribution, wave number 2 of the standing eddies dominates. This is to be expected from the land–sea distribution, which exercises a strong influence on the water-vapor distribution in the lower layers of the atmosphere. In a similar manner wave number 2 is mainly responsible for the meridional eddy transport of water vapor. Of the three latitudes, 30°N , 45°N , and 60°N , for which Peixoto and Saltzman carried out the computations, the first one shows the largest transports.

More detailed data on lower latitudes were used by Boogaard (1964) in computing the eddy water-vapor transport for Dec. 12, 1957, between the equator and latitude 40°N (for more details on mean and eddy transports revealed by this study, see Chap. 3). Results of these computations are shown in Fig. 4.23. At latitudes 15° to 20°N , wave number 2, indeed, seems to carry most of the eddy transport. Farther north, however, wave numbers 5 and 6 become dominant in this transport process, indicating the important influence of the cyclonic activity of middle latitudes.

Hemispheric Interactions

Interhemispheric mass, momentum, and energy-exchange processes, to my knowledge, have not yet been explored in the wave-number space. According to Tucker (1965a), standing and transient eddies contribute significantly to the momentum flux (see Fig. 3.70). From Tucker's statement that the standing eddy flux is mainly caused by the monsoonal circulations over the Indian Ocean and over the West Pacific, one may conclude, at least qualitatively, that wave numbers 1 and 2 should be dominant in generating the large flux values shown in Fig. 3.70. To what extent the "southern oscillation" [this term was coined by Walker (1924) to describe a standing fluctuation of opposed pressure anomalies in the eastern and western hemispheres] is involved in such mass and momentum flux has not yet been explored to my knowledge. Troup (1965) believes that the oscillation is caused by a direct circulation between the warmer eastern and the cooler western hemispheres. The temperature anomalies characterizing the southern oscillation are by no means confined to the lower troposphere but are also found near tropopause level (see also Schove, 1963). For effects on sea–surface temperatures, see Bjerknes (1969).

Lagrangian Coordinates

Chapter 3 mentions briefly that widespread and routine use of constant-density balloons in a global atmospheric sounding system may necessitate the adoption of a quasi-Lagrangian coordinate system to describe the motions and dynamics of the atmosphere. The impact of such a change in the reference frame on spectral statistics may be realized by considering the (nondimensional) wave number (measured in an Eulerian coordinate system)

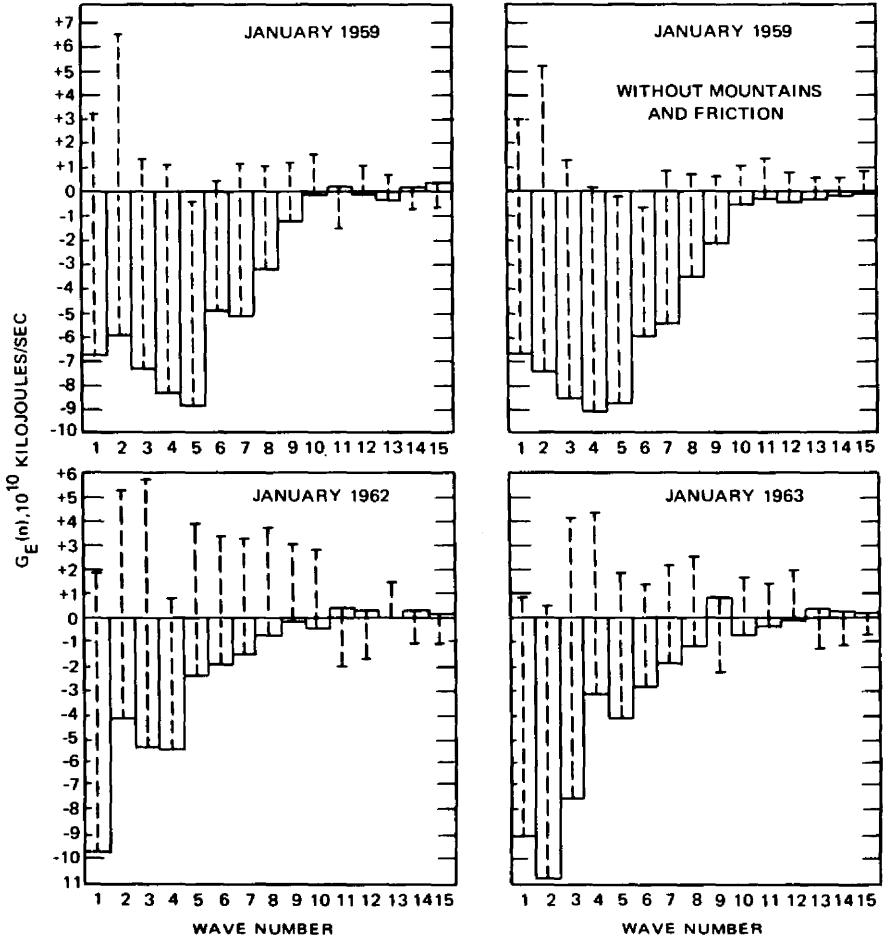


Fig. 4.22 (See facing page for legend.)

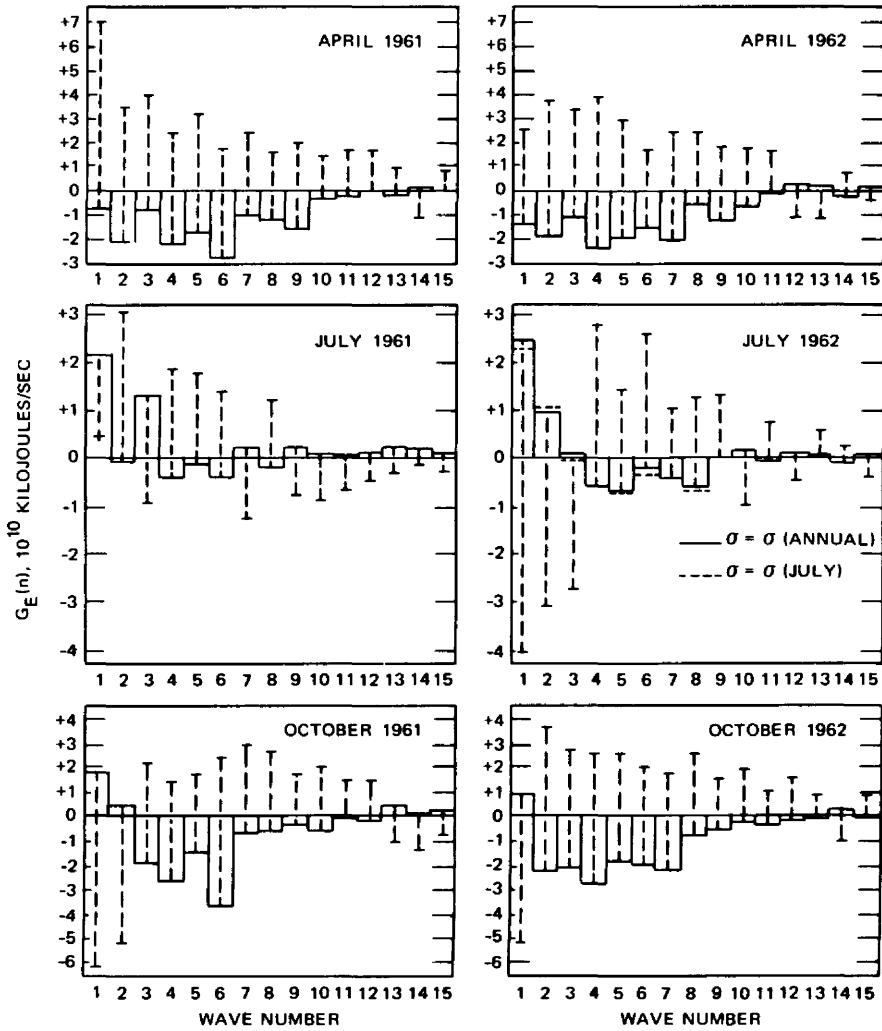


Fig. 4.22 Monthly means and standard deviations of $G_E(n)$ for wave numbers 1 to 15 and for months as indicated for the 1000- to 200-mb layer. [From J. A. Brown, Jr., *Tellus*, 16(3): 382; 383 (1964).]

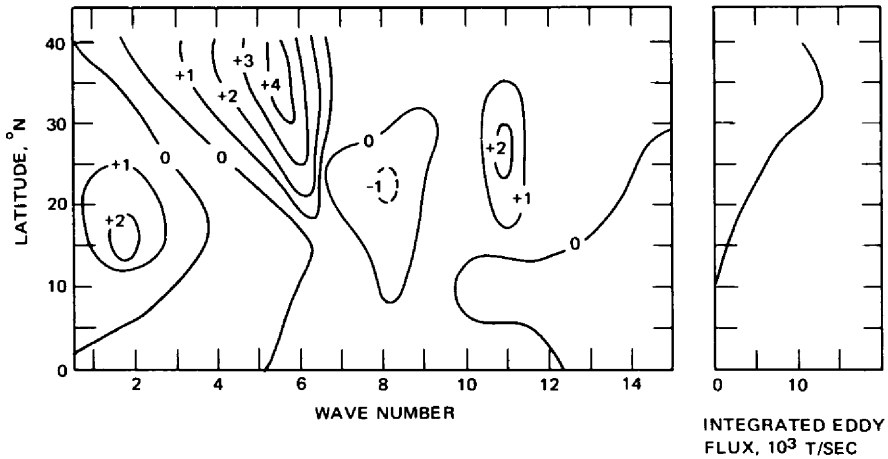


Fig. 4.23 Eddy flux of water vapor as a function of latitude and wave number. [From H. M. E. Van de Boogaard, *Tellus*, 16(1): 53 (1964).]

$$n = \frac{2\pi a \cos \phi}{L} \quad (4.27)$$

and the frequency observed in a quasi-Lagrangian system

$$\omega = \frac{[u]_{(\lambda)} - C}{L} = \frac{([u]_{(\lambda)} - C)n}{2\pi a \cos \phi} \quad (4.28)$$

of atmospheric flow perturbations (a is the earth's radius and L is the wavelength). Equation 4.28 contains the additional variables of the mean zonal wind speed, $[u]_{(\lambda)}$, which will vary with latitude and with time, and of the speed, C , of the propagating wave disturbances, which, in itself, is a function of n . Thus transient and stationary eddies will produce different frequency distributions in Lagrangian wind fluctuations. More research is needed to correlate the various atmospheric energy-conversion and energy-transport terms in the wave-number space with those in the frequency space.

There is an additional implication of these considerations which has an immediate bearing on radioactive-debris dispersal: The spreading and dispersal of a cloud of nuclear debris, such as that produced by an atomic bomb explosion, may be described in a Lagrangian coordinate system, which follows the "center of gravity" of this cloud. As the horizontal and vertical dimensions of the cloud increase by the effect of microscale and mesoscale eddy-transport processes, its rate of dispersion will increasingly be affected by large-scale disturbances whose amplitudes and frequencies (see Eq. 4.28) both are functions of location, wave number, and time. Statistical treatment of atmospheric transport processes in a Lagrangian coordinate system or in the frequency space would greatly enhance the understanding of large-scale dispersion processes in the atmosphere.

5 GEOGRAPHIC AND CURVILINEAR COORDINATE SYSTEMS

In Chap. 1 it was mentioned that mean meridional and eddy-transport characteristics in a geographic coordinate system may be drastically different from those in a curvilinear one. Riehl and Fultz (1957, 1958) pointed toward this fact, using experimental results from a steady three-wave dishpan experiment. In the real atmosphere, comparisons between these two coordinate systems are sparse because of the nonsteady atmospheric flow patterns which make it exceedingly difficult to define curvilinear coordinates and to follow the movement of the coordinate axes. Those flux computations in a curvilinear system that have come to my attention deal with regions in which flow patterns and jet streams change slowly, e.g., the subtropics and the polar-night stratosphere.

From a case study of December 1955 and January–February 1956, Krishnamurti (1961a) concluded that the day-to-day variability of the subtropical jet stream is remarkably small. It hardly affects the low wave numbers (1 to 3). The dominant three-wave pattern appears on mean charts of the winter season (Fig. 5.1) as well as on daily charts. The important role of wave number 3 is also evident from Fig. 5.2. In this diagram the wave pattern of the subtropical jet stream (STJ) appears to run antiparallel to the contour pattern in middle latitudes: The STJ has a tendency to shift northward wherever a deep trough cuts from middle into subtropical latitudes.

Krishnamurti (1961a) computed the “mean mass circulation” (in a curvilinear coordinate system) about the mean jet-stream position. It can be defined as $[\bar{v}_n]_{(t,s)}$, where subscript n indicates the velocity component normal to the jet axis, t extends over one month (the diagrams shown here are for December 1955), and the averaging process for s (measured parallel to the main jet axis) extends around the globe. The term “mass circulation” is used here in contrast to the “mean meridional circulation,”

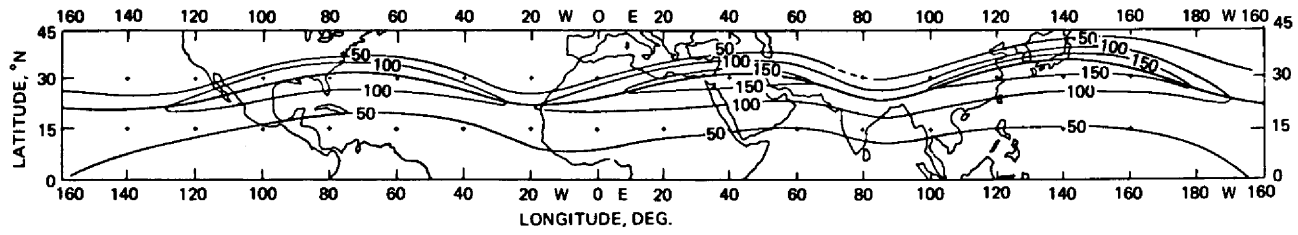


Fig. 5.1 Mean subtropical jet stream for winter 1955–1956. Isotach analysis at 200-mb surface. Isotachs are drawn for every 50 knots. The mean latitude of the jet axis is 27.5°N. [From T. N. Krishnamurti, *Journal of Meteorology*, 18(2): 176 (1961).]

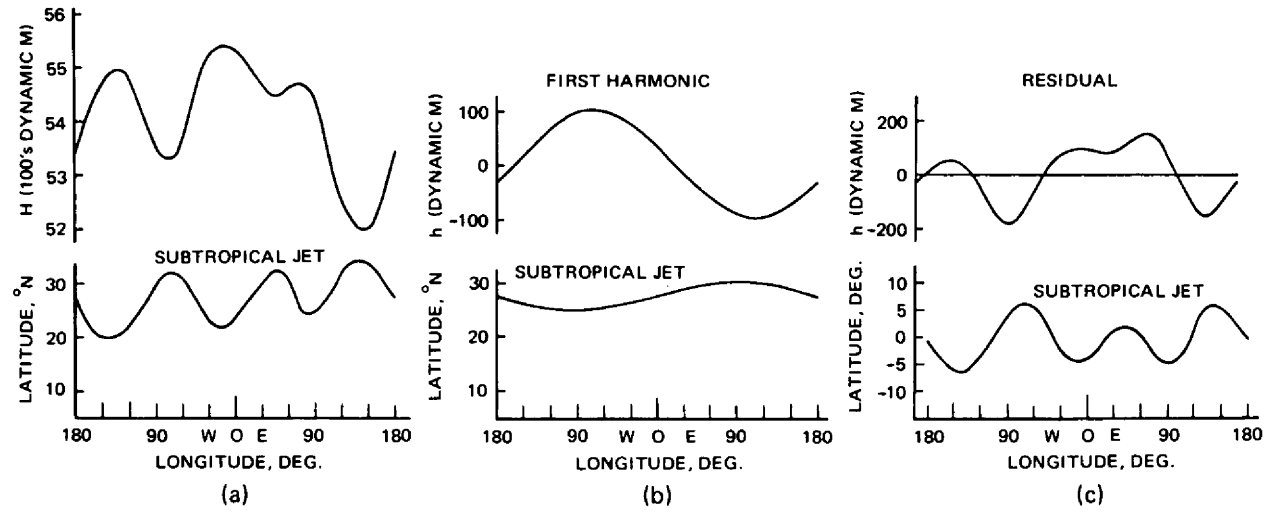


Fig. 5.2 (a) The 500-mb height (mean for winters 1945 to 1953) at 47.5°N latitude and the mean latitude of the subtropical jet-stream axis for winter 1955–1956. (b) The first harmonic of the curves on Part a. (c) Residual, obtained by subtracting the first harmonic from the curves on Parts a and b. [From T. N. Krishnamurti, *Journal of Meteorology*, 18(2): 176 (1961).]

which refers to a geographic coordinate system. By analogy, $[v_s]_{(t,s)}$ is the mean velocity component along the jet axis in a curvilinear system. Figures 5.3 and 5.4 show the computational results. The "quasi-mean zonal" speeds of the jet core in this representation are approximately 20 m/sec, or 40 knots, higher than those computed by Mintz (1954) (see also Wiin-Nielsen, Brown, and Drake, 1964) in a geographic coordinate system. This is to be expected since the meanders of the jet axis in a geographic coordinate system will reduce the peak zonal wind speed in a mean meridional wind profile. The mean mass circulation clearly reveals the presence of a direct-circulation cell to the south of the subtropical jet stream, as postulated by Palmén (1954) (Fig. 1.2) and by Miegheem and Hamme (1962) (Fig. 2.2). From mass balance requirements, Stokes's stream function can be defined. Its distribution is shown in Fig. 5.5.

By applying the equation

$$\frac{d[T]_{(t,s)}}{dt} = \frac{[T]_{(t,s)}}{[\theta]_{(t,s)}} \left\{ [v_n]_{(t,s)} \frac{\partial [\theta]_{(t,s)}}{\partial n} + [\omega]_{(t,s)} \frac{\partial [\theta]_{(t,s)}}{\partial p} \right\} \quad (5.1)$$

Krishnamurti (1961a) estimated the warming and cooling that should take place near the STJ because of advective processes. Results are shown in Fig. 5.6 and are compared with London's (1957) computations of the radiational heat balance. Part b of Fig. 5.6 shows integrated values for a belt extending from 10° latitude south of the jet axis to 10° latitude north of the jet axis. This diagram shows that the mean mass circulation has the correct strength needed to balance the radiational heat loss of the troposphere. Part a of this diagram can be compared with Fig. 5.7. The latter shows the change of the zonal mean temperature computed by Wiin-Nielsen, Brown, and Drake (1963) from the meridional heat-flux convergence. Although the results shown here are for a different period (January 1963), in a geographic coordinate system a more complex pattern results than Krishnamurti's (1961a) values indicate for a curvilinear coordinate system. Also, the zonally averaged values show maximum cooling in the lower troposphere, whereas the results in a curvilinear system show the main cooling processes in the upper troposphere, in good agreement with London's estimates. A comparison of Fig. 5.6 with Fig. 5.7 reveals, furthermore, that in a geographic coordinate system the low-tropospheric cooling takes place slightly to the north of the mean jet-stream position (see Fig. 5.2). A secondary maximum of cooling ($-\frac{1}{2}^\circ\text{C}/\text{day}$) is located underneath the zonally averaged jet axis and corresponds to Krishnamurti's area of maximum cooling. (As pointed out earlier, the zonally averaged jet stream is considerably weaker than the jet stream in a curvilinear system and thus its zonally averaged effect on temperature changes should also be weaker.)

The release of potential energy by the mass circulation in a curvilinear coordinate system was computed from

$$\frac{RS}{g} \int_{\ln(p)} \int_n [\omega]_{(t,s)} [T]_{(t,s)} dn d(\ln p) \quad (5.2)$$

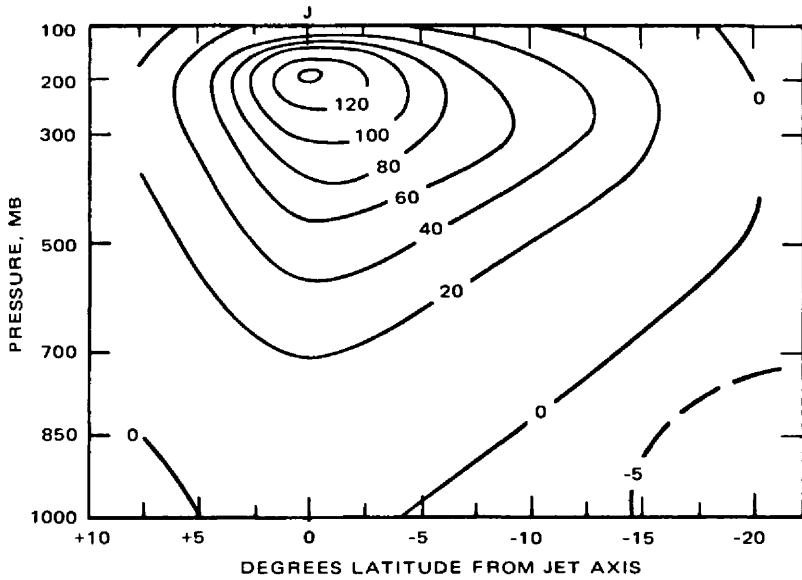


Fig. 5.3 Mean cross section of $[v_s]_{(t,s)}$, the wind component along the jet axis (knots), for December 1955. [From T. N. Krishnamurti, *Journal of Meteorology*, 18(2): 178 (1961).]

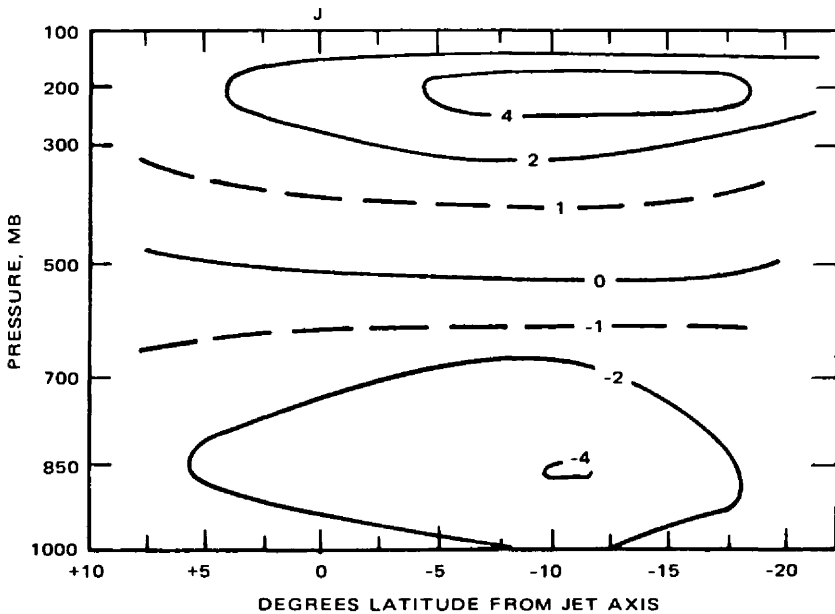


Fig. 5.4 Mean cross section of $[v_n]_{(t,s)}$, the wind component normal to the jet axis (knots), for December 1955. [From T. N. Krishnamurti, *Journal of Meteorology*, 18(2): 178 (1961).]

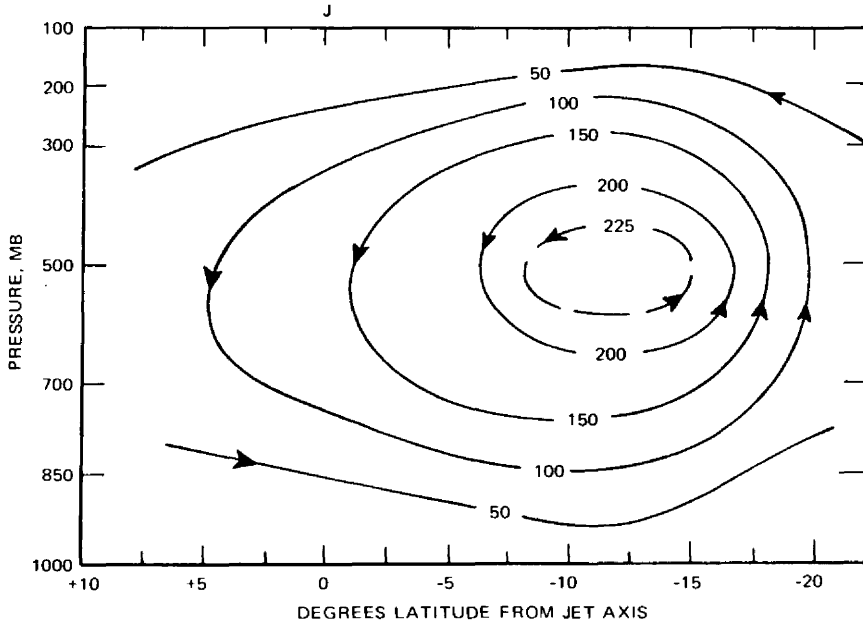


Fig. 5.5 Mean cross section of Stokes's stream function, $[\psi]_{(t,s)}$ (g/sec), for December 1955. [From T. N. Krishnamurti, *Journal of Meteorology*, 18(2): 179 (1961).]

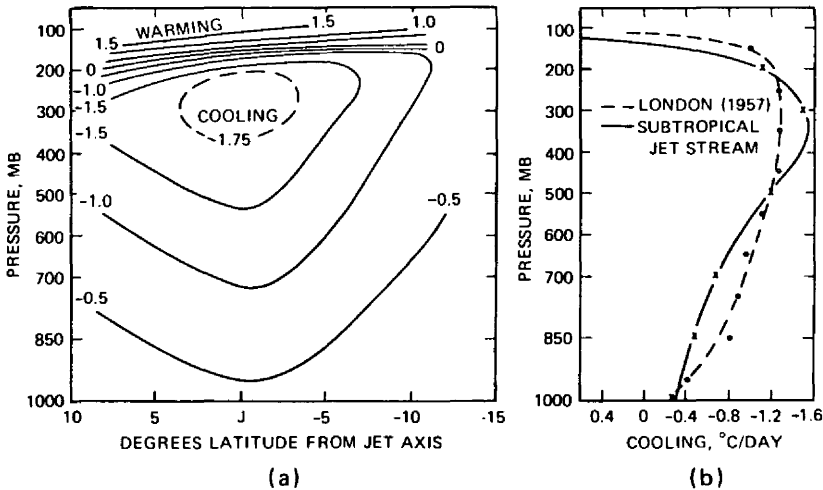


Fig. 5.6 (a) Cooling (or warming) ($^{\circ}\text{C}/\text{day}$) computed from Eq. 5.1. (b) Cooling (or warming) ($^{\circ}\text{C}/\text{day}$) integrated between the latitude belts -10° to 10° curve (solid). London's estimate of radiational cooling for the troposphere, as a function of pressure, is shown by the dashed curve. [From T. N. Krishnamurti, *Journal of Meteorology*, 18(2): 188 (1961).]

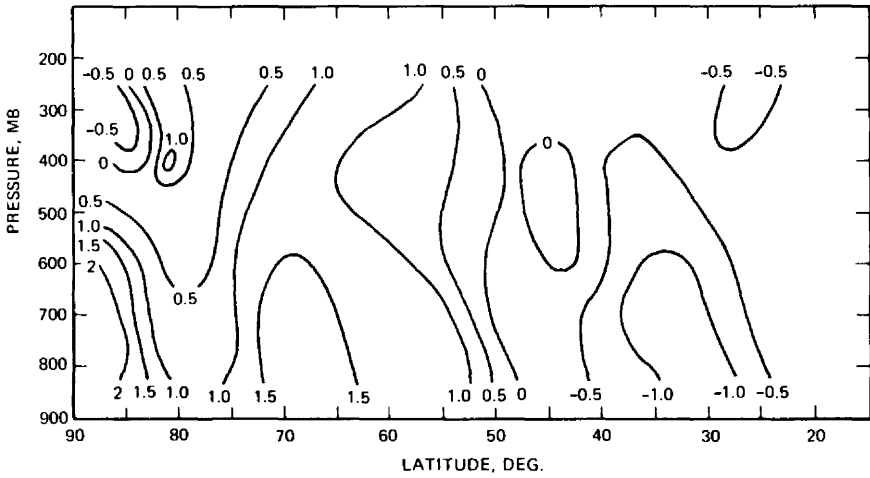


Fig. 5.7 The change in the zonal mean of the temperature ($^{\circ}\text{C}/\text{day}$) due to meridional convergence of the heat transport as a function of latitude and pressure. Averaged values for the month of January 1962. [From A. Wiin-Nielsen, J. A. Brown, and M. Drake, *Tellus*, 15(3): 273 (1963).]

where n refers to the distance normal to the jet axis and s is the length of the meandering jet axis measured around the hemisphere. Results for volumes of a width of 5° of latitude are shown in Fig. 5.8. Most of the potential energy is released in the immediate vicinity of the jet-stream position. As shown in Chap. 3, the conversion (K_Z, A_Z) in a geographic coordinate system, which, according to Table 3.1, is similar to Eq. 5.2, is mostly in the sense of an indirect circulation (see Fig. 3.20).

Figure 5.6 describes the cooling effects that are counterbalanced by the heat transport from the mean mass circulation only. As shown previously, eddy effects in a geographic coordinate system dominate in the transport processes, even in subtropical latitudes. Krishnamurti (1961b) computed the eddy transports in a curvilinear system. Results for the heat transport (i.e., the flux of the quantity $h = gz + c_p T + Lq$, where L is the latent heat of evaporation and q is the specific humidity of air) are shown in Fig. 5.9. Three types of eddies are considered separately in this representation:

1. Standing eddies, given by

$$[(\overline{h})_{(t)}]_{(s)} \quad [(\overline{v_n})_{(t)}]_{(s)} \quad (5.3)$$

where (t) again extends over a one-month period and (s) indicates averages of and departures from hemispheric mean values computed along lines parallel to the jet axis.

2. Five-day eddies [defined as in Eq. 5.3 except that (t) now extends over five-day periods].

3. Daily eddies, given by

$$[(h)_{(t,s)}] \quad [(v_n)_{(t,s)}] \quad (t,s) \quad (5.4)$$

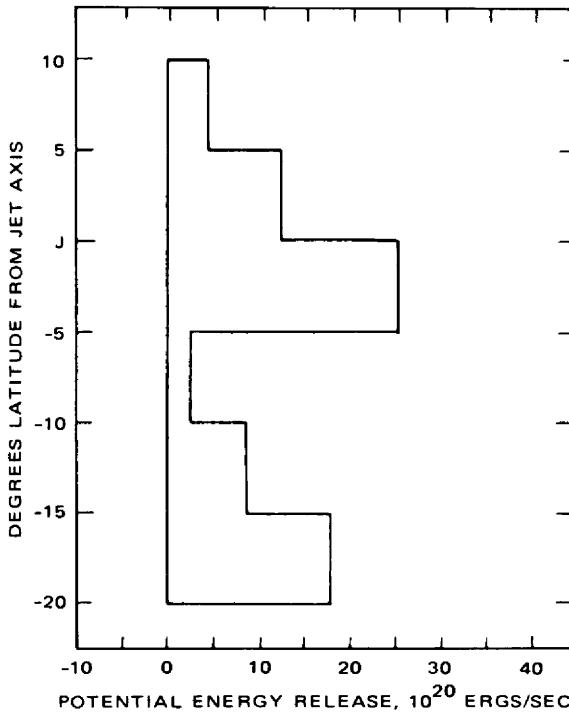


Fig. 5.8 Release of potential energy over volumes 5° of latitude wide, computed from Eq. 5.2. [From T. N. Krishnamurti, *Journal of Meteorology*, 18(2): 189 (1961).]

where (t) again refers to the departures from the monthly mean values of h and v_n .

As expected, the transport by standing eddies is zero in the jet axis (expressed by the fact that in Fig. 5.9 at this point the mass circulation is equal to mass circulation plus standing eddies) since a curvilinear coordinate system filters out these eddy motions which are followed around by the coordinate system. At some distance from the mean jet axis, the flow is no longer parallel to this axis. Therefore there is some slight transport by standing eddies in these regions. South of the jet axis, the heat flux produced by the standing eddies is northward, in support of the flux by the mean mass circulation. North of the jet axis, however, the standing eddy flux counteracts the mean mass circulation by transporting heat southward.

The five-day eddies contribute positively everywhere to the northward flux of sensible and latent heat. North of, and at some distance from, the jet axis, these eddies carry the bulk of the transport against the action of the standing waves. No estimates have been made of the transport by daily eddies. Their effect probably is quite appreciable north of the mean jet axis because here large discrepancies occur between the "total flux" (not incorporating daily eddy effects) computed by Krishnamurti (1961b) and the poleward heat flux estimated by London (1957) from radiation requirements. See Fig. 5.9 for a comparison.

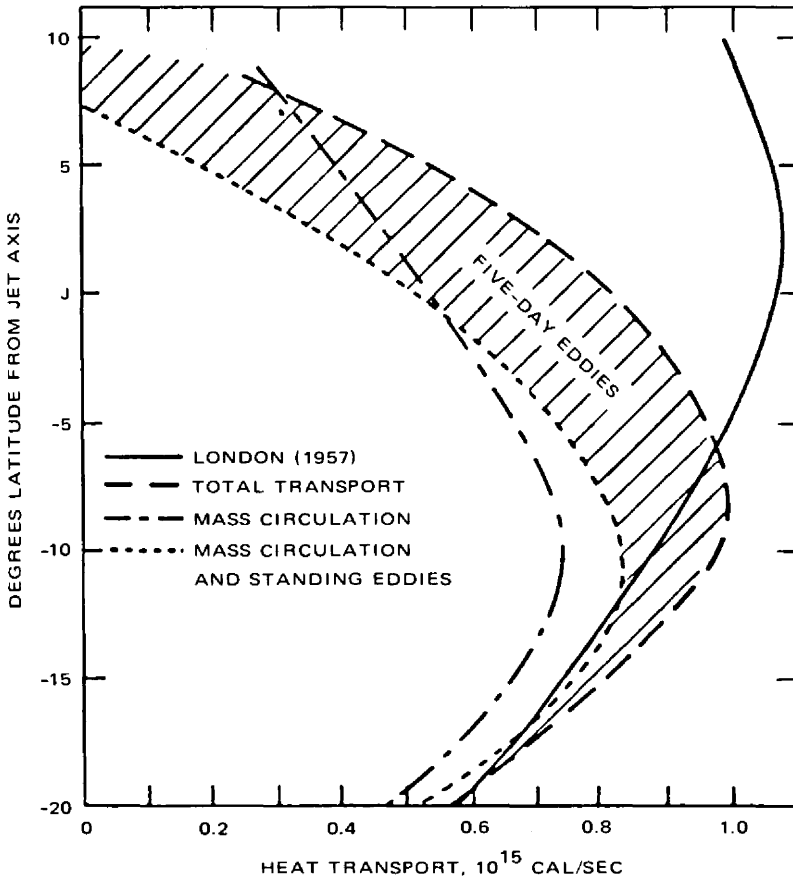


Fig. 5.9 Heat transport for winter 1955–1956. London's (1957) estimate of the transport requirement is shown by the solid curve. The mean latitude of the jet axis is 27.5°. [From T. N. Krishnamurti, *Journal of Meteorology*, 18(5): 659 (1961).]

Separate estimates have been made by Krishnamurti (1961b) of the poleward flux of latent heat (Fig. 5.10). For this quantity, the mean mass circulation in a curvilinear coordinate system provides the bulk of the flux. Agreement with values obtained by Jacobs (1951), in general, is good. In Chap. 4, it was pointed out that wave number 2 of the standing eddies transports most of the water vapor poleward in a geographic coordinate system (Peixote and Saltzman, 1958). This wave number is mainly governed by the land–sea distribution. Largest values of northward vapor flux were found near 30°N, which roughly corresponds to the latitude of the STJ. Since the standing wave number 2 of the geographic coordinate frame will be absorbed in the mass circulation of the curvilinear coordinate system, the results of Fig. 5.10 can be considered in good agreement with those reported in Chap. 4. The curvilinear system, however, reveals more clearly the role of the STJ in this transport process.

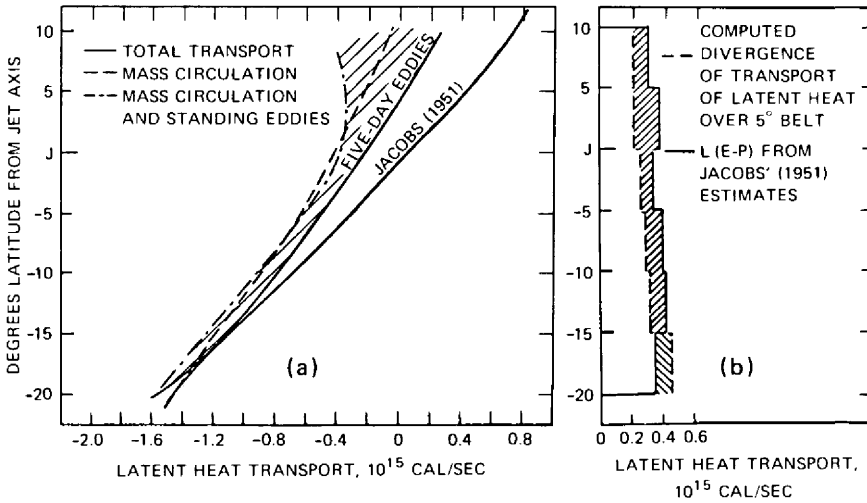


Fig. 5.10 (a) Latent heat transport for winter 1955–1956. The estimate of the transport requirement by Jacobs (1951) is also included. (b) Divergence of flux of latent heat, computed for winter of 1955–1956, compared with the values obtained by Jacobs. Note that the Jacobs flux curve in Part a was obtained with an assumed zero flux at -17.5° from the jet axis. [From T. N. Krishnamurti, *Journal of Meteorology*, 18(5): 661 (1961).]

The flux of relative angular momentum in a curvilinear coordinate system is shown in Fig. 5.11. The total flux (not including daily eddies) agrees well with earlier estimates by Bjerknes (1957). The largest transports, again, are accomplished by the mean mass circulation. The contribution by standing eddies is positive everywhere and is quite appreciable north of the jet axis. The standing eddy flux does not vanish in the position of the mean jet axis because of velocity fluctuations along the jet axis, which are correlated with fluctuations $([v_s]_t)_{(s)}$. This is in contrast with Fig. 1.5 for the dishpan experiment; however, hardly any velocity fluctuations along the jet axis (i.e., no distinct jet maxima) were observed there. We can conclude, therefore, that the flux of relative angular momentum produced by standing eddies near the position of the mean jet axis is due to the presence of jet maxima and thus is an effect of quasi-inertial oscillations of the flow in the STJ (Newton, 1959; for further details consult Reiter, 1961, 1963b).

Five-day eddies, and presumably daily eddies, contribute relatively little toward the total relative momentum flux. This is in agreement with results from computations in a geographic coordinate system (reported in Chap. 4) according to which a peak in momentum transport occurs in the domain of low wave numbers that may be recognized as standing eddies. Again, the effect of these large eddies will be absorbed by the mean mass circulation of a curvilinear coordinate system.

The transport of kinetic energy (Fig. 5.12) in a curvilinear coordinate system reveals a similar distribution between mean mass circulation, standing eddies, and five-day eddies. There is considerable variation from month to month, however, in the

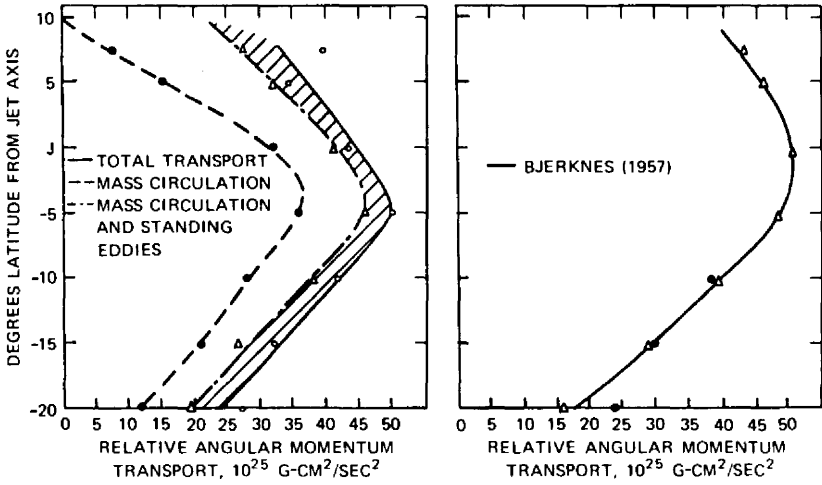


Fig. 5.11 Relative angular momentum transport for winter 1955-1956. On the right the estimates from Bjerknes (1957) are shown. [From T. N. Krishnamurti, *Journal of Meteorology*, 18(5): 662 (1961).]

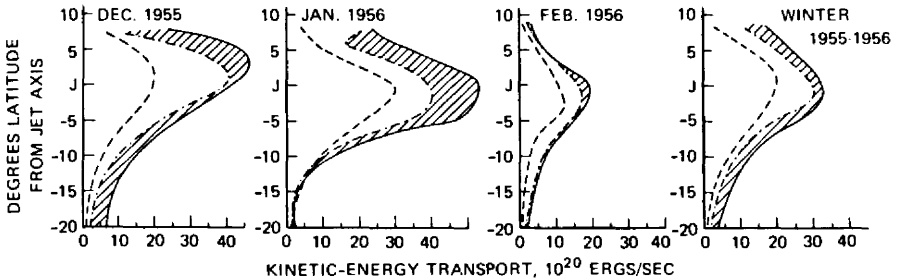


Fig. 5.12 Transport of kinetic energy for winter 1955-1956. —, total transport. ---, mass circulation. - · -, mass circulation and standing eddies. [From T. N. Krishnamurti, *Journal of Meteorology*, 18(5): 665 (1961).]

relative contribution of each of these terms toward the total flux. This would indicate that even in a jet-stream system as well defined as the STJ the atmosphere has a variety of combinations of transport modes at its disposal. During December 1955, for instance, the kinetic-energy transport by standing eddies was equal in magnitude, even in the mean jet axis, to the transport by the mean mass circulation. This would indicate that during this month the maximums in the STJ were especially strong. During January 1956 the flux in the five-day eddies became quite significant.

Results reported so far pertain to conditions in the troposphere. Mahlman (1966) investigated the polar-night jet stream of the stratosphere during a major breakdown period (Jan. 10 to Feb. 19, 1958). The indirect mean meridional circulation in a

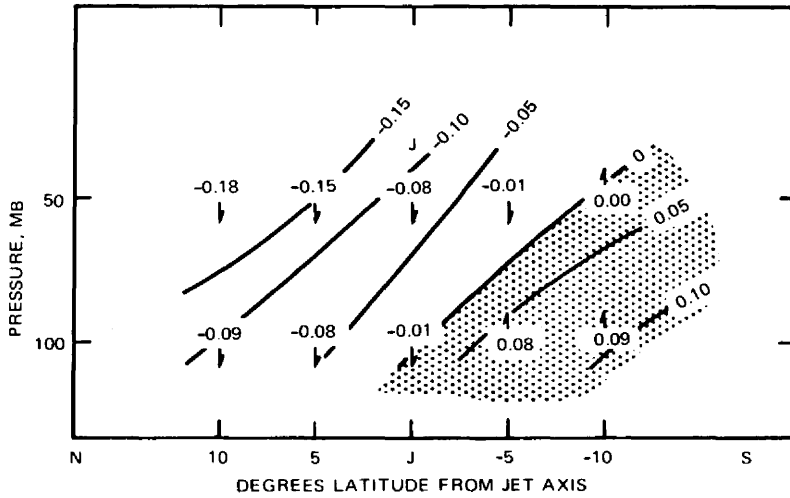


Fig. 5.13 Time composite of adiabatically computed mean vertical motion (km/day) with respect to coordinate system oriented along line of maximum circulation intensity at 50 mb. Composite is for the period Jan. 10 to 27, 1958. Hatching denotes area of rising motion $[w]_{(t,s)}$ (Mahlman, 1966).

geographic coordinate system, which resulted during this period, is shown in Fig. 3.10. A curvilinear frame of reference was defined by Mahlman by taking the height contour of maximum wind speeds at the 50-mb surface as coordinate origin. The mean direct mass circulation shown in Fig. 5.13, resulted from these computations for the time period January 10 to 27. After the breakdown of the polar-night vortex, a curvilinear system could no longer be defined, and therefore no estimates of a mass circulation could be made.

As mentioned in the preceding chapters, long planetary waves, characteristic of standing eddies, provide the heat and momentum transport necessary to maintain the stratospheric flow patterns against the indirect mean meridional circulation. If a curvilinear coordinate system is adopted, the effects of these large eddies are absorbed in the mean mass circulation, as has been the case in Krishnamurti's studies of the STJ.

Mahlman (1967) also studied a minor breakdown of the stratospheric circumpolar vortex that was followed by re-formation of the vortex (Nov. 15 to Dec. 15, 1958). In this case the geographic coordinate system revealed a direct mean meridional circulation and the curvilinear system indicated a weak indirect mass circulation: mean sinking motion was observed in the belt 10° of latitude north to 10° of latitude south of the jet axis. However, the strongest sinking took place to the south of the axis.

For motion patterns more complex than those described so far, it is difficult to define curvilinear coordinates, mainly because of the nonlinear movements that such systems would undergo. Reiter, Glasser, and Mahlman (1967) have made a preliminary attempt to compute motions on an isentropic surface across the intersection line of the tropopause with this surface. From such computations, one may be able to

estimate the outflow of (contaminated) air from and the inflow into the stratosphere. However, it is difficult to define the curvilinear reference line, i.e., the intersection line of the tropopause, and its movement with time. Reiter et al. felt justified in assuming that the tropopause would move in a direction parallel to the wind vectors observed at the intersection line with the isentropic surface. This yields a wind vector in the curvilinear system

$$\mathbf{V}_C = \mathbf{V}_T - \mathbf{C}_T \quad (\text{for } \mathbf{C}_T \parallel \mathbf{V}_T) \quad (5.5)$$

where \mathbf{V}_T is the wind velocity at the tropopause intersection line in the geographic coordinate frame and \mathbf{C}_T is the velocity of this intersection line. The flow across the tropopause on the isentropic surface Θ is then given by

$$(\mathbf{V}_T - \mathbf{C}_T)_\Theta \sin \alpha \quad (5.6)$$

where α is the angle between the vector \mathbf{V}_T and the tropopause intersection line.

Preliminary results from this study indicated the following: An exchange of stratospheric and tropospheric air can take place (1) by irreversible intrusion processes, (2) by re-formation of the tropopause at a new level, and (3) by smaller scale mixing processes in the region of strong horizontal wind shears and of large potential absolute vorticity gradients. Outflow of stratospheric air appears to take place throughout the vertical depth of the tropopause gap near well-developed jet streams, although this process is best defined within the stable region of the jet-stream front. Return flow of tropospheric air into the stratosphere seems to occur in significant amounts at and above jet core level.

Statistical studies of such flow processes are still lacking. Even global estimates have yet to be made. Such studies will have to be based on careful hemispheric isentropic analyses (Danielsen, 1967a, b). As pointed out by Reiter, Glasser, and Mahlman (1967), the magnitude of cross-tropopause transports depends strongly on the careful definition and analysis of the tropopause itself and on the identification of its intersection line with the isentropic surface under consideration. Coded tropopause values, as, for instance, analyzed by Defant (1958) and by Defant and Taba (1958a, 1958b), will not suffice for accurate mass-flow estimates.

6 CONCLUSIONS AND OUTLOOK

The foregoing chapters describe in detail the conversions between available potential and kinetic energies in the atmosphere and the transports of these quantities by both mean meridional circulations and large-scale eddies and the role of these transport processes in maintaining the general circulation. The energy exchanges between the atmosphere, the earth's surface, and space through diabatic processes have been considered to the extent to which they influence these energy transformations and transfers. From these discussions it is quite obvious that the balance requirements for energy in the atmosphere and the energy fluxes resulting from these requirements provide interesting aspects of atmospheric transport processes that have far-reaching implications. Even though for a given air parcel a specific form of energy, e.g., its kinetic energy, is not conserved but can, at least in part, be transformed into other forms of energy, certain conclusions about the transfer of conservative properties, such as of radioactive contaminants or ozone, can be reached from detailed energy considerations. Many of the conclusions reached in the foregoing discussions are opposed by a number of challenging questions that arise either from contradictory results from research or from yet unexplored aspects that may merit further investigation.

As has been pointed out, the general circulation has at its disposal various modes of interplay between mean and eddy motions for maintaining itself. The degrees of freedom within the wave-number space of motions and of energy transformations further complicate the understanding of the general circulation. Why is it that certain flow patterns and their associated energy-transformation processes prevail during certain periods of one year but not during the same periods of the next year? Are there certain efficiency levels associated with certain modes of energy transfer which

the atmosphere chooses to adopt during such periods? Can such modes be predicted? A "yes" to the last question might mean a dramatic advancement in our long-range forecasting capabilities.

As has been pointed out, the net conversions between available potential and kinetic energy, averaged around the hemisphere, do not give the complete picture of the turnover rate of the atmosphere. A large fraction of the eddy kinetic energy that is generated from potential energy within a jet-stream system is transferred back again into eddy potential energy within the same system. Even though it is the net conversion that maintains the general circulation, the *absolute amount* of conversion between eddy available potential and kinetic energies determines the large-scale mixing processes that prevail in the latitude belt under consideration.

The data in the foregoing chapters indicate large interdiurnal variations in the energy-transfer and energy-transformation processes of the troposphere and, maybe to a lesser extent, also of the stratosphere. From synoptic evidence we know that such variations characterize not only the day-to-day aspects of the general circulation but also various sectors of the globe. Whereas one part of the hemisphere may find itself under high index conditions with nearly zonal flow, another section of the same hemisphere may reveal deep troughs and strong ridges in its mid and upper tropospheric contour patterns. Hemispheric mean values of transfer processes, therefore, may not always give an adequate picture of the global circulation.

Because of the sparsity of data for the southern hemisphere, we do not know if certain anomalies in the energy cycles of one hemisphere have their counterparts in the other hemisphere. Even though preliminary studies described in the foregoing chapters have indicated a significant flow of kinetic energy, especially in the standing eddy domain, across the equator, the details of such processes, especially their time and space variations, remain to be investigated. Satellite data, especially from the Applications Technology Satellite, may serve as valuable tools in such a study. Even a preliminary investigation of such data reveals striking differences in the aspects of the intertropical convergence zone (ITC) within relatively short time periods. There are occasions when cloud bands extend from the ITC outward into the temperate latitudes of one or both hemispheres. At times even two ITC's are visible on satellite pictures. This could be taken as evidence of a strong dynamic interaction between tropical and subtropical regions of one or both hemispheres in the eddy domain, at least during certain periods of time. The implications of such interactions on atmospheric transport processes are quite obvious: List, Telegadas, and Ferber (1964) and Reiter and Mahlman (1965) have shown that at least on one occasion radioactive debris from the Christmas Island region in the equatorial Pacific was swept into a strong westerly current in the lower stratosphere and reached the continental United States within a few days after its injection into the atmosphere. From such radiochemical evidence and from data made available by satellites, it would appear desirable to combine statistical results, such as those described in the foregoing chapters, with details derived from synoptic studies. Such a combined approach would help in answering the question of whether or not certain characteristic periods in

atmospheric energy conversions are associated with certain characteristic trajectory patterns.

Preliminary studies, especially those by Julian and Labitzke (1965), have established certain energy fluxes between the troposphere and the stratosphere. Although it is well recognized by now that the lower stratospheric circulation is driven mainly by tropospheric processes, we are still lacking knowledge on the time and space variations of such fluxes. The question of the extent to which the breakdown of the polar-night stratospheric vortex may be caused by tropospheric triggering of a dynamically unstable flow configuration cannot be answered satisfactorily before such detailed investigations are made.

As pointed out in the text, we should not *a priori* assume that the northern and southern hemispheres contain the same basic circulation patterns. There is suspicion that the southern stratosphere during winter may show one meridional circulation cell, whereas the northern hemisphere during the same season reveals two cells, with rising motion prevailing over both pole and equator. Further investigations will be needed, possibly making use of atmospheric tracer studies, to either confirm or reject this suspicion.

The discussions in the preceding chapters are restricted mainly to the large-scale circulation aspects. The atmospheric mesoscale, however, may have considerable bearing on atmospheric energetics and transport processes. This can be recognized from the fact that in tropical regions most of the vertical heat and moisture transport directed against the mean gradient of these properties occurs in the hot towers of cumulus convection. Again, satellite data may become instrumental in extending atmospheric energy studies from the synoptic into the mesoscale. The latter constitutes the vital bridge between the planetary processes in the atmosphere and the small-scale diffusion and energy dissipation processes. As the atmospheric mesoscale is taken into consideration, it will become necessary to include the kinetic energy of vertical motions in a full three-dimensional treatment of atmospheric energetics because, especially in strong convective motions as well as in orogenic lee waves, the vertical components of perturbation (eddy) motions may reach the same orders of magnitude as the horizontal components.

The atmospheric mesoscale will also be of importance in a more complete understanding of the energy dissipation processes in the atmosphere. From turbulence theory we know that within the inertial subrange the smaller eddies feed on the larger ones. Such a redistribution of kinetic energy over smaller eddy sizes takes place in the wavelength region between tens of meters and a few millimeters or centimeters at the most. Still smaller disturbances in the flow, characteristic of the processes in the "frictional dissipation range" of turbulence, convert their kinetic energy into internal energy. As has been discussed at length, on a planetary scale (wavelengths of thousands of kilometers) the eddy disturbances appear to feed some of their energy into the mean zonal flow. Thus the flow of energy is in a direction opposite to the one postulated by turbulence theory. Probably somewhere in the mesoscale range of atmospheric disturbances a decisive separation in these energy-transfer processes to

other wavelengths, or eddy sizes, takes place. These processes, however, have not yet been studied in detail.

We may envision, for instance, the following: Convective motions in cumulus clouds draw their kinetic energy of perturbation motion mostly from buoyant forces, aided by the release of latent heat of condensation (and/or sublimation). At the same time latent and sensible heat is transported upward in the atmosphere by such convective motions. This may lead to the generation of large-scale eddy available potential energy if such transports by "hot towers" are more prevalent in warm air than in cold air. Part of the available potential energy thus generated may be transformed into large-scale eddy kinetic energy. At the same time, however, at least some, if not most, of the perturbation kinetic energy associated with the convective motions in these cumulus clouds will be dissipated into smaller eddies and into internal energy of the environment. Thus it appears, at least under certain conditions, that mesoscale systems in the atmosphere may lead to energy transfers to smaller as well as to larger eddy sizes.

For a better understanding of the general circulation of the atmosphere, the role of the mesoscale in the energy budget will have to receive considerable attention. Since the synoptic observation network does not lend itself to such investigations of the mesoscale, other inputs will have to be sought, such as satellite observations and measurement flights by specially instrumented aircraft. With a more thorough understanding of the atmospheric mesoscale, its function in the energy-transfer and energy-transformation processes may be properly taken into account in numerical models of the atmosphere and in objective medium- and long-range forecasting schemes. The transport of atmospheric admixtures, such as radioactive contaminants, upon which the mesoscale motions of the atmosphere also exercise their influence, can be predicted more accurately if such an understanding is reached. The complex washout processes by convective cloud systems and the mixing of radioactive debris and of industrial air pollution, through deep atmospheric layers under neutral or unstable conditions especially will be comprehended better once we know more about the energetic processes in the wide spectrum range of motions between the synoptic scale and the small-scale turbulence.

REFERENCES

- Adem, J., 1967, On the Relations Between Outgoing Long-wave Radiation, Albedo, and Cloudiness, *Mon. Weather Rev.*, **95**(5): 257-260.
- , 1968, A Parametric Method for Computing the Mean Water Budget of the Atmosphere, *Tellus*, **20**(4): 621-632.
- Albrecht, F., 1961, Der jährliche Gang der Komponenten des Wärme- und Wasserhaushalts der Ozeane, *Ber. Deut. Wetterdienstes*, **11**(79): 24 pp.
- Allison, L. J., and G. Warnecke, 1966, The Interpretation of TIROS Radiation Data for Practical Use in Synoptic Weather Analysis, *Beitr. Phys. Atmos.*, **39**(2-4): 165-181.
- Anderson, C. E., 1964, Stratospheric Heat Transport Values and Derived Vertical Velocities, 1st American Institute of Aeronautics and Astronautics Annual Meeting, Washington, D. C., June 29–July 2, 1964, AIAA Paper No. 64-313.
- Angell, J. K., 1960, An Analysis of Operational 300-mb Transosonde Flights from Japan in 1957-58, *J. Meteorol.*, **17**(1): 20-35.
- , 1964, Some Velocity and Momentum-Flux Statistics Derived from Transosonde Flights, *Quart. J. Roy. Meteorol. Soc.*, **90**(386): 472-477.
- , and J. Korshover, 1962, The Biennial Wind and Temperature Oscillations of the Equatorial Stratosphere and Their Possible Extension to Higher Latitudes, *Mon. Weather Rev.*, **90**(4): 127-132.
- , and J. Korshover, 1963, Harmonic Analysis of the Biennial Zonal-Wind and Temperature Regimes, *Mon. Weather Rev.*, **91**(10-12): 537-548.
- , and J. Korshover, 1964, Quasi-biennial Variations in Temperature, Total Ozone and Tropopause Height, *J. Atmos. Sci.*, **21**(5): 479-492.
- , J. Korshover, and T. H. Carpenter, 1966, Note Concerning the Period of the Quasi-biennial Oscillation, *Mon. Weather Rev.*, **94**(5): 319-323.
- Anthes, R. A., and D. R. Johnson, 1968, Generation of Available Potential Energy in Hurricane Hilda (1964), *Mon. Weather Rev.*, **96**(5): 291-302.

- Arakawa, H., 1953, On the Time Rate of Work Done by the Eddy Stresses in the Free Air and the Maintenance of the Westerlies in Middle Latitudes, *J. Meteorol.*, 10(5): 392-393.
- Arking, A., and J. S. Levine, 1967, Earth Albedo Measurements: July 1963 to June 1964, *J. Atmos. Sci.*, 24(6): 721-724.
- Asakura, T., and A. Katayama, 1964, On the Normal Distribution of Heat Sources and Sinks in the Lower Troposphere over the Northern Hemisphere, *J. Meteorol. Soc. Jap.*, 42(4): 209-244.
- Ashbel, D., A. Eviatar, and E. Doron, 1961, Radiation Maps and High Altitude Temperature for the Globe (During the I.G.Y., I.G.C.), Report from the Hebrew University, Department of Climatology and Meteorology, Jerusalem, Israel.
- Aubert, E. J., and J. S. Winston, 1951, A Study of Atmospheric Heat-Sources in the Northern Hemisphere for Monthly Periods, *J. Meteorol.*, 8(2): 111-125.
- Auer, A. H., Jr., and J. D. Marwitz, 1968, Estimates of Air and Moisture Flux into Hailstorms on the High Plains, *J. Appl. Meteorol.*, 7(2): 196-198.
- Ball, F. K., 1961, Viscous Dissipation in the Atmosphere, *J. Meteorol.*, 18(4): 553-557.
- Bannon, J. K., and L. P. Steele, 1960, Average Water Vapor Content of the Air, *Geophys. Memoirs, London*, No. 102.
- Barnes, A. A., Jr., 1963, Kinetic and Potential Energy Between 100 mb and 10 mb During the First Six Months of the I.G.Y., Final Report, Massachusetts Institute of Technology Planetary Circulation Project.
- , 1965, Atmospheric Water Vapor Divergence: Measurements and Applications, in *Humidity and Moisture*, Vol. II, pp. 513-522, Reinhold Publishing Corporation, New York.
- Barrett, E. W., 1961, Some Applications of Harmonic Analysis to the Study of the General Circulation. I. Harmonic Analysis of Some Daily and Five-day Mean Hemispheric Contour Charts. II. Calculations of Some Product-Spectra and Related Quantities, *Beitr. Phys. Atmos.*, 33: 280-355.
- Barry, R. G., 1967, Variations in the Content and Flux of Vapour over Northeastern North America During Two Winter Seasons, *Quart. J. Roy. Meteorol. Soc.*, 93(398): 535-543.
- Belmont, A. D., and D. G. Dartt, 1968, The Variation with Longitude of the Quasi-biennial Wave, in Proceedings of the (Seventh) Stanstead Seminar on the Middle Atmosphere, McGill University, *Meteorology*, 90: 161-167.
- , G. W. Nicholas, and W. C. Shen, 1968, Comments on "Midwinter Stratospheric Warmings in the Southern Hemisphere: General Remarks and a Case Study," *J. Appl. Meteorol.*, 7(2): 300-302.
- Benton, G. S., and M. A. Estoque, 1954, Water Vapor Transfer over the North American Continent, *J. Meteorol.*, 11(6): 462-477.
- , and A. B. Kahn, 1958, Spectra of Large-scale Atmospheric Flow at 300 mb, *J. Meteorol.*, 15(4): 404-410.
- Berggren, R., and A. Nyberg, 1967, Eddy Vertical Transport of Latent and Sensible Heat, *Tellus*, 19(1): 18-23.
- Berliand, T. G., 1956, The Heat Balance of the Atmosphere over the Northern Hemisphere (in Russian), in *A. I. Voeikov and Modern Problems of Climatology*, M. I. Budyko (Ed.), Hygrometeorology Publishing House, Leningrad.
- Bernard, E. A., 1962, Théorie des Oscillations Annuelles et Diurnes de la Température à la Surface des Continents et des Océans, *Arch. Meteorol. Geophys. Bioklimatol., Ser. A*, 12: 502-543.
- Berson, F. A., and A. J. Troup, 1961, On the Angular Momentum Balance in the Equatorial Trough Zone of the Eastern Hemisphere, *Tellus*, 13(1): 66-78.
- Bjerknes, J., 1957, Large Scale Synoptic Processes, Final Report, University of California at Los Angeles.
- , 1960, Ageostrophic Corrections to the Computed Poleward Flux of Angular Momentum, in *Dynamics of Climate*, R. L. Pfeffer (Ed.), pp. 67-70, Pergamon Press, Inc., New York.
- , 1969, Atmospheric Teleconnections from the Equatorial Pacific, *Mon. Weather Rev.*, 97(3): 163-172.

- , and Y. Mintz, 1955, Investigations of the General Circulation of the Atmosphere, Final Report, University of California at Los Angeles.
- Blackadar, A. K., 1950, Transformation of Energy by the Large-scale Eddy Stress in the Atmosphere, *Meteorological Papers*, Vol. 1, No. 3, New York University.
- Blaes, C. E., 1961, A Study of Geostrophic Angular Momentum Transport by Waves with Periods 1 to 30 Days at the 500 mb Surface and a Mid-latitude Station, Thesis, U. S. Naval Postgraduate School.
- Böhme, W., 1967, Eine 26-monatige Schwankung der Häufigkeit meridionaler Zirkulationsformen über Europa, *Z. Meteorol.*, 19(3-4): 113-115.
- Bolin, B., 1950, On the Influence of the Earth's Orography on the General Character of the Westerlies, *Tellus*, 2(3): 184-195.
- Boogaard, H. M. E. van de, 1964, A Preliminary Investigation of the Daily Meridional Transfer of Atmospheric Water Vapour Between the Equator and 40°N, *Tellus*, 16(1): 43-54.
- Boville, B. C., C. V. Wilson, and F. K. Hare, 1961, Baroclinic Waves of the Polar-night Vortex, *J. Meteorol.*, 18(5): 567-580.
- Boville, B. W., 1963, What Are the Causes of the Aleutian Anticyclone?, *Meteorol. Abhandl.*, 36: 107-119.
- Bradford, R., C. Frasch, C. Huang, M. D. Lethbridge, H. A. Panofsky, and A. Schwalb, 1965, Synoptic Applications of Infrared Satellite Data, Interim Report, Pennsylvania State University.
- Bradley, J. H. S., 1968, The Transient Parts of the Atmospheric Planetary Waves, in Proceedings of the (Seventh) Stanstead Seminar on the Middle Atmosphere, McGill University, *Meteorology*, 90: 61-70.
- Brewer, A. W., 1949, Evidence for a World Circulation Provided by the Measurements of Helium and Water Vapour Distribution in the Stratosphere, *Quart. J. Roy. Meteorol. Soc.*, 75(326): 351-363.
- Brier, G. W., 1969, Long-range Prediction of the Zonal Westerlies and Some Problems in Data Analysis, *Rev. Geophys.*, 6(4): 525-551.
- Brown, J. A., Jr., 1964, A Diagnostic Study of Tropospheric Diabatic Heating and the Generation of Available Potential Energy, *Tellus*, 16(3): 371-388.
- , 1967, On Atmospheric Zonal to Eddy Kinetic Energy Exchange for January 1963, *Tellus*, 19(1): 14-17.
- Brunt, D., 1926, Energy in the Earth's Atmosphere, *Phil. Mag.*, 7(1): 523-532.
- , 1934, *Physical and Dynamical Meteorology*, Cambridge University Press, New York.
- Buch, H. S., 1954, Hemispheric Wind Conditions During the Year 1950, Final Report, Part 2, Massachusetts Institute of Technology.
- Budyko, M. I., 1956, *The Heat Balance of the Earth's Surface*, Gidrometeorologicheskoe Izdatel'sto, Leningrad.
- , 1963, *Atlas of the Heat Balance of the Earth* (in Russian), U.S.S.R. Glarnaia geofizicheskaja Observatorria, Moscow.
- , and K. Y. Kondratiev, 1964, The Heat Balance of the Earth, in *Research in Geophysics*, Vol. 2, H. Odishaw (Ed.), pp. 529-554, Massachusetts Institute of Technology Press, Cambridge, Mass.
- Cehak, K., 1962, Die Verwendung von orthogonalen Polynomen in der Meteorologie, I. Mitteilung, *Arch. Meteorol. Geophys. Bioklimatol., Ser. A.*, 12: 40-61.
- Charney, J. G., 1947, The Dynamics of Long Waves in a Baroclinic Westerly Current, *J. Meteorol.*, 4(5): 135-162.
- , 1951, Dynamic Forecasting by Numerical Process, *Compendium Meteorol.*, pp. 470-482.
- , and P. G. Drazin, 1961, Propagation of Planetary-scale Disturbances from the Lower into the Upper Atmosphere, *J. Geophys. Res.*, 66(1): 83-110.
- , and J. Pedlosky, 1963, On the Trapping of Unstable Planetary Waves in the Atmosphere, *J. Geophys. Res.*, 68(24): 6441-6442.

- Chiu, Wan-Cheng, and H. L. Crutcher, 1966, The Spectrums of Angular Momentum Transfer in the Atmosphere, *J. Geophys. Res.*, **71**(4): 1017-1032.
- Clapp, Ph. F., 1961, Normal Heat Sources and Sinks in the Lower Troposphere in Winter, *Mon. Weather Rev.*, **89**(5): 147-162.
- , 1962, Comments on "Analysis of Infrared Radiation Measurements on a Synoptic Scale" and "Synoptic Use of Radiation Measurements from Satellite TIROS II," *Mon. Weather Rev.*, **90**(7): 287-288.
- , 1964, Global Cloud Cover for Seasons Using TIROS Nephanalyses, *Mon. Weather Rev.*, **92**(11): 495-507.
- , and F. Winniehoff, 1963, Tropospheric Heat Sources and Sinks at Washington, D. C., Summer 1961, Related to the Physical Features and Energy Budget of the Circulation, *Mon. Weather Rev.*, **91**(10-12): 494-504.
- Comité International de Géophysique—International Year of the Quiet Sun (CIG-IQSY) Committee, 1963, Details of the IQSY Plan for Alerts of Stratospheric Warmings, IQSY Notes, Nos. 5 and 6.
- Corcoran, J. L., and L. H. Horn, 1965, The Role of Synoptic Scale Variations of Infrared Radiation in the Generation of Available Potential Energy, *J. Geophys. Res.*, **70**(18): 4521-4528.
- Craig, R. A., and W. S. Hering, 1959, The Stratospheric Warming of January–February 1957, *J. Meteorol.*, **16**(2): 91-107.
- , and M. A. Lateef, 1962, Vertical Motion During the 1957 Stratospheric Warming, *J. Geophys. Res.*, **67**(5): 1839-1854.
- Cressman, G. P., 1959, An Operational Objective Analysis System, *Mon. Weather Rev.*, **87**(10): 367-374.
- , 1960, Improved Terrain Effects in Barotropic Forecasts, *Mon. Weather Rev.*, **88**(9-12): 327-342.
- Crossley, A. F., 1950, Relation Between the Standard Deviations of Temperature at Constant Pressure and at Constant Height, *Quart. J. Roy. Meteorol. Soc.*, **76**(329): 337-340.
- Crutcher, H. L., 1958, Upper Wind Distribution Statistical Parameter Estimates, U. S. Weather Bureau, Technical Paper No. 43.
- , 1959, Upper Wind Statistics Charts of the Northern Hemisphere, Office of the Chief of the U. S. Naval Operations.
- , 1961, Meridional Cross-sections, Upper Winds Over the Northern Hemisphere, U. S. Weather Bureau, Technical Paper No. 41.
- Danard, M. B., 1964, On the Influence of Release of Latent Heat on Cyclone Development, *J. Appl. Meteorol.*, **3**(1): 27-37.
- Danielsen, E. F., 1967a, Synoptic Distribution of Radioactivity over the Northern Hemisphere Based on the Distribution of Potential Vorticity on Isentropic Surfaces, paper presented at 14th General Assembly of the International Union of Geodesy and Geophysics, Lucerne, Switzerland, Sept. 25–Oct. 7, 1967.
- , 1967b, Transport and Diffusion of Stratospheric Radioactivity Based on Synoptic Hemispheric Analyses of Potential Vorticity, USAEC Report NYO-3317-3, Pennsylvania State University.
- Davis, N. E., 1951, The Mean Position of the Jet Stream, Great Britain Meteorological Research Committee, Meteorological Research Paper 615.
- Davis, P. A., 1963, An Analysis of the Atmospheric Heat Budget, *J. Atmos. Sci.*, **20**(1): 5-22.
- , 1965, TIROS III Radiation Measurements and Some Diabatic Properties of the Atmosphere, *Mon. Weather Rev.*, **93**(9): 535-545.
- Deardorff, J. W., 1966, The Counter-Gradient Heat Flux in the Lower Atmosphere and in the Laboratory, *J. Atmos. Sci.*, **23**(5): 503-506.
- , 1967, Empirical Dependence of the Eddy Coefficient of Heat upon Stability Above the Lowest 50 m, *J. Appl. Meteorol.*, **6**(4): 631-643.

- Defant, A., 1921, Die Zirkulation der Atmosphäre in den gemässigten Breiten der Erde, *Geogr. Annaler*, 3: 209-266.
- , 1949, Neuere Ansichten über die allgemeine Zirkulation der Atmosphäre in mittleren Breiten, *Arch. Meteorol. Geophys. Bioklimatol., Ser. A.*, 1(3-4): 273-294.
- Defant, F., 1958, Die allgemeine Atmosphärische Zirkulation in neuerer Betrachtungsweise, *Geofisica (Helsinki)*, 6(3-4): 189-217.
- , and H. M. E. van de Boogaard, 1963, The Global Circulation Features of the Troposphere Between the Equator and 40°N Based on a Single Day's Data, *Tellus*, 15(3): 251-260.
- , and H. Taba, 1958a, The Details of Wind and Temperature Field and the Generation of the Blocking Situation over Europe (Jan. 1-4, 1956), *Beitr. Phys. Atmos.*, 31(1-2): 69-88.
- , and H. Taba, 1958b, The Breakdown of Zonal Circulation During the Period January 8 to 13, 1956, the Characteristics of Temperature Field and Tropopause and Its Relation to the Atmospheric Field of Motion, *Tellus*, 10(4): 430-450.
- Deland, R. J., 1964, Traveling Planetary Waves, *Tellus*, 16(2): 271-273.
- , 1965a, On the Scale Analysis of Traveling Planetary Waves, *Tellus*, 17(4): 527-528.
- , 1965b, Some Observations of the Behavior of Spherical Harmonic Waves, *Mon. Weather Rev.*, 93(5): 307-312.
- , 1965c, Addendum to "Some Observations of the Behavior of Spherical Harmonic Waves," *Mon. Weather Rev.*, 93(8): 494.
- , and K. W. Johnson, 1968, A Statistical Study of the Vertical Structure of Traveling Planetary-scale Waves, *Mon. Weather Rev.*, 96(1): 12-22.
- , and Y.-J. Lin, 1967, On the Movement and Prediction of Traveling Planetary-scale Waves, *Mon. Weather Rev.*, 95(1): 21-31.
- Derome, J., 1966, Some Dynamical Effects of Topography and Diabatic Heating, *Meteorology*, 80: 75-81.
- Dickinson, R. E., 1962, Momentum Balance of the Stratosphere During the IGY, Final Report, pp. 132-167, Massachusetts Institute of Technology.
- , 1969, Vertical Propagation of Planetary Rossby Waves Through an Atmosphere with Newtonian Cooling, *J. Geophys. Res.*, 74(4): 929-938.
- Dickson, R. R., 1964, Synoptic Characterization of the Thermal Nature of the Earth's Surface, *Mon. Weather Rev.*, 92(5): 195-201.
- Doberitz, R., H. Flohn, and K. Schütte, 1967, Statistical Investigations of the Climatic Anomalies of the Equatorial Pacific, *Bonner Meteorol. Abhandl.*, No. 7.
- Döös, B. R., 1962, The Influence of Exchange of Sensible Heat with the Earth's Surface on the Planetary Flow, *Tellus*, 14(2): 133-147.
- , 1969, The Influence of the Large-scale Heat Sources on the Dynamics of the Ultra-long Waves, *Tellus*, 21(1): 25-39.
- Dopporto, M., 1964, Nodal Surfaces in the Atmosphere with Special Reference to Isopycnic and Horizontal Motion Levels, *Arch. Meteorol. Geophys. Bioklimatol., Ser. A.*, 14(1): 14-29.
- Drozdov, O. A., and A. S. Grigor'eva, 1965, *The Hydrologic Cycle in the Atmosphere* (translated from Russian), Israel Program for Scientific Translations, Jerusalem.
- Dungen, F. H. van den, J. F. Cox, and J. van Mieghem, 1950, Variations in the Earth's Angular Velocity Resulting from Fluctuations in Atmospheric and Oceanic Circulation, *Tellus*, 2(4): 319-320.
- , J. F. Cox, and J. van Mieghem, 1952, Les Fluctuations Saisonnières de la Rotation du Globe Terrestre et la Circulation Atmosphérique Générale, *Tellus*, 4(1): 1-7.
- , J. F. Cox, and J. van Mieghem, 1956, Seasonal Fluctuations in the Rate of Rotation of the Earth, in *Vistas in Astronomy*, A. Beer (Ed.), Pergamon Press Ltd., Oxford, England.
- , J. F. Cox, and J. van Mieghem, 1959, Sur les Irrégularités de la Rotation de la Terre, Brussels, *Acad. Roy. Belg., Bull. Classe Sci., Ser. 5*, 65(1): 69-71.
- Dütsch, H. U., 1966, Two Years of Regular Ozone Soundings over Boulder, Colorado, Technical Notes, January, pp. 36-40, National Center for Atmospheric Research.

- Dutton, J. A., and D. R. Johnson, 1967, The Theory of Available Potential Energy and a Variational Approach to Atmospheric Energetics, in *Advan. Geophys.*, **12**: 333-463.
- Dyer, A. J., and B. B. Hicks, 1965, Radioactive Fallout in Southern Australia During the Years 1958-1964, *J. Geophys. Res.*, **70**(16): 3879-3884.
- Eady, E. T., 1949, Long Waves and Cyclone Waves, *Tellus*, **1**(3): 33-52.
- , 1950, The Cause of the General Circulation of the Atmosphere, in *Centenary Proceedings of the Royal Meteorological Society, 1950*, pp. 156-172, Royal Meteorological Society.
- Eliassen, E., 1958, A Study of the Long Atmospheric Waves on the Basis of Zonal Harmonic Analysis, *Tellus*, **10**(2): 206-215.
- , 1961, On the Interactions Between the Long Baroclinic Waves and the Mean Zonal Flow, *Tellus*, **13**(1): 44-55.
- , and B. Machenhauer, 1965, A Study of the Fluctuations of the Atmospheric Planetary Flow Patterns Represented by Spherical Harmonics, *Tellus*, **17**(2): 220-238.
- Eliassen, A., 1956, A Procedure for Numerical Integration of the Primitive Equations of the Two-parameter Model of the Atmosphere, Final Report, University of California at Los Angeles.
- Ellsasser, H. W., 1963, Expansion of Geophysical Scalar Fields in Surface Spherical Harmonics, USAEC Report UCRL-7617-T, University of California at Los Angeles.
- Ertel, H., 1942, Der vertikale Turbulenz-Wärmestrom in der Atmosphäre, *Meteorol. Zeitschr.*, **59**: 250-253.
- Faust, H., 1960, Die Schwachwindsschicht der unteren Stratosphäre als Nullschicht, *Meteorol. Rundsch.*, **13**: 77-85.
- , 1961, Die Höhenlage der hochtroposphärischen Nullschicht, *Geofis. Pura Appl.*, **49**: 191-196.
- , 1963a, Planetarische Heizflächen und Zirkulationssysteme, *Meteorol. Rundsch.*, **16**(1): 5-9.
- , 1963b, Evaluation of Rocket Measurements in View of the Circulation in Stratosphere and Mesosphere, *Meteorol. Abhandl.*, **36**: 411-423.
- , 1963c, Neue Raketen-Windauswertungen, *Geofis. Pura Appl.*, **55**: 209-216.
- , 1967, Interaction Between the Different Layers of the Homosphere, *Arch. Meteorol. Geophys. Bioklimatol., Ser. A.*, **16**(1): 12-30.
- , and W. Attmannspacher, 1961, Die allgemeine Zirkulation der außertropischen Breiten bis 60 km Höhe auf der Basis der Nullschichtkonzeption, *Meteorol. Rundsch.*, **14**: 6-10.
- et al., 1959, Cell Structure of the Atmosphere, Final Report, Offenbach, Deutscher Wetterdienst.
- Finger, F. G., and S. Teweles, 1964, The Mid-winter 1963 Stratospheric Warming and Circulation Change, *J. Appl. Meteorol.*, **3**(1): 1-15.
- , and H. M. Woolf, 1967, Southern Hemisphere Stratospheric Circulation as Indicated by Shipboard Meteorological Rocket Observations, *J. Atmos. Sci.*, **24**(4): 387-395.
- Fjørtoft, R., 1953, On the Changes in the Spectral Distribution of Kinetic Energy for Two-dimensional Nondivergent Flow, *Tellus*, **5**(3): 225-230.
- Fleagle, R. G., 1947, The Fields of Temperature, Pressure and Three-dimensional Motion in Selected Weather Situations, *J. Meteorol.*, **4**: 165-185.
- Flohn, H., 1961, Meridional Transport of Particles and Standard Vector Deviation of Upper Winds, *Geofis. Pura Appl.*, **50**: 229-234.
- , 1964, Zur Interpretation und räumlichen Verteilung statistischer Parameter der Höhenwindverteilung, *Beitr. Phys. Atmos.*, **37**: 17-29.
- , 1967, Thermische Unterschiede zwischen Arktis und Antarktis, *Meteorol. Rundsch.*, **20**(5): 147-149.
- , D. Henning, and H. C. Korff, 1965, Studies on the Water-Vapor Transport over Northern Africa, *Bonner. Meteorol. Abhandl.*, **6**.
- Fortak, H., 1957, Über beschleunigungsfreie Luftbewegungen in äquatorialen Breiten, *Geofis. Pura Appl.*, **38**: 141.

- Friedman, D. G., 1955, Specification of Temperature and Precipitation in Terms of Circulation Patterns, *J. Meteorol.*, **12**: 428-435.
- Fritz, S., 1958, Seasonal Heat Storage in the Ocean and Heating of the Atmosphere, *Arch. Meteorol. Geophys. Bioklimatol., Ser. A.*, **10**: 291-300.
- , 1963, The Variable Appearance of the Earth from Satellites, *Mon. Weather Rev.*, **91**(10-12): 613-620.
- , and J. S. Winston, 1962, Synoptic Use of Radiation Measurements from Satellite TIROS II, *Mon. Weather Rev.*, **90**(1): 1-9.
- Garstang, M., 1967, Sensible and Latent Heat Exchange in Low Latitude Synoptic Scale Systems, *Tellus*, **19**(3): 492-508.
- Gilchrist, A., 1957, The Representation of Circumpolar 500 mb Charts by a Series of Spherical Harmonics, Meteorology Research Paper No. 1040, British Meteorology Office.
- Gilman, P. A., 1964, On the Vertical Transport of Angular Momentum in the Atmosphere, *Pure Appl. Geophys.*, **57**: 161-166.
- , 1965, The Mean Meridional Circulation of the Southern Hemisphere Inferred from Momentum and Mass Balance, *Tellus*, **17**(3): 277-284.
- Godson, W. L., 1963, A Comparison of Middle-Stratosphere Behaviour in the Arctic and Antarctic, with Special Reference to Final Warmings, *Meteorol. Abhandl.*, **36**: 161-206.
- Goldie, N., J. G. Moore, and E. E. Austin, 1957, Upper Air Temperature over the World, *Geophys. Memoirs*, No. 101.
- Green, J. S. A., 1960, A Problem in Baroclinic Stability, *Quart. J. Roy. Meteorol. Soc.*, **86**(368): 237-251.
- Griggs, M., 1963, Measurements of the Vertical Distribution of Atmospheric Ozone at Nairobi, *Quart. J. Roy. Meteorol. Soc.*, **89**(380): 284-286.
- Haar, T. H. Vonder, and V. E. Suomi, 1969, Satellite Observations of the Earth's Radiation Budget, *Science*, **163**(3868): 667-669.
- Haines, D. A., and J. S. Winston, 1963, Monthly Mean Values of Spatial Distribution of Meridional Transport of Sensible Heat, *Mon. Weather Rev.*, **91**(7): 319-328.
- Haney, R. L., 1961, Behavior of the Principal Harmonics of Selected Five-day Mean 500 mb Charts, *Mon. Weather Rev.*, **89**(10): 391-396.
- Hanson, K. J., Th. H. V. Haar, and V. E. Suomi, 1967, Reflection of Sunlight to Space and Absorption by the Earth and Atmosphere over the United States During Spring 1962, *Mon. Weather Rev.*, **95**(6): 354-362.
- Hare, F. K., 1965, Stratospheric Dynamics North of 40°N, *Quart. J. Roy. Meteorol. Soc.*, **91**(390): 417-420.
- Hassan, E. S. M., 1961, Fluctuations in the Atmospheric Inertia, 1873-1950, *Meteorol. Monographs*, **4**(24): 1-40.
- Hastenrath, St. L., 1966, On General Circulation and Energy Budget in the Area of the Central American Seas, *J. Atmos. Sci.*, **23**(6): 694-711.
- Haurwitz, B., 1961, Frictional Effects and the Meridional Circulation in the Mesosphere, *J. Geophys. Res.*, **66**(8): 2381-2391.
- , and R. A. Craig, 1952, Atmospheric Flow Patterns and Their Representation by Spherical Surface Harmonics, Geophysics Research Paper No. 14, Air Force Cambridge Research Center.
- Hawkins, H. F., and D. T. Rubsam, 1968, Hurricane Hilda, 1964: II. Structure and Budgets of the Hurricane on October 1, 1964, *Mon. Weather Rev.*, **96**(9): 617-636.
- Hawkins, R. S., 1964, Analysis and Interpretation of TIROS II Infrared Radiation Measurements, *J. Appl. Meteorol.*, **3**(5): 564-572.
- Hay, J. S., and F. Pasquill, 1959, Diffusion from a Continuous Source in Relation to the Spectrum and Scale of Turbulence, *Advan. Geophys.*, **6**: 345-365.
- Hayden, Ch. M., and A. C. Wiin-Nielsen, 1968, Objective Analysis Inconsistencies in Geostrophic Wind and Momentum Transport Calculations, Technical Report 087 59-4-T, University of Michigan.

- Heastie, H., and P. M. Stephenson, 1960, Upper Winds over the World, *Geophys. Memoirs*, No. 103.
- Hellerman, S., 1967, An Updated Estimate of the Wind Stress on the World Ocean, *Mon. Weather Rev.*, **95**(9): 607-626.
- Hennig, H., 1958, 40-jährige Monatsmittel der absoluten Topographien der 850 mb-, 700 mb-, und 300 mb- Flächen über der Nordhemisphäre für den Zeitraum 1900-1939, *Meteorol. Abhandl.*, **4**(3): 60 pp.
- Henry, R. M., and S. L. Hess, 1957, A Study of the Large-scale Spectra of Atmospheric Kinetic Energy, Wave Speed, Momentum Flux, and Heat Flux, Technical Report No. 9, Florida State University.
- , and S. L. Hess, 1958, A Study of Large-Scale Spectra of Some Meteorological Parameters, *J. Meteorol.*, **15**(4): 397-403.
- Hering, W. S., 1963, Preliminary Analysis of Ozone-Sonde Network Observations over North America, Paper Presented at 13th General Assembly of the International Union of Geodesy and Geophysics, Berkeley, Aug. 17-31, 1963.
- Hinich, M. J., and C. S. Clay, 1968, The Application of the Discrete Fourier Transform in the Estimation of Power Spectra, Coherence, and Bispectra of Geophysical Data, *Rev. Geophys.*, **6**(3): 347-363.
- Hirota, I., 1967, The Vertical Structure of the Stratospheric Sudden Warming, *J. Meteorol. Soc. Jap.*, **45**(5): 422-435.
- , 1968, Planetary Waves in the Upper Stratosphere in Early 1966, *J. Meteorol. Soc. Jap.*, **46**(5): 418-430.
- Högström, U., 1968, Studies of the Natural Evaporation and Energy Balance, *Tellus*, **20**(1): 65-75.
- Hollmann, G., 1955, Über die Beziehung zwischen Wind- und Druckfeld in Abhängigkeit von der geographischen Breite, *Meteorol. Rundsch.*, **8**: 79-82.
- , 1959, Der thermodynamische Wirkungsgrad der atmosphärischen Zirkulation, *Beitr. Phys. Atmos.*, **31**(3-4): 177-188.
- Holopainen, E. O., 1963, On the Dissipation of Kinetic Energy in the Atmosphere, *Tellus*, **15**(1): 26-32.
- , 1964, Investigation of Friction and Diabatic Processes in the Atmosphere, Paper No. 101, University of Helsinki.
- , 1965, On the Role of Mean Meridional Circulations in the Energy Balance of the Atmosphere, *Tellus*, **17**(3): 285-294.
- , 1966, A Diagnostic Study of the Maintenance of Stationary Disturbances in the Atmosphere, Technical Report No. 3, University of Michigan.
- , 1967, On the Mean Meridional Circulation and the Flux of Angular Momentum over the Northern Hemisphere, *Tellus*, **19**(1): 1-13.
- Horn, L. H., and R. A. Bryson, 1963, An Analysis of the Geostrophic Kinetic Energy Spectrum of Large-scale Atmospheric Turbulence, *J. Geophys. Res.*, **68**(4): 1059-1064.
- Houghton, D. D., 1962, A Calculation of the Large-scale Three-dimensional Distribution of Diabatic Heating in the Atmosphere, *Arch. Meteorol. Geophys. Bioklimatol., Ser. A*, **12**: 407-425.
- Houghton, H. G., 1954, On the Annual Heat Balance of the Northern Hemisphere, *J. Meteorol.*, **11**(1): 1-9.
- Huang, Ch.-H., H. A. Panofsky, and A. Schwalb, 1967, Some Relationships Between Synoptic Variables and Satellite Radiation Data, *Mon. Weather Rev.*, **95**(7): 483-486.
- Hutchings, J. W., 1957, Water Vapor Flux and Flux-divergence over Southern England: Summer 1954, *Quart. J. Roy. Meteorol. Soc.*, **83**(355): 30-48.
- , 1961, Water Vapour Transfer over the Australian Continent, *J. Meteorol.*, **18**(5): 615-634.
- Ichiye, T., and E. J. Zipser, 1967, An Example of Heat Transfer at the Air-Sea Boundary Over the Gulf Stream During a Cold Outbreak, *J. Meteorol. Soc. Jap.*, **45**(3): 261-270.

- Iida, M., 1968, Computations of the Transports of Momentum, Sensible and Latent Heat Across the Equator, *J. Meteorol. Soc. Jap.*, **46**(1): 1-13.
- International Council of Scientific Unions/International Union on Geodesy and Geophysics Committee on Atmospheric Sciences and Committee on Space Research, 1967, The Global Atmospheric Research Program (GARP), Report of the Study Conference held at Stockholm, June 28–July 11, 1967.
- Isacker, J. van, and J. van Mieghem, 1956, De selectieve rol van de atmosferische storingen in de algemene luchtcirculatie, *Meded. Koninkl. Vlaam. Acad., Wetenschap., Belg.*, 18 pp.
- Jacobs, I., 1958, 5-bzw. 40-jährige Monatsmittel der absoluten Topographien der 1000 mb-, 850 mb-, 500 mb- und 300 mb- Flächen sowie der Relativen Topographien 500/1000 mb und 300/500 mb über der Nordhemisphäre und ihre Monatlichen Änderungen; Folge 2, *Meteorol. Abhandl.*, **4**(2).
- Jacobs, W. C., 1949, The Energy Acquired by the Atmosphere over the Oceans Through Condensation and Through Heating from the Sea Surface, *J. Meteorol.*, **6**(4): 266-272.
- , 1950, Distribution and Some Effects of the Seasonal Quantity E-P over the North Atlantic and North Pacific, *Arch. Meteorol. Geophys. Bioklimatol., Ser. A*, **2**: 1-16.
- , 1951, Large-scale Aspects of Energy Transformations over the Oceans, *Compendium Meteorol.*, pp. 1057-1069.
- Jaw, J.-J., 1946, The Formation of Semipermanent Centers of Action in Relation to the Horizontal Solenoidal Field, *J. Meteorol.*, **3**(4): 103-114.
- Jeffreys, H., 1933, The Function of Cyclones in the General Circulation, *Proces-Verbaux de l'Association de Météorologie, Part II (Memoirs)*, pp. 219-230, Union of Geodesy and Geophysics, Lisbon.
- Jensen, C. E., 1960, Energy Transformation and Vertical Flux Processes over the Northern Hemisphere, Planetary Circulation Project, Scientific Report No. 1, Massachusetts Institute of Technology.
- , 1961, Energy Transformation and Vertical Flux Processes over the Northern Hemisphere, *J. Geophys. Res.*, **66**(4): 1145-1156.
- Johnson, D. R., 1965, The Role of Terrestrial Radiation in the Generation of Available Potential Energy, Ph.D. Thesis, University of Wisconsin.
- , 1966, The Effect of Bias and Random Radiometersonde Temperature Errors in the Estimation of Atmospheric Downward, Upward, Net and Equivalent Infrared Irradiance, *J. Geophys. Res.*, **71**(24): 5815-5826.
- , 1967, The Role of Terrestrial Radiation in the Generation of Zonal and Eddy Available Potential Energy, *Tellus*, **19**(4): 517-539.
- , and W. C. Shen, 1968, Profiles of Infrared Irradiance and Cooling Through a Jet Stream, *Mon. Weather Rev.*, **96**(8): 559-572.
- Julian, P. J., 1965, Some Aspects of Tropospheric Circulation During Midwinter Stratospheric Warming Events, *J. Geophys. Res.*, **70**(4): 757-767.
- Julian, P. R., 1966, The Index Cycle: A Cross-spectral Analysis of Zonal Index Data, *Mon. Weather Rev.*, **94**(5): 283-293.
- , 1967, Mid-winter Stratospheric Warmings in the Southern Hemisphere: General Remarks and a Case Study, *J. Appl. Meteorol.*, **6**(3): 557-563.
- , and K. Labitzke, 1965, A Study of Atmospheric Energetics During the January–February 1963 Stratospheric Warming, *J. Atmos. Sci.*, **22**(6): 597-610.
- Jurica, G. M., 1966, Radiative Heating in the Troposphere and Lower Stratosphere, *Mon. Weather Rev.*, **94**(9): 573-579.
- Kahn, A. B., 1962, Large-scale Atmospheric Spectra at 200 mb, *J. Atmos. Sci.*, **19**(2): 150-158.
- Kao, S.-K., 1953, On Total Momentum Vorticity with Application to the Study of the General Circulation in the Atmosphere, Scientific Report No. 1, University of California at Los Angeles.
- , 1954a, An Analysis of the Longitudinal Spectrum of Large-scale Atmospheric Motion, Final Report, pp. 235-244, Johns Hopkins University.

- , 1954b, The Meridional Transport of Kinetic Energy in the Atmosphere, *J. Meteorol.*, **11**(5): 352-361.
- , 1960, Transfer of Momentum Vorticity and the Maintenance of Zonal Circulation in the Atmosphere, *J. Meteorol.*, **17**(2): 122-129.
- , 1962, Large-scale Turbulent Diffusion in a Rotating Fluid with Application to the Atmosphere, *J. Geophys. Res.*, **67**(6): 2347-2359.
- , 1965, Some Aspects of the Large-scale Turbulence and Diffusion in the Atmosphere, *Quart. J. Roy. Meteorol. Soc.*, **91**(387): 10-17.
- , 1968, Governing Equations and Spectra for Atmospheric Motion and Transports in Frequency, Wave-number Space, *J. Atmos. Sci.*, **25**(1): 32-38.
- , and G. R. Farr, 1966, Turbulent Kinetic Energy in Relation to Jet Streams, Cyclone Tracks, and Ocean Currents, *J. Geophys. Res.*, **71**(18): 4289-4296.
- , and W. P. Hurley, 1962, Variations of the Kinetic Energy of Large-scale Eddy Currents in Relation to the Jet Streams, *J. Geophys. Res.*, **67**(11): 4233-4242.
- , and V. R. Taylor, 1964, Mean Kinetic Energies of Eddy and Mean Currents in the Atmosphere, *J. Geophys. Res.*, **69**(6): 1037-1049.
- Karsten, F., G. Korb, G. Manier, and F. Möller, 1959, On the Heat Balance of the Troposphere, Final Report, Meteorologisch Geophysikolisches Institut, Johannes Gutenberg Universität, Mainz.
- Kasahara, A., 1967, The Influence of Orography on the Global Circulation Patterns of the Atmosphere, Atmospheric Science Paper No. 122, pp. 194-221, Colorado State University.
- Katayama, A., 1966, On the Radiation Budget of the Troposphere Over the Northern Hemisphere (1), *J. Meteorol. Soc. Jap.*, **44**(6): 381-401.
- Keegan, T. G., 1961, Observed Variability of Winds and Circulations in the Mesosphere, in *Space Research II*, pp. 1061-1079, North Holland Publishing Co., Amsterdam.
- , 1962, Large-scale Disturbances of Atmospheric Circulation Between 30 and 70 km in Winter, *J. Geophys. Res.*, **67**(5): 1831-1838.
- Kellogg, W. W., 1961, Warming of the Polar Mesosphere and Lower Ionosphere in the Winter, *J. Meteorol.*, **18**(3): 373-381.
- , and G. F. Schilling, 1951, A Proposed Model of the Circulation in the Upper Stratosphere, *J. Meteorol.*, **8**(4): 222-230.
- Kennedy, J. S., 1964, Energy Generation Through Radiative Processes in the Lower Stratosphere, Report No. 11, USAEC Report TID-21471, Massachusetts Institute of Technology.
- Keshava, Murti, R. N., 1968, On the Maintenance of the Mean Zonal Motion in the Indian Summer Monsoon, *Mon. Weather Rev.*, **96**(1): 23-31.
- Kidson, J. W., and R. E. Newell, 1969, Exchange of Atmospheric Angular Momentum Between the Hemispheres, *Nature*, **221**(5178): 352-353.
- Korb, G., and F. Möller, 1962, Theoretical Investigations of Energy Gain by Absorption of Solar Radiation in Clouds, Ludwig-Maximilian Universität, Meteorologisches Institut, München, Germany.
- Koteswaram, P., 1958, The Easterlie Jet Stream in the Tropics, *Tellus*, **10**(1): 43-57.
- Kress, Chr., 1965, Untersuchungen Über Zonale Windprofile in der 850 mb Fläche, *Arch. Meteorol. Geophys. Bioklimatol., Ser. A*, **14**(4): 409-419.
- Krishnamurti, T. N., 1961a, The Subtropical Jet Stream of Winter, *J. Meteorol.*, **18**(2): 172-191.
- , 1961b, On the Role of the Subtropical Jet Stream of Winter in the Atmospheric General Circulation, *J. Meteorol.*, **18**(5): 657-670.
- Krueger, A. F., J. S. Winston, and D. Haines, 1965, Computations of Atmospheric Energy and Its Transformation for the Northern Hemisphere for a Recent Five-year Period, *Mon. Weather Rev.*, **93**(4): 227-238.
- Kubota, S., and M. Iida, 1954, Statistical Characteristics of the Atmospheric Disturbances, Papers in *Meteorol. and Geophys.*, **5**: 22-34.
- , and M. Iida, 1955, Transfer of Angular Momentum in the Atmosphere, Papers in *Meteorol. and Geophys.*, **5**: 224-232.

- Kuhn, P. M., 1963, Measured Effective Long-wave Emissivity of Clouds, *Mon. Weather Rev.*, **91**(10-12): 635-640.
- , 1968, Nimbus II and Balloon Infrared Radiation Analyses over the Antarctic, *J. Atmos. Sci.*, **25**(5): 908-911.
- , and V. E. Suomi, 1960, Infrared Radiometer Soundings on a Synoptic Scale, *J. Geophys. Res.*, **65**(11): 3669-3677.
- Kulkarni, R. N., 1966, Breakdown of the Biennial Variation of Ozone and of Lower Stratospheric Temperature in the Middle Latitudes of the Southern Hemisphere, *Nature*, **210**: 286-287.
- Kung, E. C., 1963, Climatology of Aerodynamic Roughness Parameters and Energy Dissipation in the Planetary Boundary Layer over the Northern Hemisphere, Annual Report, pp. 37-98, University of Wisconsin.
- , 1966a, Kinetic Energy Generation and Dissipation in the Large-scale Atmospheric Circulation, *Mon. Weather Rev.*, **94**(2): 67-82.
- , 1966b, Large-scale Balance of Kinetic Energy in the Atmosphere, *Mon. Weather Rev.*, **94**(11): 627-640.
- , 1967, Diurnal and Long-term Variations of the Kinetic Energy Generation and Dissipation for a Five-year Period, *Mon. Weather Rev.*, **95**(9): 593-606.
- , 1968, On the Momentum Exchange Between the Atmosphere and Earth over the Northern Hemisphere, *Mon. Weather Rev.*, **96**(6): 337-341.
- Kuo, H. L., 1951a, A Note on the Kinetic Energy Balance of the Zonal Wind System, *Tellus*, **3**(3): 205-207.
- , 1951b, Dynamical Aspects of the General Circulation and the Stability of Zonal Flow, *Tellus*, **3**(4): 268-284.
- , 1952, Three-dimensional Disturbances in a Baroclinic Zonal Current, *J. Meteorol.*, **9**(4): 260-278.
- , 1953, On the Production of Mean Zonal Currents in the Atmosphere by Large Disturbances, *Tellus*, **5**(4): 475-493.
- , 1956, Forced and Free Meridional Circulation in the Atmosphere, *J. Meteorol.*, **13**(6): 561-568.
- , 1959, Application of Energy Integrals to Thermally Driven Motions, *Beitr. Phys. Atmos.*, **31**: 189-199.
- , 1960, Theoretical Findings Concerning the Effects of Heating and Rotation on the Mechanism of Energy Release in Rotating Fluid Systems, in *Dynamics of Climate*, R. L. Pfeffer (Ed.), pp. 78-85, Pergamon Press, Inc., New York.
- Labitzke, K., 1965a, On the Mutual Relation Between Stratosphere and Troposphere During Periods of Stratospheric Warmings in Winter, Technical Note No. 66, pp. 249-261, World Meteorological Organization.
- , 1965b, On the Mutual Relation Between Stratosphere and Troposphere During Periods of Stratospheric Warmings in Winter, *J. Appl. Meteorol.*, **4**(1): 91-99.
- , and H. van Loon, 1965, A Note on Stratospheric Mid-winter Warmings in the Southern Hemisphere, *J. Appl. Meteorol.*, **4**(2): 292-295.
- Laby, J. E., J. G. Sparrow, and E. L. Unthank, 1964, Wind Studies to 120,000 Ft over Australia, *J. Atmos. Sci.*, **21**(3): 249-259.
- LaCruz, H., 1962, Stratospheric Temperature Variation over the Tropical Pacific, Report No. 23, Hawaii Institute of Geophysics, University of Hawaii.
- Lahey, J. F., R. A. Bryson, H. A. Corzine, and Ch. W. Hutchins, 1960, Atlas of 300 mb Wind Characteristics for the Northern Hemisphere, Final Report, University of Wisconsin.
- Lamb, H., 1932, *Hydrodynamics*, 6th edition, Cambridge University Press, New York.
- Landsberg, H. E., J. M. Mitchell, Jr., H. L. Crutcher, and F. T. Quinlan, 1963, Surface Signs of the Biennial Atmospheric Pulse, *Mon. Weather Rev.*, **91**(10-12): 549-556.
- Langlois, W. E., 1968, Total Potential Energy of Finite Columns, *Tellus*, **20**(4): 654-658.
- Lateef, M. A., 1964, The Energy Budget of the Stratosphere over North America During the Warming of 1957, *J. Geophys. Res.*, **69**(8): 1481-1495.

- Leovy, C., 1964, Simple Models of Thermally Driven Mesospheric Circulations, *J. Atmos. Sci.*, **21**(4): 327-341.
- Lettau, H. H., 1962, Theoretical Wind Spirals in the Boundary Layer of a Barotropic Atmosphere, *Arch. Meteorol. Geophys. Bioklimatol., Ser. A*, **7**: 133-157.
- List, R. J., K. Telegadas, and G. J. Ferber, 1964, Meteorological Evaluation of the Sources of Iodine-131 in Pasteurized Milk, *Science*, **146**: 59-64.
- London, J., 1957, A Study of the Atmospheric Heat Balance, Final Report, New York University.
- , 1963, Ozone Variations and Their Relation to Stratospheric Warming, *Meteorol. Abhandl.*, **36**: 299-310.
- , 1967, The Worldwide Distribution of Atmospheric Ozone, Paper Presented at 14th General Assembly of the International Union of Geodesy and Geophysics, Lucerne, Switzerland, Sept. 25–Oct. 7, 1967, Report IAMAP-CI-2, International Association of Meteorology and Atomic Physics.
- Loon, H. van, 1967, The Half-yearly Oscillations in Middle and High Southern Latitudes and the Coreless Winter, *J. Atmos. Sci.*, **24**(5): 472-486.
- Lorenz, E. N., 1951, Computations of the Balance of Angular Momentum and the Poleward Transport of Heat, Scientific Report No. 6, Massachusetts Institute of Technology.
- , 1953, A Multiple Index Notation for Describing Atmospheric Transport Processes, Technical Report 53-35, pp. 154-156, Air Force Cambridge Research Center.
- , 1955a, Available Potential Energy and the Maintenance of the General Circulation, *Tellus*, **7**(2): 157-167.
- , 1955b, Generation of Available Potential Energy and the Intensity of the General Circulation, in *Large Scale Synoptic Processes*, Final Report, 1957, University of California at Los Angeles.
- , 1960, Generation of Available Potential Energy and the Intensity of the General Circulation, in *Dynamics of Climate*, R. L. Pfeffer (Ed.), pp. 86-92, Pergamon Press, Inc., New York.
- , 1967, The Nature and Theory of the General Circulation of the Atmosphere, World Meteorological Organization No. 218.TP.115.
- Ludlam, F. H., 1967, Characteristics of Billow Clouds and Their Relation to Clear-air Turbulence, *Quart. J. Roy. Meteorol. Soc.*, **93**(398): 419-435.
- Lufkin, D. H., 1959, Atmospheric Water Vapor Divergence and the Water Balance at the Earth's Surface, Scientific Report No. 4, Massachusetts Institute of Technology.
- Maeda, K., 1963, On the Heating of Polar Night Mesosphere, *Meteorol. Abhandl.*, **36**: 451-506.
- , 1967, Quasi-biennial Cycles in Cosmic Ray Intensity, *J. Atmos. Sci.*, **24**(3): 320-323.
- Maenhout, A. G., and J. van Mieghem, 1964, Aanhoudende stratosferische verwarming in de Lente Hoven de Koning Boudewijn Basis, *Koninkl. Vlaam. Acad. Wetenschap., Letter. Schone Kunsten Belg., Klasse Wetenschap.*, **26**(10): 30 pp.
- Mahlman, J. D., 1964a, On the Feasibility of Relating Seasonal Fallout Oscillations to Hemispheric Index Patterns, Atmospheric Science Paper No. 58, pp. 55-58, Colorado State University.
- , 1964b, Relation of Upper-air Index Patterns to Seasonal Fallout Fluctuations, in *Radioactive Fallout from Nuclear Weapons Tests*, Germantown, Md., 1964, AEC Symposium Series, No. 5 (CONF-765), 1965.
- , 1965, Relation of Tropopause-level Index Changes to Radioactive Fallout Fluctuations, USAEC Report COO-1340-2, pp. 84-109, Colorado State University.
- , 1966, Atmospheric General Circulation and Transport of Radioactive Debris, Atmospheric Science Paper No. 103, USAEC Report COO-1340-7, Colorado State University.
- , 1967, Further Studies on Atmospheric General Circulation and Transport of Radioactive Debris, Atmospheric Science Paper No. 110, USAEC Report COO-1340-10, Colorado State University.
- Malone, T. F., 1956, Studies in Synoptic Climatology, Final Report No. N 5 ori-07883, Massachusetts Institute of Technology.
- Manabe, S., and F. Möller, 1961, On the Radioactive Equilibrium and Heat Balance of the Atmosphere, *Mon. Weather Rev.*, **89**(12): 503-532.

- Margules, M., 1903, Über die Energie der Stürme, *Jahrbuch kais.-königl. Zent. Meteorol., Vienna*, translated by C. Abbee in *Smithsonian Inst. Misc. Collections*, 51: 1910.
- Martin, D. W., 1956, Contribution to the Study of Atmospheric Ozone, Science Report No. 6, Massachusetts Institute of Technology.
- Maruyama, T., 1968a, Upward Transport of Westerly Momentum Due to Large-scale Disturbances in the Equatorial Lower Stratosphere, *J. Meteorol. Soc. Jap.*, 46(5): 404-417.
- , 1968b, Time Sequence of Power Spectra of Disturbances in the Equatorial Lower Stratosphere in Relation to the Quasi-biennial Oscillation, *J. Meteorol. Soc. Jap.*, 46(5): 327-342.
- Matsuno, T., and I. Hirota, 1966, On the Dynamic Stability of Polar Vortex in Wintertime, *J. Meteorol. Soc. Jap.*, 44(2): 122-128.
- Meinardus, W., 1934, Die Niederschlagsverteilung auf der Erde, *Meteorol. Z.*, 51: 345-350.
- Merilees, P. E., 1966, Harmonic Representation Applied to Large Scale Atmospheric Waves, McGill University, Montreal, *Meteorology*, 83: 174 pp.
- , 1968, On the Linear Balance Equation in Terms of Spherical Harmonics, *Tellus*, 20(1): 200-202.
- Merritt, E. S., 1967, Atlantic Upper Tropospheric Circulations and Tropical Cyclone Development, Final Report, Allied Research Associates, Inc.
- Mieghem, J. van, 1952a, Energy Conversion in the Atmosphere on the Scale of the General Circulation, *Tellus*, 4(4): 334-351.
- , 1952b, Seasonal Fluctuations of the Earth's Rotation and the General Circulation of the Atmosphere, *Ber. Deut. Wetterdienstes*, 35: 24-26.
- , 1955, Note on Energy Transfer and Conversion in Large Atmospheric Disturbances, *Quart. J. Roy. Meteorol. Soc.*, 81(347): 18-22.
- , 1956a, Réflexions sur le transport et la production du moment et de l'énergie cinétiques dans l'atmosphère et sur l'existence de circulations méridiennes moyennes, *Beitr. Phys. Atmos.*, 29: 55-82.
- , 1956b, The Energy Available in the Atmosphere for Conversion into Kinetic Energy, *Beitr. Phys. Atmos.*, 29: 129-142.
- , 1957, Energies potentielle et interne convertibles en énergie cinétique dans l'atmosphère, *Beitr. Phys. Atmos.*, 30: 5-17.
- , 1958, On the Interpretation of the Energy Equations in Dynamic Meteorology, *Geophysica*, 6: 559-576.
- , 1962, Pour une exploration synoptique du champ du rayonnement dans l'atmosphère, *Arch. Meteorol. Geophys. Bioklimatol., Ser. A*, 13(2): 129-143.
- , 1963, New Aspects of the General Circulation of the Stratosphere and Mesosphere, *Meteorol. Abhandl.*, 36: 1-62.
- , 1966, La dynamique et l'énergétique de la circulation a grande echelle. les problèmes météorologiques de la stratosphère et de la mésosphère, Publications du Centre National d'Études Spatiales, Presses Universitaires de France, Paris.
- , 1967, Energy Transport Across Internal Boundaries, *Beitr. Phys. Atmos.*, 40: 1-6.
- , and J. van Hamme, 1962, Sur la production, la redistribution et la dissipation de l'énergie cinétique dans la circulation meridienne moyenne, *Beitr. Phys. Atmos.*, 35: 213-233.
- , P. Defrise, and J. van Isacker, 1959, On the Selective Role of the Motion Systems in the Atmospheric General Circulation, in *The Atmosphere and the Sea in Motion*, B. Bolin (Ed.), pp. 230-239, Rockefeller Institute Press and Oxford University Press, Inc., New York.
- , P. Defrise, and J. van Isacker, 1963, Utilisation du diagramme polaire par la représentation des harmoniques zonaux de la circulation atmosphérique générale, *Beitr. Phys. Atmos.*, 36: 24-28.
- , P. Defrise, and J. van Isacker, 1966, Analyse harmonique zonale des températures stratosphériques Janvier-Février 1958, *Tellus*, 18(4): 814-819.
- Miller, A. J., 1967, Note on Vertical Motion in the Lower Stratosphere, *Beitr. Phys. Atmos.*, 40: 29-48.

- , 1969, On the Interannual Variability of the Tropospheric Energy Cycle and the Quasi-biennial Oscillation, *Mon. Weather Rev.*, **97**(2): 142-149.
- , S. Teweles, and H. M. Woolf, 1967, Seasonal Variation of Angular Momentum Transport at 500 mb, *Mon. Weather Rev.*, **95**(7): 427-439.
- , H. M. Woolf, and S. Teweles, 1967, Quasi-biennial Cycles in Angular Momentum Transports at 500 mb, *J. Atmos. Sci.*, **24**(3): 298-304.
- Miller, J. E., 1950, Energy Transformation Functions, *J. Meteorol.*, **7**(2): 152-159.
- Mintz, Y., 1951, The Geostrophic Poleward Flux of Angular Momentum in the Month of January 1949, *Tellus*, **3**(3): 195-200.
- , 1954, The Observed Zonal Circulation of the Atmosphere, *Bull. Amer. Meteorol. Soc.*, **35**(2): 208-214.
- , 1955a, Final Computations of the Mean Geostrophic Poleward Flux of Angular Momentum and of Sensible Heat in the Winter and Summer of 1949, Final Report, University of California at Los Angeles.
- , 1955b, The Total Energy Budget of the Atmosphere, Final Report, pp. 1-6, University of California at Los Angeles.
- , and S.-K. Kao, 1952, A Zonal-index Tendency Equation and Its Application to Forecasts of the Zonal Index, *J. Meteorol.*, **9**(2): 87-92.
- , and J. Lang, 1955, A Model of the Mean Meridional Circulation, Final Report, University of California at Los Angeles.
- Miyakoda, K., 1963, Some Characteristic Features of Winter Circulation in the Troposphere and Lower Stratosphere, Technical Report No. 14, University of Chicago.
- Molla, A. C., Jr., and C. J. Loisel, 1962, On the Hemispheric Correlations of Vertical and Meridional Wind Components, *Geofis. Pura Appl.*, **51**: 166-170.
- Möller, F., 1951a, Long-wave Radiation, in *Compendium of Meteorology*, Thomas F. Malone (Ed.), pp. 34-49, American Meteorological Society.
- , 1951b, Vierteljahreskarten des Niederschlags für die ganze Erde, *Geogr. Mitt.*, **95**: 1-7.
- , 1960, Der Strahlungshaushalt der Troposphäre, *Meteorol. Rundsch.*, **13**: 65-77.
- , 1967, Eine Karte der Strahlungsbilanz des Systems Erde-Atmosphäre für einen 14tägigen Zeitraum, *Meteorol. Rundsch.*, **20**(4): 97-98.
- Muench, H. S., 1965a, Stratospheric Energy Processes and Associated Atmospheric Long-wave Structure in Winter, Environmental Research Paper No. 95, Air Force Cambridge Research Laboratory.
- , 1965b, On the Dynamics of the Winter-time Stratospheric Circulation, *J. Atmos. Sci.*, **22**(4): 349-360.
- , 1966, The Energetics of the Wintertime Stratosphere, *Meteorology*, **80**: 11-35.
- Murakami, T., 1960, On the Maintenance of Kinetic Energy of the Large-scale Stationary Disturbances in the Atmosphere, Scientific Report No. 2, Massachusetts Institute of Technology.
- , 1962, Stratospheric Wind, Temperature, and Isobaric Height Conditions During the IGY Period, Report No. 5, USAEC Report TID-15476(Pt. I), Massachusetts Institute of Technology.
- , 1963, Maintenance of the Kinetic Energy of the Disturbances Appearing on the Monthly Mean Weather Charts, *J. Meteorol. Soc. Jap.*, **41**(1): 15-28.
- , 1965, Energy Cycle of the Stratospheric Warming in Early 1958, *J. Meteorol. Soc. Jap.*, **43**(5): 262-283.
- , 1967, Vertical Transfer of Energy Due to Stationary Disturbances Induced by Topography and Diabatic Heat Sources and Sinks, *J. Meteorol. Soc. Jap.*, **45**(3): 205-231.
- , and K. Tomatsu, 1964, The Spectrum Analysis of the Energy Interaction Terms in the Atmosphere, *J. Meteorol. Soc. Jap.*, **42**(1): 14-25.
- , and K. Tomatsu, 1965a, Energy Cycle in the Lower Troposphere, World Meteorological Organization—International Union of Geodesy and Geophysics Symposium on Research and

- Development Aspects of Long-Range Forecasting, Tech. Note No. 66, pp. 295-331, World Meteorological Organization.
- , and K. Tomatsu, 1965b, Energy Cycle in the Lower Atmosphere, *J. Meteorol. Soc. Jap.*, **43**(2): 73-89.
- Murgatroyd, R. J., 1957, Winds and Temperatures Between 20 km and 100 km—A Review, *Quart. J. Roy. Meteorol. Soc.*, **83**(358): 417-458.
- , 1969, A Note on the Contributions of Mean and Eddy Terms to the Momentum and Heat Balances of the Troposphere and Lower Stratosphere, *Quart. J. Roy. Meteorol. Soc.*, **95**(403): 194-202.
- , and R. M. Goody, 1958, Sources and Sinks of Radiative Energy from 30 to 90 km, *Quart. J. Roy. Meteorol. Soc.*, **84**(361): 225-234.
- , and F. Singleton, 1961, Possible Meridional Circulations in the Stratosphere and Mesosphere, *Quart. J. Roy. Meteorol. Soc.*, **87**(372): 125-135.
- , and F. Singleton, 1962, Possible Meridional Circulations in the Stratosphere and Mesosphere, *Quart. J. Roy. Meteorol. Soc.*, **88**(375): 105-107.
- Murray, R., A. E. Parker, and P. Collison, 1969, Some Computations of Meridional Flow, Angular Momentum and Energy in the Atmosphere Based on IGY Data for Latitude 30°N, *Quart. J. Roy. Meteorol. Soc.*, **95**(403): 92-103.
- Namias, J., 1950, The Index Cycle and Its Role in the General Circulation, *J. Meteorol.*, **7**(2): 130-139.
- , 1962, Influences of Abnormal Surface Heat Sources and Sinks on Atmospheric Behavior, in Proceedings of the International Symposium on Numer. Weather Prediction, Nov. 7-13, 1960, pp. 615-627, Meteorological Society of Japan.
- , 1963, Interactions of Circulation and Weather Between Hemispheres, *Mon. Weather Rev.*, **91**(10-12): 482-486.
- , 1969, Seasonal Interactions Between the North Pacific Ocean and the Atmosphere During the 1960's, *Mon. Weather Rev.*, **97**(3): 173-192.
- , and P. F. Clapp, 1951, Observational Studies of General Circulation Patterns, in *Compendium of Meteorology*, Thomas F. Malone (Ed.), pp. 551-567, American Meteorological Society.
- Newell, R. E., 1961, The Transport of Trace Substances in the Atmosphere and Their Implications for the General Circulation of the Stratosphere, *Geofis. Pura Appl.*, **49**: 137-158.
- , 1963a, Transfer Through the Tropopause and Within the Stratosphere, *Quart. J. Roy. Meteorol. Soc.*, **89**(380): 167-204.
- , 1963b, Preliminary Study of Quasi-horizontal Eddy Fluxes from Meteorological Rocket Network Data, *J. Atmos. Sci.*, **20**(3): 213-225.
- , 1963c, The General Circulation of the Atmosphere and Its Effects on the Movement of Trace Substances, *J. Geophys. Res.*, **68**(13): 3949-3962.
- , 1964a, A Note on the 26-Month Oscillation, *J. Atmos. Sci.*, **21**(3): 320-321.
- , 1964b, Further Ozone Transport Calculations and the Spring Maximum in Ozone Amount, *Pure Appl. Geophys.*, **59**: 191-206.
- , 1964c, The Circulation of the Upper Atmosphere, *Sci. Amer.*, **210**(3): 62-74.
- , 1964d, Stratospheric Energetics and Mass Transport, *Pure Appl. Geophys.*, **58**: 145-156.
- , 1965a, A Review of Studies of Eddy Fluxes in the Stratosphere and Mesosphere, Report No. 12, USAEC Report MIT-2241-3, Massachusetts Institute of Technology.
- , 1965b, The Energy and Momentum Budget of the Atmosphere Above the Tropopause, Proceedings of the 6th International Space Science Symposium, Mar-del-Plata, Argentina, May 11-19, 1965, in *Problems of Atmospheric Circulation*, R. U. Garcia and T. F. Malone (Eds.), Spartan Books Inc., Washington, D. C.
- , and A. J. Miller, 1965, Some Aspects of the General Circulation of the Stratosphere, in *Radioactive Fallout from Nuclear Weapons Tests*, Alfred W. Klement, Jr. (Ed.), AEC Symposium Series, No. 5 (CONF-765), Germantown, Md., 1964, pp. 392-404, 1965.

- , J. M. Wallace, and J. R. Mahoney, 1966, The General Circulation of the Atmosphere and Its Effects on the Movement of Trace Substances, Part 2, *Tellus*, **18**(2-3): 363-380.
- Newton, C. W., 1954, Frontogenesis and Frontolysis as a Three-dimensional Process, *J. Meteorol.*, **11**(6): 449-461.
- , 1959, Axial Velocity Streaks in the Jet Stream, Ageostrophic "Inertial" Oscillations, *J. Meteorol.*, **16**(6): 638-645.
- Ninomiya, T., 1968, Heat and Water Budget over the Japan Sea and the Japan Islands in Winter Season—With Special Emphasis on the Relation Among the Supply from Sea Surface, the Convective Transfer and the Heavy Snowfall, *J. Meteorol. Soc. Jap.*, **46**(5): 343-372.
- Nitta, T., 1967, Dynamical Interactions Between the Lower Stratosphere and the Troposphere, *Mon. Weather Rev.*, **95**(6): 319-339.
- Nyberg, A., T. Duvedal, and S. Fryklund, 1954, Transport of Heat and Momentum by Horizontal Large Scale Eddies in November 1957, July 1949, and February 1950, North of 40°N, Swedish Meteorological and Hydrological Institute Notiser och Prel. Rapporter, Vol. I, No. 4.
- Obasi, G. O. P., 1963a, Poleward Flux of Atmospheric Angular Momentum in the Southern Hemisphere, *J. Atmos. Sci.*, **20**(6): 516-528.
- , 1963b, Atmospheric Momentum and Energy Calculations for the Southern Hemisphere During the IGY, Scientific Report No. 6, Massachusetts Institute of Technology.
- , 1965, On the Maintenance of Kinetic Energy of Mean Zonal Flow in the Southern Hemisphere, *Tellus*, **17**(1): 95-105.
- Ogura, Y., 1957, Spectrum Modifications Due to the Use of Finite Differences, *J. Meteorol.*, **14**(1): 77-80.
- , 1958, On the Isotropy of Large-scale Disturbances in the Upper Troposphere, *J. Meteorol.*, **15**(4): 375-382.
- Ohring, G., 1958, The Radiation Budget of the Stratosphere, *J. Meteorol.*, **15**(5): 440-451.
- Oort, A. H., 1962, Direct Measurement of the Meridional Circulation in the Stratosphere During the IGY, Report No. 6, USAEC Report TID-17467, Massachusetts Institute of Technology.
- , 1964a, On the Energetics of the Mean and Eddy Circulations in the Lower Stratosphere, *Tellus*, **16**(3): 309-327.
- , 1964b, On Estimates of the Atmospheric Energy Cycle, *Mon. Weather Rev.*, **92**(11): 483-493.
- , 1964c, Computations of the Eddy Heat and Density Transport Across the Gulf Stream, *Tellus*, **16**(1): 55-63.
- , 1964d, Direct Measurement of the Meridional Circulation in the Stratosphere During the IGY, *Arch. Meteorol. Geophys. Bioklimatol., Ser. A*, **14**(2): 131-148.
- , 1965, The Climatology of the Lower Stratosphere During the IGY and Its Implications for the Regime of Circulation, *Arch. Meteorol. Geophys. Bioklimatol., Ser. A*, **14**(3): 243-278.
- Palmén, E., 1951, The Role of Atmospheric Disturbances in the General Circulation, *Quart. J. Roy. Meteorol. Soc.*, **77**(333): 337-354.
- , 1954, Über die atmosphärischen Strahlströme, *Meteorol. Abhandl.*, **2**(3): 35-50.
- , 1955, On the Mean Meridional Circulation in Low Latitudes of the Northern Hemisphere and the Associated Meridional and Vertical Flux of Angular Momentum, *Soc. Sci. Fenn., Comm. Phys.-Math.*, **XVII**(8): 1-33.
- , 1958, Vertical Circulation and Release of Kinetic Energy During the Development of Hurricane Hazel Into an Extratropical Storm, *Tellus*, **10**(1): 1-23.
- , 1959, On the Maintenance of Kinetic Energy in the Atmosphere, in *The Atmosphere and the Sea in Motion*, B. Bohn (Ed.), pp. 212-224, The Rockefeller Institute Press and Oxford University Press, New York.
- , 1960, On Generation and Frictional Dissipation of Kinetic Energy in the Atmosphere, *Soc. Sci. Fenn., Comm. Phys.-Math.*, **XXIV**(11).
- , 1961, On Conversion Between Potential and Kinetic Energy in the Atmosphere, *Geofis. Pura Appl.*, **49**: 167-177.

- , 1966a, On the Interhemispheric Mass Circulation Across the Equator, *Quart. J. Roy. Meteorol. Soc.*, **92**(391): 157-158.
- , 1966b, On the Mechanism of the Vertical Heat Flux and Generation of Kinetic Energy in the Atmosphere, *Tellus*, **18**(4): 838-845.
- , and M. A. Alaka, 1952, On the Budget of Angular Momentum in the Zone Between Equator and 30°N, *Tellus*, **4**(4): 324-331.
- , and E. O. Holopainen, 1962, Divergence, Vertical Velocity, and Conversion Between Potential and Kinetic Energy in an Extratropical Cyclone, *Geophysica*, **8**: 89-113.
- , H. Riehl, and L. A. Vuorela, 1958, On the Meridional Circulations and Release of Kinetic Energy in the Tropics, *J. Meteorol.*, **15**(3): 271-277.
- , and L. A. Vuorela, 1963, On the Mean Meridional Circulations in the Northern Hemisphere During the Winter Season, *Quart. J. Roy. Meteorol. Soc.*, **89**(379): 131-138.
- Palmer, C. E., and R. C. Taylor, 1960, The Vernal Breakdown of the Stratospheric Cyclone over the South Pole, *J. Geophys. Res.*, **65**(11): 3319-3329.
- Paulin, G., 1968, Spectral Atmospheric Energetics During January 1959, *Meteorology*, **91**: 256 pp.
- Peixoto, J. P., 1958, Hemisphere Humidity Conditions During the Year 1950, Scientific Report No. 3, Massachusetts Institute of Technology.
- , 1959, A Campa da Divergencia do Campa do Fluxo do Vapor do Agua na Atmosfera, *Rev. Fac. Cienc. 2A Ser., B-Cienc. Fis.-Quim.*, **VII**: 25-56.
- , 1960, Hemispheric Temperature Conditions During the Year 1950, Scientific Report No. 4, Massachusetts Institute of Technology.
- , 1961, Contribuição Para o Estudo dos Campos da Entalpia na Atmosfera, Paper presented at Congresso Luso-Espanhol para o Progresso das Ciencias, Porto.
- , and A. R. Crisi, 1965, Hemisphere Humidity Conditions During the IGY, Scientific Report No. 6, Massachusetts Institute of Technology.
- , and B. Saltzman, 1958, Harmonic Analysis of the Mean Northern Hemisphere Water Vapor Distribution for the Year 1950, *Geofis. Pura Appl.*, **41**: 183-188.
- , B. Saltzman, and S. Teweles, 1964, Harmonic Analysis of the Topography Along Parallels of the Earth, *J. Geophys. Res.*, **69**(8): 1501-1505.
- Peng, L., 1963, Stratospheric Wind Temperature and Isobaric Height Conditions During the IGY Period. Part II, Planetary Circulations Project, Scientific Report No. 10, Massachusetts Institute of Technology.
- , 1965a, A Modeling Study of the Meridional Temperature Profile and Energy Transformations in the Lower Stratosphere, Planetary Circulations Project, Report No. 13, Massachusetts Institute of Technology.
- , 1965b, Stratospheric Wind, Temperature, and Isobaric Height Conditions During the IGY Period, Part III, Planetary Circulations Project, Report No. 15, Massachusetts Institute of Technology.
- , 1965c, A Simple Numerical Experiment Concerning the General Circulation of the Lower Stratosphere, *Pure Appl. Geophys.*, **61**: 191-218.
- Perry, J. S., 1967, Long-wave Energy Processes in the 1963 Sudden Stratospheric Warming, *J. Atmos. Sci.*, **24**(5): 539-550.
- Petterssen, S., 1950, Some Aspects of the General Circulation of the Atmosphere, in *Centenary Proceedings of the Royal Meteorological Society, 1950*, pp. 120-155, Royal Meteorological Society.
- , D. L. Bradbury, and K. Pedersen, 1962, The Norwegian Cyclone Models in Relation to Heat and Cold Sources, *Geofis. Publ.*, **24**: 243-280.
- Pfeffer, R. L., 1964, The Global Atmospheric Circulation, *Trans. N. Y. Acad. Sci.*, Ser. 11, **26**(8): 984-997.
- , and Y. Chiang, 1967, Two Kinds of Vacillation in Rotating Laboratory Experiments, *Mon. Weather Rev.*, **95**(2): 75-82.
- Phillips, N. A., 1954, Energy Transformations and Meridional Circulations Associated with Simple Baroclinic Waves in a Two-level Quasi-geostrophic Model, *Tellus*, **6**(3): 273-286.

- , 1956, The General Circulation of the Atmosphere: A Numerical Experiment, *Quart. J. Roy. Meteorol. Soc.*, **82**(352): 123-164.
- , 1958, Geostrophic Errors in Predicting the Appalachian Storm of November 1950, *Geophysica*, **6**(3-4): 389-405.
- Phillipot, H. R., 1964, The Springtime Accelerated Warming Phenomenon in the Arctic Stratosphere, International Antarctic Analysis Center, Technical Report No. 3, Commonwealth Bureau of Meteorology, Melbourne.
- Pisharoty, P. R., 1955, The Kinetic Energy of the Atmosphere, Final Report, University of California at Los Angeles.
- Priestley, C. H. B., 1949, Heat Transport and Zonal Stress Between Latitudes, *Quart. J. Roy. Meteorol. Soc.*, **75**(323): 28-40.
- , 1951, A Survey of the Stress Between the Ocean and the Atmosphere, *Aust. J. Sci. Res.*, **44**: 315-328.
- , and P. A. Sheppard, 1952, Turbulence and Transfer Processes in the Atmosphere, *Quart. J. Roy. Meteorol. Soc.*, **78**(338): 489-529.
- , and W. C. Swinbank, 1947, Vertical Transport of Heat by Turbulence in the Atmosphere, *Proc. Roy. Soc. (London), Ser. A*, **189**: 543-561.
- , and A. J. Troup, 1954, Further Studies of the Physical Interaction Between Tropical and Temperate Latitudes, Commonwealth Scientific and Industrial Research Organization, Technical Paper No. 1.
- , and A. J. Troup, 1964, Strong Winds in the Global Transport of Momentum, *J. Atmos. Sci.*, **21**(4): 459-460.
- Raethjen, P., 1966, Zur Energetik kräftiger Frontogenesis, *Beitr. Phys. Atmos.*, **39**(2-4): 182-198.
- Ramanadham, K. R., 1965, The 26-Month Cycle and Atmospheric Ozone, in *International Atmospheric Ozone Symposium*, Albuquerque, Aug. 31, 1964, pp. 1-6, World Meteorological Organization, Geneva.
- Rao, M. Sankar, 1965, Continental Elevation Influence on the Stationary Harmonics of the Atmospheric Motion, *Pure Appl. Geophys.*, **60**: 141-159.
- , and R. Ramanadham, 1963, On the Meridional Local Eddy Flux of Relative Momentum over India, *J. Atmos. Sci.*, **20**(4): 350-353.
- Rao, P. K., and J. S. Winston, 1963, Investigation of Some Synoptic Capabilities of Atmospheric "Window" Measurements from Satellite TIROS II, *J. Appl. Meteorol.*, **2**(1): 12-23.
- Rao, Y. P., 1960, Interhemispheric Features of the General Circulation of the Atmosphere, *Quart. J. Roy. Meteorol. Soc.*, **86**(368): 156-166.
- , 1962, Transequatorial Exchange of Angular Momentum, *Quart. J. Roy. Meteorol. Soc.*, **88**(375): 96-99.
- , 1964, Interhemispheric Circulation, *Quart. J. Roy. Meteorol. Soc.*, **90**(384): 190-194.
- , 1967, Mean Meridional Circulation and Large-scale Eddies, *Tellus*, **19**(3): 483-491.
- Raschke, E., 1965a, Auswertungen von infraroten Strahlungsmessungen des meteorologischen Satelliten TIROS III, Teil I, Generalisierte Transmissionsfunktionen für die Konstruktion von Strahlungsrechendiagrammen, *Beitr. Phys. Atmos.*, **38**: 97-120.
- , 1965b, Auswertung von infraroten strahlungsmessungen des Meteorologischen Satelliten TIROS III, Teil II, *Beitr. Phys. Atmos.*, **38**: 153-187.
- , 1966, Über den Einfluss hoher Wolkenoberflächen auf Satellitenmessungen der Strahlungstemperatur der Stratosphäre, *Meteorol. Rundsch.*, **19**(6): 173-174.
- , F. Möller, and W. R. Bandeen, 1968, The Radiation Balance of the Earth-atmosphere System over Both Polar Regions Obtained from Radiation Measurements of the Nimbus II Meteorological Satellite, *Medd. Sveriges Meteorol. Hydrol. Inst.*, Ser. B, No. 28: 42-57.
- Rasmusson, E. M., 1967, Atmospheric Water Vapor Transport and the Water Balance of North America: Part I. Characteristics of the Water Vapor Flux Field, *Mon. Weather Rev.*, **95**(7): 403-426.

- , 1968, Atmospheric Water Vapor Transport and the Water Balance of North America: II. Large-scale Water Balance Investigations, *Mon. Weather Rev.*, **96**(10): 720-734.
- Reed, R. J., 1963a, On the Cause of the 26-Month Periodicity in the Equatorial Stratospheric Winds, *Meteorol. Abhandl.*, **36**: 245-257.
- , 1963b, On the Cause of the Stratospheric Sudden Warming Phenomenon, *Meteorol. Abhandl.*, **36**: 315-334.
- , 1964, A Tentative Model of the 26-Month Oscillation in Tropical Latitudes, *Quart. J. Roy. Meteorol. Soc.*, **90**(386): 441-466.
- , 1966a, The Circulation of the Tropical Stratosphere, *Meteorology*, **80**: 109-133.
- , 1966b, The Origin and Structure of the 26-Month Oscillation, *Meteorology*, **80**: 135-161.
- , and K. E. German, 1965, A Contribution to the Problem of Stratospheric Diffusion by Large-scale Mixing, *Mon. Weather Rev.*, **93**(5): 313-321.
- , J. Wolfe, and H. Nishimoto, 1963, A Spectral Analysis of the Energetics of the Stratospheric Sudden Warming of Early 1957, *J. Atmos. Sci.*, **20**(4): 256-275.
- Reiter, E. R., 1961, *Meteorologie der Strahlströme (Jet Streams)*, Springer-Verlag, Vienna.
- , 1963a, Die vertikale Struktur des Strahlstromkernes aus Forschungsflügen des Project Jet Stream, *Ber. Deut. Wetterd.*, **80**: 30 pp.
- , 1963b, *Jet Stream Meteorology*, The University of Chicago Press, Chicago.
- , 1963c, Note on the Eddy Kinetic Energy Distribution in Relation to the Jet Stream, *J. Geophys. Res.*, **68**(6): 1785-1787.
- , 1967, *Jet Streams. How Do They Affect Our Weather?*, Doubleday & Co., Inc., New York.
- , 1969a, Tropospheric Circulation and Jet Streams, in *World Survey of Climatology*, Vol. 4, H. E. Landsberg (Ed.), Elsevier, Amsterdam.
- , 1969b, Mean and Eddy Motions in the Atmosphere, *Mon. Weather Rev.*, **97**(3): 200-204.
- , M. E. Glasser, and J. D. Mahlman, 1967, Role of the Tropopause in Stratospheric-Tropospheric Exchange Processes, Atmospheric Science Paper No. 107, USAEC Report COO-1340-9, Colorado State University.
- , and R. W. Hayman, 1962, On the Nature of Clear-air Turbulence (CAT), Atmospheric Science Paper No. 28, Colorado State University.
- , and J. D. Mahlman, 1965, Heavy Iodine-131 Fallout over the Midwestern United States, May 1962, Atmospheric Science Paper No. 70, USAEC Report COO-1340-2, pp. 1-53, Colorado State University.
- Reynolds, O., 1895, On the Dynamical Theory of Incompressible Viscous Fluids and the Determination of the Criterion, *Phil. Trans. Roy. Soc. London, Ser. A*, **186**: 123-164.
- Richards, M. E., 1967, The Energy Budget of the Stratosphere During 1965, Planetary Circulations Project, Scientific Report No. 21, Massachusetts Institute of Technology.
- Riehl, H., 1950, On the Role of the Tropics in the General Circulation of the Atmosphere, *Tellus*, **2**(1): 1-17.
- , 1954, *Tropical Meteorology*, McGraw-Hill Book Company, Inc., New York.
- , 1962a, Radiation Measurements over the Caribbean During the Autumn of 1960, *J. Geophys. Res.*, **67**(10): 3935-3942.
- , 1962b, General Atmospheric Circulation of the Tropics, *Science*, **135**(3497): 13-22.
- , and D. Fultz, 1957, Jet Stream and Long Waves in a Steady Rotation-Dishpan Experiment, Structure of the Circulation, *Quart. J. Roy. Meteorol. Soc.*, **83**(356): 215-231; **84**(360): 186-187.
- , and D. Fultz, 1958, The General Circulation in a Steady Rotating-dishpan Experiment, *Quart. J. Roy. Meteorol. Soc.*, **84**(362): 389-417.
- , and R. Higgs, 1960, Unrest in the Upper Stratosphere over the Caribbean Sea During January 1960, *J. Meteorol.*, **17**(5): 555-561.
- , and J. S. Malkus, 1957, On the Heat Balance and Maintenance of Circulation in the Trades, *Quart. J. Roy. Meteorol. Soc.*, **83**(355): 21-29.
- , and J. S. Malkus, 1958, On the Heat Balance in the Equatorial Trough Zone, *Geophysica*, **6**(3-4): 503-537.

- , and T. C. Yeh, 1950, The Intensity of the Net Meridional Circulations, *Quart. J. Roy. Meteorol. Soc.*, **76**(328): 182-188.
- , T. C. Yeh, and N. E. LaSeur, 1950, A Study of Variations of the General Circulation, *J. Meteorol.*, **7**(3): 181-194.
- Rogers, D. G., 1962, An Investigation of the Angular Momentum Flux as Related to Stratospheric Wind Reversals in the Equatorial Belt, M.S. Thesis, University of Washington.
- Roper, R. G., and W. G. Elford, 1963, Seasonal Variation of Turbulence in the Upper Atmosphere, *Nature*, **197**: 963-964.
- Rosenthal, S. L., 1967, On the Development of Synoptic-scale Disturbances over the Subtropical Oceans, *Mon. Weather Rev.*, **95**(6): 341-346.
- Rossby, C.-G., 1947, On the Distribution of Angular Velocity in Gaseous Envelopes Under the Influence of Large-scale Horizontal Mixing Processes, *Bull. Amer. Meteorol. Soc.*, **28**(2): 53-68.
- , 1949, On a Mechanism for the Release of Potential Energy in the Atmosphere, *J. Meteorol.*, **6**(3): 163-180.
- Rubin, M. J., 1964, Antarctic Weather and Climate, in *Research in Geophysics*, Vol. 2, H. Odishaw (Ed.), pp. 461-478, Massachusetts Institute of Technology Press, Cambridge, Mass.
- , and W. Weyant, 1963, The Mass and Heat Budget of the Antarctic Atmosphere, *Mon. Weather Rev.*, **91**(10-12): 487-493.
- Rudloff, W., 1950, Zur jährlichen Schwankung der Erddrehung (Vorläufige Mitteilung), *Ann. Meteorol.*, **3**(11-12): 376-378.
- , 1963, Geophysikalische Einflüsse auf die Länge des Sterntages, *Deut. Hydrogr. Z.*, **16**(2): 76-85.
- Sabatini, R. R., and V. E. Suomi, 1962, On the Possibility of Atmospheric Infrared Cooling Estimates from Satellite Observations, *J. Atmos. Sci.*, **20**(1): 62-65.
- Saltzman, B., 1957, Equations Governing the Energetics of the Larger Scales of Atmospheric Turbulence in the Domaine of Wave Number, *J. Meteorol.*, **14**(6): 513-523.
- , 1958, Some Hemispheric Spectral Statistics, *J. Meteorol.*, **15**(3): 259-263.
- , 1961a, The Zonal Harmonic Representation of the Atmospheric Energy Cycle, Report TRC-9, Travelers Research Center.
- , 1961b, Note on the Role of Mountains in the Energy Budget of the Atmosphere, *Tellus*, **13**(2): 291-292.
- , 1967, On the Theory of the Mean Temperature of the Earth's Surface, *Tellus*, **19**(2): 219-229.
- , and A. Fleisher, 1960a, Spectrum of Kinetic Energy Transfer Due to Large-scale Horizontal Reynolds Stresses, *Tellus*, **12**(1): 110-111.
- , and A. Fleisher, 1960b, The Modes of Release of Available Potential Energy in the Atmosphere, *J. Geophys. Res.*, **65**(4): 1215-1222.
- , and A. Fleisher, 1960c, The Exchange of Kinetic Energy Between Large Scales of Atmospheric Motion, *Tellus*, **12**(4): 374-377.
- , and A. Fleisher, 1961, Further Statistics of the Modes of Release of Available Potential Energy, *J. Geophys. Res.*, **66**(7): 2271-2273.
- , and A. Fleisher, 1962, Spectral Statistics of the Wind at 500 mb, *J. Atmos. Sci.*, **19**(2): 195-204.
- , R. M. Gottuso, and A. Fleisher, 1961, The Meridional Eddy Transport of Kinetic Energy at 500 mb, *Tellus*, **13**(2): 293-295.
- , and S. Teweles, 1964, Further Statistics on the Exchange of Kinetic Energy Between Harmonic Components of the Atmospheric Flow, *Tellus*, **16**(4): 432-435.
- , and A. D. Vernekar, 1968, A Parameterization of the Large-scale Transient Eddy Flux of Relative Angular Momentum, *Mon. Weather Rev.*, **96**(12): 854-857.
- Sawyer, J. S., 1961, Quasi-periodic Wind Variations with Height in the Lower Stratosphere, *Quart. J. Roy. Meteorol. Soc.*, **87**(371): 24-33.

- , 1965, The Dynamical Problems of the Lower Stratosphere, *Quart. J. Roy. Meteorol. Soc.*, **91**(390): 407-416.
- Scherhag, R., 1948, *Neue Methoden der Wetteranalyse und Wetterprognose*, Springer-Verlag Ohg., Berlin.
- Schmitz, H. P., 1963, Zu den Beziehungen für den fluktuativen und mittleren Wassertransport in der Atmosphäre, *Geofis. Pura Appl.*, **55**: 217-238.
- Schove, D. J., 1963, Models of the Southern Oscillation in the 300–100 mb Layer and the Basis of Seasonal Forecasting, *Geofis. Pura Appl.*, **55**: 249-261.
- Schwerdtfeger, W., 1960, Der südliche Polarwirbel, *Meteorol. Rundsch.*, **13**: 89-93.
- , 1962, Die halbjährige Periode des meridionalen Temperaturgradienten in der Troposphäre und des Luftdruckes am Boden im Südpolargebiet, ihre Erscheinungsform und kausalen Zusammenhänge, *Beitr. Phys. Atmos.*, **35**: 234-244.
- , 1963, The Southern Circumpolar Vortex and the Spring Warming of the Polar Stratosphere, *Meteorol. Abhandl.*, **36**: 207-224.
- , 1967, Annual and Semi-annual Changes of Atmospheric Mass over Antarctica, *J. Geophys. Res.*, **72**(14): 3543-3548.
- , and D. W. Martin, 1964, The Zonal Flow of the Free Atmosphere Between 10°N and 80°S in the South American Sector, *J. Appl. Meteorol.*, **3**(6): 726-733.
- Sekiguchi, Y., 1963, Energy Variation in the Stratosphere During the Winter Season and Its Relation to Dynamic Stability of the Polar Vortex, Report ARL-1277-3, University of Oklahoma.
- Serra, A., 1964, Comments on Interactions of Circulation and Weather Between Hemispheres, *Mon. Weather Rev.*, **92**(9): 427.
- Shah, G. M., 1967, Quasi-biennial Oscillation in Ozone, *J. Atmos. Sci.*, **24**(4): 396-401.
- , and W. L. Godson, 1966, The 26-Month Oscillation in Zonal Wind and Temperature, *J. Atmos. Sci.*, **23**(6): 786-790.
- Shapiro, R., 1964, A Mid-latitude Biennial Oscillation in the Variance for the Surface-pressure Distribution, *Quart. J. Roy. Meteorol. Soc.*, **90**(385): 328-331.
- , and F. Ward, 1963, The Kinetic Energy Spectrum of Meridional Flow in the Mid-troposphere, *J. Atmos. Sci.*, **20**(4): 353-358.
- Shaw, D. B., 1966, Note on the Computation of Heat Sources and Sinks in the Atmosphere, *Quart. J. Roy. Meteorol. Soc.*, **92**(391): 55-66; **93**(396): 271-272.
- Shen, W. C., 1963, The Generation of Available Potential Energy Due to Horizontal Variations in Terrestrial Radiation as Measured by the Satellite Explorer VII, Ph.D. Thesis, University of Wisconsin.
- , G. W. Nicholas, and A. D. Belmont, 1968, Antarctic Stratospheric Warmings During 1963 Revealed by TIROS VII, 15-Micron Data, in Proceedings of the (Seventh) Stanstead Seminar on the Middle Atmosphere, McGill University, *Meteorology*, **90**: 169-185.
- Shenk, W. E., 1963, TIROS II Window Radiation and Large-scale Vertical Motion, *J. Appl. Meteorol.*, **2**(6): 770-775.
- Sheppard, P. A., 1953, The Vertical Transfer of Momentum in the General Circulation, *Arch. Meteorol. Geophys. Bioklimatol., Ser. A*, **7**: 114-124.
- Sherr, P. E., A. H. Glasen, J. C. Barnes, and J. H. Willand, 1968: World-wide Cloud Cover Distribution for Use in Computer Simulations, Report NASA-CR-61226, National Aeronautics and Space Administration, George C. Marshall Space Flight Center.
- Shuman, F. G., 1957, Numerical Methods in Weather Prediction. II. Smoothing and Filtering, *Mon. Weather Rev.*, **85**(11): 357-361.
- Smagorinsky, J., 1963, General Circulation Experiments with the Primitive Equations. I. The Basic Experiment, *Mon. Weather Rev.*, **91**(3): 99-164.
- Smith, E. K., 1968, Some Unexplained Features in the Statistics for Intense Sporadic E, paper given at the Second Seminar on the Cause and Structure of Temperature Latitude Sporadic E, Vail, Colorado, June 19–22, 1968.

- Smith, W. L., L. H. Horn, and D. R. Johnson, 1966, TIROS Radiation Measurements and the Infrared Cooling of the Atmosphere, *J. Appl. Meteorol.*, 5(4): 526-531.
- Spar, J., 1949, Energy Changes in the Mean Atmosphere, *J. Meteorol.*, 6(6): 411-415.
- Sparrow, J. G., 1965, A Southern Hemisphere Zonal Wind Cross Section, *J. Appl. Meteorol.*, 4(5): 635-637.
- , and E. L. Unthank, 1964, Biennial Stratospheric Oscillations in the Southern Hemisphere, *J. Atmos. Sci.*, 21(6): 592-596.
- Staley, D. O., 1965, An Evaluation of Certain Forms of Momentum Transfer in the 26-Month Oscillation, *Mon. Weather Rev.*, 93(3): 157-162.
- Stark, L. P., 1965, Position of Monthly Mean Troughs and Ridges in the Northern Hemisphere, 1949-1963, *Mon. Weather Rev.*, 93(11): 705-720.
- Starr, V. P., 1948, An Essay on the General Circulation of the Earth's Atmosphere, *J. Meteorol.*, 5(1): 39-43; Selected Meteorology Papers, No. 1, Gen. Circulation Part I, Meteor. Soc. Japan.
- , 1951a, A Note on the Eddy Transport of Angular Momentum, *Quart. J. Roy. Meteorol. Soc.*, 77(331): 44-50.
- , 1951b, Applications of Energy Principles to the General Circulation, in *Compendium Meteorology*, Thomas F. Malone (Ed.) pp. 568-574, American Meteorological Society.
- , 1953, Note Concerning the Nature of the Large-scale Eddies in the Atmosphere, *Tellus*, 5(4): 494-498.
- , 1954a, Commentaries Concerning Research on the General Circulation, *Tellus*, 6(6): 268-272.
- , 1954b, Studies of the Atmospheric General Circulation, Final Report, Part I, Massachusetts Institute of Technology.
- , 1956, Modern Developments in the Study of the General Circulation of the Atmosphere, *J. Geophys. Res.*, 61: 334-340.
- , 1959a, Further Statistics Concerning the General Circulation, *Tellus*, 11(4): 481-483.
- , 1959b, Trends of Thought Concerning Meteorological Research, *Geofis. Pura Appl.*, 43: 269-277.
- , 1968, *Physics of Negative Viscosity Phenomena*, McGraw-Hill Book Company, Inc., New York.
- , and R. E. Dickinson, 1963, Large-scale Vertical Eddies in the Atmosphere and the Energy of the Mean Zonal Flow, *Geofis. Pura Appl.*, 55: 133-136.
- , and J. P. Peixoto, 1958, On the Global Balance of Water Vapour and the Hydrology of Deserts, *Tellus*, 10(2): 188-194.
- , and J. P. Peixoto, 1960, On the Zonal Flux of Water Vapor in the Northern Hemisphere, *Geofis. Pura Appl.*, 47: 199-203.
- , and J. P. Peixoto, 1964, The Hemispheric Eddy Flux of Water Vapor and Its Implications for the Mechanics of the General Circulation, *Arch. Meteorol. Geophys. Bioklimatol., Ser. A*, 14(2): 111-130.
- , J. P. Peixoto, and G. C. Livadas, 1958, On the Meridional Flux of Water Vapor in the Northern Hemisphere, *Geofis. Pura Appl.*, 39(1): 174-185.
- , and J. M. Wallace, 1964, Mechanics of Eddy Processes in the Tropical Troposphere, *Pure Appl. Geophys.*, 58: 138-144.
- , and R. M. White, 1951, A Hemispherical Study of the Atmospheric Angular Momentum Balance, *Quart. J. Roy. Meteorol. Soc.*, 77(332): 215-225.
- , and R. M. White, 1952a, Two Years of Momentum Flux Data for 31°N, *Tellus*, 4(4): 332-333.
- , and R. M. White, 1952b, Meridional Flux of Angular Momentum in the Tropics, *Tellus*, 4(2): 118-125.
- , and R. M. White, 1952c, Note on the Seasonal Variation of the Meridional Flux of Angular Momentum, *Quart. J. Roy. Meteorol. Soc.*, 78(335): 62-69.
- , and R. M. White, 1952d, Schemes for the Study of Hemispheric Exchange Process, *Quart. J. Roy. Meteorol. Soc.*, 78(337): 407-410.

- , and R. M. White, 1954, Balance Requirements of the General Circulation, Geophysics Research Paper No. 35, G. R. D., Cambridge.
- Suomi, V. E., and W. C. Shen, 1963, Horizontal Variation of Infrared Cooling and the Generation of Eddy Available Potential Energy, *J. Atmos. Sci.*, **20**(1): 62-65.
- Sutcliffe, R. C., 1950, Variations in the Length of the Day, *Meteorol. Mag.*, **79**(942): 353-354.
- , 1956, Water Balance and the General Circulation of the Atmosphere, *Quart. J. Roy. Meteorol. Soc.*, **82**(354): 385-395.
- Syono, S., A. Kasahara, and Y. Sekiguchi, 1955, Some Statistical Properties of the Atmospheric Disturbance at 500 mb Level, *J. Meteorol. Soc. Jap.*, **33**: 23-30.
- Teweles, S., 1961, Time Section and Hodograph Analysis of Churchill Rocket and Radiosonde Winds and Temperatures, *Mon. Weather Rev.*, **89**(4): 125-136.
- , 1963a, Spectral Aspects of the Stratospheric Circulation During the IGY, Report No. 8, Massachusetts Institute of Technology.
- , 1963b, A Spectral Study of the Warming Epoch of January–February 1958, *Mon. Weather Rev.*, **91**(10-12): 505-519.
- , 1964, Stratospheric–Mesospheric Circulation, in *Research in Geophysics*, Vol. 2, H. Odishaw (Ed), pp. 509-528, Massachusetts Institute of Technology Press, Cambridge, Mass.
- , and F. G. Finger, 1958, An Abrupt Change in Stratospheric Circulation Beginning in Mid-January 1958, *Mon. Weather Rev.*, **86**(1): 23-28.
- , and F. G. Finger, 1962, Synoptic Studies Based on Rocketsonde Data, Space Research III, North-Holland Publishing Co., Amsterdam.
- Theon, J. S., and J. J. Horvath, 1968, Observations of the Southern Hemisphere Stratosphere and Mesosphere, *J. Geophys. Res.*, **73**(14): 4475-4480.
- Troup, A. J., 1965, The "Southern Oscillation," *Quart. J. Roy. Meteorol. Soc.*, **91**(390): 490-506.
- Tucker, G. B., 1957, Evidence of a Mean Meridional Circulation in the Atmosphere from Surface Wind Observations, *Quart. J. Roy. Meteorol. Soc.*, **83**(357): 290-302.
- , 1959, Mean Meridional Circulations in the Atmosphere, *Quart. J. Roy. Meteorol. Soc.*, **85**(365): 209-224.
- , 1960, The Atmospheric Budget of Angular Momentum, *Tellus*, **12**(2): 134-144.
- , 1964, Zonal Winds over the Equator, *Quart. J. Roy. Meteorol. Soc.*, **90**(386): 405-423.
- , 1965a, The Equatorial Tropospheric Wind Regime, *Quart. J. Roy. Meteorol. Soc.*, **91**(388): 140-150.
- , 1965b, The Divergence of Horizontal Eddy Flux of Momentum in the Lower Equatorial Stratosphere, *Quart. J. Roy. Meteorol. Soc.*, **91**(389): 356-359.
- , 1967, The Equatorial Tropospheric Wind Regime, *Quart. J. Roy. Meteorol. Soc.*, **93**(395): 137-139.
- , and J. M. Hopwood, 1968, The 26-Month Zonal Wind Oscillation in the Lower Stratosphere of the Southern Hemisphere, *J. Atmos. Sci.*, **25**(2): 293-298.
- , and D. O. Staley, 1965, Comments and Reply on "An Evaluation of Certain Forms of Momentum Transfer in the 26-Month Oscillation," *Mon. Weather Rev.*, **93**(11): 704, 720.
- University of Chicago, 1947, On the General Circulation of the Atmosphere in Middle Latitudes, *Bull. Amer. Meteorol. Soc.*, **28**: 255-280.
- Valovcin, F. R., 1968, Infrared Measurements of Jet Stream Cirrus, *J. Appl. Meteorol.*, **7**(5): 817-826.
- Vernekar, A. D., 1967, On Mean Meridional Circulations in the Atmosphere, *Mon. Weather Rev.*, **95**(11): 705-721.
- Vinnichenko, N. K., 1969, The Kinetic Energy Spectrum in the Free Atmosphere—1 Second to 5 Years (to be published).
- Vítek, V., 1962, On the Theory of Equatorial Zonal Flow, *Prague Stud. Geophys. Geod.*, **6**: 291-293.
- , and D. Vítková, 1962, On the Theory of Equatorial Westerlies, *Prague Stud. Geophys. Geod.*, **6**: 102.

- Vuorela, L. A., 1957, On the Observed Zonal and Meridional Circulations at Latitudes 15°N and 30°N in Winter, *Geophysica*, **6**: 106-120.
- , and I. Tuominen, 1964, On the Mean Zonal and Meridional Circulations and the Flux of Moisture in the Northern Hemisphere During the Summer Season, *Pure Appl. Geophys.*, **57**: 167-180.
- Walker, G. T., 1924, World Weather II, *Mem. India Meteorol. Dep.*, **24**: 275.
- Wallace, J. M., 1966, Long Period Wind Fluctuations in the Tropical Stratosphere, Report No. 19, USAEC Report MIT-2241-29, Massachusetts Institute of Technology.
- , 1967a, On the Role of Mean Meridional Motions in the Biennial Wind Oscillation, *Quart. J. Roy. Meteorol. Soc.*, **93**(396): 176-185.
- , 1967b, A Note on the Role of Radiation in the Biennial Oscillation, *J. Atmos. Sci.*, **24**(5): 589-599.
- , and J. R. Holton, 1968, A Diagnostic Numerical Model of the Quasi-biennial Oscillation, *J. Atmos. Sci.*, **25**(2): 280-292.
- , and V. E. Kousky, 1969, On the Relation Between Kelvin Waves and the Quasi-biennial Oscillation, *J. Meteorol. Soc. Jap.*, **46**(6): 496-502.
- , and R. E. Newell, 1966, Eddy Fluxes and the Biennial Stratospheric Oscillation, *Quart. J. Roy. Meteorol. Soc.*, **92**(394): 481-489.
- Walts, D. S., 1968, Transport Processes During Stratospheric Warming and Cooling Episodes, M.S. Thesis, Colorado State University.
- Warnecke, G., 1966, A Synoptic Study of the Stratospheric Circulation Above 30 Kilometers, *Meteorology*, **80**: 253-284.
- Webb, W. L., 1964, Stratospheric Solar Response, *J. Atmos. Sci.*, **21**(6): 582-591.
- , 1966, *Structure of the Stratosphere and Mesosphere*, Intercontinental Geophysics Series, Vol. 9, Academic Press, Inc., New York.
- Webster, F., 1961, The Effect of Meanders on the Kinetic Energy Balance of the Gulf Stream, *Tellus*, **13**(3): 392-401.
- , 1965, Measurements of Eddy Fluxes of Momentum in the Surface Layer of the Gulf Stream, *Tellus*, **17**(2): 239-245.
- Weinstein, M., and V. Suomi, 1961, Analysis of Satellite Infrared Radiation Measurements on a Synoptic Scale, *Mon. Weather Rev.*, **89**(11): 419-428.
- Wexler, H., W. B. Moreland, and W. S. Weyant, 1960, A Preliminary Report on Ozone Observations at Little America, Antarctica, *Mon. Weather Rev.*, **88**(2): 43-54.
- White, R. M., 1949, The Role of Mountains in the Angular Momentum Balance of the Atmosphere, *J. Meteorol.*, **6**(5): 353-355.
- , 1951a, The Meridional Flux of Sensible Heat over the Northern Hemisphere, *Tellus*, **3**(2): 83-88.
- , 1951b, The Meridional Eddy Flux of Energy, *Quart. J. Roy. Meteorol. Soc.*, **77**(332): 188-189.
- , 1954, The Counter Gradient Flux of Sensible Heat in the Lower Stratosphere, *Tellus*, **6**(2): 177-179.
- , and D. S. Cooley, 1952, The Large-scale Vertical Eddy Stresses on the Free Atmosphere, *Trans. Amer. Geophys. Union*, **33**: 502-506.
- , and D. S. Cooley, 1956, Kinetic Energy Spectrum of Meridional Motion in the Mid-troposphere, *J. Meteorol.*, **13**(1): 67-69.
- , and G. F. Nolan, 1960, A Preliminary Study of the Potential to Kinetic Energy Conversion Process in the Stratosphere, *Tellus*, **12**(2): 145-148.
- , and B. Saltzman, 1956, On Conversion Between Potential and Kinetic Energy in the Atmosphere, *Tellus*, **8**(3): 357-363.
- Widger, W. K., 1949, A Study of the Flow of Angular Momentum in the Atmosphere, *J. Meteorol.*, **6**(5): 291-299.
- Wiin-Nielsen, A., 1959, A Study of Energy Conversion and Meridional Circulation for the Large-scale Motion in the Atmosphere, *Mon. Weather Rev.*, **87**(9): 319-332.

- , 1962, On Transformation of Kinetic Energy Between the Vertical Shear Flow and the Vertical Mean Flow in the Atmosphere, *Mon. Weather Rev.*, **90**(8): 311-323.
- , 1964, On Energy Conversion Calculations, *Mon. Weather Rev.*, **92**(4): 161-167.
- , 1965a, Some New Observational Studies of Energy and Energy Transformations in the Atmosphere, in *Proceedings of the Symposium on Research and Development Aspects of Long-Range Forecasting*, Tech. Note No. 66, pp. 177-202, World Meteorological Organization.
- , 1965b, Transport and Mixing in Atmosphere, in *Proceedings of the Atmospheric Biology Conference*, pp. 11-24, Report N-65-23980, University of Minnesota and National Aeronautics and Space Administration.
- , 1967, On the Annual Variation and Spectral Distribution of Atmospheric Energy, *Tellus*, **19**(4): 540-559.
- , 1968, On the Intensity of the General Circulation of the Atmosphere, *Rev. Geophys.*, **6**(4): 559-579.
- , and J. A. Brown, 1962, On Diagnostic Computations of Atmospheric Heat Sources and Sinks and Generation of Available Potential Energy, in *Proceedings of the International Symposium of Numerical Weather Prediction, Tokyo, 1960*, pp. 593-613, Meteorology Society of Japan.
- , J. A. Brown, and M. Drake, 1963, On Atmospheric Energy Conversions Between Zonal Flow and Eddies, *Tellus*, **15**(3): 261-279.
- , J. A. Brown, and M. Drake, 1964, Further Studies of Energy Exchange Between the Zonal Flow and the Eddies, *Tellus*, **16**(2): 168-180.
- , and M. Drake, 1965, On the Energy Exchange Between the Baroclinic and Barotropic Components of Atmospheric Flow, *Mon. Weather Rev.*, **93**(2): 79-92.
- , and M. Drake, 1966a, The Contribution of Divergent Wind Components to the Energy Exchange Between the Baroclinic and Barotropic Components, *Mon. Weather Rev.*, **94**(1): 1-8.
- , and M. Drake, 1966b, An Observational Study of Kinetic Energy Conversions in the Atmosphere, *Mon. Weather Rev.*, **94**(4): 221-230.
- , and L. Steinberg, 1967, The Maintenance of Temperature Amplitude in the Atmosphere, *J. Geophys. Res.*, **72**(2): 461-467.
- , and A. D. Vernekar, 1967, On the Influence of the Mean Meridional Circulation on the Zonal Flow, *Mon. Weather Rev.*, **95**(11): 723-732.
- Wilkins, E. M., 1960, Dissipation of Energy by Atmospheric Turbulence, *J. Meteorol.*, **17**(1): 91-92.
- Williams, B. H., and B. T. Miers, 1968, The Synoptic Events of the Stratospheric Warming of December 1967–January 1968, Report ECOM-5216, Atmospheric Sciences Research Office.
- Winston, J. S., 1961, Preliminary Study of Atmospheric Energy Parameters, Report No. 3, Meteorological Satellite Laboratory.
- , 1967a, Zonal and Meridional Analysis of 5-Day Averaged Outgoing Long-wave Radiation Data from TIROS IV over the Pacific Sector in Relation to the Northern Hemisphere Circulation, *J. Appl. Meteorol.*, **6**(3): 453-463.
- , 1967b, Planetary-scale Characteristics of Monthly Mean Long-wave Radiation and Albedo and Some Year-to-Year Variations, *Mon. Weather Rev.*, **95**(5): 235-256.
- , 1968, Global Distribution of Cloudiness and Radiation for Seasons as Measured from Weather Satellites, in *World Survey of Climatology*, Vol. III, American Elsevier Publishing Co., New York.
- , and A. F. Krueger, 1961, Some Aspects of a Cycle of Available Potential Energy, *Mon. Weather Rev.*, **89**(9): 307-318.
- , and P. K. Rao, 1962, Preliminary Study of Planetary-scale Outgoing Long-wave Radiation as Derived from TIROS II Measurements, *Mon. Weather Rev.*, **90**(8): 307-310.

- , and P. K. Rao, 1963, Temporal and Spatial Variations in the Planetary-scale Outgoing Long-wave Radiation as Derived from TIROS II Measurements, *Mon. Weather Rev.*, **91**(10-12): 641-657.
- Wippermann, F., 1956, Numerische Untersuchungen der zeitlichen Änderung der Spektralverteilung kinetischer Energie für eine zweidimensionale, divergenz- und reibungsfreie Strömung, *Arch. Meteorol. Geophys. Bioklimatol., Ser. A*, **9**: 1-18.
- , 1957, Die Transformation potentieller und innerer Energie in die Energie rotorloser und diejeniger divergenzfreier Bewegung, *Beitr. Phys. Atmos.*, **29**: 269-275.
- , P. Gburčik, and W. Klug, 1963, Zur Eulerschen und Lagrangeschen Statistik sehr grossräumiger atmosphärischer Bewegungen, *Beitr. Phys. Atmos.*, **36**: 36-69.
- World Meteorological Organization, 1967, *World Weather Watch*.
- Zubyan, G. D., 1959, On the Inter-latitudinal Exchange of Warm and Cold Air Masses in the Stratosphere in Winter, *Meteorol. Gidrol.*, **1**(3-12), translated by Meteorological Branch, Department of Transport, Canada.

AUTHOR INDEX

- Adem, J., 122, 138, 217
Alaka, M. A., 12, 13, 15, 16, 233
Albrecht, F., 114, 217
Allison, L. J., 122, 217
Anderson, C. E., 59, 65, 217
Angell, J. K., 12, 145, 166, 217
Anthes, R. A., 139, 217
Arakawa, H., 49, 218
Arking, A., 122, 218
Asakura, T., 129, 218
Ashbel, D., 126, 218
Attmannspacher, W., 70, 222
Aubert, E. J., 114, 218
Auer, A. H., 139, 218
Austin, E. E., 24, 98, 223
Ball, F. K., 141, 218
Bandeep, W. R., 126, 128, 234
Bannon, J. K., 138, 218
Barnes, A. A., Jr., 27, 68, 136, 218
Barnes, J. C., 237
Barrett, E. W., 169, 171, 218
Barry, R. G., 136, 218
Belmont, A. D., 145, 152, 218, 237
Benton, G. S., 136, 165, 166, 218
Berggren, R., 130, 131, 132, 218
Berliand, T. G., 129, 218
Bernard, E. A., 116, 218
Berson, F. A., 159, 218
Bjerknes, J., 12, 72, 145, 149, 197, 209,
210, 218, 219
Blackadar, A. K., 177, 219
Blaes, C. E., 171, 219
Böhme, W., 145, 219
Bolin, B., 174, 219
Boogaard, H. M. E. van de, 20, 21, 136,
137, 138, 140, 158, 159, 197, 200, 219,
221
Boville, B. C., 180, 219
Boville, B. W., 78, 219
Bradbury, D. L., 132, 134, 233
Bradford, R., 122, 219
Bradley, J. H., 20, 97, 219
Brewer, A. W., 70, 219
Brier, G. W., 145, 219
Brown, J. A., Jr., 13, 78, 85, 86, 94, 103,
108, 109, 114, 117, 121, 123, 126, 128,
129, 177, 179, 180, 190, 195, 196, 199,
203, 206, 219, 241
Brunt, D., 94, 135, 219
Bryson, R. A., 169, 224, 227
Buch, H. S., 13, 18, 94, 150, 219
Budyko, M. I., 114, 128, 132, 219
Carpenter, T. H., 145, 217
Cehak, K., 187, 219
Charney, J. G., 78, 79, 106, 165, 219
Chiang, Y., 86, 233

- Chiu, Wan-Cheng, 171, 220
 Clapp, Ph. F., 86, 114, 115, 122, 220, 231
 Clay, C. S., 165, 224
 Collison, P., 231
 Comité International de Géophysique,
 152, 220
 Cooley, D. S., 20, 165, 240
 Corcoran, J. L., 122, 220
 Corzine, H. A., 227
 Cox, J. F., 9, 10, 221
 Craig, R. A., 52, 59, 165, 220, 223
 Cressman, G. P., 196, 220
 Crisi, A. R., 136, 139, 233
 Crossley, A. F., 24, 220
 Crutcher, H. L., 24, 94, 98, 171, 220, 227
 Danard, M. B., 174, 220
 Danielsen, E. F., 31, 212, 220
 Dartt, D. G., 145, 218
 Davis, N. E., 13, 101, 220
 Davis, P. A., 122, 129, 130, 220
 Deardorff, J. W., 116, 133, 220
 Defant, A., 1, 27, 221
 Defant, F., 20, 21, 158, 159, 212, 221
 Defrise, P., 165, 229
 Deland, R. J., 165, 187, 221
 Derome, J., 114, 221
 Dickinson, R. E., 20, 21, 23, 68, 78, 221,
 238
 Dickson, R. R., 114, 221
 Doberitz, R., 152, 154, 221
 Döös, B. R., 115, 171, 221
 Doporto, M., 72, 183, 221
 Doron, E., 126, 218
 Drake, M., 13, 78, 85, 86, 87, 89, 90, 91, 92,
 93, 94, 103, 108, 109, 114, 121, 177, 179,
 180, 183, 184, 185, 190, 195, 196, 203,
 206, 241
 Drazin, P. G., 78, 79, 219
 Drozdov, O. A., 136, 221
 Dungen, F. H. van den, 9, 10, 221
 Dütsch, H. U., 145, 221
 Dutton, J. A., 33, 36, 40, 122, 125, 171, 222
 Duvedal, T., 130, 232
 Dyer, A. J., 145, 222
 Eady, E. T., 34, 173, 222
 Elford, W. G., 79, 236
 Eliassen, E., 86, 165, 171, 187, 222
 Eliassen, A., 89, 114, 222
 Ellsaesser, H. W., 165, 222
 Ertel, H., 133, 222
 Estoque, M. A., 136, 218
 Eviatar, A., 126, 218
 Farr, G. R., 101, 226
 Faust, H., 24, 68, 70, 183, 222
 Ferber, G. J., 214, 228
 Finger, F. G., 27, 59, 74, 152, 222, 239
 Fjørtoft, R., 186, 222
 Fleagle, R. G., 173, 222
 Fleisher, A., 48, 49, 50, 53, 85, 86, 94, 130,
 141, 150, 164, 165, 171, 172, 173, 174,
 175, 176, 178, 186, 187, 236
 Flohn, H., 24, 25, 136, 152, 154, 156, 221,
 222
 Fortak, H., 148, 222
 Frasch, C., 219
 Friedman, D. G., 187, 223
 Fritz, S., 114, 122, 223
 Fryklund, S., 130, 232
 Fultz, D., 1, 2, 3, 4, 5, 201, 235
 Garstang, M., 131, 133, 223
 Gburčik, P., 168, 242
 German, K. E., 133, 235
 Gilchrist, A., 165, 223
 Gilman, P. A., 13, 150, 223
 Glasen, A. H., 237
 Glasser, M. E., 211, 212, 235
 Godson, W. L., 145, 152, 223
 Goldie, N., 24, 98, 223
 Goody, R. M., 70, 81, 231
 Gottuso, R. M., 186, 236
 Green, J. S. A., 34, 223
 Griggs, M., 70, 223
 Grigor'eva, A. S., 136, 221
 Haar, Th. H. V., 125, 128, 223
 Haines, D. A., 86, 94, 108, 115, 223, 226
 Hamme, J. van, 13, 17, 203, 229
 Haney, R. L., 173, 223
 Hanson, K. J., 125, 223
 Hare, F. K., 142, 180, 219, 223
 Hassan, El Sayed Mohammed, 9, 223
 Hastenrath, St. L., 117, 223
 Haurwitz, B., 79, 80, 81, 83, 165, 223
 Hawkins, H. F., 139, 223
 Hawkins, R. S., 122, 223
 Hay, J. S., 168, 223
 Hayden, Ch. M., 75, 223
 Hayman, R. W., 162, 235
 Heastie, H., 98, 224
 Hellerman, S., 20, 152, 224
 Hennig, H., 98, 224
 Henning, D., 136, 222
 Henry, R. M., 165, 166, 190, 224
 Hering, W. S., 52, 70, 220, 224
 Hess, S. L., 165, 166, 190, 224

- Hicks, B. B., 145, 222
 Higgs, R., 147, 235
 Hinich, M. J., 165, 224
 Hirota, I., 49, 51, 60, 145, 224, 229
 Högström, U., 116, 224
 Hollmann, G., 37, 148, 224
 Holopainen, E. O., 12, 13, 18, 94, 97, 99, 129, 132, 142, 143, 150, 159, 174, 186, 224, 233
 Holton, J. R., 148, 240
 Hopwood, J. M., 145, 239
 Horn, L. H., 122, 169, 220, 224, 238
 Horvath, J. J., 152, 239
 Houghton, D. D., 125, 224
 Houghton, H. G., 128, 129, 224
 Huang, C., 122, 219, 224
 Hurley, W. P., 101, 105, 226
 Hutchings, J. W., 136, 224
 Hutchins, Ch. W., 227
 Ichiye, T., 117, 224
 ICSU/IUGG Committee on Atmospheric Sciences and COSPAR, 100, 225
 Iida, M., 156, 165, 177, 225, 226
 Isacker, J. van, 165, 177, 225, 229
 Jacobs, I., 98, 225
 Jacobs, W. C., 114, 136, 208, 209, 225
 Jaw, J.-J., 170, 225
 Jeffreys, H., 1, 225
 Jensen, C. E., 27, 94, 225
 Johnson, D. R., 33, 36, 40, 122, 125, 139, 171, 222, 225, 238
 Johnson, K. W., 187, 221
 Julian, P. J., 225
 Julian, P. R., 51, 54, 55, 68, 72, 73, 74, 75, 76, 77, 78, 85, 86, 101, 107, 152, 180, 215, 225
 Junge, C. E., 60
 Jurica, G. M., 129, 130, 225
 Kahn, A. B., 165, 166, 218, 225
 Kao, S.-K., 6, 13, 20, 27, 30, 85, 101, 105, 162, 166, 167, 168, 169, 177, 225, 226, 230
 Karsten, F., 130, 226
 Kasahara, A., 165, 171, 226, 239
 Katayama, A., 122, 129, 218, 226
 Keegan, T. G., 27, 226
 Kellogg, W. W., 68, 79, 226
 Kennedy, J. S., 129, 147, 226
 Keshava, Murti, R. M., 13, 226
 Kidson, J. W., 156, 226
 Klug, W., 168, 242
 Kondratiev, K. Y., 114, 128, 219
 Korb, G., 122, 226
 Korff, H. C., 136, 222
 Korshover, J., 145, 217
 Koteswaram, P., 159, 226
 Kousky, V. E., 148, 240
 Kress, Chr., 86, 226
 Krishnamurti, T. N., 21, 24, 201, 202, 203, 204, 205, 206, 207, 208, 209, 210, 211, 226
 Krueger, A. F., 86, 94, 226, 241
 Kubota, S., 165, 177, 226
 Kuhn, P. M., 122, 130, 227
 Kulkarni, R. N., 145, 227
 Kung, E. C., 20, 106, 125, 142, 143, 144, 227
 Kuo, H. L., 12, 44, 49, 53, 74, 86, 106, 177, 227
 Labitzke, K., 51, 54, 55, 60, 68, 72, 73, 74, 75, 76, 77, 78, 85, 101, 107, 145, 146, 152, 180, 183, 215, 225, 227
 Laby, J. E., 145, 227
 La Cruz, H., 148, 227
 Lahey, J. F., 24, 227
 Lamb, H., 177, 227
 Landsberg, H. E., 145, 227
 Lang, J., 98, 230
 Langlois, W. E., 227
 La Seur, N. E., 85, 236
 Lateef, M. A., 52, 59, 220, 227
 Leovy, C., 83, 85, 228
 Lethbridge, M. D., 219
 Lettau, H. H., 142, 228
 Levine, J. S., 122, 218
 Lin, Y.-J., 187, 221
 List, R. J., 214, 228
 Livadas, G. C., 136, 141, 238
 Loisel, C. J., 70, 71, 72, 183, 230
 London, J., 59, 65, 68, 98, 126, 128, 129, 130, 132, 145, 203, 205, 207, 208, 228
 Loon, H. van, 152, 227, 228
 Lorenz, E. N., 8, 33, 34, 35, 36, 37, 39, 40, 41, 44, 45, 177, 228
 Ludlam, F. H., 162, 228
 Lufkin, D. H., 136, 228
 Machenhauer, B., 165, 187, 222
 Maeda, K., 79, 148, 228
 Maenhout, A. G., 152, 228
 Mahlman, J. D., 59, 62, 64, 68, 74, 152, 175, 210, 211, 212, 214, 228, 235
 Mahoney, J. R., 29, 232
 Malkus, J. S., 117, 156, 235
 Malone, T. F., 187, 228

- Manabe, S., 68, 228
 Manier, G., 226
 Margules, M., 33, 34, 229
 Martin, D. W., 70, 150, 229, 237
 Maruyama, T., 148, 229
 Marwitz, J. D., 139, 218
 Matsuno, T., 49, 229
 Meinardus, W., 132, 229
 Merilees, P. E., 187, 229
 Merritt, E. S., 122, 229
 Mieghem, J. van, 9, 10, 12, 13, 17, 37, 40,
 42, 44, 49, 65, 78, 152, 165, 173, 177,
 203, 221, 225, 228, 229
 Miers, B. T., 145, 241
 Miller, A. J., 51, 70, 148, 190, 193, 229,
 230, 231
 Miller, J. E., 42, 184, 230
 Mintz, Y., 12, 13, 18, 85, 97, 98, 99, 132,
 193, 203, 219, 230
 Mitchell, J. M., Jr., 227
 Miyakoda, K., 54, 55, 68, 230
 Molla, A. C., Jr., 70, 71, 72, 183, 230
 Möller, F., 68, 122, 126, 127, 128, 129, 130,
 132, 136, 141, 226, 228, 230, 234
 Moore, J. G., 24, 98, 223
 Moreland, W. B., 155, 240
 Muench, H. S., 40, 41, 42, 43, 44, 45, 49, 51,
 52, 53, 54, 55, 183, 230
 Murakami, T., 25, 49, 59, 86, 94, 171, 186, 230
 Murgatroyd, R. J., 13, 60, 70, 72, 81, 82, 83,
 84, 231
 Murray, R., 13, 21, 231
 Namias, J., 85, 86, 117, 149, 156, 231
 Newell, R. E., 24, 25, 26, 27, 29, 34, 51, 70,
 78, 79, 83, 147, 148, 149, 156, 226, 231,
 232, 240
 Newton, C. W., 175, 209, 232
 Nicholas, G. W., 145, 152, 218, 237
 Ninomiya, T., 117, 232
 Nishimoto, H., 52, 53, 57, 58, 59, 60, 61,
 74, 106, 162, 180, 235
 Nitta, T., 173, 232
 Nolan, G. F., 51, 240
 Nyberg, A., 130, 131, 132, 218, 232
 Obasi, G. O., 150, 151, 152, 153, 154, 232
 Ogura, Y., 166, 169, 232
 Ohring, G., 70, 81, 232
 Oort, A. H., 25, 48, 49, 51, 52, 53, 54, 55,
 58, 72, 92, 94, 95, 96, 97, 232
 Palmén, E., 2, 10, 11, 12, 13, 15, 16, 20, 98,
 132, 134, 135, 142, 158, 159, 174, 175,
 176, 203, 232, 233
 Palmer, C. E., 156, 233
 Panofsky, H. A., 122, 219, 224
 Parker, E., 231
 Pasquill, F., 168, 223
 Paulin, G., 186, 233
 Pedersen, K., 132, 134, 233
 Pedlovsky, J., 79, 219
 Peixoto, J. P., 86, 94, 98, 99, 114, 136, 138,
 139, 141, 173, 197, 208, 233, 238
 Peng, L., 25, 51, 233
 Perry, J. S., 59, 74, 177, 183, 184, 233
 Pettersen, S., 16, 132, 134, 233
 Pfeiffer, R. L., 12, 86, 233
 Phillips, N. A., 44, 85, 89, 94, 106, 233,
 234
 Phillipot, H. R., 152, 234
 Pisharoty, P. R., 98, 141, 234
 Priestley, C. H. B., 12, 20, 108, 133, 158,
 234
 Quinlan, F. T., 227
 Raethjen, P., 122, 234
 Ramanadham, K. R., 12, 145, 147, 234
 Rao, M. Sankar, 12, 171, 186, 234
 Rao, P. K., 122, 234, 241
 Rao, Y. P., 24, 156, 158, 159, 234
 Raschke, E., 122, 126, 128, 234
 Rasmusson, E. M., 136, 234, 235
 Reed, R. J., 51, 52, 53, 54, 55, 57, 58, 59,
 60, 61, 70, 71, 74, 78, 106, 133, 145, 147,
 162, 180, 235
 Reiter, E. R., 1, 7, 8, 12, 13, 27, 44, 85, 89,
 97, 101, 148, 159, 162, 175, 209, 211,
 212, 214, 235
 Reynolds, O., 177, 235
 Richards, M. E., 56, 58, 235
 Richardson, L. F., 49
 Riehl, H., 1, 2, 3, 4, 5, 12, 85, 98, 117, 130,
 147, 156, 159, 201, 233, 235, 236
 Rogers, D. G., 147, 236
 Roper, R. G., 79, 236
 Rosenthal, S. L., 131, 236
 Rossby, C.-G., 27, 48, 236
 Rubin, M. J., 155, 236
 Rubsam, D. T., 139, 223
 Rudloff, W., 9, 236
 Sabatini, R. R., 122, 236
 Saltzman, B., 20, 24, 48, 49, 50, 51, 53, 85,
 86, 94, 115, 116, 119, 120, 130, 141, 148,
 150, 162, 164, 165, 171, 172, 173, 174,
 175, 176, 177, 178, 186, 187, 188, 197,
 208, 233, 236, 240
 Sawyer, J. S., 70, 142, 236, 237

- Scherhag, R., 103, 237
Schilling, G. F., 68, 226
Schmitz, H. P., 136, 237
Schove, D. J., 197, 237
Schütte, K., 152, 154, 221
Schwalb, A., 122, 219, 224
Schwerdtfeger, W., 150, 152, 237
Sekiguchi, Y., 54, 55, 68, 165, 237, 239
Serra, A., 156, 237
Shah, G. M., 145, 147, 237
Shapiro, R., 48, 147, 165, 237
Shaw, D. B., 130, 237
Shen, W. C., 94, 122, 145, 152, 218, 225, 237, 239
Shenk, W. E., 122, 237
Sheppard, P. A., 20, 133, 234, 237
Sherr, P. E., 122, 237
Shuman, F. G., 169, 237
Singleton, F., 70, 81, 82, 83, 84, 231
Smagorinsky, J., 89, 90, 92, 94, 106, 128, 129, 237
Smith, E. K., 148, 149, 237
Smith, W. L., 122, 238
Spar, J., 40, 238
Sparrow, J. G., 145, 150, 227, 238
Staley, D. O., 147, 238, 239
Stark, L. P., 171, 238
Starr, V. P., 12, 13, 20, 21, 23, 44, 48, 49, 50, 51, 92, 94, 97, 101, 103, 106, 114, 116, 117, 118, 136, 141, 152, 177, 238, 239
Steele, L. P., 138, 218
Steinberg, L., 113, 241
Stephenson, P. M., 98, 224
Suomi, V. E., 94, 122, 125, 128, 130, 223, 227, 236, 239, 240
Sutcliffe, R. C., 9, 136, 239
Swinbank, W. C., 133, 234
Syono, S., 165, 239
Taba, H., 212, 221
Taylor, R. C., 156, 233
Taylor, V. R., 101, 226
Telegadas, K., 214, 228
Teweles, S., 27, 59, 63, 74, 94, 148, 183, 186, 188, 190, 193, 222, 230, 233, 236, 239
Theon, J. S., 152, 239
Tomatsu, K., 86, 171, 186, 230
Troup, A. J., 12, 159, 197, 218, 234, 239
Tucker, G. B., 11, 12, 13, 14, 15, 16, 17, 19, 27, 68, 70, 98, 145, 147, 156, 157, 158, 159, 197, 239
Tuominen, I., 138, 141, 158, 159, 240
University of Chicago, 27, 239
Unthank, E. L., 145, 227, 238
Valovcin, F. R., 122, 239
Vernekar, A. D., 13, 24, 103, 108, 236, 239, 241
Vinnichenko, N. K., 6, 239
Vítek, V., 148, 239
Vítková, D., 148, 239
Vuorela, L. A., 12, 98, 138, 141, 158, 159, 233, 240
Walker, G. T., 197, 240
Wallace, J. M., 29, 70, 114, 116, 117, 118, 145, 147, 148, 149, 232, 238, 240
Walts, D. S., 60, 65, 67, 68, 69, 70, 240
Ward, F., 48, 165, 237
Warnecke, G., 74, 122, 217, 240
Webb, W. L., 74, 155, 240
Webster, F., 49, 240
Weinstein, M., 122, 240
Wexler, H., 155, 240
Weyant, W., 155, 236, 240
White, R. M., 11, 12, 13, 20, 51, 92, 94, 108, 117, 130, 136, 165, 238, 240
Widger, W. K., 11, 12, 240
Wiin-Nielsen, A. C., 13, 18, 48, 73, 75, 78, 85, 86, 87, 88, 89, 90, 91, 92, 93, 94, 100, 102, 103, 106, 108, 109, 112, 113, 114, 117, 119, 121, 125, 130, 141, 142, 143, 152, 164, 165, 168, 169, 170, 171, 172, 173, 174, 175, 177, 179, 180, 183, 184, 185, 187, 190, 193, 195, 196, 203, 206, 223, 240, 241
Wilkins, E. M., 142, 241
Willand, J. H., 237
Williams, B. H., 145, 241
Wilson, C. V., 180, 219
Winninghoff, F., 115, 220
Winston, J. S., 86, 94, 108, 113, 114, 115, 122, 124, 126, 195, 218, 223, 226, 234, 241, 242
Wippermann, F., 73, 86, 89, 168, 242
Wolfe, J., 52, 53, 57, 58, 59, 60, 61, 74, 106, 162, 180, 235
Woolf, H. M., 148, 152, 190, 193, 230
World Meteorological Organization, 100, 242
Yeh, T. C., 85, 236
Zipser, E. J., 117, 224
Zubyan, G. D., 12, 242

SUBJECT INDEX

- Aerosols, 10, 42, 48
- Ageostrophic components, 106
- Air pollution, 216
- Albedo, 122, 156
- Aleutian high, 145
- Anisotropy, 169
- Antarctica, 155
- Applications Technology Satellite, 214
- Arctic, 156
- Arosa, 147
- Austausch, 1
- Australia, 136
- Autocorrelation, Eulerian, 166
 - spectra, 171
- Lagrangian, 166

- Balloons, constant density, 197
 - constant level, 100
- Baroclinic atmosphere, 34 f.
- Baroclinic instability, 169
- Baroclinic processes, 108
- Baroclinic waves, 173 f.
- Baroclinicity, 89
- Barotropic processes, 92
- Beta effect, 12
- Bias, slow wind, 12

- Biennial oscillation (see Oscillation, biennial)
- Boundary layer, 142
- Bowen ratio, 133
- British Isles, 142

- Caribbean, 117, 125
- Central America, 171
- Chaff, 29
- Cheltenham, 148
- Christmas Island, 214
- Circulation, cross axis, 3
 - direct (see Hadley cell)
 - indirect (see Ferrel cell)
 - mean meridional, 2, 4, 6, 10 ff., 13, 16 f., 43 f., 48, 68, 70, 72, 74 f., 79, 81, 97 ff., 103, 136, 147, 150 f., 157, 159, 201, 210, 211, 213
- Circumpolar vortex (see Polar vortex)
- Clear-air turbulence, 161
- Cloud, noctilucent, 81, 83
- Cloudiness, 125
- Cold outbreaks, 125, 174
- Conductivity, 83
- Convection, 130 f., 215 f., 162
- Convergence (see Divergence)

- Cooling, radiational, 132
- Coordinate system, curvilinear, 2 f., 5, 20 f., 98, 201, 203, 206, 208 f., 211
- Eulerian, 100, 197
- Geographic, 3 f., 13, 20 f., 98, 201, 203, 206, 208 f., 211
- Lagrangian, 100, 197, 200
- Cosmic-ray intensity, 148
- Cyclone index, 175
- Debris, radioactive (see radioactivity)
- Density, 33
- Diabatic effects, 68, 74, 98, 126, 128 f., 140, 195, 213
- Diabatic generation of potential energy, 73
- Diffusion, 5 f., 215
- "Dishpan", 1 ff., 12 f., 86, 201
- Dispersion, rate of, 200
- Dissipation of kinetic energy, 3, 40, 51, 79, 98, 125, 134, 140 ff., 144, 171, 186, 195, 215
- in the free atmosphere, 142
- Divergence, 27, 73, 90, 175
- Domain, longitudinal, 97
- mixed space-time, 95 ff.
- space, 94, 96 f., 99
- time, 96 f., 99
- vertical, 97
- Drag, 20, 196
- East Asia, 113
- Easterlies, polar, 10
- Eddies, 1, 3 f., 6, 10 ff., 20, 24 f., 40 f., 45, 48 f., 57, 59, 65, 67, 70, 78 f., 81, 97 f., 125, 132, 137, 147 f., 150, 161, 201
- daily, 206 f., 209
- five day, 206 f., 209 f.
- standing, 6, 13, 20 f., 23 ff., 70, 97 ff., 114, 150 f., 156 f., 186, 197, 200, 206 ff.
- transient, 6, 13, 17, 20 f., 23 ff., 70 f., 97 ff., 130, 138, 147, 150 ff., 156 f., 186, 197, 200
- Eddy flow, harmonic components of the, 177
- Eddy viscosity, 83
- Efficiency factor, 40
- Energy, available potential, 34 f., 37, 40, 58 f., 76, 79, 94, 96 f., 101, 106, 148, 164, 170, 175, 188, 213
- barotropic kinetic, 86
- divergence-free kinetic, 74, 89
- divergent-flow kinetic, 74, 89
- eddy available potential, 42, 49, 60, 90, 171 f., 174, 195, 216
- eddy kinetic, 40, 48 ff., 75, 79, 101, 105, 164 f., 170 ff., 214, 216
- flux of (see Energy transfer)
- generation of available potential, 39 f., 42, 108, 115, 117, 125, 139 f.
- internal, 33 f., 73, 215 f.
- kinetic, 6, 33 ff., 40, 53, 58 f., 76 f., 89 ff., 94, 96 f., 101, 103, 105, 132, 134, 148, 150, 152, 154, 165, 175 f., 179, 183 f., 186 ff., 213, 215
- mean kinetic, 37, 48, 50, 76, 86, 88, 90, 97, 101, 106, 169, 179
- minimum total potential, 34 f.
- potential, 33, 42, 53, 60, 73 f., 99, 186, 195, 203, 206, 214
- shear-flow kinetic, 86 ff., 90, 92, 97, 169
- spectra of available potential, 171
- total potential, 33 f.
- zonal (see Energy, mean kinetic)
- Energy balance, 43
- Energy conversions (see Energy transformations)
- Energy dissipation (see Dissipation of kinetic energy)
- Energy transfer, 21, 43 f., 48 f., 76, 78, 97, 99 ff., 135, 145, 150, 152, 179, 209 f., 214, 216
- between the eddies and the mean zonal current, 177, 186
- between individual wave modes, 171
- Energy transformation, 39, 42, 44 f., 48 f., 59, 76, 93 f., 96, 98, 100 f., 103, 106 f., 112, 150, 162, 172, 184 f., 213 ff.
- Energy transport (see Energy transfer)
- England, 136
- Entropy, 171
- Equator, 48, 126, 136, 145, 147 f., 152
- geostrophic flow conditions at the, 148
- thermal, 159
- Europe, 174
- Evaporation, 136, 141, 206
- Excentricity of the tropospheric polar vortex, 78
- Explorer VII, 122
- "Explosive" warming (see Stratospheric warming)

- Ferrel cell, 13, 17, 59, 74, 98, 136
 Flux, countergradient, 49, 51, 114, 147
 Fourier analysis, 161 f., 165, 186 f.
 Fourier coefficients, 177
 Fourier transform, 163, 166
 Friction, 9 ff., 20, 34, 40, 42, 51, 79, 83,
 143, 188, 193
- Gas constant, 34
 General circulation, model of, quasi-
 nondivergent, 89
 periodicities of the, 145
 Generation of potential energy (see
 Diabatic effects)
 Geopotential, 72 f., 132
 Geostrophic approximation, 48 f., 186
 Geostrophic drag coefficient, 142
 Global Atmospheric Research Program, 100
 Gravity waves, 161
 Greenhouse effect, 122
 Gulf of Mexico, 117
 Gulf Stream, 49
- Hadley cell, 5, 12 f., 17, 20 f., 59, 74, 78,
 83, 92, 98, 103, 108, 136, 138, 156
 Harmonic analysis (see Fourier
 analysis)
 Hawaii, 117
 Heat, conduction and convection, 116
 latent, 42, 128, 130, 132 f., 139, 195,
 209, 216
 sensible, 42, 83, 99, 108, 114 f., 128,
 130 f., 134, 193, 195, 208, 216
 specific, 34
 Heat budget, 108, 115, 120, 122, 128 f.,
 132, 203
 Heat flux, countergradient, 83, 114
 horizontal, 113, 117, 121, 132 f., 147,
 156, 203
 turbulent, 132
 Heat sources, 114
 Heat transport, 3 f., 24, 70, 83, 114,
 116 f., 130 f., 133, 147, 187, 193,
 206, 208 f., 211, 215
 cross equatorial, 156
 Heating, diabatic, 40, 52 f.
 High index, 85, 177, 214
 Himalayas, 101, 125, 171, 174
 "Hot towers", 130, 139, 215 f.
 Huancayo, 148
- Humidity, specific, 136, 206
 Hurricanes, 139, 174, 176
- IGY, 53, 72, 155
 Index cycle, 86, 145, 171, 180
 Inertial oscillations, 209
 Indian Ocean, 150, 159, 197
 Interaction, hemispheric, 156
 Interhemispheric mass exchange, 159
 Intertropical convergence zone, 138,
 156, 214
 Ionosphere, 79, 148
 IQSY-1965, 58
- Japan, 117
 Jet axis, 4, 21
 Jet maxima, 3, 27, 174 f.
 Jet stream, 1, 101, 106, 108, 122, 125,
 142, 152, 174, 187, 193, 201, 203, 206,
 210, 212, 214
 arctic front, 13, 21
 polar front, 3, 13, 21, 24, 27, 136
 polar night, 25, 53, 57, 79, 83, 210
 subtropical, 13, 17, 21, 24, 98, 136,
 201 f.
 tropical easterly, 24, 159
 tropopause, 25, 83
 tropospheric, 89
 Jet-stream front, 212
 "Junge aerosol layer", 60
- Kokubunji, 148
- Land-sea distribution, 92, 150, 171, 197,
 208
 Lapse rate, dry adiabatic, 36
 Lee waves, 215
 Length of day, 9
 Level, isopycnic, 72, 108
 Low index, 86, 177
- Mass circulation, 4, 201, 203, 208 ff.
 Mass transport, interhemispheric, 156
 Mean flow, barotropic, 98, 173, 183
 Mesopause, 81, 83
 Mesosphere, 70, 81
 Meteor trail, 79

- Meteorological Rocket Network, 29, 79
 Mixing theory of jet-stream formation, 27
 Moisture transport, 139, 208, 215
 Momentum, angular, 1, 9 ff., 20, 27, 30, 79, 83, 151, 154
 of the ocean, 9
 flux of, 10, 13, 16, 18, 20 f., 23 f., 27, 30, 42, 75, 83, 98, 148, 150, 158, 187, 190, 193, 196, 209 ff.
 Momentum flux across equator, 157
 Momentum vorticity, 27, 30
 Monsoon, 13, 150, 159, 197
 Motions, mean meridional (see Circulation, mean meridional)
 vertical, 2 f., 11, 13, 25, 49, 59, 61 ff., 68, 70, 73 f., 82, 122, 131, 148, 155, 162, 183, 211
 Mountain effects (see Orography)
- Nephanalyses, 122
 NIMBUS II, 126 f.
 Nonadiabatic (see Diabatic)
 North Africa, 136
 North America, 79, 136, 142, 171
 Nuclear debris (see Radioactivity)
 Null layers, 72
- Ocean-continent effects (see Land-sea distribution)
 Omega equation, 75
 Orography, 30, 92, 101, 150, 171
 Orthogonal polynomials, 187
 Oscillation, biennial, 70 f., 145, 147 f.
 Oxygen, recombination of, 79
 Ozone, 20, 59, 68, 72, 145, 147 f., 155, 213
 biennial variations, 147
 spring maxima, 71, 83
- Pacific Ocean, 79, 169, 214
 Parseval's theorem, 163
 Poisson's constant, 35
 Poisson's equation, 35 f.
 Polar vortex, breakdown of, 52, 57 f., 62, 81, 103, 152, 177, 183, 210 f., 215
 Potential energy (see Energy, potential)
 Precipitation, 132, 136, 141
- long wave, 116, 122, 124 ff., 129
 reflected short wave, 125
 short wave, 115 f.
 Radioactive fallout (see Radioactivity)
 Radioactivity, 5 f., 10, 20, 42, 71, 83, 200, 213 f., 216
 Reynolds stresses, 177
 Rocket grenade data, 29
 Rocky Mountains, 101, 125, 171, 174
 Rotation, changes in earth's rate of, 9
- Salt Lake City, 169
 Satellite, 122, 125, 214 ff.
 Scales of turbulence, Eulerian, 168
 Lagrangian, 168
 Sea-surface temperature anomalies, 149
 Sea temperatures, equatorial, 145
 Shear flow, baroclinic, 90, 173, 183
 spectrum of the, 169
 Snow cover, interannual variability of, 117
 Southern oscillation, 197
 Specific heat (see Heat, specific)
 Spectra (see Energy spectra)
 Spectrum slopes, 169
 Speed of sound, 37
 Spherical-harmonic analysis, 165, 187
 Sporadic E-layers, 148 f.
 Stability, static, 73, 143
 Standard deviation, spatial, 24, 26
 temporal, 24 ff.
 of velocity components, 24 f.
 Stratosphere, 49, 51, 53, 59, 70, 72 f., 78, 81, 101 f., 129, 145, 152, 155 f., 169, 180, 183 f., 186, 193, 201, 210, 212, 214 f.
 dry, 83, 129
 moist, 129
 single-cell scheme, 68
 three-cell regime, 60
 tropical, 68
 two-cell structure, 60, 68, 70, 72, 74, 81, 155
 Stratospheric "sudden" cooling, 65
 Stratospheric warming, 49, 51 f., 59 ff., 72, 74 f., 78, 107, 145 f., 152, 155 f., 183
 Stream function, 73, 75
 Streamlines, 6, 17
 Surface, isentropic, 34, 212
 Surface stress, 20, 152

- Surface temperatures, biennial oscillation
of, 145
- Symbolism, mathematical, 6
- Tchebychev polynomials, 187
- Temperature, mesospheric, 79
surface, 119
variance of potential, 36
zonal mean, 64, 118
- Temperature anomalies, sea surface, 117
- Temperature gradient, meridional, 52, 59,
74 f., 108, 152
- Thermal wind, 106, 148
- Tidal effects, 79
- TIROS IV, 125, 195
- TIROS VII, 145
- Torque, due to pressure differences across
mountains, 11, 19 f.
frictional, 19 f.
- Trade winds, 9, 12, 117, 156
- Trajectories, 5 f., 83 f.
- Transosonde, 12, 169
- Transport, mean meridional (see
Circulation, mean meridional)
- Trapping of waves, 148
- Tropopause, 70, 102, 129, 173, 197, 211 f.
- Tropopause gap, 212
- Troposphere, 49, 51, 53, 70, 72, 75, 78,
101 f., 108, 129 f., 132, 136, 141, 156,
169, 173, 183 f., 193, 197, 203, 205, 212,
214 f.
- Tropospheric three-cell pattern, 60, 180
- Troughs, tilting, 27, 161, 173
- Tungsten, 133
- Turbulence, 162, 171
clear air, 161
convective, 133 f., 139
- Typhoons, 139
- Undulance, 162
- United States, 117, 125, 214
- Velocity potential, 73
- Volume, specific, 38
- Vorticity, absolute, 27, 73
potential, 1, 31, 174, 212
relative, 73, 89
- Vorticity transport, 27
- Washout, 216
- Water vapor, flux of, 136 ff., 197, 200
(See also Moisture transport)
- Wave energy flux, 78
- Wave numbers, 52, 86, 89 f., 148, 161 f.,
165 f., 169, 171 ff., 178 ff., 185 ff.,
190, 193, 195 f., 199 f., 208 f., 213
energy exchange between, 184
- Waves, lee, 215
planetary, 5, 6, 20, 27, 52, 78, 92, 114,
117, 145, 168, 171, 174, 190, 211
semiannual, 152
standing, 171
transient, 141, 171, 173
(See also Eddies)
- West Pacific, 159, 197
- Zonal index, cross spectra of the, 86

LEGAL NOTICE

This book was prepared under the sponsorship of the U. S. Atomic Energy Commission. Neither the United States, nor the Commission, nor any person acting on behalf of the Commission:

A. Makes any warranty or representation, expressed or implied, with respect to the accuracy, completeness, or usefulness of the information contained in this publication or that the use of any information, apparatus, method, or process disclosed in this book may not infringe privately owned rights; or

B. Assumes any liabilities with respect to the use of, or for damages resulting from the use of any information, apparatus, method, or process disclosed in this publication.

As used in the above, "person acting on behalf of the Commission" includes any employee or contractor of the Commission, or employee of such contractor, to the extent that such employee or contractor of the Commission, or employee of such contractor prepares, disseminates, or provides access to, any information pursuant to his employment or contract with the Commission, or his employment with such contractor.